Assessing the Compressive Strength and Elastic Modulus of High-Performance GGBS Concrete

Jingran Gao

A thesis submitted for the degree of Doctor of Philosophy to the University of Dublin, Trinity College.

Jan 2023

The Research for this thesis was conducted at the Department of Civil, Structural and Environmental Engineering University of Dublin, Trinity College, Ireland

Declaration:

I hereby declare that this thesis is entirely my own work. It has not been used to obtain any degree in this or any other university.

I hereby confirm that the library may lend or copy this thesis for academic purposes upon request.

_____

Jingran Gao

Jan 2023

Acknowledgements:

I would like to express my gratitude to a number of people who have helped and supported me through the course of my PhD.

First of all, to my parents, who sacrificed a lot through not being able to see me for the most time during these years. Their phone calls across the entire Eurasia have always been my best support and encouragement.

To my supervisor Roger West, who have been giving me constant support anytime I am in difficulties with academic problems or life. I could not imagine the writing of this thesis can be finished without his guidance and encouragement.

To Kevin, Mick, Dave, Barrie, Eoin, Sean and Chris, who provided me the with facilities and a huge amount of work to finish my long-term project in the laboratory. To Kevin, who can manage and solve any problem in the lab whenever I need his help. To Mick, who stood with me throughout the tedious work of concrete pouring every morning. To Dave, who produced excellent models and tools for my experiments. To Eoin, who taught me a lot of practical knowledge in making concrete samples.

To Banagher Concrete and Ecocem, who supported me through the funding and experimental materials for making a large amount of concrete samples.

To my friends Cong and Yishan, who made my life much easier and more comfortable with various help in the daily life. I am lucky to be your roommate for more than four years.

To my friend and colleague Lin, who are always helpful in the postgraduate office when I needed some aids.

Abstract:

The mechanical properties of High Performance Concrete are crucial for structural design to achieve expected advantages over conventional concrete. For example, the efficient prefabrication of precast concrete requires sufficient early-age strength so that early striking time and transport can be achieved. The stiffness of prestressed concrete significantly determines the prestress loss as the deformation of concrete is strongly related to the elastic modulus.

The studies of the mechanical properties of High Performance Concrete involve the correlation between the compressive strength and the elastic modulus. There are also many influencing factors that strongly affect these mechanical properties.

Ground granulated blast-furnace slag (GGBS), as a by-product from a steel plant, is a widely used supplementary cementitious material in Ireland. The advantages and disadvantages of using GGBS are both vital for assessing this material in concrete manufacture. It is necessary to quantify the influence of GGBS on both the strength and elastic modulus under various conditions.

There are many conventional methods that can be used to accelerate the development of concrete after mixing to varying degrees. Thus both the strength and elastic modulus are affected by these techniques under a faster growth rate. The individual effect of one accelerating method and the combined effect of several methods together are both of importance for determining the growth path of concrete strength and stiffness.

Numerical prediction of the compressive strength and elastic modulus is commonly introduced in many standards and books through different formulae. The comparison of calculated values and actual results provides a reliable method of determining the accuracy of those formulae. For different countries with more complicated situations, modified formulae with new variables and constants should be proposed based on experimental work for more accurate prediction.

This research recommends values for constants and indices in the predicted equations used by practitioners for both strength and stiffness using Irish aggregates and GGBS, together with rapid hardening cement, an accelerating admixture and thermal curing in the high strength precast industry.

TABLE OF CONTENTS

LIST OF ABBREVIATIONS

ACI	American Concrete Institute
ACV	Aggregate crushing value
Al_3O_2	Aluminium oxide
C_2S	Dicalcium silicate
C_3S	Tricalcium silicate
C_3A	Tricalcium aluminate
C_4AF	Tetracalcium aluminoferrate
$CaCO_3$	Calcium carbonate
CaO	Calcium oxide
CEM I	Portland cement
CEM II	Portland-composite cement
CEM II/A-L	Portland-limestone cement
CEM III	Blast furnace cement
C-S-H	Calcium silicate hydrate
EC2	Euro Code 2
E_c	Modulus of elasticity
E_{cm}	Secant modulus of elasticity of concrete at 28 days
f_c	Compressive cylinder strength of cylinder concrete
f_{ck}	Characteristic compressive cylinder strength of concrete at 28 days
$f_{ck.cube}$	Characteristic compressive cube strength of concrete at 28 days
f_{cm}	Mean compressive strength of concrete at 28 days
Fe_3O_4	Iron oxide
fib	International Federation for Structural Concrete
GGBS	Ground Granulated Blast-Furnace Slag
GPa	Gaga Pascal
HPC	High-Performance Concrete
HSP	High-Strength Concrete
LP	Limestone powder
MLS	Modified lignosulfonates
MPa	Mega Pascal
PFA	Pulverized fly ash
RHPC	Rapid Hardening Portland Cement

SCM	Supplementary cementitious materials
SF	Silica fume
SiO_2	Silicon dioxide
SMF	Sulphonated melamine-formaldehyde condensates
SNF	Sulphonated naphthalene-formaldehyde condensates
SSD	Saturated surface dry
TOC	Total organic carbon
UHPC	Ultra high strength concrete

LIST OF FIGURES

Chapter 2

Chapter 3

LIST OF TABLES

Chapter 2

Chapter 3

Chapter 4

1.INTRODUCTION

1.1 Background

Due to the constant pursuit of better constructional materials, there is a concerted move towards off-site production of concrete in order to take advantage of inherent efficiencies associated with precast concrete production. These include leaner, more environmentally friendly production of large volumes of concrete, including better quality control, less waste, improved safety and more efficient prefabrication. To provide these advantages for the building industry, special constituents and mixing techniques are essential to improve the properties of concrete in any specified scope. Concrete with improved features can be classified as High Performance Concrete (HPC) to achieve various specialist jobs.

The most valuable property of concrete as a man-made material is its strength after the hydration reaction occurs in a concrete mixture. As the direct consequence of cement hydration, strength also represents the general quality of concrete production and is strongly determined by most factors that influence the chemical reaction of the hydration process. The long-term strength and durability of concrete are the primary concerns for any structural design when using concrete as a building element. The early-age strength of concrete is also critical because striking time and early transport of precast concrete highly rely on the performance of concrete during the first few days after mixing. Therefore, it is important to fully understand the growth path of concrete strength through a continuous period after mixing.

The deformation of concrete always occurs when any stress is imposed on the concrete element. For influences on structural design issues, such as early cracking, prestress loss and maximum deflection, it is vital to study the stress-strain relationship from the elastic range to the non-linear range. When the stress is below a certain threshold and the applied period is short enough, concrete can be treated as an elastic material. Therefore, the modulus of elasticity derived from the stress-strain relationship can be used to represent the elastic property of concrete for design requirements. It is established also that the modulus of elasticity is highly related to the compressive strength. Empirical formulae have been established to predict the modulus of elasticity based on the compressive strength with acceptable accuracy in the past, but the introduction of cement alternation has changed this.

The above two mechanical properties of concrete can be affected by many factors during concrete production. The composition of cementitous materials is a core factor for

concrete development and can be heavily influenced by an addition of supplementary cementitious materials other than pure Portland cement. Ground granulate blast-furnace slag (GGBS), for example, as a common type of supplementary cementitious material, is a by-product from a steel-making plant. The rationale for using GGBS in the Irish market place has never been stronger, given the recent publication of the latest version of the Irish National Annex to the European Concrete Specification, I.S. EN-206-1 (2013). Using this document, it is now permissible, based on extensive research conducted by the Irish Concrete Society Durability Committee, and ratified by NSAI, to use up to 70% GGBS as a cement replacement in combination with CEM I Portland cement on a one-for-one basis. It may also be used in combination with certain newer CEM II/A cements now produced in Ireland, including CEM II/A-LL and CEM II/A-V. The former is the most used product in Irish concrete practice.

The quick turn-over of precast concrete requires additional techniques to accelerate both the strength and stiffness of concrete to a high degree. Rapid Hardening Portland cement (RHPC) is an alternative of normal Portland cement for a higher rate of early-age strength development. This accelerating ability of RHPC is mainly due to its higher fineness of ground cement clinker.

Admixtures are not an essential component for concrete but can provide significant benefits in various properties at a controlled dosage. There is a wide range of chemical admixtures for achieving different functions, such as accelerating, retarding, water-reducing etc. In particular, the application of an accelerating admixture can help the precast concrete manufacturer with a quicker striking time and early service in construction.

The temperature effects on cement hydration can cause significantly different results of strength and stiffness at both early-age and long-term. Concrete produced under a low-temperature environment grows at a reduced rate of strength development. On the other hand, a higher temperature speeds up the hydration reaction, and therefore accelerates the growth of strength during the early age. However, this accelerating effect leads to poorer microstructure of cement paste and consequently can reduce the long-term strength to some extent.

The nature of aggregates is of great importance to the properties of concrete due to their high proportion of total concrete mass. It is agreed that both strength and modulus of elasticity are affected by the mechanical properties of aggregates. However, the influence of coarse aggregate on strength is sometimes insignificant when the ultimate strength of concrete is largely lower than the strength of the coarse aggregate used. The reason is that

the strength testing of concrete cannot reach the strength limit of coarse aggregate due to a weak cement paste. The modulus of elasticity, on the other hand, is heavily related to the elastic property of coarse aggregate no matter how strong the strength and stiffness of concrete are.

1.2 Objective

The general aim of this research is to investigate the mechanical properties of a novel recipe HPC produced under various conditions. Two phases of experimental work were designed to achieve the goals by monitoring the growth of the compressive strength and elastic modulus through a long period of concrete development. Different constituents and techniques were selected to establish an overall picture of influencing factors on HPC. Then, experimental results can be used for numerical analysis to indicate the effects of individual or combined factors. Based on the analysis of experiments, it is also necessary to propose variable empirical formulae for theoretical predictions of compressive strength and elastic modulus to guide concrete design. The research objectives in each step are:

-Review past literature of concrete mechanical properties to plan appropriate experimental schemes and design concrete constituents.

-Investigate the influence of five different types of coarse aggregate in terms of compressive strength and elastic modulus through laboratory tests.

-Investigate the retardation effect of the GGBS content on concrete growth from a low to high proportion.

-Investigate the individual and combined effects of three well-established different accelerating methods from 1 day to 56 days.

-Investigate the individual and combined effects of these different accelerating methods on concretes containing different proportions of GGBS content from 1 day to 56 days.

-Compare the experimental results and theoretical predictions of compressive strength to derive more accurate coefficients in different situations.

-Predict the elastic modulus based on the 28-day compressive strength. Compare the experimental results and theoretical predictions to improve the empirical formula for different situations.

-Predict the elastic modulus based on the 28-day elastic modulus. Compare the experimental results and theoretical predictions to improve the empirical formula for different situations.

1.3 Thesis Structure

The chapters of this thesis are written in the following structure:

Chapter 2 is a general literature review of high-performance concrete. The nature and performance of HPC and each main constituent of HPC will be discussed to demonstrate the existing knowledge of concrete. The theoretical modelling of compressive strength and elastic modulus are also introduced in this chapter for analysing the experimental work in later chapters.

Chapter 3 introduces the materials and experimental methods involved in this research. The technical specifications of cementitious materials, aggregates and chemical admixtures are of importance in experimental designs. The mix setup and proportions of each experimental phase are outlined in detail. There are full explanations of mixing and testing methods in this chapter for each phase. The pouring scheme is also properly planned to suit the capability of the concrete laboratory.

Chapter 4 mainly demonstrates the experimental results of phase 1. The measures of compressive strength and elastic modulus for five different types of coarse aggregates are discussed to show the influences of each rock type. The predicted values of elastic modulus are compared with the actual test ones to evaluate the formula proposed by EC2 and Model Code 2010. Modified values of a coefficient in this formula will be proposed for Irish local aggregates.

Chapter 5 involves the numerical analysis of experimental results under various proportions of GGBS and different combinations of accelerating methods. By comparing the results in a general picture, the quantitative effects of GGBS, three accelerating methods and their possible combinations can be acquired and shown in tables.

Chapter 6 focuses on the theoretical predictions of compressive strength and elastic modulus through empirical formulae proposed by EC2. With the original formulae and coefficients, the calculated results have significant errors compared to the test values.

Therefore, varying the values of coefficient can improve the accuracy of prediction. In this case, these coefficients can be used as indicators that reflect the effects of different influencing factors. A further improved prediction can be achieved by modifying the structure of those formulae by introducing new coefficients.

Chapter 7 draws the conclusions from the experimental and calculated results of previous chapters. It also discusses the recommendations for further studies.

CHAPTER 2. LITERATURE REVIEW

2.1 Introduction

This chapter presents a general review of the properties of high-performance precast concrete in several respects. Section 2.2 mainly introduces the nature and performance of precast concrete and its advantages over conventional concrete in terms of efficiency, durability and functionality. The relevant mechanical properties of precast concrete, namely the compressive strength and elastic modulus, are crucial for structural design to meet the requirement of high-performance.

The following sections 2.3 to 2.5 discuss the nature of each constituent of precast concrete and how they interact with other materials to affect the performance of a concrete mix. Cementitious materials and their hydration processes are the primary factors that determine the development of concrete to a large extent. Aggregates and additional admixtures also have significant roles in concrete production depending on their physical/chemical properties.

Section 2.6 presents the past research on theoretical predictions of concrete's mechanical properties over time. Predicting the compressive strength and elastic modulus will be the objective of this research in later chapters, and the numerical influence of temperature effects will also be discussed in a mathematical form based on past empirical equations.

2.2 High-Performance Precast Concrete

Concrete is the most widely used construction material all over the world for various applications. The properties of concrete have advantages which ensure its leading role as a building material in the 21st century. These advantages, including the low cost of raw materials and manufacturing, high resistance and durability, easy maintenance, etc., are inherited and magnified by introducing High Performance Concrete (HPC) in a precast plant to replace the conventional concrete poured on-site.

The American Concrete Institute (ACI) defines high-performance concrete (HPC) as a concrete meeting special combination of performance and uniformity requirements that cannot always be achieved routinely using conventional constituents and normal mixing, placing and curing practices. The primary feature of HPC is its high compressive strength from a compact matrix. Concretes with a cylinder compressive strength over 42MPa are normally considered as high-strength concretes (Nawy 2001). However, high-strength

concrete and high-performance concrete are not synonymous. The compressive strength of HPC is not the only criteria for design. Long-term durability and serviceability are more important properties for particular requirements. Thus, the term high-performance has been used to describe for concrete mixtures possessing high workability, high durability and high ultimate strength (Mehta and Aitcin 1990).

Precast concrete is manufactured in a factory mould and cured in controlled environments other than its on-site position. The production process of precast concrete can be monitored and controlled more consistently in a precast plant than conventional concrete produced in-situ on a construction site. The finished concrete components are transported to and lifted in the construction site for their designed application. A precast plant also provides controlled conditions for the application of prestressing reinforcement where the steel wires, strands or cables can be either pre-tensioned or post-tensioned in the precast concrete for extra flexural strength.

2.2.1 Economics

HPC resists structural loads that cannot be resisted by ordinary concretes in most cases. It also increases the strength per unit cost, per unit weight, and per unit volume compared with normal-strength concretes. Thus, the volume of structural elements, such as columns under compression loads, can be significantly reduced by using HPC because its higher bearing capacity requires less cross-sectional area. This advantage also brings economic benefits for the construction industry. Furthermore, HPC typically has an increased modulus of elasticity, which increases the stability of structures and reduces deflections and deformations (Malaikah 2005).

2.2.2 Sustainability

When considering the sustainability of the concrete industry, HPC can be helpful in reducing the energy consumption and raw materials to some extent. Generally speaking, the entire concrete industry is not sustainable for several reasons. For example, the process of Portland cement manufacturing is irreversible and generates a large amount greenhouse gas. The demand for non-renewable raw materials used for concrete production is unavoidable and is increasing year by year, while the rate of use of recycled concrete is not yet increasing proportionately (Changming Bu et al. 2022).

The advantages of HPC in solving sustainability problems come from two sources. Firstly, HPC reduce the total volumes of concrete and extends the service life to a longer period. Traditionally, normal concrete structures are designed for a service life of 50 years

approximately (I.S EN-206-1, 2013). With the advent of HPC, the service lives of these new designed structures can be doubled to about 100 years (Mehta 2004). The increasing productivity of the concrete industry results in a significant reduction in consumption of energy and raw materials. Consequently, the total carbon footprint of concrete industry is lowered.

Another way to solve sustainability issues by using HPC is to re-use the industrial wastes to replace certain proportions of cement used in concrete mixtures. These industrial by-products are called supplementary cementitious materials (SCM) and are generated from various industries which are unable to recycle them in their own manufacturing process. Portland cement contents in HPC mixtures are largely reduced by blending with these supplementary cementitious materials, meanwhile the structural properties of HPC are improved in various respects depending on the types of cementitious materials used in the concrete mixtures. It is now possible to produce HPC mixtures containing up to 60% pulverised fly ash (PFA) or 70% ground granulated blast-furnace slag (GGBS) by mass of the blended cementitious material.

2.2.3 Architectural Applications

HPC has a dense microstructure that makes it quite suitable for certain types of architectural applications. It can be cut into a smooth surface and polished easily using similar methods as other architectural materials, such as granite and marble. Even though polished high-performance concrete cannot compete with natural materials from an aesthetic point of view (see Figure 2.1), it can present some unique technical advantages over other building materials, such as high resistance and reinforcement with steel or fibres (Aitcin 1995).

Figure 2.1 Smooth surface of C40/50 cylinder sample due to its dense microstructure

2.2.4 Durability

To some extent, durability rather than high strength appears to be the principal characteristic for the use of HPC. This character of HPC is especially required for concretes used in hostile environments such as seafloor tunnels, offshore and coastal marine structures, and confinement for solid and liquid wastes containing hazardous materials (Mehta and Aitcin 1990).

For HPC, it is often required to develop the early-age strength at a faster rate. However, in the long-term, concrete with high early-age strength may not turn out to be durable and maintenance-free to meet the requirements for HPC. A typical reason is that these concrete mixtures generate extra heat at an early age and are characterized by drying shrinkage at low water/cement ratios, and therefore are prone to autogenous cracking (Jiang et al. 2022). Under severe exposure conditions, concrete structures containing internal microcracks cannot provide sufficient durability in the long-term.

Chloride attack is caused by calcium chloride and sodium chloride within sea or de-icing water migrating through the concrete by a diffusion process. Therefore, a lower diffusion rate is highly necessary for HPC which is exposed to severe conditions. With the additions of supplementary cementitious materials, such as PFA and GGBS, HPC can be significantly more durable to this type of chemical attack due to lower permeability and chloride binding (Neville 2012).

Carbonation is the process whereby calcium hydroxide in concrete reacts with carbon dioxide in air to form calcium carbonate. The alkalinity of concrete is lowered due to the subsequent weak carbonic acid in the concrete. Thus, this process is a major cause of the corrosion of steel reinforcement. HPC incorporating supplementary cementitious materials (such as PFA) is less resistant to carbonation reaction due to a large loss of calcium hydroxide through the PFA's pozzolanic reaction (Sulapha et al. 2003). Furthermore, proper curing is significantly important to the carbonation resistance of HPC with supplementary cementitious materials due to slower hydration (Navdeep et al. 2022).

Alkali-silica reaction is a common type of alkali-aggregate reaction that takes place between the hydroxyl ions from the calcium hydroxide in the concrete and reactive forms of silica in the aggregate. It can cause severe expansion and cracking in concrete, resulting in serious structural problems. Replacing part of the Portland cement with pozzolanic materials is an effective solution to reducing the expansion of altered

aggregates due to less amount of alkali in the concrete. PFA, GGBS and silica fume (SF) are suitable ingredients in resisting the alkali-silica reaction (Lindgård et al. 2012).

2.2.5 Workability

Appropriate workability of HPC requires the mixture to be easily vibrated and compacted through closely placed reinforcement. The formwork of concrete structures should be filled completely without voids and segregation.

In practice, this workability is mainly determined by the slump of the fresh mixture of HPC. Sufficient slump is essential for HPC to achieve a compact and dense matrix. For high-flowing concrete mixtures, such as self-compacting concrete, the workability needs to be tested by a flow-measuring method, such as the slump-flow test (IS EN-12350-8, 2010).

Workability of HPC depends on several factors during the concrete producing process. The first one is the condition of the aggregates. Under the condition of saturated surface dry (SSD), the surface of aggregate particles is relatively dry while the inter-particle voids are saturated with water content. The SSD aggregate does not influence workability because the free water content is not affected by such aggregates. The moisture content within aggregate beyond or under this condition is required to be determined and taken into account in the modification of the total free water content (Neville 2012).

Temperature is another important factor that determines the workability through the hydration process of concrete. A higher temperature causes lower setting time and faster loss of slump. Therefore, a low temperature is necessary to keep the slump value for a longer period (Neville 2012).

Plasticizers and superplasticizers are chemical admixtures which are significantly effective in maintaining the workability of concrete when the water/cement is reduced to a lower value that is usually not practical for conventional concrete. Thus, they are also called mid-range water reducers or high-range water reducers respectively (Neville 2012).

The increase of cement fineness has a positive effect on the workability (Ahmad 2002). For example, Rapid Hardening Portland cement (RHPC) has a higher fineness of cement particles than normal Portland cement, and consequently a better cohesiveness under the same mix proportions. The supplementary cementitious material, PFA, also improves the workability by partially replacing the normal Portland cement due to the high fineness and spherical shape of its particles.

The workability of HPC also involves the requirement of stability to prevent the segregation of concrete mixtures. To improve the stability of HPC, a higher quantity of fines content in the concrete is needed by increasing the cement quantity, adding supplementary cementitious materials or increasing the fineness of the fine aggregates (Zhang et al. 2021).

2.3 Cementitious Materials

Cementitious materials are the binding components of concrete that hold all the materials together. The traditional cement, Portland cement, can be used alone or blended with other supplementary cementitious materials, such as limestone powder (LP), PFA, GGBS or SF (I.S. EN-197-1, 2011).

2.3.1 Portland Cement

Portland cement is the primary binding material of HPC that produces a strong water-resisting compound which comprises a hardened matrix of concrete after the hydration reactions are completed. It consists of a powdered crystalline mixture of oxides of calcium, silicon and aluminium. There are four dominating compounds formed from these oxides shown in Table 2.1 that comprise Portland cement in various proportions.

Name	Chemical composition	Abbreviation
Tricalcium Silicate	$3CaO.SiO_2$	C_3S
Dicalcium Silicate	$2CaO.SiO_2$	C_2S
Tricalcium Aluminate	$3CaO.Al_2O_3$	C_3A
Tetracalcium Aluminoferrate	$4CaO.Al_2O_3.Fe_2O_3$	C_4AF

Table 2.1 Compounds of Portland Cement

The strength development of HPC is determined by the hydration reactions that take place between Portland cement and water if no supplementary cementitious material is added. Figure 2.2 shows the development of compressive strength of each pure compound with time. C_3S and C_2S are significantly stronger than the other two compounds during the entire period of concrete development. Therefore, C_3S and C_2S make up over 75% of the whole cement by mass; they contribute most to the strength growth. During the first 28 days, C_3S has a faster rate of reaction than that of C_2S and generates more heat as seen in Figure 2.2. Thus early-age strength develops faster with a high percentage of C_3S, while

C_2S has a slower strength development with high long-term compressive strength (Neville 2012).

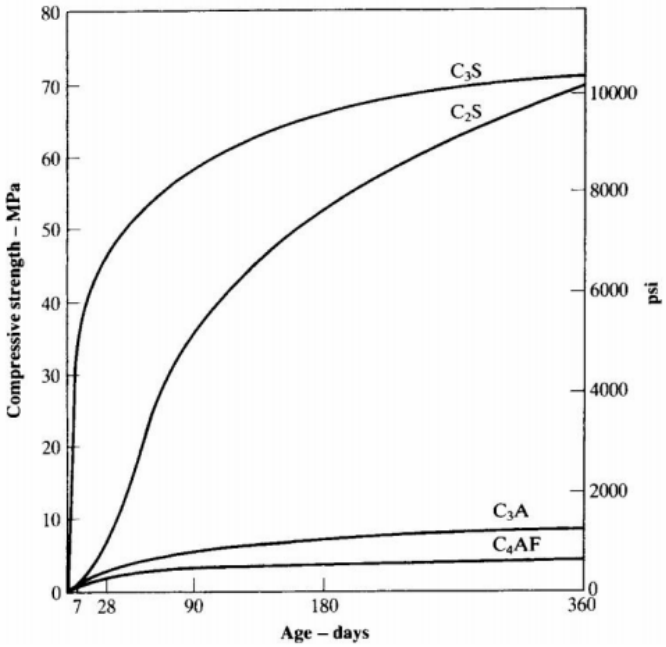

Figure 2.2. Development of compressive strength of pure compounds (Neville 2012)

A harmonised European Standard defines five classes of common cement that comprise cement clinker in varying amounts from up to 100% (CEM I) down to 10% (CEM III/C) (I.S. EN-197-1, 2011). These cement types, termed as CEM cements, should conform to the requirements of this Irish standard. By appropriately batching and mixing with aggregate and water, the CEM cements should be capable of producing concrete or mortar which retains its workability for a sufficient time and possess long-term volume stability. The ages at which concrete attains specified strength levels should be defined. The cementitious materials that are permitted to be added in type II to type V CEM cements are artificial pozzolanic materials (GGBS, SF and PFA) or natural pozzolanic materials (volcanic ash glasses, calcined clays and shale), together with LP in some cases.

I: Portland cement	Comprising ground Portland cement clinker and up to 5% of minor additional constituents
II: Portland-composite cement	Ground Portland cement clinker and up to 35% of other single constituents
III: Blastfurnace cement	Ground Portland cement clinker and higher percentages of blastfurnace slag
IV: Pozzolanic cement	Ground Portland cement clinker and up to 55% of pozzolanic constituents (volcanic ashes)
V: Composite cement	Ground Portland cement clinker, blastfurnace slag or fly ash and pozzolana

Table 2.2 Classifications of common cements

The fundamental principle of classifying cement types by EN-197 is based on the percentage proportions by mass of Portland cement clinker and other mineral constituents (I.S. EN-197-1, 2011). Particularly, Portland cement CEM I and Portland-Limestone cement CEM II/A-L are involved in this research.

Further experiments will also involve the blending of CEM I or CEM II/A-L with GGBS. Combinations of CEM I and GGBS are equivalent to CEM II/A or CEM III/B if the percentage of GGBS is between 36% and 80% (I.S. EN-197-1, 2011). Combinations of CEM II/A-L and GGBS do not equate to any blended cements permitted under IS EN 197-1, but are deemed to satisfy the requirements of IS EN 206 if restricted to a maximum of 70% GGBS.

2.3.1.1 CEM I: Portland cement

CEM I cement is manufactured to contain over 95% Portland cement clinker which consists of predominant compounds C_3S, C_2S, C_3A and C_4AF. Minor additional constituents are controlled below 5% by mass and mixed with Portland cement clinker to produce the finished product. These additional constituents are necessary for particular reasons, such as Calcium Sulphate that is added as gypsum to control the fast setting time caused by C_3A hydration (Neville 2012).

The standard 28-day compressive strength of CEM I Portland cement has 3 classes, which are class 32,5, class 42,5 and class 52,5. The figure of each corresponding class indicates that the characteristic 28-day compressive strength of cube prism made from this cement type should be not less than this figure in MPa.

By testing the early-age strength of the above cement classes at 2 days and 7 days, each strength class can be divided into 3 levels, depending on the early-age performance in Table 2.3.

-Ordinary early strength: N

-High early strength: R

-Low early strength: L

Thus, for one particular type of CEM I Portland cement, there are 9 different strength classes as shown in Table 2.3. These classes of cement are used to determine the early-age and long-term performance for concrete designs. This table also indicates the initial setting of different strength classes and their soundness (expansion) performances.

For HPC with a specific requirement of high early-age strength, CEM I classed as 42.5R and 52.5R are recommended to achieve this goal. These cement types are called Rapid Hardening Portland Cement (RHPC) as a more specific term.

Strength class	Compressive strength MPa				Initial setting time	Soundness (expansion)
	Early strength		Standard strength			
	2 days	7 days	28 days		min	mm
32,5 L[a]	-	≥ 12,0	≥ 32,5	≤ 52,5	≥ 75	≤ 10
32,5 N	-	≥ 16,0				
32,5 R	≥ 10,0	-				
42,5 L[a]	-	≥16,0	≥ 42,5	≤ 62,5	≥ 60	
42,5 N	≥ 10,0	-				
42,5 R	≥ 20,0	-				
52,5 L[a]	≥ 10,0	-	≥ 52,5	-	≥ 45	
52,5 N	≥ 20,0	-				
52,5 R	≥ 30,0	-				
a Strength class only defined for CEM III cements.						

Table 2.3 Strength classes of CEM Portland cement (I.S. EN-197-1, 2011)

Rapid Hardening Portland Cement (RHPC) is a specially manufactured cement for concrete construction to achieving a higher rate of early-age strength, compared to using ordinary Portland cement. The early-age performance of Portland cement can be improved by modification of the mineral phase composition, addition of admixtures, multi-component mixtures and increasing the fineness of the cement powder (Srinivasan et al. 2003). The most common method is achieved through increased fineness. The specific surface area of RHPC is 450 to 600 m^2/kg compared to 300 to 400 m^2/kg of normal Portland cement (Neville 2012).

2.3.1.2 CEM II/A-L: Portland-Limestone cement

Portland-Limestone cement is produced by grinding a combination of cement clinker, selected LP and a controlled quantity of gypsum up to 5% by mass. The addition of limestone content replaces Portland cement clinker by 6% to 20% by mass. The selected limestone added in CEM II/A-L is finely ground powder of limestone and shale. The requirements of the limestone addition are (I.S. EN-197-1, 2011):

-The calcium carbonate content calculated from the calcium oxide content should be at least 75 % by mass.

-The clay content should not exceed 1.20 g/100 g.

-The total organic carbon (TOC) content should not exceed 0.5 % by mass.

The production of Portland-Limestone cement has been increasing in the cement industry in order to reduce consumption of natural raw materials for producing normal Portland cement, which consequently reduces the CO_2 emissions from the cement industry (Baron and Douvre 1987, Damtoft et al. 2008). Since the sustainable advantage of replacing Portland cement with limestone content is coupled with a sufficient supply of limestone sources, this type of CEM II cement is widely used as normal Portland cement in Ireland nowadays, where typically 8% limestone is used as clinker substitute apparently without adversely affecting strength attainment.

The strength development of limestone cement is affected by the interaction of cement clinker and limestone content rather than their individual reactions within the concrete matrix (Tsivilis et al. 1999). However, there is no overall agreement on whether the limestone content improves or reduces the strength development of CEM II/A-L cement (Sarah et al. 2022) (Gyabaah et al. 2022). The compressive strength of concrete made from Irish CEM II/A-L cement develops a similar compressive strength as the concrete made from CEM I cement, of the same strength class. Compared with normal Portland cement, no effect of limestone content on concrete setting time is observed (Irassar et al. 2011).

As far as cement hydration is concerned, it is generally agreed that limestone participates in the hydration reactions rather than being an inert filler. However, the estimation of the limestone amount that is incorporated into a cement hydration process has no widely acceptable conclusion (Klemm and Adams 1990). For example, the influence of limestone on the properties of concrete products depends on a series of factors of mixture constituents, including cement types, cement fineness and lime saturation factor. For cement clinker having a high lime saturation, the addition of limestone mainly influences the early compressive strength. On the other hand for cement clinker having a low lime saturation, long-term compressive strength after 28 days and the initial setting time are influenced considerably by the addition of limestone (Vuk et al. 2001).

The participation of limestone during the hydration process is proved to be the reaction between $CaCO_3$ from the limestone content and C_3A from the cement content. When considering the fresh properties of concrete with limestone cement, there is a reducing water demand of using CEM II/A-L for particular slump, compared to the corresponding pure CEM I cement (Tsivilis et al. 1999). This is because limestone powder is not as fine as Portland cement, typically.

2.3.2 Supplementary Cementitious Materials

Supplementary Cementitious Materials (SCM) are common by-products from other industrial processes with various degrees of cementitious capability. These materials have little or no reactivity in moist conditions by themselves but can present cementitious properties by reacting with one of the products of the hydration Portland cement, namely calcium hydroxide. Pozzolanic materials consist essentially of siliceous or alumino-siliceous contents that chemically react with the calcium hydroxide released by the hydration of Portland cement to form new hardened products, calcium silicate hydrate (C-S-H) gel (Neville 2012).

For the pozzolanic activity, supplementary cementitious materials are added to a concrete mixture as part of the cementitious system. They can be used as a partial replacement of Portland cement in concrete, depending on the properties of the materials and the desired effects on concrete, or as an addition. These specific effects of using supplementary cementitious materials improve particular concrete properties, such as high chemical resistance, less early-age heat generation and low permeability/slow diffusion (Neville 2012).

Concrete containing an SCM, such as PFA, GGBS and SF, provide better resistance to attack under seawater conditions compared to normal Portland cement concrete (Memon et al. 2002), but, generally, poorer carbonation resistance.

2.3.2.1 Pulverised Fly Ash

Pulverised Fly Ash is a finely divided by-product from the combustion process of coal-fired power stations. The large demand of electricity also results in the generation of large quantities of fly ash (I.S. EN 450-1, 2012). In Europe, it is widely known as PFA.

PFA contains various compounds, which includes silicon dioxide (SiO_2), aluminium oxide (Al_3O_2), iron oxide (Fe_3O_4), calcium oxide (CaO) and small amounts of crystalline compounds. The particles of PFA are generally spherical in shape and range in size from 1 to 100 µm, and the specific surface is usually between 250 to 600 m^2/kg by the Blaine method compared to 300-400 m^2/kg for normal Portland cement (Neville 2012). The specific density of PFA generally ranges between 1.9 and 2.8 compared to 3.1 for normal Portland cement and the typical colour is grey.

This pozzolanic material can be used as a component of blended Portland cements or a mineral admixture in concrete. In European standards, the dosage of fly ash is suggested

to be 6-35% by mass of the total cementitious material (I.S. EN-197-1, 2011). The limit can be raised to 55% for Type IV CEM cement, or even 70% in certain situations, but above 35% PFA acts as a filler rather than as a cement due to the lowered amount of calcium hydroxide available from cement hydration process to execute the pozzolanic reaction (Swamy and Lambert 1983).

Using PFA in concrete mixtures enhances some of the fresh and hardened properties of concrete. These advantages include (Neville 2012):

-Improved workability and lower water demand

-Less bleeding and segregation

-High sulphate and alkali aggregate resistance

-Reduced early-age thermal cracking

-Reduced permeability and adsorption, and slower diffusivity

Furthermore, PFA is economical and more environmentally friendly because the total carbon footprint is reduced by replacing some proportions of normal Portland cement with PFA. The influence of PFA on compressive strength cannot be quantified by any specific method or formula (Neville 2012). In general, the early-age strength of concrete is decreased by using PFA, since the pozzolanic reaction take places over a longer period after mixing. The long-term strength of concrete, particularly over a year, is improved considerably with the addition of PFA. However, this beneficial influence is not clear when PFA content exceeds 35% by mass of the total cementitious material (Odler 1991).

2.3.2.2 Ground Granulated Blast-furnace Slag

Ground Granulated Blast-furnace Slag (GGBS) is made from iron blast-furnace slag which is a by-product of the iron and steel production process. It is a hydraulic cementitious material consisting essentially of silica, lime and alumina developed in a molten condition simultaneously with iron in a blast furnace. These oxide materials, similar to the components of Portland cement, comprise over 70% by mass of GGBS. Irish practice requires that GGBS contains at least two thirds by mass of glassy slag and possesses hydraulic properties when suitably activated (I.S. EN-197-1, 2011).

This granulated material, which is ground to less than 45 μm, has a surface area fineness of about 250 to 500 m^2/kg by the Blaine method (Neville 2012). Thus, the specific area fineness of GGBS is generally higher than that of Portland cement and shall not be less

than 260 m^2/kg (I.S. EN 15167-1, 2006). The specific gravity of GGBS is in the range of 2.85 to 2.95, and the typical colour is white or light-grey.

Since GGBS has hydraulic properties, it can be used on its own for particular constructions with water and alkali activators, such as Sodium Hydroxide or Calcium Hydroxide. However, the most common application of GGBS is using it with Portland cement in certain proportions by various methods. This type of cement, normally called Portland Blastfurnace cement (CEM III), is produced by blending ground cement clinker and dry GGBS together. Alternatively, a recognised cement (e.g. CEM I) may be combined with GGBS powder at the mixer on site or at the ready-mixed concrete plant. Both blended cement (CEM III/B) and combinations (CEM I or CEM II/A and GGBS) are used in Ireland.

The hydraulic activity of GGBS is conditional on its surface fineness and quantified as an activity index by I.S. EN 15167-1. This activity index, for any particular test cement, is expressed as the ratio of compressive strength of mortar prisms made from half GGBS and half test cement, to the compressive strength of mortar prisms made from 100% test cement at the same age. I.S. EN 15167-1 requires that the activity index at 7 days and at 28 days shall be not less than 45 % and 70 % respectively.

The beneficial effects of using GGBS with Portland cement into concrete mix are (Neville 2012):

-Improved workability

-Slower heat generation

-Higher long-term compressive strength

-Higher durability due to lower permeability and slower diffusion rates

-Improved resistance to steel corrosion due to chloride ingress

-Prevention of alkali-silica reaction

The strength development of Portland Blastfurnace cement is in a similar manner to cement containing pozzolanic materials. The initial hydration rate is very slow since the GGBS requires the alkali hydroxides to activate its hydraulic properties, while alkali hydroxides are released from the hydration of Portland cement at a slow rate. Thus, the early-age strength of Portland Blastfurnace cement is lower than normal Portland at a ratio that depends on the proportion of GGBS used in the mix. Especially for concrete within 1 day of mixing, the compressive strength is mainly determined by the hydration of Portland cement on its own, and the peak rate of heat generation decreases linearly

with increasing addition of GGBS (Ballim and Graham 2009). Figure 2.3 demonstrates the influence of GGBS on the heat generation on varying replacement levels from 20% to 70%. The increasing replacement of GGBS causes a significant reduction of mortar temperature depending on the proportions of GGBS. Resulting from the slow rate of early-age hydration, the setting time of concrete with GGBS is also retarded and thus increases the specified curing times. Using GGBS at 40% by mass of total cementitious materials causes extreme retardation in setting times as the initial and final setting times can be increased to 11 and 17 hours from 5 and 7.5 hours respectively (Brooks et al. 2000).

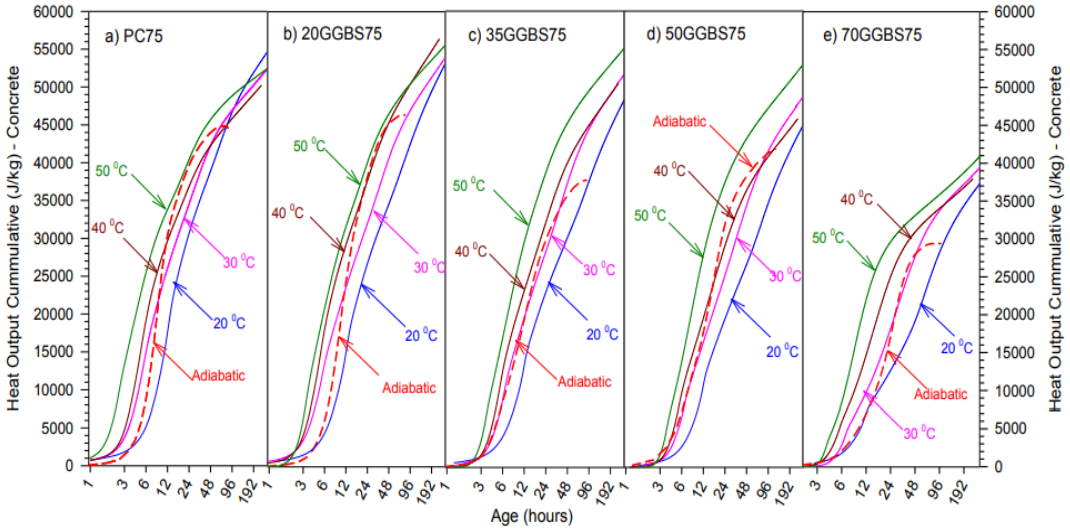

Figure 2.3 Cumulative heat output of concrete with different proportions of GGBS (Gidion 2013)

On the other hand, for GGBS containing more silica content and less lime, the resulting products of this type of cement have more calcium silica hydrates (C-S-H) than normal Portland cement and a denser pore structure. Therefore, the long-term structure of the cement paste is expected to be stronger and denser than CEM I or CEM II/A-L concretes (Neville 2012).

2.3.2.3 Silica Fume

Silica fume, often used as a pozzolan, is a by-product material of the manufacture of silicon or ferrosilicon alloy from high-purity quartz and coal in an electric arc furnace. The history of using silica fume is relatively short compared with other SCMs. Nowadays, silica fume is increasingly acting an important role for various applications of HPC.

Silica fume, in essence, consists of silicon dioxide (usually more than 85%) in amorphous form. It has extremely fine particles (usually less than 1 μm) in spherical shape (I.S. EN-197-1, 2011). The specific surface area of silica fume is about 20,000 m^2/kg (using the nitrogen adsorption method), which is about 50 times higher than that of Portland cement particles (Neville 2012). The specific gravity of silica fume, on the other hand, is about 2.2 and is relatively light compared with Portland cement. The colour of silica fume can be either light or dark grey depending on the remaining carbon contents.

The physical properties of silica fume make it more reactive than the other SCMs. Due to its high reactivity, the replacement of Portland cement by silica fume at small proportions, normally 5-15% by mass, can improve the early-age strength of concrete significantly. The early-age strength loss due to inclusion of PFA also can be compensated for by the incorporation of silica fume at certain mixing proportions (Khan 2012). The small particles of silica fume can enter the gaps between Portland cement particles to reduce permeability, and thus enhancing the durability, of concrete to a large extent.

Normally, silica fume is used with Portland cement by the batcher in situ. Portland-silica fume cement containing 6-10% silica fume by mass is produced by blending silica fume and Portland cement together and is categorized as CEM II/A-D in the European standard. The cost of silica fume is considerably higher than other SCMs which is prohibitive to its wider use. Consequently, it is mostly used for HPC with specific and strict quality requirements. Furthermore, due to its extreme fineness it is hard/dangerous to handle and often is used in slurry form (Runxiao et al. 2022).

2.4 Aggregates

Aggregates, occupying approximately 70% by mass of total concrete volume, significantly influencing the properties of concrete, such as shrinkage, strength limits and elastic behaviour, as well as workability (Neville 2012).

From an economical point of view, aggregates are cheaper than any other constituent in concrete, except water. Incorporating more aggregates in concrete design can considerably reduce the cost of concrete construction and improve its performance.

2.4.1 Fine aggregate

Aggregates are generally divided into 2 main groups by their sizes. Fine aggregate, often named as sand, have particles less than 4mm in size; while the dimensions of coarse

aggregates are required to be greater than 4mm (I.S. EN 12620, 2013). Fine aggregate is the main constituent that comprises cement mortar during the concrete mixing process. Fine aggregate with good quality should have a proper grading, as shown in Table 2.4 and be free of organic impurities or any other deleterious materials. Fine aggregates can be categorized into natural sand and crushed sand. HPC containing crushed sand performs similar or better with regard to its mechanical properties than natural sand, while fresh mixtures with crushed sand are less workable due the shape and texture (and thus water demand) of sand particles (Donza et al. 2002).

Sieve size	Tolerances in percentages passing by mass		
mm	0/4	0/2	0/1
4	± 5 [a]	–	–
2	–	± 5 [a]	–
1	± 20	± 20	± 5 [a]
0,250	± 20	± 25	± 25
0,063 [b]	± 3	± 5	± 5

Table 2.4 Tolerances on typical grading for general use fine aggregates (I.S. EN 12620, 2013)

2.4.2 Coarse Aggregate

The properties of coarse aggregates are important factors that influence the long-term strength and durability of concretes, depending on their physical and mineral nature. Three common types of coarse aggregates are widely used and classified by their sources, which are crushed stones, natural gravels and artificial aggregates.

Coarse aggregates from crushed stones are made from various types of natural rocks, such as igneous, sedimentary and metamorphic rocks. They are generally stronger than natural gravels produced by weathering actions, but less workable in fresh concrete. Artificial coarse aggregates are normally by-products from other manufacturing processes and are used for light-weight concretes (Ravindra et al 2018).

2.4.3 Influence of Aggregate

The shape and texture of aggregate have significant effects on both the fresh and hardened properties of concrete. An increase in roughness and angularity of aggregate particles would result in lower workability. On the other hand, a rough surface and angular shape are beneficial to form strong bond between cement paste and aggregate

which improves the hardened strength of concrete. The overall strength is increased by using irregular-shaped aggregate (Piotrowska et al. 2014).

The grading/size distribution of aggregate is an important factor for mix design of concrete. The control of segregation and bleeding of fresh concrete is affected by the grading of aggregate largely. However, the relationship between the aggregate grading and concrete proportions has not been established in a mathematical form to control the above behaviour of concrete (Neville 2012). An appropriate grading of aggregate should conform to the requirements in the Irish standard (I.S. EN 12620, 2013).

The strength of aggregate is not considered to be a key factor that determines the strength of normal concrete because the failure strength of normal concrete is mainly decided by the cement paste which is far below the strength of aggregate. However, for HPC with extraordinary high strength, the strengths of cement paste and aggregate could be close to each other and in such cases, the mechanical properties of aggregate can be the limiting factor for concrete strength. In ultra-high strength concrete (UHPC), the interfacial transition zone between the cement paste and surface of the aggregate plays a significant part in its enhanced mechanical properties.

The deformation properties of aggregate, especially coarse aggregate, have significant influence on the elastic modulus of concrete. The elastic modulus of concrete is increased when using aggregate with higher elastic modulus. Concretes made from different types of coarse aggregate may have similar strength due to the same design of cement paste. However, these concretes can be significantly different in their elastic modulus because these aggregate types have different elastic modulii. To represent the differences mathematically among different types of aggregates, a coefficient α is introduced in a prediction formula for elastic modulus in the European concrete design standard (I.S. EN-1992-1-1, 2005). This formula and values of coefficient α for common rock types will be examined in further discussions.

2.5 Chemical Admixtures

An admixture is made from a specific chemical material that can be added to a concrete mix in a small quantity (normally less than 5% by mass of cement content) to modify a particular property of concrete. There is an increasing demand for different types of chemical admixtures for the design of HPC with various quality requirements. These chemical admixtures provide considerable benefits for HPC through the fresh states to hardened properties. The effectiveness of admixtures is highly determined by its dosage

in the concrete mix and other mixing constituents. Ideally, the variation of admixture effectiveness with different dosages should be controlled within an acceptable range (Neville 2012).

A series of chemical admixtures are defined and specified by the European standard (I.S. EN 934-2, 2012) for various functions as follows:

-Water reducing/plasticizing admixtures

-High range water reducing/superplasticizing admixtures

-Water retaining admixtures

-Air entraining admixtures

-Set accelerating admixtures

-Hardening accelerating admixtures

-Set retarding admixtures

-Water resisting admixtures

-Set retarding/plasticizing admixtures

-Set retarding/superplasticizing admixtures

-Set accelerating/plasticizing admixtures

-Viscosity modifying admixtures

The above admixtures can provide beneficial effects for concrete with a single function or multiple functions. Superplasticizing admixtures and hardening accelerating admixtures are particularly of interest in this research and shall be considered further.

2.5.1 Superplasticizer

A superplasticizer, also termed as a high range water reducer, has become a common admixture for concrete productions, especially in high performance and self-compacting concrete. This chemical admixture is significantly water reducing and more effective than a normal water reducer (Neville 2012). Superplasticizers are linear polymers containing sulphonic acid groups attached to the polymer backbone at regular intervals. There exist four main types of superplasticizers:

-Sulphonated melamine-formaldehyde condensates (SMF)

-Sulphonated naphthalene-formaldehyde condensates (SNF)

-Modified lignosulfonates (MLS)

-Carbohydrate esters

Superplasticizers with long molecules can wrap around cement particles and give them negative charges on their surfaces. Thus, the cement particles repel each other by steric repulsion (Cartuxo et al. 2015). This action by superplasticizers results in deflocculation and dispersion of cement particles, thus releasing the water tied up in the cement particles and thereafter reducing the viscosity of fresh concrete mixtures. The sulphonic acid groups attached on these polymers are the functional components of superplasticizers for neutralizing the surface charges on the cement particles.

Using superplasticizers affects fresh concrete properties resulting in flowing concrete mixtures with very high slump where sufficient compaction cannot otherwise be easily achieved. The other major application of superplasticizers is to produce high strength concrete at low water/cement ratio ranging from 0.3 to 0.4 (Ramachandran and Malhotra 1984). The effectiveness of using superplasticizers to improve the workability of concrete depends on such factors as chemical types, dosages, water/cement ratios and cement types.

With a high initial slump, a fast rate of slump loss with time often appears with the application of superplasticizers in concrete (Ramachandran and Malhotra 1984). The slump loss problem can be overcome by adding the admixture to the concrete just before the concrete is placed.

2.5.2 Hardening accelerating/retarding admixtures

Hardening accelerating admixtures, referred to simply as accelerators, are mainly used to accelerate the rate of strength growth of concrete at an early age. The chemical ingredients of accelerators include some inorganic compounds such as calcium chlorides, carbonates and silicates, and some organic compounds such as triethanolamine. On the other hand, a retarding admixture, or retarder, comprises of sugar, carbohydrate derivatives, soluble zinc salts, soluble borates and some other salts (Ramachandran and Malhotra 1984). This chemical admixture can counteract the accelerated hydration process due to hot conditions, slow down the slump loss and keep the concrete workable for a longer period.

Figure 2.4 shows the influences of an accelerator and a retarder on the rate of heat of hydration during the early age of concrete compared with a standard mix. The significantly increased amount of heat generation when using an accelerator has a great impact on the initial setting time of Portland cement concrete. Although the rates of heat

liberation of the accelerated mix and non-accelerated mix are similar to each other after 10 hours, the extra heat generation before 10 hours can result in a higher early-age compressive strength for the accelerated mix. The effect of a retarder, also shown in Figure 2.4, demonstrates lower rate of heat generation during the first 10 hours. Figure 2.4 also shows that the retarded mix has a slightly higher rate of heat generation than the normal and accelerated mix (Schindler 2004).

The most common type of accelerator that has been used over a long time period is calcium chloride. This chemical compound was dissolved in concrete mixtures as a catalyst that effectively speeded up the hydration reaction of calcium silicate in Portland cement. Calcium chloride has been used for concrete produced in cold weather since 1885 to achieve equivalent strength gain to concrete cured under normal curing temperatures (Rixom and Mailvaganam 1986). Originally, under normal temperatures, calcium chloride was used to accelerate the setting and hardening process for fast mould turnaround of precast concrete. The early-age compressive strengths of concrete are considerably improved by using calcium chloride at a dosage of 2% by mass of cement, while the long-term strength is usually unaffected but is sometimes reduced, especially at high temperature conditions. Aside from the accelerating effect, calcium chloride had a minor effect on fresh concrete properties. It was observed that addition of calcium chloride slightly improved the workability and reduced the water demand (Ramachandran 1984).

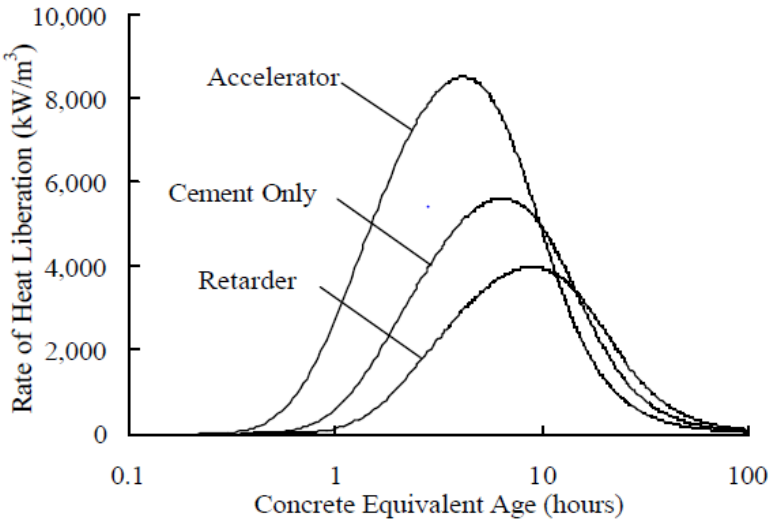

Figure 2.4 The effect of a retarder and accelerator on the rate of heat of hydration (Schindler 2004)

However, calcium chloride introduces chloride ions to the mix that can corrode reinforcing steels in the presence of moisture and oxygen (Sluijter and Kreijger 1997).

This detrimental effect makes it prohibited for reinforced concrete and prestressed concrete by various standards and codes.

Considering the risk of using calcium chloride, non-chloride accelerators have become standard. These alternatives are chemical compounds containing sulphate, formate, nitrate or triethanolamine ions. Compared with calcium chloride, these non-chloride accelerators are generally less effective and economical, thus none of these options is widely accepted as preferential at present (Neville 2012).

2.6 Mechanical Properties of HPC

HPC is designed to satisfy a series of special requirements that cannot be commonly achieved by mixing normal structural materials or applying normal concrete practices. The compressive strength and elastic modulus of HPC are the main properties that will be focused on in this research. There are a series of fresh and hardened properties that are required to be discussed for analysing these mechanical properties of HPC.

2.6.1 Compressive Strength

The compressive strength of precast HPC is a primary property that needs to be designed properly for various performance requirements. The striking time of concrete formwork and the early construction loads that can be applied to the structure are primarily determined by the early-age strength of the HPC, and this is critical for the efficiency of precasting operation. This early-age strength also affects the strength development over the entire life of the HPC, and consequently determines the long-term compressive strength of the HPC to some extent. There are various factors that control the compressive strength of the HPC from the mixing proportions to mixing conditions shown in Table 2.5 (Neville 2012).

Mixing proportions	Manufacturing processes
-Water/binder ratio -Chemical admixtures -Mineral admixtures -Aggregate Strength (For HPC)	-Temperature and moisture of raw materials -Room temperature and humidity -Compaction process -Curing condition

Table 2.5 Key factors that control the compressive strength

2.6.1.1 Hydration process:

The strength development of HPC is a result of the hydration reactions that take place between the water and cementitious materials right after the mixing processes and lasts

continuously for a long period of many years at a decreasing rate if water continues to be available. The resulting hydration products form and provide the solid and hardened properties for concrete.

The compressive strength is highly dependent on the degree of hydration which is the fraction of total cementitious materials that has already reacted. This chemical reaction is exothermic and, therefore, the heat generated from the hydration reaction can be used to represent the degree of hydration. A higher rate of heat generation results in a faster development of compressive strength. Figure 2.5 describes several possible factors that can affect the heat of hydration through various mixing constituents and procedures.

The SCMs have little hydraulic activity and require alkalinity (such as calcium hydroxide) as an activator to initiate the reaction. For example, GGBS needs to be blended with Portland cement which is the source of calcium hydroxide when hydrated. As a result, the early-age hydration of this blended cement is significantly slower than that of pure Portland cement depending on the percentage of GGBS. Consequently, the compressive strength growth is slower when replacing some Portland cement with GGBS (Kourounis et al. 2007). Different types and compositions of SCMs also cause significantly different variations to the heat of hydration in the blended cement paste (Beushausen et al. 2012). These influences of SCMs are also varying at different stages of concrete development.

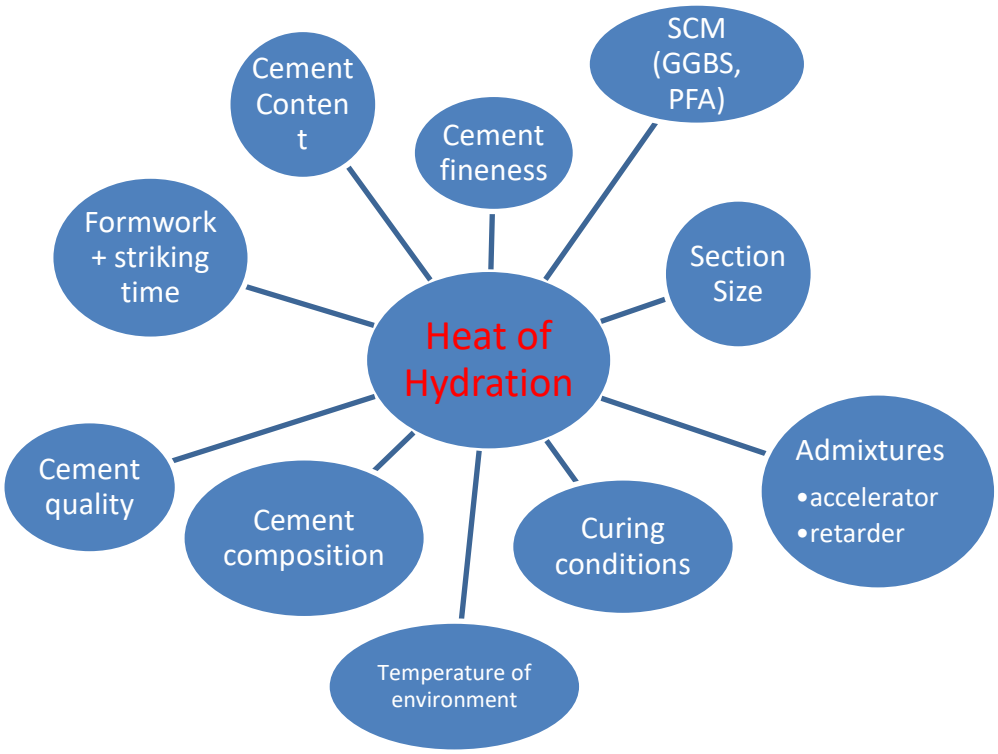

Figure 2.5 Key factors that influence the heat of hydration

2.6.1.2 Water/Binder ratio

At a given age and curing condition, the strength and concrete is primarily determined by the water/cement ratio and the degree of compaction (Neville 2012). The water/cement ratio has a great impact on the capillary porosity of hardened cement paste. Consequently, the volume of porosity within the cement paste determines the strength of concrete because it is highly related to the microstructure and failure of concrete. Thus, the strength is considered to be inversely proportional to the water/cement ratio. The mathematical relationship between the concrete strength and water/cement ratio was established by Duff Abrams in 1919 and is described in Equation 2.1 (Neville 2012).

$$f_c = \frac{K_1}{K_2^{w/c}} \qquad \text{(Eqn 2.1)}$$

where f_c and w/c are the strength of concrete and water cement ratio, and K_1 and K_2 are empirical constants.

This ideal relationship given by Equation 2.1 is drawn in Figure 2.6 with a solid line to represent fully compacted concrete. The degree of compaction significantly influences the larger voids within the concrete. Therefore, the compaction method is also important for the strength of concrete. Although the numerical influence of compaction cannot be determined clearly, the dashed line in Figure 2.6 shows the possible effect of incomplete compaction on the compressive strength of concrete.

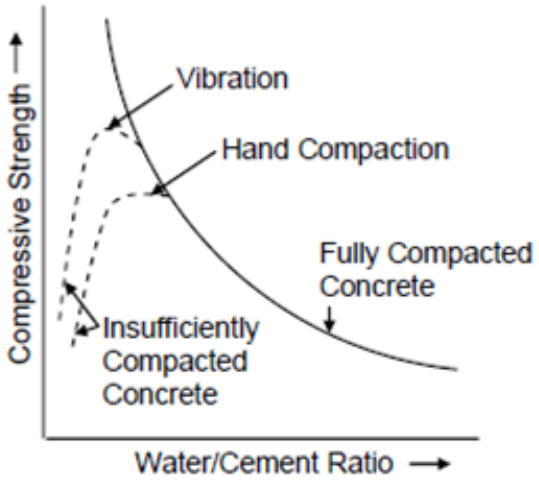

Figure 2.6 Relation between strength and water to cement ratio of concrete (Neville 2012)

2.6.1.3 Curing Condition

Curing is an important process for concrete development as it provides adequate moisture content and temperature over a required period of time to ensure timely and continued hydration. Figure 2.7 demonstrates the influence of the curing process at different levels. The concrete without any curing stops gaining any strength quickly after it dries out. Thus, the 28-day strength of non-cured concrete can only reach about 50% of the potential 28-day strength of concrete which is continuously cured for 28 days (Mamlouk and Zaniewski 2010). Short-term curing is helpful for strength development to a limited degree. As the curing condition is continuously provided for concrete, the hydration reaction will also continue to increase the strength of concrete gradually over a long period of time.

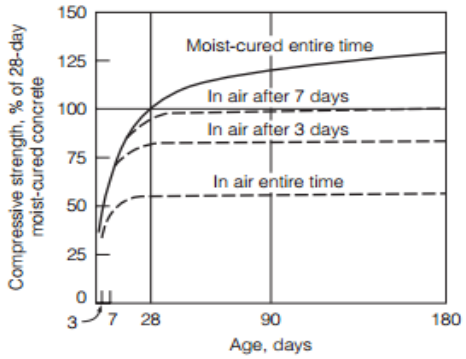

Figure 2.7 Compressive strength of concrete at different ages and curing levels (Mamlouk and Zaniewski 2010)

As an example, Table 2.6 demonstrates that uncontrolled moisture conditions would cause a significant loss of compressive strength, approximately 25%-35%. From a high water/cement ratio (0.55) to a low water/cement ratio (0.30), wet cured concretes have consistently higher compressive strengths than those uncured concrete specimens at any particular age from 3 days to 90 days. When the water/cement ratio is 0.40, the increment of compressive strength from 3 days to 90 days is also greater if concrete is wet cured (increased by 17.5MPa in this case), while the uncured concrete only gained 6.2MPa during the same period of time.

Free	Plasticizer	Slump	Uncured compressive strength (N/mm^2)					Wet cured compressive strength (N/mm^2)				
w/c	(l/m^3)	(mm)	3 days	7 days	14 days	28 days	90days	3 days	7 days	14 days	28 days	90 days
0.30	6.8	30	29.43	30.85	31.91	32.84	32.95	36.04	40.02	47.38	49.18	49.75
0.35	5.7	90	29.03	34.24	36.64	37.63	39.50	35.42	41.68	45.73	52.71	61.71
0.40	2.4	120	28.79	30.36	33.60	34.78	35.01	32.49	34.95	40.42	44.53	49.96
0.45	1.1	200	22.13	29.96	31.00	33.40	33.34	23.82	27.68	33.69	33.94	40.11
0.50	0	200	19.19	20.45	25.54	25.79	26.75	20.89	24.18	28.13	30.39	34.85
0.55	0	200	13.29	16.25	18.56	20.39	21.21	15.20	16.99	21.01	21.34	26.37

Table 2.6. Typical effects of curing conditions on compressive strength of concrete (Abalaka and Okoli 2012)

2.6.1.4 Temperature

Figure 2.8 is a comparison of compressive strength of concretes cured at different temperatures and tested at 1 and 28 days. The 1-day tests demonstrate the powerful effect of high-temperature curing. As a result, the 1-day compressive strength is increased from 3MPa to 15MPa when the curing temperature is heated from 12˚C to 48˚C. However, the beneficial effect of high curing temperature at 1 day becomes detrimental at 28 days. Compared with the early-age enhancement, there is an equivalent reduction in the compressive strength at 28 days.

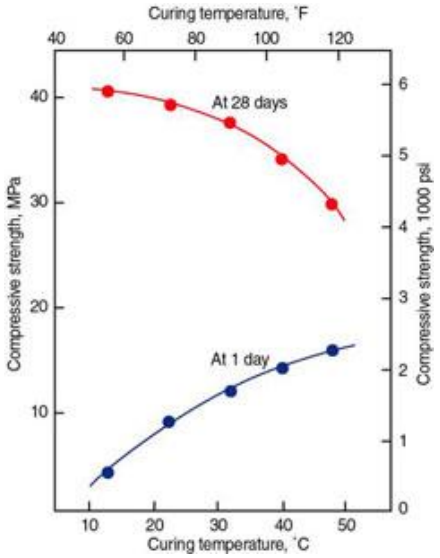

Figure 2.8 Influence of curing temperature on the compressive strength at 1 and 28 days (Neville 2012)

To control the temperature of concrete, there are several methods which can be used before or after the mixing process. Heating or cooling the concrete materials (cement, aggregate and water) before the start of mixing can ensure a constant temperature throughout the entire thermal treatment. The control of temperature after mixing can be achieved through water curing or steam curing. Concrete is stored in the designed curing conditions for a certain period of time.

2.6.1.5 Strength development with time

The long-term compressive strength of concretes is denoted by the characteristic cylinder strength f_{ck}, which is determined by testing cylindrical specimens at 28 days (I.S. EN-1992-1-1, 2005). Less than 5% of test result are expected to be lower than this characteristic compressive strength. When cylindrical specimens are not available, the test results of cube specimens can be used to represent the compressive strength of concrete and expressed as $f_{ck,cube.}$ However, for any particular concrete mixture, the test results of

cube specimens are consistently higher than those of cylinders due to different aspect ratios of the specimen types. The platens of the compression machine have a confining effect at the ends of concrete specimens to restraint the lateral expansion, and this confining effect by the platens increases the recorded axial strength of concrete. The entire part of a cube specimen is affected by this confinement, but the middle part of a cylindrical specimen is not affected due to a higher aspect ratio. Therefore, a cube specimen has a higher compressive strength than a cylindrical specimen made of the same concrete (Kumavat and Patel. 2014). Table 2.7 demonstrates the relationship between f_{ck} and $f_{ck,cube}$ across most strength classes of concrete from normal to high-strength concrete.

$f_{ck,cylinder}$ (MPa)	12	16	20	25	30	35	40	45	50	55	60	70	80	90
$f_{ck,cube}$ (MPa)	20	24	28	33	37	45	50	55	60	67	75	85	95	105

Table 2.7 Strength classes of cylinders and cubes (I.S. EN-1992-1-1, 2005)

EuroCode 2 (EC2) also introduces a method to predict the mean compressive strength at various ages. Under a mean temperature of 20°C and curing in accordance with the European specification (IS EN-12390-1, 2012), the compressive strength of concrete $f_{cm}(t)$ may be estimated by Equations 2.2 and 2.3. The original source of the EC2 formula is considered to be fib Model Code 1990 when EC2 was first published in 1990s. Model Code 1990 was superseded by a newer version Model Code 2012 later.

$$f_{cm}(t) = \beta(t)\, f_{cm} \qquad \text{(Eqn 2.2)}$$

where:

$$\beta(t) = \exp[s[1-(\frac{28}{t})^{0.5}] \qquad \text{(Eqn 2.3)}$$

$$f_{cm} = f_{ck} + 1.64\times\Delta \qquad \text{(Eqn 2.4)}$$

where:

$f_{cm}(t)$ is the mean concrete compressive strength at an age of t days

f_{cm} is the mean compressive strength at 28 days

Δ is the standard deviation

$\beta(t)$ is a coefficient which depends on the age of the concrete

t is the age of the concrete in days

s is a coefficient which depends on various factors, such as the types of cement, temperature history, addition of SCM and admixtures.

As shown in Figure 2.9, characteristic strength is defined as the strength below which a specified proportion of all valid test results is expected to fail. For conventional data, this proportion is taken to be 5%. The later chapters in this thesis are based on the mean values of testing results rather than the characteristic ones.

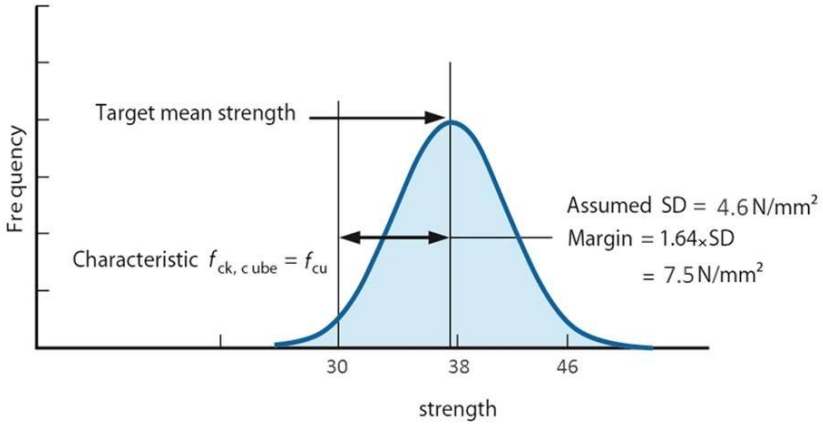

Figure 2.9 Characteristic strength vs Target mean strength (Crook and Day 2016)

A theoretical curve of strength development derived from Equation 2.2 and 2.3 is drawn in Figure 2.10 to demonstrate the estimated behaviour of strength growth with time. If the concrete does not conform with the EC2 specification for compressive strength at 28 days, the use of Expressions (2.1) and (2.2) may not be appropriate. For example, if the early-age curing temperature is far above 20°C to achieve extreme high early-age strength, the compressive strength cannot be estimated by the age of concrete alone. The magnitude of the curing temperature also needs to be considered for more precise prediction.

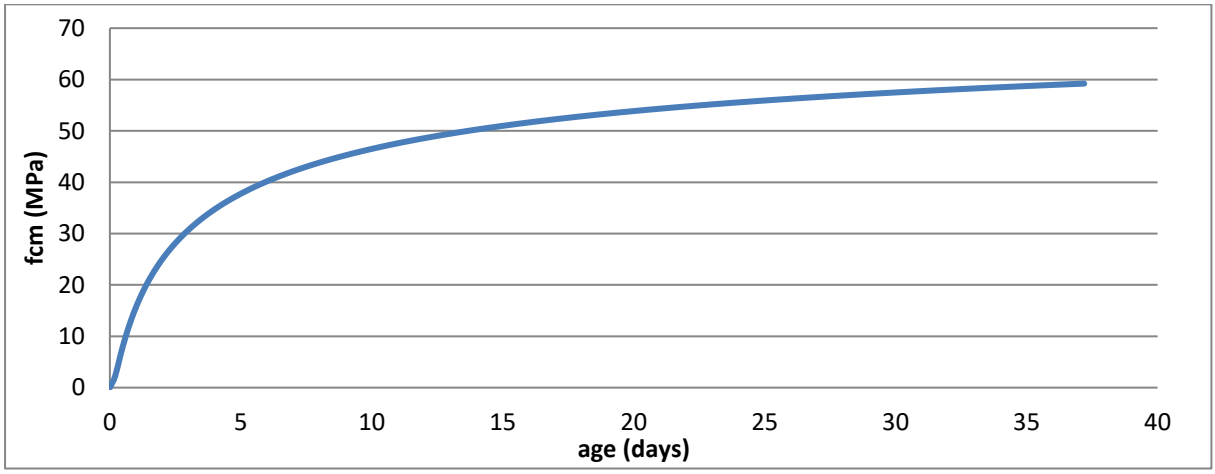

Figure 2.10 Typical strength development with time based on EC2 model of strength prediction

2.6.2 Modulus of elasticity

Elastic stiffness of concrete, often measured as modulus of elasticity, is a fundamental property that determines the deformation behaviour of structural concrete, particularly used for the design of reinforced and prestressed concrete. The loss at transfer of the prestress force due to the elastic shortening of the concrete should be calculated by taking into account the elastic modulus of the concrete at the time of transfer. The prestress loss is equal to the concrete stress at the centroid multiplying a ratio of $E_p/E_{cm,}$ where E_p and E_{cm} are the elastic modulus of steel and concrete respectively (I.S. EN-13369, 2018). Therefore, and 24-hour elastic modulus is a critical factor when calculating the loss at transfer. To control deflections and dimensions of cracks, it is important to measure or predict an accurate value of elastic modulus for design calculation. For example, the tensile stresses, which cause early-age cracking, can be predicted through the tensile modulus of elasticity in some situations (Yoshitake et al. 2013). The calculation of prestress loss on transfer also requires this elastic property to determine the actual elastic shortening of concrete elements. It is stated that using 50% GGBS replacement of cement is acceptable in precast industry which requires early-age demoulding (Korde 2020). In practice, the direct measurement of the elastic modulus is difficult to achieve on-site. Early-age elastic modulus can be inferred by achieving the early-age compressive strength due to the correlation of the two mechanical properties..

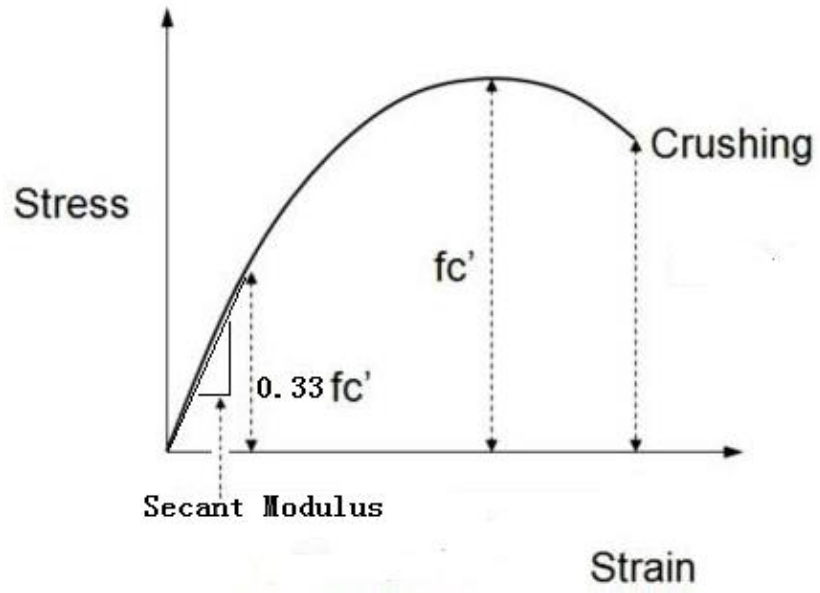

Figure 2.11 Determination of secant modulus of elasticity

The modulus of elasticity, E, is determined by the composition of concrete, aggregate type and age, especially the characteristics of the coarse aggregates used in the concrete mixture (Baalbaki. et al. 1991). However, the direct measurement of the values of the

modulus of elasticity is time-consuming and is more complicated than the direct measurement of uniaxial compressive strength. To directly measure this property of concrete, the stress and strain of a concrete cylinder with a 150mm diameter and 300mm height are recorded simultaneously until the stress reaches 33% of the ultimate compressive strength (see Figure 2.11), as previously determined in BS 1881-121 (1983). The secant modulus of elasticity, E_{cm}, can be calculated from the mean recorded strains and stresses after 3 cycles of loading and unloading procedures.

The elastic properties of coarse aggregate and cement paste also influence E_{cm} of concrete to a large extent. Therefore, it is possible to predict E_{cm} of concrete through the elastic modulus of each component. Some theoretical models proposed mathematical relationships between E_{cm} of concrete and the elastic modulii of coarse aggregate and cement paste (Zhou et al. 1995). However, direct testing of the elastic modulus of aggregate particles is not practical under most situations.

To avoid time-consuming testing, researchers and design standards have proposed a series of different mathematical formulae to predict the value of modulus of elasticity, E_{cm}, based on various design factors. The most common method is to express the modulus of elasticity as a function of compressive strength in a given range. There is no precise form of the relationship between the modulus of elasticity and compressive strength, however, it is generally agreed that E_{cm} increases with an increase in compressive strength (Sideris et al. 2004). Previous researchers show that it is not reliable to precisely predict the modulus of elasticity for high strength concrete from its compressive strengths (Baalbaki et al. 1992). Thus, experimental measurement is still necessary to ascertain the modulus of elasticity with appropriate accuracy.

In most standards and publications, a power relationship between the compressive strength and elastic modulus has been established to predict E_{cm} based on f_{ck} or f_{cm}. The general forms of these equations are similar with slightly different constants and a power index of compressive strength (0.3 to 0.33). The application ranges are also different in these standards as most of them are not viable for high-strength concrete. Equation 2.5 is proposed by EC2 and assumes that the elastic modulus is proportional to the mean compressive strength to the power of 0.3. However, an alternative (Equation 2.6) from Model Code 2010 (*fib*-bulletin-66 2012) is based on the characteristic strength and the power index is increased to 0.33.

$$E_{cm} = 22(f_{cm}/10)^{0.3} \text{ (GPa)} \qquad \text{(Eqn 2.5)}$$

where f_{cm} is the mean cylinder strength in MPa.

$$E_{cm} = E_{c0}\,\alpha[(f_{ck} + 8MPa)/10]^{0.33}\ (GPa) \qquad \text{(Eqn 2.6)}$$

where E_{c0} = 21.5 GPa; f_{ck} is the characteristic strength; (f_{ck} + 8MPa) is assumed the same as f_{cm} if the standard deviation Δ is assumed equal to 5MPa. In an earlier version (*fib*-bulletin-42 2008), Ec_0 was equal to 20.5 GPa. The coefficient α is introduced in Equation 2.6 to represent the influence of coarse aggregate type. A similar suggestion for different aggregates is also discussed in EC2. Details of α for each aggregate type will be discussed in later chapters.

However, some research has shown that design values of elastic modulus predicted by Equation 2.5 overestimate the actual stiffness of concrete (Nielsen 2015). Figure 2.12 demonstrates the comparison of predicted values of EC2 model and the test results of elastic modulus at three different curing ages. In general, the experimental measures of elastic modulus are 25%-40% lower than the calculated values based on the cylinder compressive strength. This overestimation by EC2 may cause serious problems for structural design in terms of cracking, deflection, prestress losses and etc. This thesis will examine the accuracy of prediction of elastic modulus.

2.6.3 Maturity

Temperature and age both have significant influences on the development of concrete due to their relationships to the rate of hydration of cement. The prediction of concrete development with time can be based on the combined effect of temperature and age. The maturity method is therefore established by analysing the effect of the temperature history on the compressive strength of concrete. Due to the correlation between the compressive strength and the elastic modulus, the maturity of concrete also has an impact on the development of stiffness.

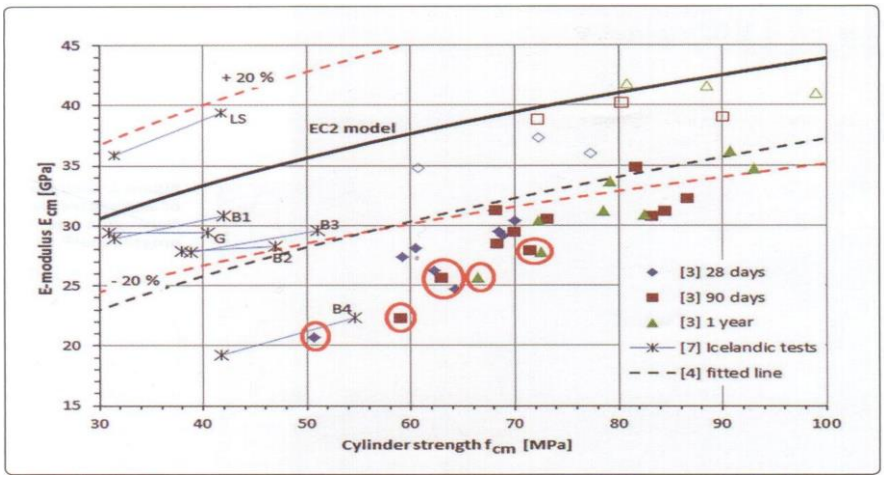

Figure 2.12 Comparison of EC2 model and test results (Nielsen 2015)

In practice, a concrete maturity method is necessary to investigate the effect of curing temperatures on the strength development of concrete from early-age to long-term. The maturity method is an appropriate solution that deals with the combined effects of time and temperature on the strength development of concrete. The origin of the method can be traced to the work on steam curing of concrete carried out in England in the late 1940s and early 1950s (Carino and Lew 2001).

Under variable temperature conditions, the curing regimes are referred to as the temperature history of concrete. Together with the corresponding periods for each curing regime, the maturity index can be calculated by the temperature history. This maturity index is directly related to the prediction of strength because for two similar concretes with similar maturities, their strengths of them will be approximately the same.

The Nurse-Saul maturity function, just one of several available, introduces a mathematical equation to calculate the maturity index shown in Equation 2.7 (Neville 2012).

$$M = \int_0^t (T - T_0) \times \Delta t \qquad \text{(Eqn 2.7)}$$

Where:

M = maturity index (°C-days).

T = average concrete temperature, during the time interval Δt (days).

T_o = datum temperature (°C).

t = elapsed time (days).

Δt = time interval (days).

A typical temperature history calculated by the Nurse-Saul function is displayed in Figure 2.13 as the sum of the shaded areas. From a mathematical point of view, it is an integration of the products of the temperature and the relative time interval.

A typical value for the datum temperature is -10°C when the strength development stops. However, this value may not be accurate for some situations and could lead to a significant inaccuracy of the final strength prediction. This method is based on the assumption that the strength-maturity relationship is relatively linear at different temperatures (Nicholas and Hai 2001).

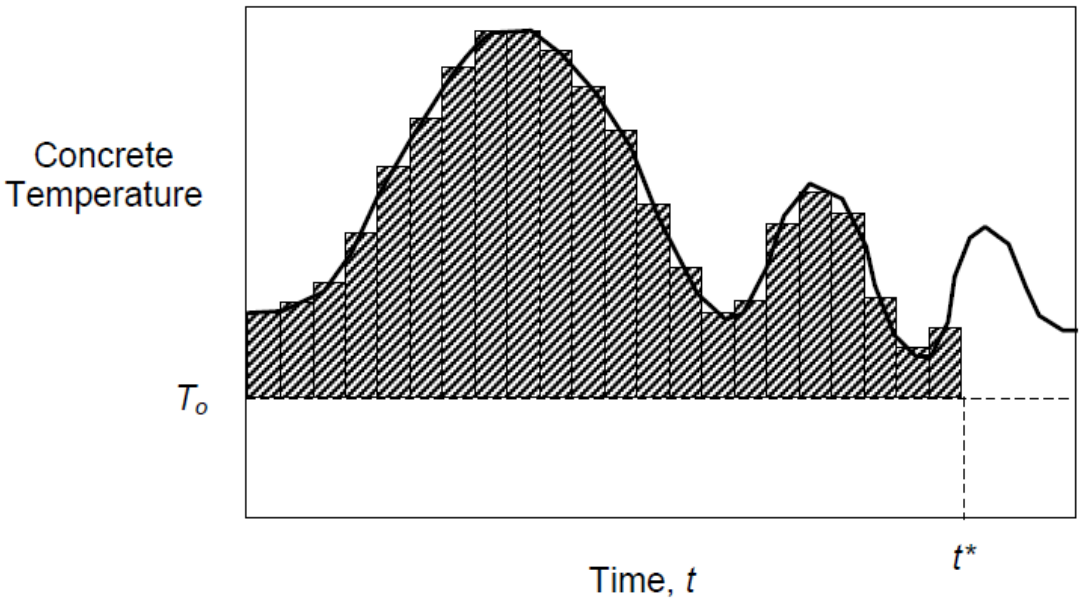

Figure 2.13 Temperature history and maturity factor (Carino and Lew 2001)

However, Equation 2.7 may generate inaccurate results of strength prediction if the initial temperatures are significantly different at early-age. Figure 2.14 shows that at the same maturity index in early-age, the compressive strength of concrete with a high temperature is stronger than that with a low temperature. On the other hand, the long-term comparison between different temperatures shows an opposite result.

An improved function was proposed by Freiesleben Hansen and Pedersen after the Nurse-Saul function for more accurate estimation, which is based on the Arrhenius equation (Neville 2012). The early-age errors of strength-maturity relationship shown in Figure 2.13 can be eliminated by Equation 2.8 because a non-linear relationship is established between the maturity and strength gain.

$$t_e = \sum_0^t e^{\frac{-En}{R}\left(\frac{1}{T}-\frac{1}{T_r}\right)}\Delta t \qquad \text{(Eqn 2.8)}$$

where:

t_e = the equivalent age at the reference temperature (days).

E_n = apparent activation energy (J/mol).

R = universal gas constant, 8.314 J/mol-K.

T = average absolute temperature (Kelvin).

T_r = absolute reference temperature (Kelvin).

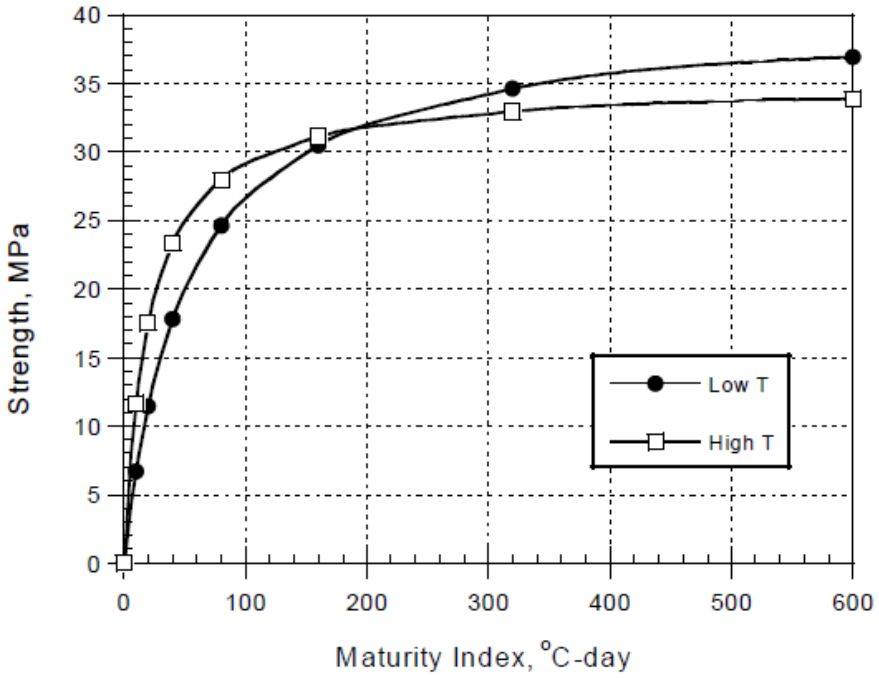

Figure 2.14 Maturity Index for different early-age temperature (Carino and Lew 2001)

To achieve an equivalent strength which is developed through a certain period of time t and reference temperature T_r at an average temperature T which is different from T_r, Equation 2.8 can be used to determine the equivalent age if the apparent activation energy E_n is known. The reference temperature is typically set at 20°C, which is the standard curing condition. The parameter E_n determines the effect of temperature on the rate of strength development. Thus, the value of E_n varies for different cement types and cementitious materials.

2.7 Effects of GGBS on Precast Industry

With the growing demand of precast concrete products and the increased global focus on reducing carbon footprint, the industry is investigating more sustainable alternative cementitious materials such as GGBS as a partial replacement of Portland cement. It is well known that GGBS has limited use in precast manufacturing due to the low early age strength development (Korde et al. 2018). The early age demoulding and lifting are crucial for productivity of precast concrete, sometimes an early time of cutting of pre-stressed strands are also required.

Because the turnover period of precast concrete is mostly required to be 1 day for competitive production, it requires precasters develop the minimum compressive strength for stripping and handling at 24 hours or earlier. To ensure safe stripping and handling of precast concrete, the manufacturers commonly wait until compressive strength reaches at

least 20MPs before they could strip the forms and handle the product. This value also depends on the application and shape of the precast members.

A novel accelerating admixture (ECOCEM AcceleR8 Plus) has proved to be significantly effective for mixing concrete with high proportions (up to 50%) of GGBS while still achieving the target early age strength and stiffness (Korde 2020).

Using thermal curing is another way to accelerate the early-age development of concrete with a high GGBS content. Replacing 30% Portland cement with GGBS appears to be a practical proposition in relation to precast factory use because activation using higher temperatures and admixtures can close the gap in the strength development loss due to its inclusion. Within 1 day, concrete with 30% GGBS can achieve 94% compressive strength. Concrete with more than 30% GGBS can be also accelerated with thermal curing and admixtures, however the 1-day development of strength and stiffness are significantly reduced in any case (Korde 2019).

In terms of compressive strength, the key design requirement for a precast element at stress transfer prior to lifting is a minimum of 25 MPa between 20 and 24 hours after pouring, whereas the production plant personnel can have a target cube compressive strength of 30 MPa (Korde 2019).

Therefore, it is important to investigate numerically the decelerating effect of GGBS at various proportions. Meanwhile, the accelerating effects of different measures are also introduced to compensate for the loss of concrete growth. With compressive strength and elastic modulus tested, these effects can be evaluated to determine whether an acceptable and affordable demould time can be achieved for Irish precasters when producing concrete with high GGBS content.

.

CHAPTER 3. MATERIALS AND EXPERIMENTAL METHODS

To achieve the aims of this research, laboratory data were necessarily acquired by testing a significant quantity of concrete specimens. These concrete specimens mainly consist of Portland and other cements, coarse and fine aggregates, water and chemical admixtures as appropriate. These materials were supplied from various local sources in Ireland.

During the experimental procedures, from concrete mixing and curing to strength and elastic modulus tests, all concrete specimens underwent controlled procedures following the required European Standards. These experimental procedures were carried out in the Structural Engineering Laboratory at Trinity College Dublin.

3.1 Materials

3.1.1 Cementitous Materials

Portland-composite Cement CEM II/A-L:

Portland-composite cement (CEM II/A-L 42.5N) was supplied in bulk by Irish Cement Ltd and was used to make the baseline concrete specimens. Complying with the requirements of the European Standard (I.S. EN-197-1, 2011), CEM II/A-L is produced by blending together the cement clinker and a controlled amount of limestone (6%-20% by mass) at high temperatures. In this case, approximately 8% of limestone by mass is present. CEM II/A-L is eco-friendlier and more popular than CEM I in Ireland. The details of chemical composition of CEM II/A-L 42.5N is shown in Table 3.1. This type of cement is also suitable for use with a wide range of approved admixtures.

SiO_2	**Al_2O_3**	**Fe_2O_3**	**CaO**	**SO_3**	**F.Cao**	**LOI**	**Na_2O**
19.7	4.9	2.9	66.3	2.3	1.4	6.0	0.5

Table 3.1 Chemical composition of CEM II/A-L 42.5N in percentage (Irish Cement Ltd)

At present the role of limestone content in the strength development is still not clear. Concretes made with CEM II/A-L cement develop similar 28-day compressive strengths as those concretes made with CEM I (Fatma et al 2018). The early-age setting time shows minor differences (a slight increase) caused by the addition of limestone, compared with normal Portland cement (Irassar et al. 2011). In I.S. EN-197-1, the initial setting time determined by the Vicat tests (I.S. EN-196-3, 2008) for CEM II/A-L 42.5N is required to be over 60 minutes. The initial setting time of CEM II/A-L produced by Irish Cement typically exceeds 90 minutes, which complies with the corresponding European Standard.

Rapid Hardening Portland Cement:

Rapid Hardening Portland cement (CEM I 42.5R) was supplied in 25kg bags or in bulk by Irish Cement Limited and is designed for the special purpose of concrete manufacture where a higher rate of early strength development is required. The chemical composition of RHPC is almost identical to normal Portland cement CEM I 42.5N, shown in Table 3.2, while the improved early performance of RHPC is achieved principally through longer grinding process which increases the fineness of the cement particles. The typical range of the specific surface area of RHPC is from 450 to 600 m^2/kg, compared with 300 to 400 m^2/kg of normal Portland cement (Neville 2012). The initial setting time of RHPC 42.5R produced by Irish Cement Limited exceeds 75 minutes, which complies with the minimum 60-minute requirement from I.S. EN-197-1.

SiO_2	**Al_2O_3**	**Fe_2O_3**	**CaO**	**SO_3**	**F.Cao**	**LOI**	**Na_2O**
20.1	5.1	3.1	65.3	2.9	1.4	2.46	0.6

Table 3.2 Chemical composition of CEM I 42.5R in percentage (Source: Irish Cement Ltd)

Ground Granulated Blast-furnace Slag (GGBS):

Ground Granulated Blast-furnace Slag (GGBS) is supplied in bulk in Ireland primarily by Ecocem Ltd and is used as the main supplementary cementitious material for this research. Ecocem GGBS is manufactured in a closed-circuit drying and grinding facility in Ireland in accordance with the European Standard (I.S. EN-15167, 2006).

This white powder material contains similar chemical constituents as normal Portland cement, although the proportions of these constituents are different in several respects (shown in Table 3.3). GGBS is suitable for blending with normal Portland cement on a one-to-one basis of substitution. In accordance with I.S. EN 197-1, the proportion of GGBS in total cementitious materials can be up to 95% in concrete mixes. I.S. EN 206-1 allows mix designs containing up to 70% slag content with a CEM I or CEM II cement, mixed at the ready-mixed plant (e.g. CEM I + 70% GGBS or CEM II/A-S + 50% GGBS).

The application of GGBS into concrete mixtures in the precast industry is developing in Ireland. Replacing a certain proportion of CEM II/A-L or RHPC with GGBS can cause a dramatic decreased rate of hydration depending on the amount of GGBS used. This side effect of using GGBS at various replacement proportions needs practical data for quantitative analysis as it can cause a significant detrimental effect on the productivity at precast concrete plants.

SiO_2	Al_2O_3	Fe_2O_3	CaO	MgO	MnO	TiO_2	SO_3	Cl-	S^{2-}	Na_2O
36.5	10.4	0.7	42.4	8.1	0.4	0.5	0.1	0.01	0.7	0.5

Table 3.3 Chemical composition of GGBS in percentage (Source: Ecocem Ireland)

3.1.2 Coarse Aggregates

To investigate the influence of aggregates on the mechanical properties of concrete, principally the strength and stiffness, five rock types of aggregates were selected to be used in the concrete mixes under identical conditions. These aggregates are commonly used as construction materials and are produced from different quarries throughout Ireland.

From a geological point of view, the general distribution of Irish natural bedrocks is shown in Figure 3.1 with a wide variety of different rock types across the island. This geological map of Ireland also indicates the possible sources where any particular type of aggregate can be found.

All coarse aggregates used in this research are crushed rock with angular shapes and well-defined edges. For the first phase of the experiments discussed in Chapter 4, 14mm aggregate size was chosen. For the second phase of experiment discussed in Chapters 5 and 6, 20mm and 8mm aggregates were used together for mix designs.

Limestone

Limestone is a sedimentary rock composed mainly of calcium carbonate ($CaCO_3$) in crystal forms. As a building material, limestone is a suitable type of coarse aggregate (shown in Figure 3.2) for concrete mixtures, base of roads, etc. Limestone is the most widely distributed natural rock overlaying on the central lowlands across Ireland. The typical 10% fines value of limestone is about 165 kN (Neville 2012).

Sandstone

Sandstone is also a sedimentary rock composed mainly of quartz or rock grains with a large variety of colours depending on the original rocks. From ancient times, sandstone has been used as a building material in many construction projects. In the southern part of Ireland, a large area is covered by the Old Red Sandstone, particularly in County Kerry.

As a type of coarse aggregate (shown in Figure 3.2) in concrete work, sandstone is not as strong as quartzite or basalt. Typically, the 10% fines value of sandstone is about 160 kN.

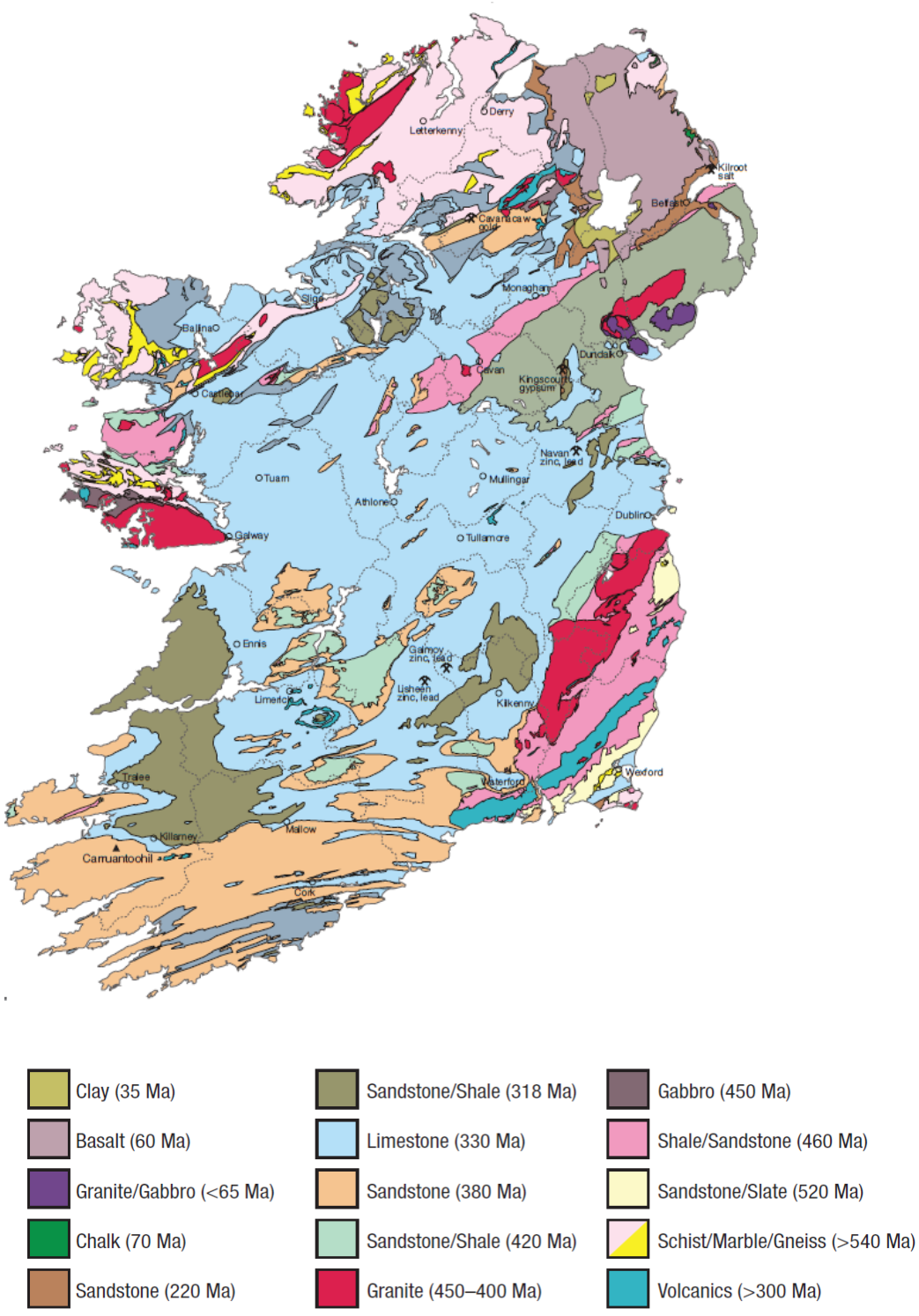

Figure 3.1 Geology of Ireland: Ma = millions of years (http://www.gsi.ie)

Basalt

Basalt is a common volcanic rock formed from the rapid cooling of lava. Basalt is usually grey or black in colour as shown in Figure 3.2. The rapid cooling effect makes basalt finely grained in mineral texture and suitable for construction works. In the north-east of Ireland, basaltic lavas were formed on the Antrim-Derry plateau and provide the sources of basalt rocks.

Basalt has very strong mechanical properties. The 10% fines value of basalt can reach 400 kN (Neville 2012).

Figure 3.2 (a)Limestone, (b)Sandstone, (c)Basalt, (d)Quartzite and (e)Granite

Quartzite

Quartzite is a metamorphic rock which was originally quartz sandstone. The similarity between sandstone and quartzite can be found by comparing the pictures in Figure 3.2. Crushed quartzite is suitable for construction works due to its hardness and angular shapes. The 10% fines value of quartzite is strong, around 250 kN, and its angular shapes and rough texture provide good bonding characteristics.

Quartzite is commonly found around the eastern and northern parts of Ireland, mostly in Counties Wicklow and Donegal.

Granite

Granite is a common type of igneous rock formed from magma with a granular texture. It is composed mainly of quartz, mica and feldspar, and these composites can be visually distinguished in Figure 3.2. The mechanical properties of granite confirm it as a proper building material, from decorative rocks to concrete aggregates. The 10% fines value of granite is about 185MPa. Granite sources can be found in several different places in Ireland, from Country Wicklow to Galway.

3.1.3 Fine Aggregates

Washed river sand was used as the fine aggregates for all the concrete mixes throughout this research. This filler material was supplied and delivered by Banagher Concrete in County Offaly. The grading of this sand is shown in Table 3.4. The percentages of passing are within the grading limits and is typical for a medium sand (I.S. EN 12620, 2013).

The moisture content of the aggregates is an important factor that determines the water/cement ratio. Both coarse and fine aggregates usually contain some moisture based on the porosity of the particles and the moisture conditions. Since coarse aggregates used in this project were close to an air-dry state, the effects of moisture content within the coarse aggregates can be neglected. However, the moisture condition of sand in each bag varied during the mixing program that lasted for several months depending on moisture conditions in the laboratory and drying time till it was used in a mix. From saturated and surface-dry to moist conditions, the values of moisture content can range from 1% to 20%. Thus, the actual values of moisture content were needed to be measured by the Speedy moisture test (BS 812-109, 1990) before each concrete mixing.

Sieve Size	% of passing	Grading limits
4.75mm	100	-
2.36mm	70	65-100
1.18mm	53	45-100
0.6mm	30	25-80
300 μm	11	5-48
150 μm	3	-

Table 3.4 Grading of washed sand from Banagher Concrete Ltd and grading limits (I.S. EN 12620, 2013)

3.1.4 Chemical Admixtures

To produce high-strength concrete with the designed qualities, chemical admixtures are necessary to improve the properties of concrete from the mixing process to the hardened state. In this research, good workability at low water/cement ratio and high early-age strength are particularly desired to be achieved by adding specific admixtures.

Superplasticizer

CHRYSO Fluid Premia 196 produced by CHRYSO Limited is the superplasticizer used in this research for each concrete mixing. This superplasticizer was produced by CHRYSO UK Limited and supplied by Banagher Concrete. Its ingredients are based on a modified polycarboxylate. For high strength concrete with low water/cement ratio, this admixture provides sufficient workability for concrete mixtures to allow full compaction.

CHRYSO Fluid Premia 196 is a milky liquid with a grey/brown colour. It is slightly heavier than water in density. The dosage of this type of superplasticizer is suggested to be 0.8% by weight of total binder content. In practice, the actual dosage varies depending on different cementitious materials. It is preferable to add this solution to the water before mixing the concrete. However, it can be added into the mixtures afterwards prior to discharge.

Accelerator

CHRYSO Xel 650 produced by CHRYSO Limited is a non-chloride accelerating admixture (based on Sodium Thiocyanate) which speeds up the first reactions of hydration especially at low temperature. This accelerator was produced by CHRYSO UK Limited and supplied by Banagher Concrete. Adding this admixture into concrete mixes

is known to reduce the setting time significantly and improves early compressive strengths. CHRYSO Xel 650 is a completely water-soluble admixture with suggested dosage of 1.5% by weight of total binder content. It can be added to the mixing water in advance or directly into the mixer.

3.2 Experimental Methods

3.2.1 Experimental Setup

The general objective of this project is to establish the relationship between the development of concrete strength and stiffness and various influencing factors. Secondly, this research was designed to investigate a practical method of accelerating the early-age strength of precast concrete made with high GGBS content. To achieve these purposes, a series of concrete mixes with different combinations of constituents selected to build a broad matrix for further analysis.

Phase 1:

In the first phase of experiment, the primary objective is to investigate the concrete mechanical properties using different coarse aggregates under a series of strength classes.

Five Irish local rock types, introduced in 3.1.2, were chosen as the coarse aggregates for comparisons. The designed strength classes are C40/50, C50/60, C60/75 and C70/85 which represent an appropriate range for high strength and pre-stressed concrete in Ireland. To reflect the practice in the pre-cast industry, the testing ages of concrete specimens were chosen at 3 days and 28 days. A bulk CEM I 42.5R cement complying with EN197-1 was used for all concrete mixes.

Phase 2:

The second phase of experimental work focused on the development of compressive strengths and elastic modulii of high-strength concrete made from different proportions of GGBS content using a selected aggregate type.

To investigate the changing mechanical properties of concrete with time, each mix has 6 sets of specimens to be tested at different ages, namely 1, 2, 3, 7, 28 and 56 days. 1, 2 and 3-day results are especially important because the main influence of GGBS on the strength development occurs during this period. To precisely acquire the data at these

early-age times, tests of concrete specimens started at exactly 24, 48 and 72 hours after pouring with a 30-minute tolerance to control the experimental errors. For the long-term tests, 56-day results were also collected to compare with 28-day results both of which can be used to establish concrete strength compliance in practice.

As the early-age strengths of concrete are reduced by introducing GGBS content, three commonly used strength accelerating methods are investigated to compensate for this drawback of GGBS, comprising RHPC, an accelerator and thermal treatment. These methods were applied singly or with each other. Table 3.5 includes the details of the experimental setups.

Except for the last mix design, designated "RHA" (RHPC + thermal curing + accelerator), all the other mix designs have tested 30%, 50% and 70% replacements of GGBS content to compare with a baseline set of pure CEM II/A-L or RHPC. The last mix design, "RHA", only tested 70% replacement of GGBS with the baseline specimens. The result of CHA is expected to be similar to that of RHA, therefore this combination was not chosen to be tested.

Specimen Label	CEM II/A-L	RHPC	Accelerator	Thermal Curing
C	✓			
R		✓		
CA	✓		✓	
RA		✓	✓	
CH	✓			✓
RH		✓		✓
RHA		✓	✓	✓

Table 3.5 Experimental setup for phase 2

3.2.2 Mix Proportions

A series of established mix designs for precast concretes with different strength classes were provided by Banagher Concrete. For example, according to I.S. EN 206-1, concrete C40/50 is supposed to have a 40MPa characteristic compressive strength at 28 days for 150 mm diameter by 300 mm cylinders, or a 50MPa characteristic compressive strength at 28 days for 150 mm cubes. The materials used in the laboratory mixes were identical to those used in Banagher Concrete Ltd.

In the first phase of the experiments, the influence of coarse aggregates was required to be tested at different strength levels. The details of mix designs for four successive strength classes are given in Table 3.6. To reach a higher strength at an early age, the cement type is CEM I 42.5R RHPC. The maximum size of coarse aggregates is 14 mm in accordance with the mix design of precast concrete by Banagher Concrete.

In the second phase of the experiments, the aim is to monitor the concrete development over time at different proportions of GGBS used. Only the C40/50 mix was chosen to be tested in this case because it is the most common precast strength in Ireland. The type of coarse aggregate was decided to be limestone for the mixes and 14mm aggregate size was replaced by a combination of 20mm and 8mm. To investigate the influence of GGBS content, GGBS replaces, in a 1:1 ratio, the CEM II/A-L or RHPC at certain proportions. Then, the two types of cementitious materials are blended in the mixer with the other materials.

Materials	C40/50	C50/60	C60/75	C70/85
Cement (kg/m^3)	375	425	475	525
14 mm Coarse aggregate (kg/m^3)	900	900	900	900
Sand (kg/m^3)	960	900	840	780
Water (l/m^3)	155	155	153	152
Water/cement ratio	0.41	0.36	0.32	0.28
Superplasticizer (L/m^3)	2.6	3.0	3.6	4.1

Table 3.6 Mix proportions for influence of coarse aggregates at different strength levels

Material	Mass per cubic metre (kg/m^3 unless stated)	Mass per pour (kg unless stated)
Cement	400	25.2
20mm aggregate	765	48.2
8mm aggregate	205	12.9
Sand	850	53.6
Max free water	160	10.1 L
Superplasticizer	3.1 (L/m^3)	195 ml
Accelerator (if used)	5.1 (L/m^3)	321 ml
Water/cement ratio	0.4	0.4

Table 3.7 Base mix proportions for C40/50N precast concrete in phase 2

For each concrete pour in phase 2, the total volume of the concrete mixture required is $0.063m^3$ which is suitable for the pan mixer with a capacity of $0.08m^3$. The mass per m^3 and mass per pour of each material are shown in Table 3.7.

3.2.3 Pouring Scheme

To test the elastic modulus, a minimum of four cylinders are needed to obtain one result by the testing method from the British Standard (BS 1881-121, 1983). There is no equivalent European standard of test elastic modulus until now. This test has not yet been superseded by a recent European standard. Three cylinders are used to determine the actual mean compressive strength of the concrete. Based on the measured mean compressive strength, the compressive load is set at one third of this mean value to test the last cylinder and thus to obtain one result of the elastic modulus.

In the first phase of testing, six cylinders were made for each concrete pour. As a result, three values of elastic modulus can be obtained for one set of specimens. For five different aggregate types, two testing ages and four strength classes, a total number of 240 cylinders were made from 40 concrete pours in this experimental phase.

Based on the consistency of testing results from the first experimental phase, the quantity of concrete cylinders for one set of specimens was reduced to five to get two values of elastic modulus in the second phase of experiment. Thus, for each mix design with six different ages, a total number of 30 cylinders should be made to demonstrate the trend of elasticity growth with time. However, the volume of materials required for 30 cylinders exceed both the limits of the mixer capacity and the total number of moulds available. As a result, 10 cylinders are made from each pour, and 3 different pours were carried out for one particular mix design. For 26 different mix designs, a total number of 780 cylinders were made from 78 concrete pours in the second experimental phase.

The storage capacity of the two available curing tanks is approximately 100 concrete cylinders in total at one time. Since the 28-day and 56- day specimens are required to stay in curing tanks for a long period of time, the total number of cylinders may exceed the limit of storage. To optimize the pouring scheme under this limitation of storage, specific programmes were designed for each experimental phase. By using these designed schemes, all the experimental works are scheduled to specific dates. The total quantity of stored cylinder specimens is increased after each "Cleaning and Stripping" event and is reduced after each "Testing" event. The detailed pouring schemes can be found in Appendix A-C. The first phase of experiment was carried out in 2010 and followed the scheme in Appendix A. The second phase of experiment was split into two parts.

Appendix B records the details of the first half of phase 2, which does not involve any thermal curing process. The other half of phase 2, shown in Appendix C, was carried out under the thermal curing process for each pour.

Due to separating the manufacture and testing of 30 cylinders into 3 pours, the quality control of compressive strength is extremely important to ensure that these specimens are identical to each other within random experimental error. An electronic scale with 20kg capacity was used for weighing all the materials.

Another possible error source is the moisture content within the sand. Since the experiments are undergone over a period of several months, the moisture content within the sand is also changing with time. To compensate for this influencing factor, a Speedy Moisture Test is carried out to test the percentage of the water content of the sand prior to the pouring on that working day. The actual water poured into the mix and the sand quantity are then modified by calculation. As one is concerned with the ambient conditions, the laboratory in the basement provides a generally stable environment with uniform temperature (17-19˚C) and humidity (65%-75%). A detailed monitor of temperature and humidity during a period of continuous 9 days is displayed in Appendix D.

Along with each pour, four 100mm×100mm×100mm cubes were made and tested at 7 days and 28 days respectively for quality control. However, EuroCode 2 states that the compressive strength test should be carried out on a 150mm×150mm×150mm concrete cube. The European standard does not provide any related information about the difference of the compressive strength between 100mm and 150mm cubes. Generally, concrete cubes with smaller sizes are considered to be stronger than the cubes with larger sizes. A 150mm cube is about 96% the strength of a 100mm cube (Neville 2012). In total for both phases of experiment, 472 cubes were made from 118 concrete pours.

3.2.4 Experimental Procedures

The mixing process is carried out in a pan mixer with 0.08m³ capacity. Initially, all the coarse aggregates and sand are mixed together with half of the free water for 2 minutes. Then, the required cement and GGBS contents are added into the mixer with the rest of the free water. Any admixture used is dissolved into the second half of water prior to mixing for even distribution throughout the fresh concrete.

Plastic cylinder moulds are prepared on a vibration table with mould oil over the inner surface. The height of 300mm of the cylinder mould is divided equally into 6 layers

during the compaction work, and each layer is vibrated for 15sec to achieve proper compaction without voids and segregation. The last layer of a cylinder specimen requires a level surface. After pouring the 10 cylinders, 4 cubes are made on the same vibration table with 2-layer fillings (IS EN-12390-1, 2012)

As one is concerned with compressive tests, cylinder specimens require smooth and levelled upper surfaces to evenly distribute the loads on the top of them (while cubes have cast surfaces on vertical sides which are smooth enough for compressive tests). A cement paste is used for a thin capping on top of the cylinders right after the pouring. This cement paste is mixed with the same type of cement as those cylinders at the same water/cement ratio. When the cylinders are filled, approximately 3mm gaps between the concrete surface and mould top edge are left for the later capping work. It is beneficial to leave rough surfaces on the fresh concrete to achieve better bonding between the cylinder top and capping material. Before the capping process, any bleed water which is left on the upper surface of the concrete should be removed. Finally, the cement paste is applied and compacted onto the cylinders' upper surface with a slightly convex shape above the edge of the mould by using a steel float. A smooth surface without any void and bulb is required in this capping work (IS EN-12390-2, 2019).

All the concrete specimens remain in the moulds for the following 22 hours under the room temperature and moist condition. Both cylinder and cube specimens are striped by pumping air through the bottom of plastic moulds with an air compressor. Then, stripped concrete specimens are immediately stored in a water curing tank at standard 20°C until testing at specific ages.

3.2.5 Thermal Curing

The thermal curing method was introduced to determine the effects of curing temperature on concrete strength development. Since concrete has a high thermal conductivity, using hot water to bring up the temperature of specimens is quite efficient and thorough. To find out the influence of temperature solely, concrete specimens were made under identical mixing proportions and procedures as previous experiments. After the initial setting time, normally 4 hours long, concrete cylinders and cubes were moved into a 2.2m×0.8m×1.2m tank while still in their plastic moulds. This water tank is filled with hot water and the water temperature is controlled by a thermostat and a heating unit at 35°C constantly. The efficiency of the thermostat and the heating unit was monitored by a thermocouple, and the reading showed that the actual temperature of water was controlled in the range of 34.5°C ~ 35°C. The curing scheme took 20 hours after the specimens were placed into the tank. After the one-day thermal curing, all the concrete cylinders and

cubes were demoulded normally and placed in a conventional curing tank at 20°C until the testing day.

3.2.6 Test of Elastic Modulus

To test the static modulus of elasticity, the method from BS 1881-121 (1983) is used for this research. The European Standard does not provide a new version of this method to date.

This method of testing involves two measuring procedures, the ultimate compressive strength of concrete and the strain measuring. The ultimate compressive strength of concrete is measured on three cylinders first under the strength testing procedure in accordance with I.S. EN 12390-3 (2019).

The strain measuring of concrete is carried out by a pair of transducers which are located on the surface in the middle third of the cylinders. A testing control system (shown in Figure 3.3) connected to the load machine can calculate and show the result of the modulus of elasticity on the screen by its pre-implanted programme.

Figure 3.3 Control System of Young's modulus testing

After placing the test specimen with the measuring transducers (shown in Figure 3.4) centrally in the machine, this programme starts to apply a base load of 1 MPa. Then, the load is steadily increased at a constant rate of 0.6 N/(mm^2·s) until one third of the ultimate cylinder compressive strength of the concrete is reached. This maximum load is maintained for 60s. The strain readings from both transducers are shown on the screen of the testing control system. If the individual strains are not within a range of ± 10 % of their mean value, it is required to restart the test by re-centring the test specimen or re-locating the transducers. When the centring is sufficiently accurate, the programme is allowed to continue into the unloading process at the same rate as the loading process. Then, the load is held at the base 1MPa for another 60s. Three loading and unloading cycles are carried by this programme to achieve an accurate result of elastic modulus. The testing result is calculated by this programme and shown on the screen. When the elasticity measurements of one particular cylinder have been completed, the ultimate strength of this cylinder is also required to be tested for a comparison with the mean compressive strength of the first three cylinders. In case where more than a 20% difference exists, this should be noted for consideration of testing validation.

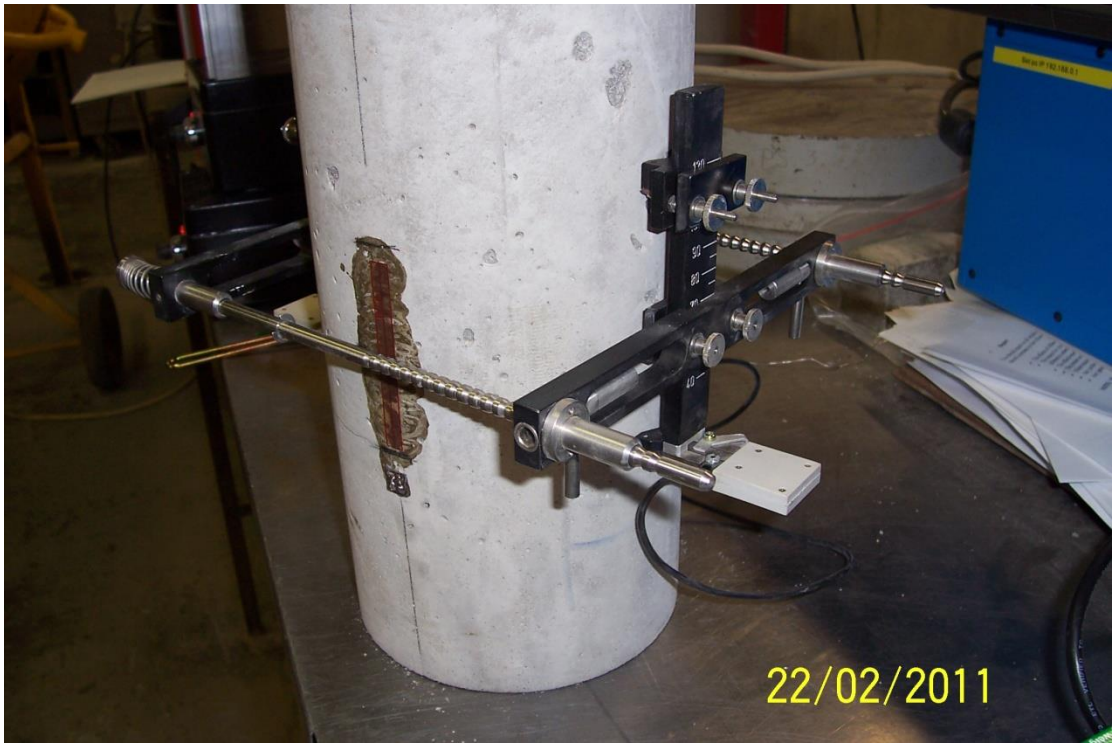

Figure 3.4 Setting of the measuring transducers on a cylinder specimen

CHAPTER 4. INFLUENCES OF COARSE AGGREGATE TYPES

4.1. Introduction

Different types of coarse aggregates have different mineralogical characteristics which are determined by the nature of their original rocks and formation methods. In the designing process of High-Strength Concrete (HSC), physical properties of coarse aggregates, such as strength, modulus of elasticity, texture and shape, can have a significant impact on the strength performance of HSC. Compared with natural gravel, crushed aggregates generally have better mechanical properties in concrete performance with higher strength and elastic modulus (Aitcin. and Mehta. 1990).

The strength of coarse aggregate mainly determines the limitation of compressive strength of the concrete that is mixed using this type of aggregate. Generally, concrete cannot be significantly stronger than its own coarse aggregate. Although the strength of coarse aggregate can exceed the design strength of concrete by a large amount, it still has some influence on the compressive strength of concrete due to its bond characteristics and surface absorption. To determine the mechanical performance of aggregates, most tests aim to investigate bulk aggregates as a whole rather than the properties of individual particles. The resistance of an aggregate to crushing under compressive load is an important criterion of this aggregate type. There are two test methods provided by the British Standards which can be used to determine this property of coarse aggregates used in different situations, namely the Aggregate Crushing Value (ACV) test and the Ten Percent Fines Value test (TFV) (BS 812-110, 1990, BS 812-111, 1990). However, the Los Angeles test as a newer practical method is introduced by the European Standard to replace the two former testing methods (IS EN 1097-2, 2010).

The influence of the type of coarse aggregate on the compressive strength of concrete is more noticeable in HSC. For normal-strength concrete, the influence of coarse aggregate on compressive strength may not be the major concern because of the low-strength bond and cement paste. Cracks occur through these bonds and cement paste before the coarse aggregates experience any critical load (Wu et al. 2001). As the bonding strength is improved in high-strength concrete, cracks may start appearing in the coarse aggregates first. In such cases, it is important to consider the strength of coarse aggregate as one of main factors of concrete mix design. From the point of view of the cracking mechanism, HSC behaves similarly to a homogeneous material, compared with normal strength concrete (Beshr et al. 2003). HSC exhibits more linear elastic behaviour and is more brittle than normal strength concrete.

4.2. Influence of Coarse Aggregates on Modulus of Elasticity

The modulus of elasticity of concrete is a fundamental property that determines the deformation behaviour of structural concrete, particularly for the design of reinforced and pre-stressed concrete. This property of concrete is significantly influenced by the characteristics of the coarse aggregates used in the concrete mixture (Baalbaki. et al. 1991). In general, concrete made from stiffer aggregates will have a higher modulus of elasticity. There is no standard method to test the elastic modulus of individual particles of coarse aggregates directly though extracted cylinders of the parent rock can be tested. The ordinary way of investigating this elastic property of coarse aggregates is to measure the elastic modulus of the concrete which is mainly determined by this coarse aggregate.

However, the direct measurement of the modulus of elasticity, E_c, is time-consuming and is more complicated than the direct measurement of compressive strength. The standard method requires one to record the stress and strain of a concrete cylinder simultaneously until the stress reaches 33% of the cylinder ultimate compressive strength (BS 1881-121, 1983). The secant modulus of elasticity can be calculated from the mean recorded strains after 3 cycles of loading and unloading procedures.

To avoid time-consuming testing, researchers and design standards have proposed a series of mathematical formulae to predict the value of modulus of elasticity based on various design factors. The most common method is to express the modulus of elasticity as a function of compressive strength in a given range. There is no precise form of the relationship between the modulus of elasticity and compressive strength, however, it is generally agreed that E_c increases with an increase in compressive strength (Sideris et al. 2004). While the strength of concrete increases by 100% from 50MPa to 100MPa, the elastic modulus, on the other hand, may only be enhanced by 20% (Zhou et al. 1995). In this research, the formulae proposed by IS EN 1992-1-1:2004 and *fib* Bulletins 42 (2008) and 65 (2012) are considered as the reference methods for predicting the modulus of elasticity, while there are also formulae from other standards with similar forms but different coefficients and ranges of application.

The theoretical formulae give relatively satisfactory results for normal strength concrete, but researchers show that it is not reliable to precisely predict the modulus of elasticity HSC from its compressive strengths (Baalbaki et al. 1992). Thus, experimental measurement is still necessary to ascertain the modulus of elasticity with appropriate accuracy. This practice will be explored in this research.

The five types of aggregates examined in this research are commonly produced and used as construction materials in Ireland. In EC2 (2004), quartzite aggregates are considered as the standard type for the modulus formula. Limestone and sandstone are treated as weaker aggregates with 10% and 30% reduction factors, α, respectively. On the other hand, basalt has a 20% increase in factor for adjusting the modulus due its stiffer response. However, there is no indication for granite aggregates. As one is concerned with the structural performance of these Irish local aggregates, they were all selected to be tested for a comprehensive evaluation of the compatibility of EC2 and *fib* bulletins 42 and 65.

The testing setup and methods were discussed in Chapter 3 with all the details of mixing designs, pouring schemes, etc.

4.3 Results and Discussion

4.3.1 Compressive strength

The test results of cube specimens are generally consistent for most mix designs. The compressive strengths of most individual cubes are valid within the range of ±15% of the mean results from that batch.

Table 4.1 and Table 4.2 show the mean cube strengths for each mix at different ages. Unexpectedly, the final results considerably exceeded the initial design strengths. At the lower end, the C40/50 grade has an average of 86.8 MPa compressive strength at 28 days which is much higher than the designed 50 MPa characteristic strength. The C70/85 concrete also has a reasonably high average 28-day strength at 104.8 MPa. However, the magnitude of measured strength for the C70/85 mix is not as high above the grade as for the lower strength classes.

The possible reasons of these unexpected high strengths may be due to the advantages of laboratory conditions. The procedures of sampling, mixing, compaction and pouring were all executed with good quality controls. A temperature-controlled curing tank can provide constant moisture content and temperature for hardened concrete specimens to gain more.

At the same mix proportion, Table 4.2 shows that concrete cubes made from sandstone, basalt and quartzite are stronger than the other two types of aggregate to some extent. This variation in the compressive strength caused by coarse aggregates is not as prominent as expected but does exist occasionally.

(In MPa)	C40/50	C50/60	C60/75	C70/85
w/c ratio	0.41	0.36	0.32	0.29
Sandstone	55.8	76.8	72.4	90.1
Basalt	70.4	74.1	85.4	87.7
Limestone	58.6	68.3	75.0	83.3
Quartzite	69.8	75.1	91.2	90.6
Granite	56.7	73.3	76.5	87.9

Table 4.1 Mean cube compressive strength at 3 days (MPa)

(In MPa)	C40/50	C50/60	C60/75	C70/85
w/c ratio	0.41	0.36	0.32	0.29
Sandstone	87.4	101.9	101.7	106.9
Basalt	89.6	94.9	99.7	111.1
Limestone	85.2	92.1	97.0	97.0
Quartzite	90.5	99.3	110.8	108.7
Granite	81.4	89.8	95.7	99.7

Table 4.2 Mean cube compressive strength at 28 days (MPa)

By plotting the mean compressive strengths against the corresponding water/cement ratios in Figure 4.1, there are apparent trends of increasing strengths with decreasing water/cement ratios for each aggregate type. Duff Abrams in 1918 presented an empirical formula that relates the strength of concrete with the water/cement ratio as given in Equation 4.1.

$$f_c = \frac{A}{B^{w/c}} \qquad \text{(Eqn 4.1)}$$

where f_c stands for the strength of concrete, A and B are empirical constants.

Based the Equation 4.1, five exponential trend lines can be added on Figure 4.1 for each aggregate type. These trend lines demonstrate a summarized performance of each aggregate type under different water/cement ratios. The trend of the line of the quartzite aggregate, which is above the other trend lines, indicates that the concrete cubes made from quartzite are generally the strongest compared with the other aggregates. Sandstone and basalt have a similar strength level because of their overlapping trend lines. Limestone and granite are considered to be 10% weaker than the other three types of aggregates by comparing their performance in Figure 4.1.

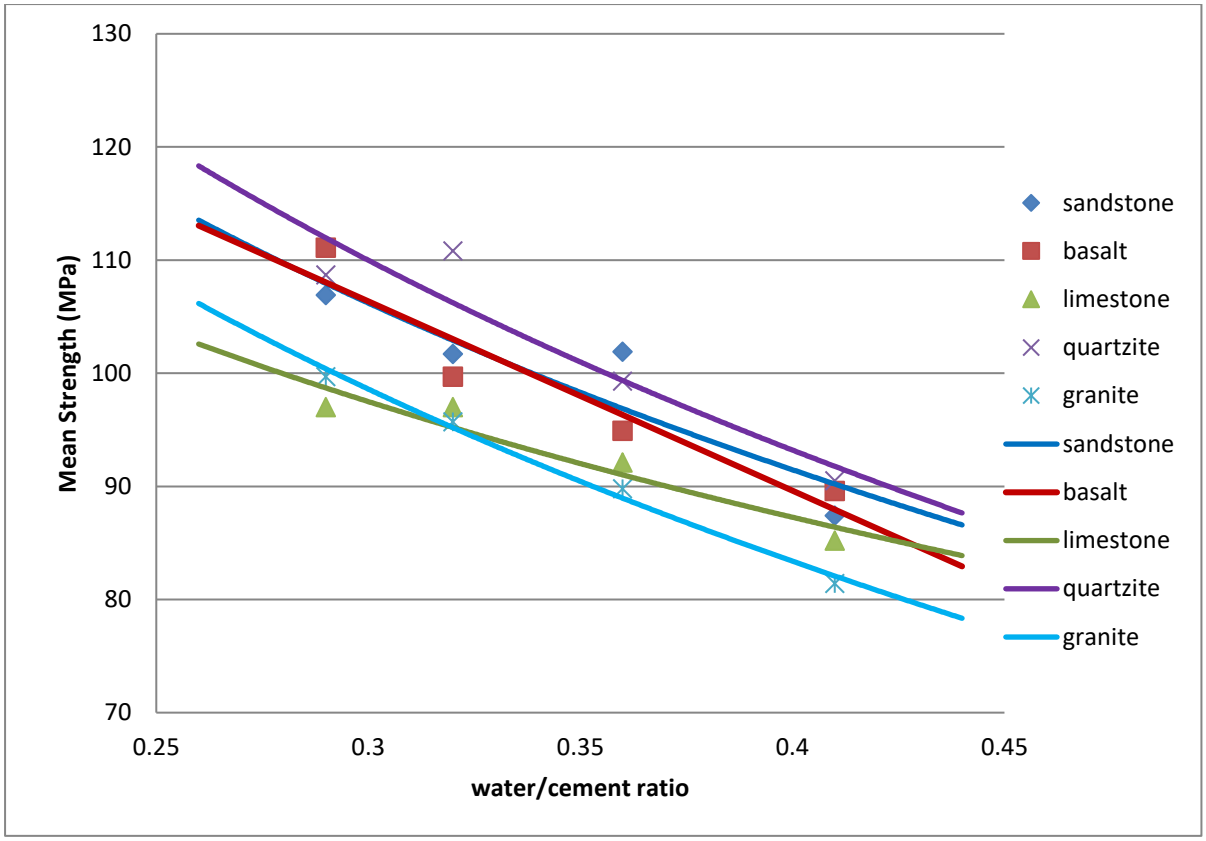

Figure 4.1 W/C ratios vs mean compressive strengths of cube at 28 days

Comparing the 3-day and 28-day results, the effect of using RHPC significantly improves the early age strengths for most mixes. For concrete made from limestone aggregates, the ratios between 3-day/28-day results increase from 63.8% at C40/50 to 88.2% at C70/85. This feature also can be found from the remaining aggregate types except basalt. In general, Table 4.3 indicates that the 3-day strengths of mixes with lower w/c ratios is closer to their 28-day strengths than those mixes with higher w/c ratio. In the early age of the strength development, a lower water/cement ratio can result in a higher rate of heat of hydration (Hu et al. 2014). Thus, within 3 days, the maturity development of concrete with a lower water/cement ratio can be considerably faster than that with a higher water/cement ratio, as evidenced in Table 4.3.

In EC2 (2004), the strength development with time is predicted by:

$$\beta(t) = \exp[s(1-(28/t)^{0.5})] \qquad \text{(Eqn 4.2)}$$

	C40/50	C50/60	C60/75	C70/85
Sandstone	63.8%	75.4%	71.1%	84.3%
Basalt	78.6%	78.1%	85.7%	78.9%
Limestone	68.8%	74.2%	77.3%	85.9%
Quartzite	77.1%	75.6%	82.3%	83.3%
Granite	69.7%	81.6%	80.0%	88.2%
Average	71.6%	77.0%	79.3%	84.1%

Table 4.3. Ratio of 3-day/28-day mean cube strengths

where β(t) is the coefficient of mean compressive strength at age t, that is, β(t) = $f_{cm}(t)/f_{cm}(28)$ and *s* is a coefficient which depends on the type of cement (s = 0.2 for RHPC given in EC2). Thus, at 3 days, β(3) = 66.3%. The average percentages in Table 4.3 demonstrate that the percentage strength at 3 days is a higher proportion of the 28-day strength the higher the grade. In fact, using the actual average β(3) values inserted in Equation 4.2, the range of s values to achieve agreement with the experimental results for RHPC varies from 0.16 for C40/50 to 0.08 for C70/85. This suggests that the development rate of these cement types is much faster than that predicted by the current EC2 equation, which should be reviewed, accepting that issues of repeatability and reproducibility have not been dealt with here, though the trends are clear. Furthermore, the cement type should not be the only factor which affects the value of coefficient *s*. The strength grades or water/cement ratio need to be taken into account as well.

Thus, based on a value of s = 0.2 given by EC2, the prediction of strength gain from 3 to 28 days for HSC is not currently accurate for Irish conditions. Alternative values of s (given in Table 4.4) depending on the strength grade increases should be considered for HPC when proposing changes to EC2 in the future.

	C40/50	C50/60	C60/75	C70/85
s values	0.16	0.13	0.11	0.08

Table 4.4. Suggested values of s based on experimental results

4.3.2 Modulus of Elasticity

4.3.2.1 Experimental Results:

Compared with cube specimens, the testing results obtained from the 150mm×300mm cylinders specimens have a greater variation for most mix designs. Results of compressive strengths and elastic modulii are considered to be invalid and are removed

from further analysis if they are out of the range of ±15% of the mean results for that batch (I.S. EN 12390-3 2019).

Figure 4.2 contains all the results of modulus of elasticity of granite concrete at 3 days, plotted against the corresponding compressive strength. Although the variations in results are large for some particular concrete mixes, the general trend clearly shows that the E_c value is ascending with an increase in the compressive strength. Figure 4.3, based on the 28-day test results for basalt concrete, also demonstrates this point of view.

Results of other aggregate types and testing ages can be found in Appendix E. The ascending trend of E_c with an increasing compressive strength is also observed in each graph in Appendix E for all the types of coarse aggregates and two different test ages.

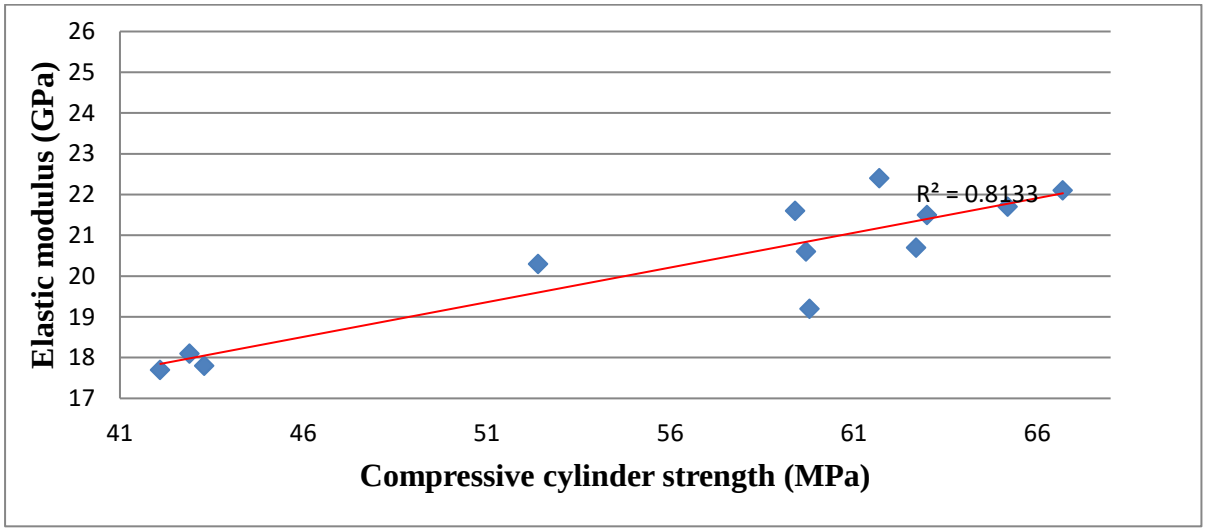

Figure 4.2 Individual modulus of elasticity (in GPa) against cylinder strength (in MPa) results for 3-day granite specimens

4.3.2.2 Numerical Prediction:

To predict the elastic modulus of concrete, it is necessary to follow an empirical relationship between the compressive strength and elastic modulus. This empirical formula used to predict the modulus of elasticity in EC2 is given as:

$$E_{cm} = 22(f_{cm}/10)^{0.3} \text{ (GPa)} \qquad \text{(Eqn 4.3)}$$

where f_{cm} is the mean cylinder strength in MPa.

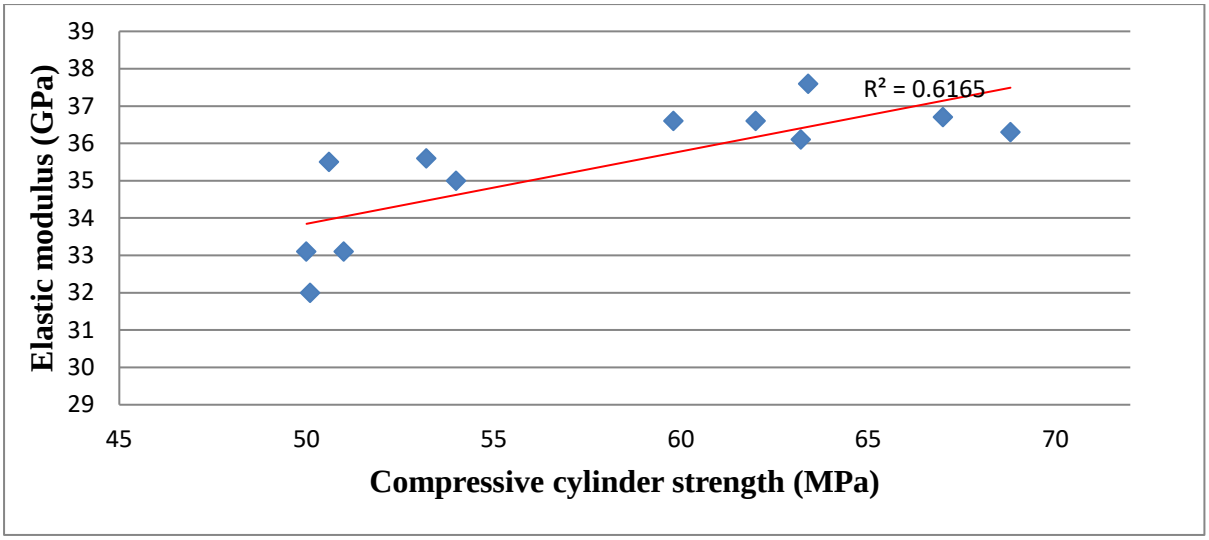

Figure 4.3 Cylindrical modulus of elasticity (in GPa) against cylinder strength (in MPa) results for 28-day basalt specimens

Concerning the accuracy of prediction, this standard formula is restricted to be used for quartzitic aggregates. For other types of aggregates, there is an adjustment coefficient, α, varying in value from +20% for basalt to -30% for sandstone. The α value of limestone is 0.9 which is 10% lower than that of the standard quartzite. However, EC2 does not give any suggestion for granite, thus granite is presently assumed to have a similar property as quartzite with an adjustment to be evaluated here.

fib bulletin 42 (2008) and the recently released *fib* Bulletin 65 (Model Code 2012) propose a similar formula with relatively small differences in the parameters.

$$E_{cm} = E_{c0}\,\alpha[(f_{ck} + 8\text{MPa})/10]^{0.33} \qquad \text{(Eqn 4.4)}$$

where E_{c0} = 20.5GPa in bulletin 42 and 21.5 GPa in bulletin 65, and f_{ck} is the characteristic strength (in MPa). For conventional situations, (f_{ck} +8MPa) can be assumed to be the same as the mean compressive strength f_{cm} because $f_{cm} = f_{ck} + 1.64\sigma$, where the standard deviation of σ is normally considered to be 5MPa. However, this assumption may not be appropriate because the actual mean compressive strength from experiment is much higher than the expected design strength. Considering the need for accuracy of calculation, (f_{ck} +8MPa) is therefore replaced by the mean compressive strength f_{cm}, and Equation 4.4 is transformed into Equation 4.5. The assumed quantitative values of α can be found in Table 4.5, and are the same as the suggestions given by EC2 (2005).

$$E_{cm} = 21.5\alpha[(f_{cm})/10]^{0.33} \qquad \text{(Eqn 4.5)}$$

Sandstone	Basalt	Limestone	Quartzite	Granite
0.7	1.2	0.9	1	n/a

Table 4.5 Quantitative values of α for different aggregates (EuroCode 2, 2005)

4.3.2.3 Comparison between Experiment and Prediction:

To compare the results between experimental data and theoretical predictions, the first step is to calculate the predicted values of the elastic modulus, based on the formulae in Equation 4.3 and Equation 4.5 respectively. Then, both experimental and predicted results of the elastic modulus are plotted on the same graph against the compressive strength. The predicted results form a power function curve with an index of either 0.3 or 1/3 determining the nature of equations from EC2 or model code 2010. A trend line with a power function form can be also applied on the experimental results to compare with the curve drawn using the predicted values.

Figure 4.4 shows the comparison of E_c values obtained from different methods, based on all the cylinder specimens made from the basalt aggregate at different ages and strength classes. The predicted curves calculated by the numerical formulae from both EC2 and model code 2010 are almost identical to each other. The variation between these two curves is mainly caused by different coefficients, and the results from EC2 are slightly greater than those from model code 2010.

On the other hand, the trend line of practical results lies well below the predicted curves to a significant degree. Considering that both the predicted curves and the practical trend line have a similar shape from a lower compressive strength to a higher compressive strength, the possible reason causing this large gap can be assumed to be the inaccurate value of adjustment coefficients α applied in both Equation 4.3 and Equation 4.5. The α value of 1.2 for the basalt aggregate might overestimate the stiffness of basalt by approximately 30%.

Figure 4.5 based on the results of cylinders specimens made from quartzite aggregates shows a similar situation as that in Figure 4.4, although a larger deviation between practical results and predicted values exists here. Therefore, the α value 1.0 proposed by EC2 is inaccurate for numerical calculation. For a more accurate prediction, the coefficients α for quartzite needs to be reduced by approximately 30%, from 1.0 to 0.7.

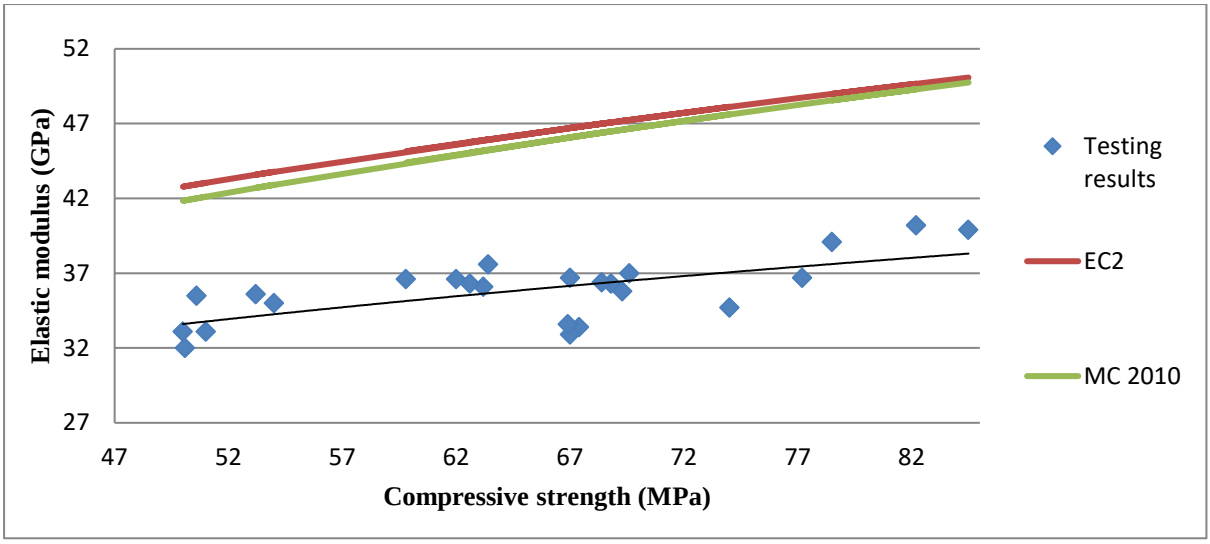

Figure 4.4 Comparison of experimental results and predictions of elastic modulus for basalt specimens

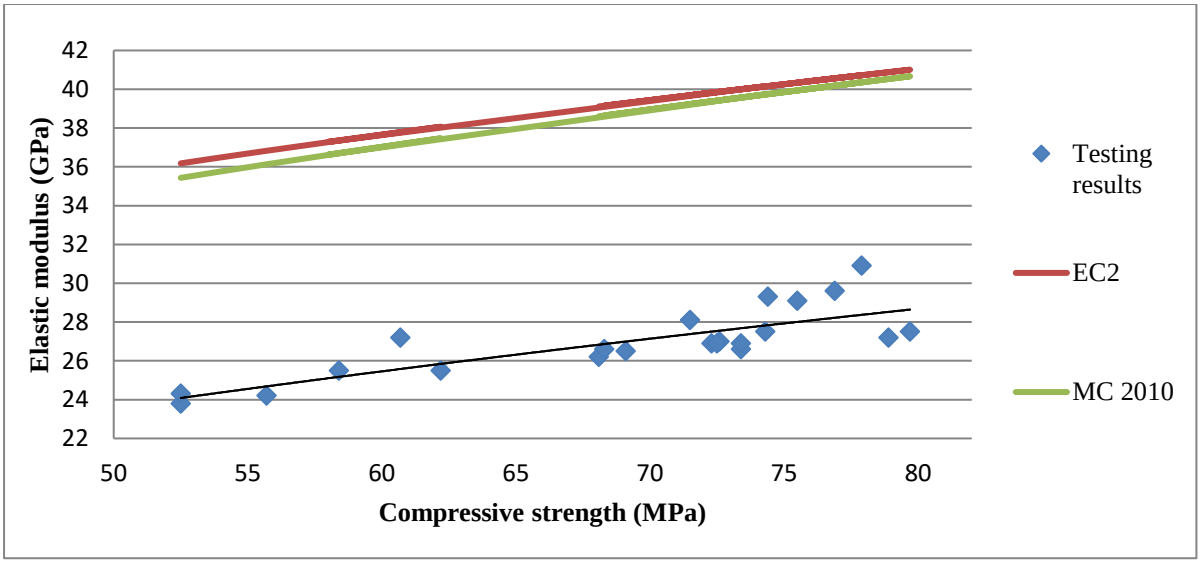

Figure 4.5 Comparison of experimental results and predictions of elastic modulus for quartzite specimens

The assumed α value of 1.0 for granite aggregate is apparently not valid due to the large variation of curves shown in Figure 4.6. The practical results show that concretes made from granite aggregate have the smallest stiffness compared with other aggregate types. However, the range of compressive strength in Figure 4.6 is similar to the previous Figure 4.5. Therefore, aggregates with different stiffness can produce concretes with similar compressive strength under an identical mix design and experimental procedure. A more accurate value of α will be discussed later.

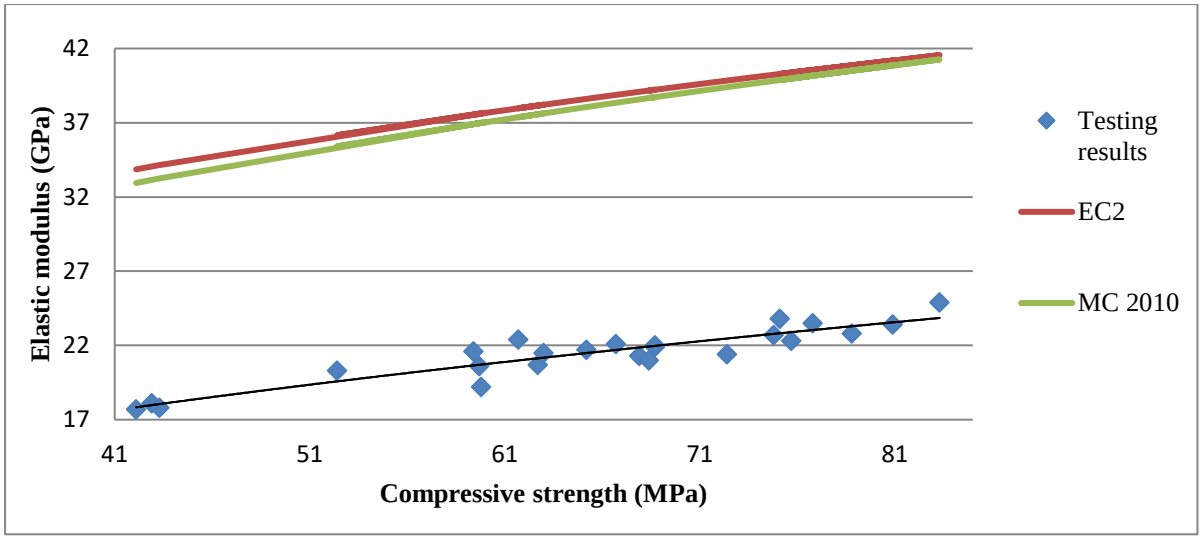

Figure 4.6 Comparison of experimental results and predictions of elastic modulus for granite specimens

In Figure 4.7 and 4.8, the test results and predicted values for limestone and sandstone are relatively close to each other, compared with previous figures. This indicates that the assumed α values for limestone and sandstone aggregates are appropriate for practical predictions.

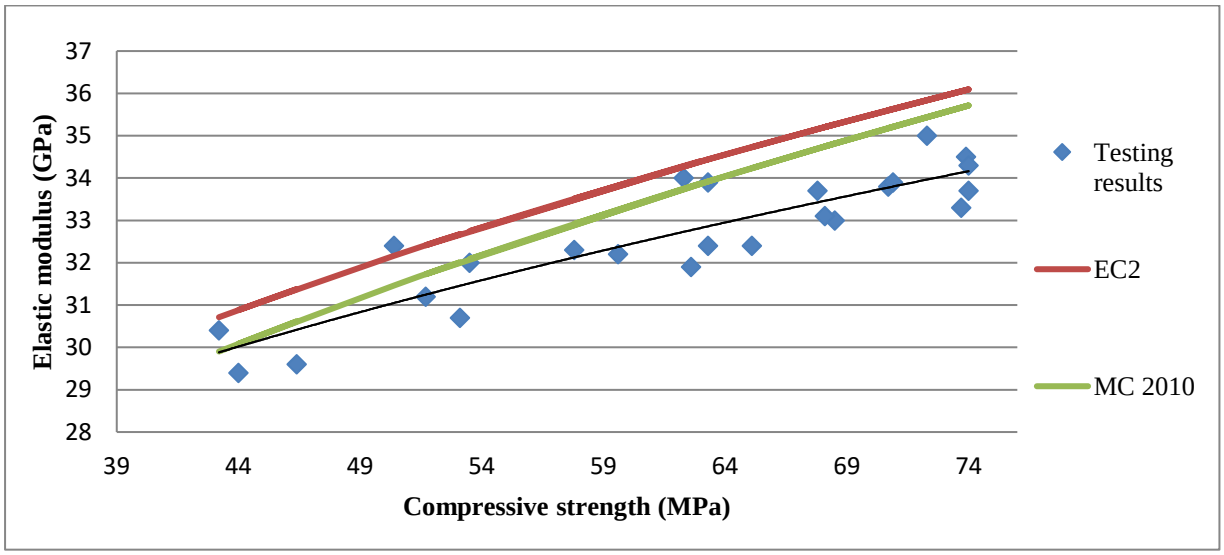

Figure 4.7 Comparison of experimental results and predictions of elastic modulus for limestone specimens

From Figure 4.4 to 4.8, there is a common phenomenon that the two predicted curves by EC2 and model code 2010 converge at a higher compressive strength. The difference between the two sources becomes insignificant as the compressive strength is getting higher.

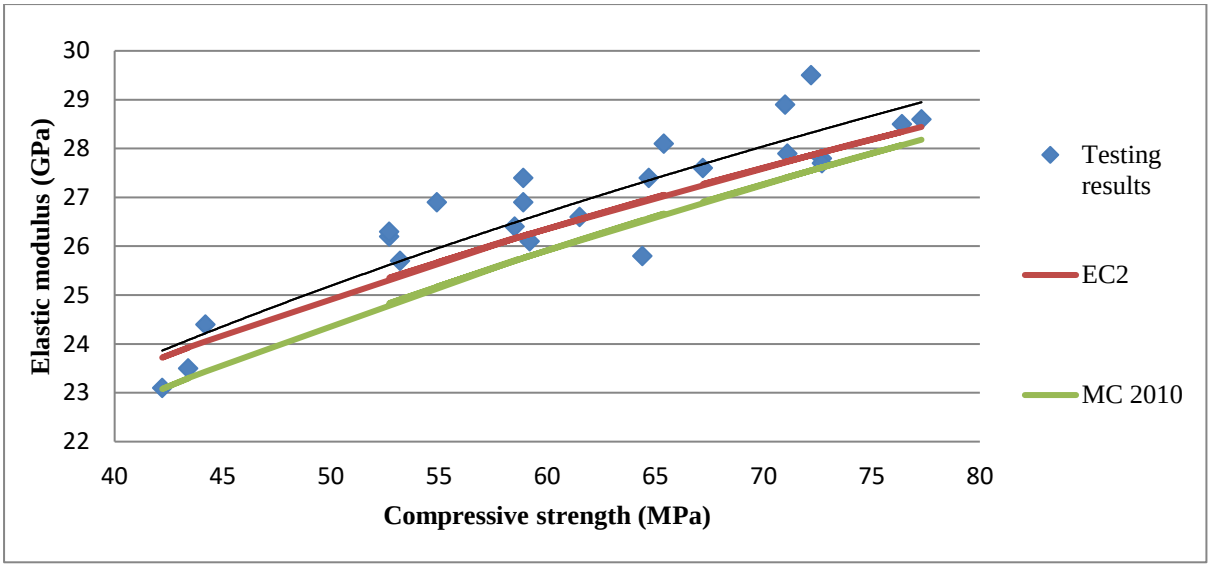

Figure 4.8 Comparison of experimental results and predictions of elastic modulus for sandstone specimens

Tables 4.6 and 4.7 give two examples of comparisons between the measured and calculated values of elastic modulus using the formulae from EC2 (2004), with and without α, and *fib* bulletins 42 and 65 (2008, 2012) at two extreme situations which have the smallest and largest mean cylinder strengths. Table 4.6, with Grade C40/50 at 3 days, has a minimum f_{cm}, while Table 4.7, with C70/85 at 28 days, has a maximum f_{cm}. The percentage difference, δ, between measured and calculated values, as shown in the tables, and can be calculated by Equation 4.6

$$\Delta = 100\% \times (E_{cm}' - E_{cm})/ E_{cm} \qquad \text{(Eqn 4.6)}$$

where E_{cm}' is the calculated value and E_{cm} is the test value.

Both of the Tables 4.6 and 4.7 indicate similar trends for the accuracy of the theoretical predictions among different types of aggregates. The remaining result of comparisons at the other ages and strength classes can be found in Appendix F. As the compressive strength is increasing from the lower class C40/50 to higher class C70/85, the accuracy of theoretical predictions by using the formulae from EC2 and model code 2010 remains at a steady level for any particular type of aggregate. The average values of percentage difference Δ through different strength classes and ages for the five types of aggregate are summarized and shown in Table 4.8.

		Sandstone	Basalt	Limestone	Quartzite	Granite
Measured mean value	f_{cm} (MPa)	41.7	47.2	44.8	53.8	41.5
	E_{cm} (GPa)	23.7	32.7	29.8	24.1	17.9
Calculated values by EC2 without α	E_{cm}' (GPa)	33.7	35.1	34.4	36.4	33.7
Calculated values by EC2 with α	E_{cm}' (GPa)	23.6	42.1	31.0	36.4	33.7
Deviation from EC2	Δ	-0.4%	+29%	+4%	+51%	+88%
Calculated values by *fib* 42	E_{cm}' (GPa)	22.9	41.1	30.3	35.7	32.8
Deviation from *fib* 42	Δ	-3%	+26%	+2%	+48%	+83%
Calculated values by *fib* 55	E_{cm}' (GPa)	24.0	43.1	31.8	37.4	34.4
Deviation from *fib* 55	Δ	+1%	+32%	+6.7%	+55%	+92%

Table 4.6 Modulus of elasticity of grade C40/50 at 3 days, assuming α= 1 for granite

		Sandstone	Basalt	Limestone	Quartzite	Granite
Measured mean value	f_{cm} (MPa)	73.7	81.5	70.7	77.5	79.0
	E_{cm} (GPa)	29.0	39.7	33.8	30.2	24.1
Calculated values by EC2 without α	E_{cm}' (GPa)	40.0	41.3	39.6	40.7	40.9
Calculated values by EC2 with α	E_{cm}' (GPa)	28.0	49.5	35.6	40.7	40.9
Deviation from EC2	Δ	-3%	+24%	+5%	+35%	+70%
Calculated values by *fib* 42	E_{cm}' (GPa)	27.7	49.2	35.2	40.3	40.5
Deviation from *fib* 42	Δ	-4%	+24%	+4%	+33%	+68%
Calculated values by *fib* 55	E_{cm}' (GPa)	29.1	51.6	36.9	42.3	42.5
Deviation from *fib* 55	Δ	+0%	+30%	+9%	+40%	76%

Table 4.7 Modulus of elasticity of grade C70/85 at 28 days, assuming α= 1 for granite

The introduction of the new Model Code 2010 (*fib* bulletin 65) does not appear to have improved the accuracy of the predictions. The calculated results for limestone are slightly higher than the measured values. For basalt and quartzite, the deviations are significantly over the expected range which means the adjustment coefficients are heavily overestimated for these two types of aggregates. Granite has the smallest value of modulus of elasticity compared with other aggregates, thus the previous initial assumption of $\alpha = 1$ from this research, in the absence of other guidance in EC2, is obviously not valid in this case.

	Sandstone	Basalt	Limestone	Quartzite	Granite
Deviation from EC2	-1.7%	+28.7%	+4.8%	+44.7%	+79.9%
Deviation from *fib* 42	-3.3%	+26.9%	+3.2%	+42.8%	+77.2%
Deviation from *fib* 55	+1.2%	+33.1%	+8.2%	+49.8%	+85.8%

Table 4.8 Percentage difference between predictions and testing of elastic modulus

The modulus test results clearly show that the accuracy of theoretical predictions of modulus elasticity by both of EC2 (2004) and *fib* bulletin 42 (2008) strongly depend on the type of aggregates and on concrete strength to a lesser extent. The recently published bulletin 65 (2010) would appear to be less accurate than the original bulletin 42 in Irish conditions. For Irish local sandstone and limestone, the deviations between practical and theoretical results are small. Such reasonably small errors are acceptable for practical design of structures with respect to deformational behaviour.

On the other hand, the results for basalt and quartzite are overestimated by significant proportions (approximately 30% for basalt and 40% for quartzite). Such large discrepancies have implications for the actual deformation and displacements, and actual results are significantly lower than the theoretical calculation of the modulus of elasticity if predicted using the aforementioned standards.

Since granite is mentioned in neither EC2 (2004) nor the *fib* bulletins 42/65 (2008, 2012), a suggested value of α of 0.55 is arrived at by using the theoretical formulae with the experimental results.

4.3.2.4 Adjustment for Irish Aggregates:

To achieve more accurate predictions using Equation 4.3, for example, the adjustment coefficient α can be introduced to this equation. Equation 4.3 can then be re-written as:

$E_{cm} = 22 \times \alpha \, (f_{cm}/10)^{0.3}$ (GPa) (Eqn 4.7)

Now Equations 4.7 and 4.5 are used in reverse, by substituting in the measured mean strength f_{cm} and measured mean modulus of elasticity E_{cm}, to obtain more practical values of α for Irish conditions. Table 4.9 and Table 4.10 show that values of the adjustment coefficient α of sandstone and limestone are close to the reference values from EC2 (2004) and *fib* bulletin 42, 65 (2008, 2012). Basalt and quartzite have significantly lower α compared with reference values 1.2 and 1.0 respectively. The value of α of granite is suggested to be about 0.55 based on the actual results but this is inconsistent with these Irish values.

Here it can be seen that limestone, for example, has a higher α value than sandstone, quartzite and granite, unlike in the original where quartzite had the higher value. Arising from this, limestone is more favourably positioned such that design of concrete structures with limestone aggregates can now be more accurately assessed for their modulus in Ireland, leading to more economic solutions. This discrepancy will have significance in HSC design in Ireland. From the lowest mean compressive strengths in Table 4.9 to the highest ones in Table 4.10, the modified value of α remains at a reasonably consistent level for any particular type of aggregate. Thus, the suggested α values as the proposed Irish values are summarized in Table 4.11 for each aggregate type.

		Sandstone	Basalt	Limestone	Quartzite	Granite
Measured mean values	f_{cm} (MPa)	41.7	47.2	44.8	53.8	41.5
	E_{cm}(GPa)	23.7	32.7	29.8	24.1	17.9
Original α in EC2		0.7	1.2	0.9	1.0	-
modified α for EC2		0.70	0.93	0.86	0.66	0.53
modified α for *fib* 42		0.72	0.96	0.89	0.68	0.55
Proposed Irish Value α		0.7	1.0	0.9	0.7	0.6

Table 4.9 Recommended adjustment coefficient α of grade C40/50 at 3 days

		Sandstone	Basalt	Limestone	Quartzite	Granite
Measured mean values	f_{cm} (MPa)	73.7	81.5	70.7	77.5	79.0
	E_{cm}(GPa)	29	39.7	33.8	30.2	24.1
Original α for EC2		0.7	1.2	0.9	1.0	-
modified α for EC2		0.72	0.96	0.85	0.74	0.59
modified α for *fib* 42		0.73	0.97	0.87	0.75	0.59
Proposed Irish		0.7	1.0	0.9	0.7	0.6

Table 4.10 Recommended adjustment coefficient α of grade C70/85 at 28 days

	Sandstone	Basalt	Limestone	Quartzite	Granite
Proposed Irish Value	0.7	1.0	0.9	0.7	0.6

Table 4.11 Proposed Irish value of α for each aggregate type

As a footnote, it should also be recognised that Model Code 2010 recommends a further adjustment, α_i, to the predicted a reduced value of modulus, E_c, based on strength, which allows for the initial plastic strain on loading which causes irreversible deformations, as follows:

$E_c = \alpha_i \times E_{cm}$' (Eqn 4.8)

where $\alpha_i = 0.8 + 0.2 \times f_{cm}/88$ but ≤ 1.0

Typically, for C40/50, $\alpha_i = 0.93$, while for C70/80, $\alpha_i = 1$. Nonetheless, the observations in this research are not affected by this secondary factor because only the secant value of the modulus of elasticity were tested and analysed.

CHAPTER 5. INFLUENCES OF ACCELERATING TECHNIQUES IN GGBS CONCRETES

5.1 Introduction

HPC is required to provide some specified advantages over conventional concrete in various aspects, such as improved strength/stiffness, better quality control, safer and easier prefabrication etc. To attain these designed requirements, common techniques and additional materials in concrete production are necessary for particular cases. The mechanical performance under three accelerating techniques and one SCM (GGBS) will be investigated in this chapter. How they affect the concrete properties will be numerically analysed through a comprehensive scheme of experimental work.

One essential component of this improved efficiency in the production of mass, reinforced and pre-stressed concrete was a quick turn-over of units. Despite the costs involved, it was productive for pre-casters to use energy to steam and/or thermally cure components, and to pay a premium for Rapid Hardening Portland cement (RHPC) and accelerating admixtures. The goal was to strike/lift and store precast units within 18 hours of pouring, thereby freeing up valuable shuttering and factory space for future pours.

In this process, there was an implicit use of the concept of concrete maturity – the time temperature history – as a mechanism for determining when pre-stressing load-transfer operations can be undertaken or when units are strong enough to support their own self weight on lifting. This is essential in achieving the economies to be had in factory production. Strength and stiffness development with time, as the cement hydrates, are key elements to be examined in this process as they define stability and elastic shortening losses on transfer.

There is regularly a debate about using GGBS as a partial replacement of Portland cement (Korde et al. 2018). The imperative to use greener cement sources, particularly GGBS in the Irish context, is pervasive. Corporate social responsibility and meeting European and Irish commitments to stringent CO_2 emissions reduction targets are unavoidable reasons for Engineers, Architects, semi-state and public bodies to specify higher replacement rates in all concrete produced. (Higgins et al 2020). There are also compelling technical reasons why GGBS might be used, and chief amongst these are the lower heat of hydration rates, the lower diffusion rates of damaging chloride ingress, the chemical binding of such chlorides, the greater sulphate attack resistance and improved workability, amongst others (Ahmad et al 2022).

However, in the welcome broadening of the scope for inclusion of GGBS in concrete, it should be recognised that the virtue of slower hydration of the C-S-H gel in better managing thermal cracking problems in the field, also imposes more onerous curing and formwork striking times. Herein lies a potential conflict with the precast concrete industry in which early age strength enhancement and fast turn-around of pours are essential in realising the efficiencies referred to heretofore. Therefore, there is a perception in the precast concrete industry that the slower rate of strength development of GGBS concrete represents a significant impediment to its more universal use and that such concrete is mostly used only when specified by an informed client. In short, precast concrete companies have been slow to adapt high percentages of GGBS substitution in prestressed concrete elements.

Thus, it is necessary to systematically demonstrate the influence of GGBS through a thorough testing scheme. To bring this about, in essence, an extensive series of concrete pours are proposed in which the development of strength and stiffness with time, using a range of available accelerating methods, with varying GGBS contents, in high strength concrete mixes will be examined.

In this way, a comprehensive picture will emerge as to whether or not, and how, if so, equally rapid early-age strength development can be achieved through existing means for GGBS concrete (without using artificial alkali activators) as for those without GGBS. It is anticipated that the research evidence may be accumulated, after the literature review and extensive testing, to demonstrate to the precast industry whether or not high GGBS replacement rates can be used without incurring a punitive time penalty on strength and stiffness development in precast works.

5.2 Experimental Setup

The general objective of this phase of the experimental work is to establish comprehensive evidence which demonstrates the growth rates of concrete strength and stiffness with various influencing factors at different ages, especially the early-age properties. To achieve this, a series of concrete mixes with different combinations of ingredients are chosen to build a broad matrix for all-purpose comparison and, subsequently, predictions of the compressive strength and stiffness.

The fundamental idea of the experimental design is to explore the individual and collective effects of the traditional means of accelerating concrete maturity with the known decelerating effect of the addition of high replacement rates of GGBS in high-

strength precast concrete. Scientifically based research outcomes will inform the Irish and European precast industries as to what combination of readily available techniques in concrete technology can be executed to bring about acceptable and affordable striking times in pouring standard precast reinforced and prestressed concrete units. To optimize the striking times of precast concrete, the mix designs of concrete pours are required to provide sufficient compressive strength and elastic modulus at an early-age stage of concrete manufactured by particular techniques, including the utilisation of Rapid Hardening Portland cement, accelerating admixtures and thermal curing treatment.

5.2.1 Design of Concrete Composition

The primary factor to be investigated is the changing mechanical properties of concrete with time. Thus, for each mix design, six different ages are selected as testing times, namely 1, 2, 3, 7, 28 and 56 days. The 1-day to 3-day results are especially important because the rate of strength gain at early ages is the main focus for the research stakeholders. To precisely acquire the data at these early-age times, tests start at exactly 24, 48 and 72 hours after pouring within a half hour variation. In the longer term, 56-day results were also collected to compare with 28-day results as these are commonly being used to represent specification compliance with high GGBS contents.

GGBS, as a retarding factor in the growth of concrete strength and stiffness, is the main focus of this research. Replacing a significant proportion of cement with GGBS causes a dramatically decreasing rate of the hydration process depending on the amount of GGBS used. To determine the side effects of using GGBS on the early-age properties of concrete at various replacement proportions, quantitative analysis is required to establish the influence of GGBS contents. 30%, 50% and 70% of GGBS replacements were selected to compare with concrete specimens without GGBS. According to the Irish Standard, 70% replacement of GGBS content is the maximum allowed in IS EN 206-1.

As early-age strengths of concrete are reduced by introducing GGBS content, three commonly used methods in the precast industry are applied to compensate for this drawback of GGBS, comprising the use of Rapid Hardening Portland Cement, an accelerating admixture and/or thermal curing treatment. These methods are carried out in certain combinations as required.

5.2.2 Mixing Design and Materials

According to the British Standard (BS 1881-125, 2013), allow all materials to reach a temperature of (20 ±5) °C before mixing the concrete. Portland cement and GGBS are

thoroughly stirred separately before use by using a hand tool in a manner that ensures the greatest possible uniformity, avoiding the intrusion of foreign matter or loss of material. The moisture content (as a percentage of the oven dry mass) of the aggregates are determined before mixing with cementitous materials.

The mix design used is to achieve a 50MPa characteristic strength of cube specimens at 28 days. The practical mix recipe in Table 5.1, provided by Banagher Concrete who supplied the aggregates, contains the quantities of materials per cubic metre of concrete with a slump class of S3. The proportion of cementitious materials is the combined mass of CEM II/A-L Portland cement and GGBS (if appropriate) where GGBS is substituted on a one-for-one basis (I.S. EN-197-1, 2011). The coarse aggregates are crushed Irish limestone for both 20mm and 8mm sizes. Fine aggregates are a medium washed sand.

A superplasticizer (CHRYSO Fluid Premia 196) is essential for every concrete pour in the work to achieve adequate workability and maintain the consistency class. Furthermore, as appropriate, an accelerator (CHRYSO Xel 650) is added for particular concrete pours that require a faster strength development during early age.

C40/50N pre-stressed concrete	
Material description	**Mass per cubic metre**
Cementitous materials	400 kg/m^3
20mm aggregate	765 kg/m^3
8mm aggregate	205 kg/m^3
Sand	850 kg/m^3
Max free water	160 kg/m^3
Superplasticizer	3.1 L/m^3
Accelerator (if used)	5.1 L/m^3
Water/cement ratio	0.4

Table 5.1 Mix design of C40/50N prestressed concrete

5.2.3 Pouring Scheme

To test the compressive strength and elastic modulus, five 300×150mm cylinders is the required quantity to acquire suitable results at any particular age. Thus, for each mix design with 6 different ages, a total number of 30 cylinders should be made to demonstrate the trend of strength and stiffness growth with time. However, the volume and quantity of materials of 30 cylinders exceed both the limits of the mixer capacity and

the total number of moulds available. Due to the $0.08m^3$ capacity of the pan mix, 10 cylinder specimens can be made from one batch. Thus, 3 different pours are necessary for one particular mix design, and this introduces an additional factor of variability that needs to be carefully controlled.

When separating 30 cylinders into 3 pours, the quality control of compressive strength is extremely important to ensure that these samples are identical to each other within normal random variations. Rather than using a mechanical scale with 500kg capacity and low accuracy, an electronic scale with 20kg limit is used for weighing all the materials. Another possible error source is the moisture content within sand. Since the pouring schedule extends over several months, the moisture content within the sand also changes with time. To compensate for this influencing factor, a Speedy Moisture Test, following the British Standard (BS 812-109, 1990), is carried out to test the percentage of the water content of the sand prior to pouring on that working day. The actual water poured into the mix and the sand quantity are then modified by the following calculations. For the second pour on the same day, the mixing equipment is fully cleaned and prepared to ensure it has exactly the same conditions as where they were used for the first pour.

$$M_{sand}' = \frac{M_{sand}}{1-w} \qquad \text{(Eqn. 5.1)}$$

$$M_{water}' = M_{water} - w \times \frac{M_{sand}}{1-w} \qquad \text{(Eqn. 5.2)}$$

where M_{sand} = designed mass of sand

M_{sand}' = modified mass of sand

M_{water} = designed mass of water

M_{water}' = the modified mass of water

w = water content by mass in %

As regards the ambient conditions, the concrete laboratory is situated in a basement which provides a generally constant environment with stable temperature and humidity. According to an electronic monitor, the ambient temperature inside the basement is approximately 18°C to 20°C peak to peak during one full day. The humidity is around 65% to 80% consistently.

Even with careful batching and quality control for each pour, unpredictable random differences do exist among these pours from a practical point of view. Thus, 4×100mm cubes are made for each pour as a control test of compressive strength (and these mix constituents) and tested 2 each at 7 days and 28 days respectively to check the deviations between the three different pours for each mix and to ensure no unacceptable errors occurred.

5.2.4 Experimental Procedures

Initially, all the coarse aggregates and sand are mixed together with half of the free water for 2 minutes. Then, the required cement and GGBS are added into the mixer followed by the rest of the free water. Any admixture used is dissolved into the second half of the water prior to mixing for even distribution throughout the fresh concrete.

10 plastic cylinders moulds are put on a vibration table for compaction purposes. The mould height of 300mm is divided into 6 layers during the compaction work, and each layer is vibrated for 15sec to achieve proper compaction without voids and segregation (IS EN-12390-2, 2019). After the pouring of the cylinder specimens, 4×100mm cubes are made using the same vibration table on which the cube moulds are compacted with 2-layer fillings. Each layer is again compacted for 15sec (BS 1881-108, 1983).

The shape, dimensions and other requirements for both cylinder and cube specimens are governed by the Irish Standard (IS EN-12390-1, 2012). The Irish Standard (IS EN-12390-2, 2019) provides guidance on specimen making and curing procedures.

Concerning the compressive tests introduced in the Irish Standard (IS EN-12390-3, 2019), cylinder samples require smooth and level upper surfaces to evenly distribute the compressive loads (while cubes have cast surfaces on vertical sides which are smooth enough for compressive tests). Therefore, a cement paste is prepared for capping the top of cylinders immediately after the pouring. This cement paste is mixed with the same type of cement as the cylinders at the same water/cement ratio. When the cylinders are filled, roughly a 3mm gap between the concrete surface and mould top edge are left for the later capping work. It is beneficial to leave rough surfaces on the finished fresh concrete to achieve better bonding between the cylinder top surface and capping materials. Before the capping process, any free water which is left on the upper surface of the concrete through bleeding should be removed. Finally, the cement paste is applied and compacted onto the cylinders' upper surface with a slightly convex shape above the edge of the mould by using the float. A smooth surface without void or bulb is required for this capping work (BS 1881-110, 1983).

It takes 2 hours for a concrete sample to develop a relatively stiff surface to maintain the smooth finish on the top. Then, all the concrete samples are covered with wet hessian and a plastic sheet. During the following 22 hours, concrete samples in the moulds are kept under a relatively constant temperature and a moist condition until stripping (IS EN-12390-2, 2019). Stripped concrete samples are stored in a water curing tank at a standard 20±0.5°C until testing at specific ages.

For particular mixes, the thermal curing method was introduced to determine the effects of curing temperature on concrete strength development. Since concrete has a relatively high thermal conductivity, using hot water to bring up the temperature of specimens is quite efficient and thorough (Ozioko and Ohazurike 2019). To find out the influence of temperature solely, concrete specimens were made with identical mixing proportions and under procedures as previous experiments. After the final setting time, normally 4 hours long, concrete cylinders and cubes were moved into a 2.2m×0.8m×1.2m tank while still within the plastic moulds.

This water tank is filled with hot water and the water temperature is controlled by a thermostat and a heating unit at 35°C ± 0.5°C constantly. The efficiency of the thermostat and the heating unit was monitored using a thermocouple, and the reading showed that the actual temperature of water was controlled in the range of 34.5°C ~ 35°C. The curing scheme was undertaken for 20 hours after the specimens were placed into the tank. After the first-day thermal curing, all the concrete cylinders and cubes were demoulded normally and placed in another curing tank at 20°C until the testing ages.

5.3 Results Analysis of Acceleration Methods

In this section of results analysis, test values are first presented from the concrete specimens without GGBS content. The focus is thus to numerically evaluate the influences of the selected three methods of accelerating the early-age concrete development on a CEM II/A-L concrete. The major effects of early-age acceleration are expected to occur within 3 days. However, the testing ages extend to 56 days to investigate the long-term side-effects, if any, in a comprehensive analysis.

5.3.1 Concrete Development for the Baseline Mix

The concrete mix used as a baseline for further comparison follows the quantities described in the recipe of Table 5.1 with solely CEM II/A-L as the cementitious material. Both the compressive strengths and elastic modulii are plotted on graphs against time

from 1 day to 56 days to demonstrate the basic development features of high-strength concrete.

Strength development:

The results of the compressive strength testing are collected at 6 different ages with 5 cylinder specimens tested at each age. Since there were 3 concrete pours required to make 30 concrete cylinders, cubes specimens were also tested at 28 days to assess the consistency and reliability of results from different pours, as previously described.

Table 5.2 shows the numerical results of the mean cylinder compressive strength, standard deviation, coefficient of variation and 28-day cube results. The general trend of the strength growth is as expected, except the slight drop at 56 days. However, the variation of cylindrical specimens within the same pour is relatively significant based on the coefficients of variation shown in Table 5.2. The values of coefficients of variation range from 6% from 2-day to 28-day results, to 12% particularly at 1-day and 56-day due to 1 or 2 rogue values which are relatively far from the mean results. As the rate of strength growth slows down after an early age, the systematic strength gain becomes less noticeable. From 28-day to 56-day, the mean strength gain is either small or even falls, such as in Table 5.2. The standard deviations of cylinders remain around 2-4MPa which are close to, or even greater than the systematic strength gain in the long-term. As a result, the influence of these random variations has more impact on the long-term than the early-age results. For example, the standard deviation at 56-day in Table 5.2 is 7.15MPa which is too high to make this group of results decisive. Therefore, the mean strength drop from 28-day to 56-day is not reliable in this case.

Due to inevitable variations between concrete mixes poured at different times, quality control is essentially examined using the cube results to evaluate the reliabilities of the corresponding cylinder specimens. In Table 5.2, the consistency of the 3 different pours is acceptable based on the 28-day cube results, with a 4.5% difference from 75.1MPa to 78.8MPa. Further analysis might be required for specific test results if the cube strengths show an unexpectedly large difference between different pours.

Figure 5.1 contains the plots of the development of mean compressive strengths over time from 1 day to 56 days. The curve connecting all the plotted points demonstrates a typical concrete development under standard curing conditions. Compared to the 28-day strength which is normally used as the characteristic strength, the early-age strengths are higher than the predictions calculated by Equation 2.1 and 2.2 to some degree. Substituting t=1 and t=3 into the Equation 2.2, where the constant s=0.25 for cement of strength Class N,

the coefficients $\beta(t)$ of 1-day/28-day strength and 3-day/28-day strength should be 35% and 60% respectively.

However, the actual result shows that the 1-day concrete reaches 50% of its 28-day compressive strength, and the 3-day ratio rises to 82%. This improvement of early-age strength is possibly caused by the ideal conditions in the laboratory, the low w/c ratio and the particular characteristics of the CEM II/A-L cement. Replacing part of the cement clinker with limestone filler could provide additional surface for precipitation of hydration products, thereby improving the early-age hydration (Aref et al 2017).

On each plotted point of the mean strength in Figure 5.1, there is a range bar indicating the actual highest and lowest values for that 5-cylinder group. The values of range bars remain around 8MPa from 1-day to 28-day but a large range of 15.9MPa at 56 days. The lowest result for the 56-day test is 15.6% away from the mean value which makes the reliability of this result doubtable. It could also explain the slight drop in compressive strength at the later testing age of 56 days compared to the 28-day result.

	1-day	2-day	3-day	7-day	28-day	56-day
Cylinder Compressive Strength (MPa)	28.6	42.7	46.9	53.1	56.9	55.6
Standard Deviation (MPa)	3.43	2.88	3.22	3.58	2.97	7.15
Coefficient of Variation	12.1%	6.6%	6.7%	6.7%	5.2%	12.9%
28-day Cube Strength (MPa)	75.1	78.7	75.1	78.7	76.5	76.5

Table 5.2 Numerical results of the cylindrical compressive strength of baseline mix and the 28-day cube results

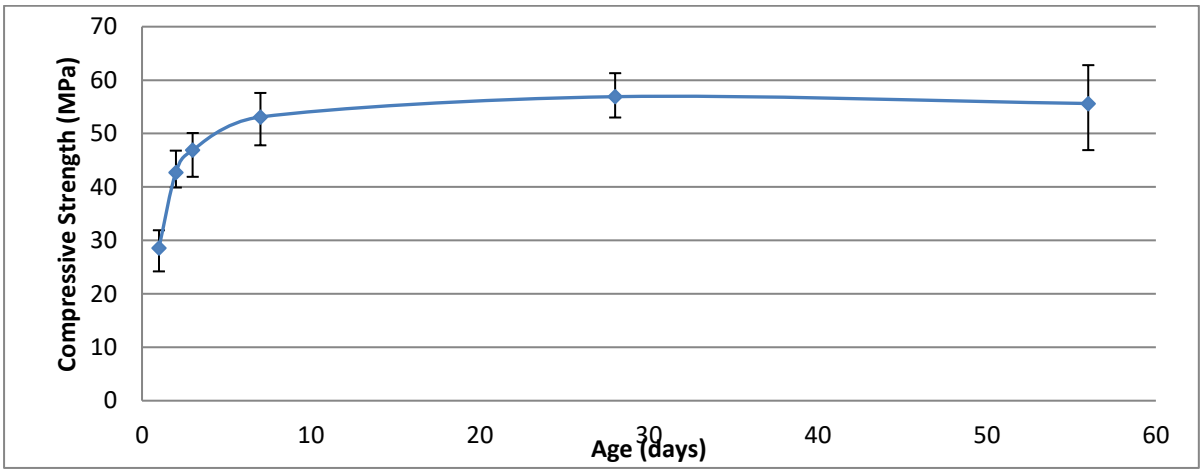

Figure 5.1 Compressive Strength vs Time for 100% CEM II/A-L

Elastic modulus development:

The development of elastic modulus over time is displayed in the graph of Figure 5.2. The growth trend of the curve in Figure 5.2 is more accentuated than the corresponding curve of strength development.

There are two main differences between the strength and elastic modulus developments. Firstly, the rate of early-age growth of elastic modulus is significantly higher than that of the compressive strength. The ratios of 1-day/28-day and 3-day/28-day results are 76% and 93% respectively, compared to 50% and 82% for the compressive strength. Based on Equation 2.5 from EuroCode 2 (I.S. EN-1992-1-1, 2005), the elastic modulus is proportional to the compressive strength to the power of 0.3. Thus, the moderate growth of the elastic modulus with time in Figure 5.2 can be explained by this numerically predicted relationship between the elastic modulus and the compressive strength.

Secondly, the variation of results from the same mix is particularly small compared to the previous graph in Figure 5.1. Since there are only two values for each testing age, the length of each range bar is the difference between the two results. As the differences are normally below 1%, except the 28-day point, most range bars are not clearly observed in the curve.

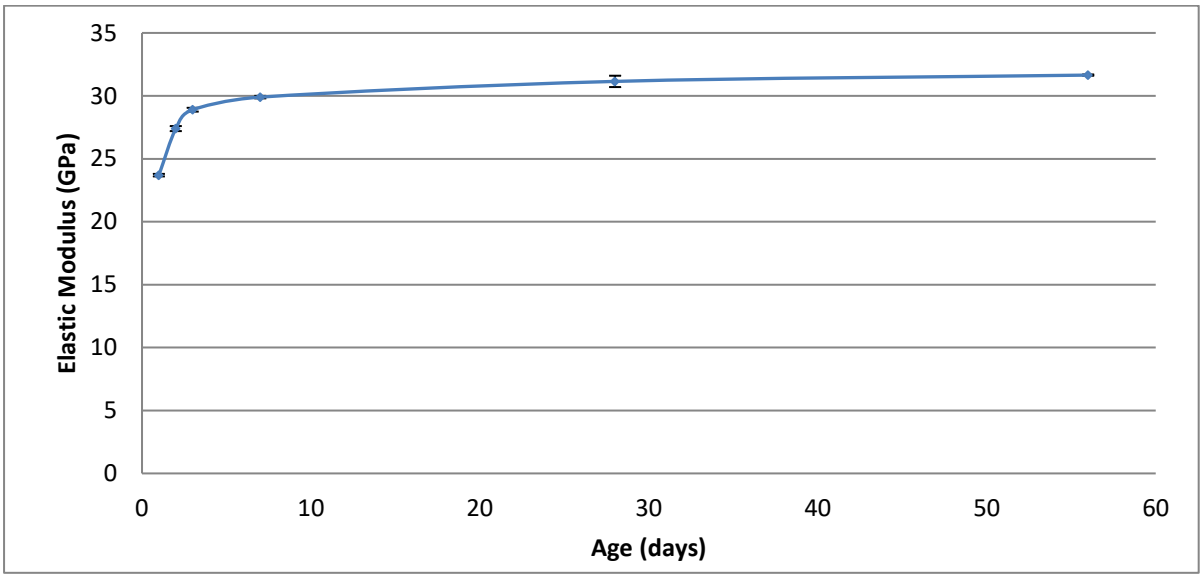

Figure 5.2 Elastic Modulus vs Time for 100% CEM II/A-L

5.3.2 Effects of Rapid Hardening Portland Cement

In this part of testing, all the conditions remained identical to the baseline mix except the replacement of the CEM II/A-L cement with RHPC.

Strength development:

The test results show some similarities between Table 5.2 and Table 5.3. The majority of the coefficients of variation for each testing group stay around 5%-6%. However, there are occasionally one or two larger variations (9-12%) occurring on some random testing ages. On the long-term side, the 56-day result once again decreased slightly from 28 days, but this is not significant.

The consistency of cube results is similar to the previous ones, ranging from 78.3MPa to 81MPa. However, the average values are generally higher by 3MPa here, which is not significant or unexpected (as strengths are accelerated at an early age).

Figure 5.3 shows the comparison of the strength development between the RHPC mix and baseline mix. There is a 20% increase in the compressive strength at 1 day by replacing the CEM II/A-L with the RHPC. However, this effect of strength improvement diminished quickly, after 2 days. On the long-term side of Figure 5.3, the RHPC mix has a slight disadvantage compared to the baseline mix, but the difference is still within random variations.

To avoid the confusion on the graph, only the range bars of RHPC mixes are drawn in Figure 5.3. The range bar of the 1-day result is the only one that is generally higher than the mean result of the baseline mix. All the remaining range bars crossover the corresponding mean results of the baseline mix. Thus, the practical effect of RHPC is not significantly obvious in Figure 5.3 after day 2. Therefore, there is no demonstrable systematic difference between the two types of cements except for the 1-day results.

	1-day	2-day	3-day	7-day	28-day	56-day
Compressive Strength (MPa)	34.2	42.2	48.1	50.1	55.7	53.0
Standard Deviation (MPa)	1.92	2.07	2.48	3.68	5.26	3.62
Coefficient of Variation	5.6%	4.9%	5.2%	7.3%	9.5%	6.8%
28-day cube Strength (MPa)	81.0	78.3	78.3	81.0	78.7	78.7

Table 5.3 Numerical results of the compressive strength of 100% RHPC

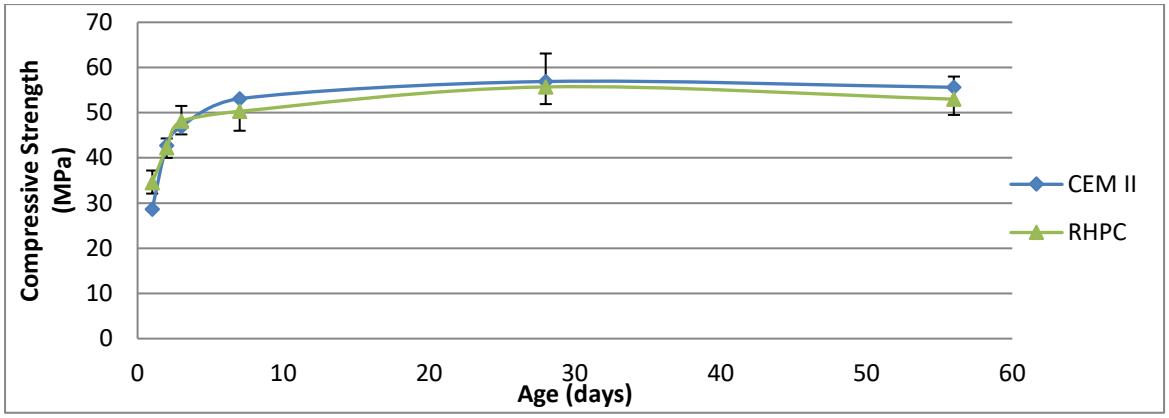

Figure 5.3 Compressive Strength vs Time for 100% CEM II/A-L and 100% RHPC

Elastic modulus development:

Figure 5.4 shows the comparison of the elastic modulus development between the RHPC mix and baseline mix. These two curves are practically identical to each other with minor difference at particular points. Even on the first day of testing, the effect of RHPC only enhanced the elastic modulus by 4%. Based on the empirical Equation 2.5, the variation of the elastic modulus is expected to be less significant than that of the compressive strength. By numerical calculation, the 20% increase of the compressive strength at 1-day should cause a 6% increase of the elastic modulus which is relatively close to the observed 4% testing result.

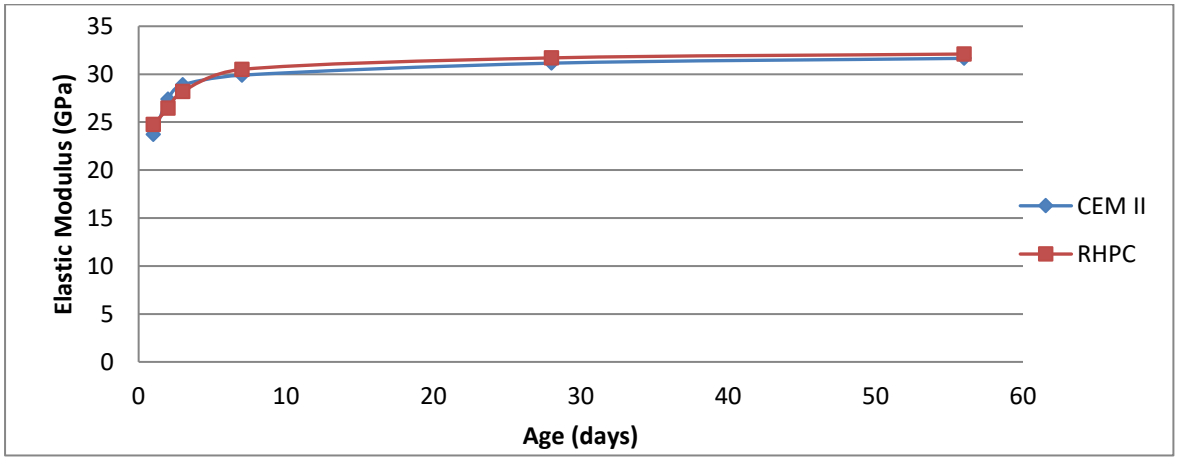

Figure 5.4 Elastic Modulus vs Time for 100% CEM II/A-L and 100% RHPC

5.3.3 Effects of Accelerator

In this part of testing, an accelerating admixture was added into the baseline mix to evaluate the effects on strength and elasticity accelerations. The dosage of the accelerator Chryso Xel 650 is 3 litres per cubic metre of the concrete mix, which is 1.1% by weight of cementitious materials. The rest of the conditions remain the same as the baseline mix.

Strength development:

In Table 5.4, cube results are generally consistent with previous mixes and almost the same as the baseline mix due to the same type of CEM II/A-L cement being used. The coefficients of variation of cylinder specimens still show a random distribution within a certain range (3%-8%).

Both of Table 5.4 and Figure 5.5 demonstrate that the effects of an accelerator on the compressive strength are similar to that of RHPC, particularly in the early age. The 1-day strength was, once again, improved by approximately 20%, and this improvement diminished after 2 days again. After 1 day, the length of error bars is wide enough to cross the mean strength difference between the baseline mix and the mix with an accelerator. Therefore, the systematic difference between two mixes is not significant compared with the random variations after day 2. The actual effects of the accelerator after 1 day cannot be accurately determined by the difference between the mean compressive strengths, if there is any, in Figure 5.5.

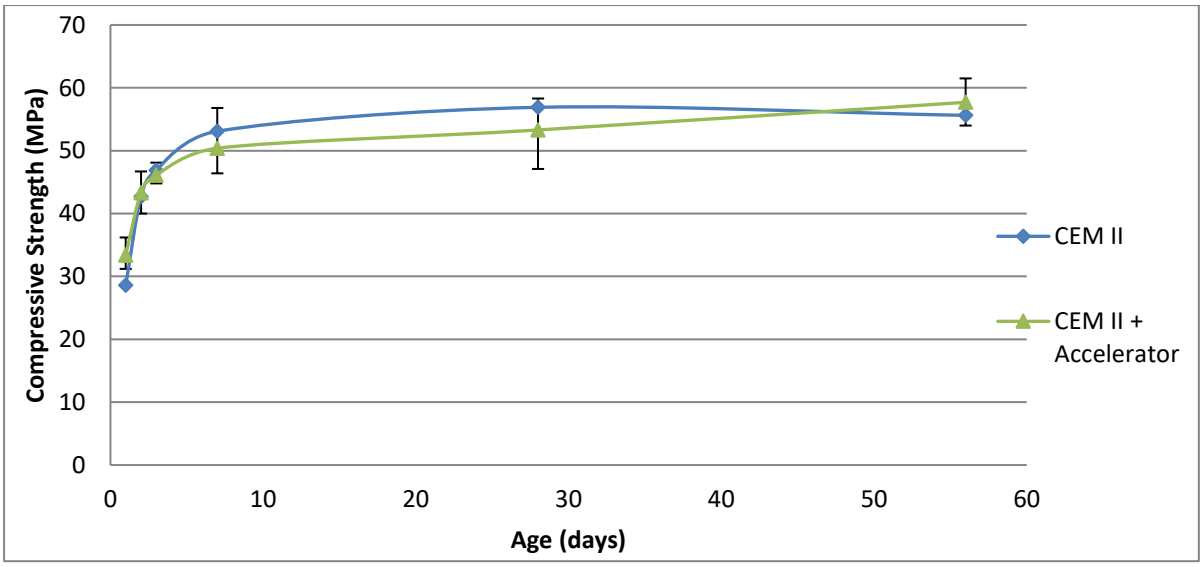

Figure 5.5 Compressive Strength vs Time for CEM II and CEM II+Accelerator

On the long-term side, the side effect of the accelerator remains ambiguous because of the unexpected results at 28-day and 56-day. The baseline mix has a slightly decreased strength from 28 days to 56 days, while the mix with the accelerator has a small growth, which is to be expected. Thus, the long-term effect of the accelerator cannot be definitively concluded from Figure 5.5, which is expected to be similar to the baseline mix.

	1-day	2-day	3-day	7-day	28-day	56-day
Compressive Strength (MPa)	33.4	43.3	46.1	50.4	53.3	57.7
Standard Deviation (MPa)	1.94	2.85	1.42	4.07	4.43	3.23
Coefficient of Variation	5.8%	6.6%	3.1%	8.1%	8.3%	5.6%
28-day cube Strength (MPa)	77.2	77.2	78.0	78.0	75.6	75.6

Table 5.4 Numerical results of the compressive strength of 100% CEM II/A-L + Accelerator

Elastic modulus development:

Figure 5.6 shows that the effect of accelerator on the elastic modulus is not as significant as that on the compressive strength, similar to Figure 5.4. Even on the first day, the improvement in the mean value is less than the variations between cylinder specimens. With the exception of a couple of unexpected points at 56 days, these two curves almost overlap each other.

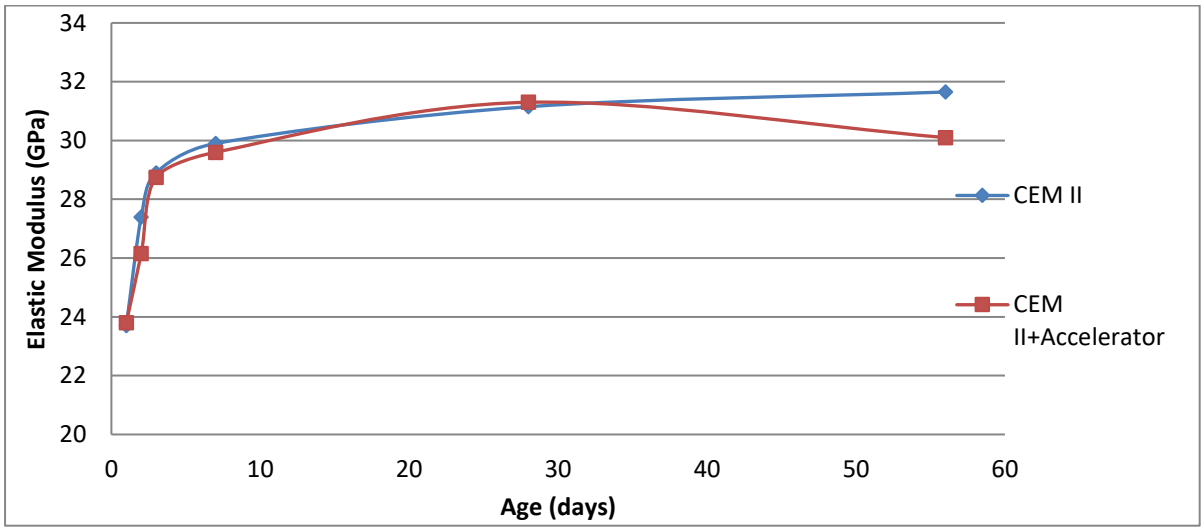

Figure 5.6 Elastic Modulus vs Time for CEM II and CEM II + Accelerator

Comparing Figure 5.6 and Figure 5.4, the effects on the elastic modulus of both methods are similarly benign. Theoretically, if the strength is improved by 20%, the increase of the elastic modulus should be around 6% based on Equation 2.5. However, the results indicate that the actual difference is smaller than the theoretical prediction, principally due to marginal random variations in test results.

5.3.4 Effects of Thermal Curing

In this part of testing, the concrete specimens of the baseline mixes undertook a thermal curing process in a hot water tank. After the 4-hour initial setting time, concrete specimens retained within their plastic moulds were brought into a temperature-controlled water tank at a constant temperature of 35°C. Specimens were stripped from the moulds after 20 hours of thermal treatment. Then, they were either tested for the 1-day results or kept in a normal curing tank at 20°C until the scheduled testing ages.

Strength development:

Again, cube results are consistent and reliable for the quality control between different pours, ranging from 74.1 MPa to 78.5 MPa cured under normal curing conditions. In sections 5.3.1, 5.3.3 and 5.3.4, mixes with CEM II/A-L cement show that the ranges of 28-day cube results are almost the same as each other. However, the results in 5.3.2 indicates that RHPC has a small advantage of 3MPa on the long-term mean strength.

The main difference in this case is that the effectiveness of thermal curing is significantly greater than the previous two methods. The 1-day improvement of the compressive strength is more than 40%, and 1-day mean compressive strength reached 40.9MPa compared to 34.2 and 33.4 MPa for RHPC and an accelerator respectively. Under 35°C curing conditions, the maturity of concrete development is growing at a significantly higher rate. The high efficiency of this water-curing method is due to the high thermal conductivity of concrete. The duration of this improving effect is also longer than previously. The 2-day strength of thermally cured specimens still has a significant advantage compared to the normally cured ones (45.9 MPa and 42.7 MPa respectively).

On the long-term side, the side-effect of this accelerating method is significantly noticeable in Figure 5.7. The compressive strength of thermal cured cylinders after 7 days is considerably lower than that of the normal cured ones by 10% to 17% due to the reduced surface area of the hydrated products and a coarser pore structure (Kjellsen 1996). However, this side-effect did not change the 28-day cube results strongly based on the values in Table 5.5. Thus, the ratio of the cube to cylinder strengths at 28 days is lower than previously.

The decrease of 56-day result from the 28-day result occurred to a more severe degree. A more detailed discussion of the comparison between 28-day and 56-day results will be included later.

	1-day	2-day	3-day	7-day	28-day	56-day
Compressive Strength (MPa)	40.9	45.9	46.4	47.1	50.8	45.8
Standard Deviation(MPa)	2.43	4.28	4.09	2.99	6.44	0.99
Coefficient of Variation	5.9%	9.3%	8.8%	6.3%	12.7%	2.2%
28-day cube Strength (MPa)	74.1	74.1	78.5	78.5	77.1	77.1

Table 5.5 Numerical results of the compressive strength of 100% CEM II/A-L + Thermal Curing

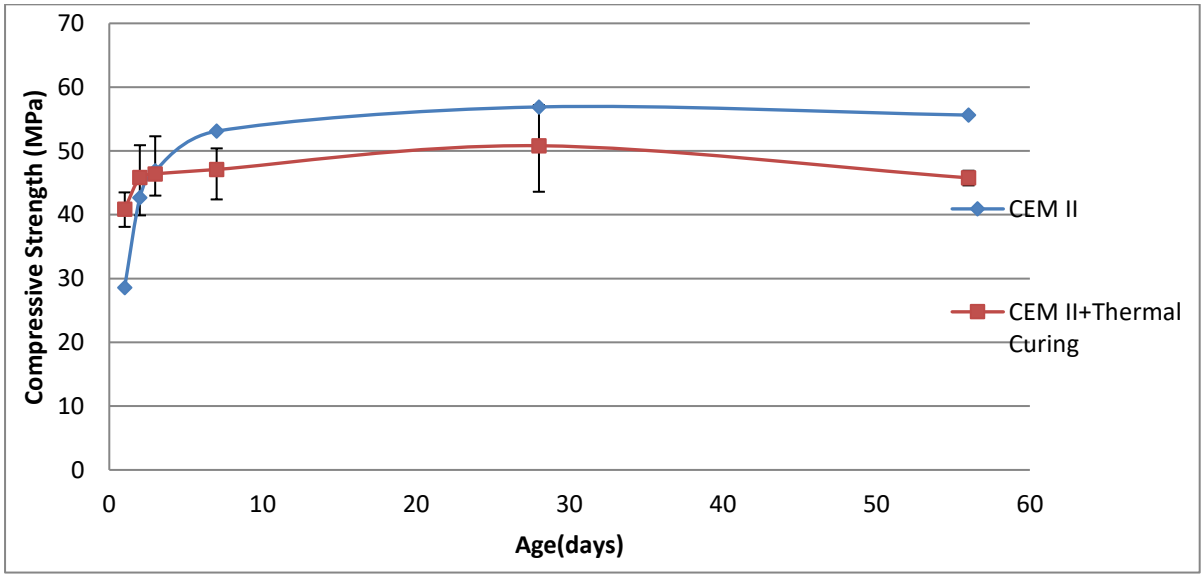

Figure 5.7 Compressive Strength vs Time for CEM II and CEM II+ Thermal Curing

Elastic modulus development:

Early-age elasticity has been improved significantly by enhancing the thermal curing treatment. As shown in Figure 5.8, the 1-day elastic modulus is 16% higher than that of the baseline mix. Again, by using Equation 2.5, the increase of the elastic modulus is predicted to be of the order of 12% when the compressive strength is 40% higher. Unlike the previous two methods, the predicted value is smaller than the actual result. However, the growth of the elastic modulus almost stopped after 3 days and ended at lower values at long-term ages compared with the baseline mix. This trend of elasticity development corresponds with the strength curve which has a lower slope.

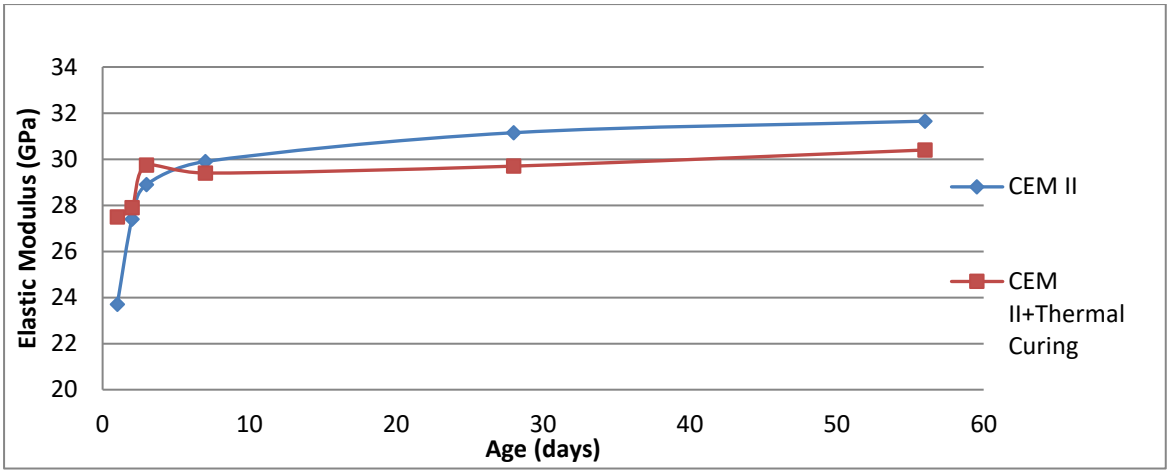

Figure 5.8 Elastic Modulus vs Time for CEM II and CEM II + Thermal Curing

5.3.5 Combined Effects of RHPC and Accelerator

In this section of testing, RHPC and accelerator were used simultaneously in the concrete mix to evaluate the combined effects of these two methods. The testing procedure was performed in the same way as section 5.3.3, except the CEM II/A-L cement was replaced by RHPC.

Strength development:

Figure 5.9 shows that the combination of RHPC and an accelerator provides a significant improvement on the compressive strength within 3 days. The 1-day compressive strength is approximately 40% higher than the result of the baseline mix. This 40% strength enhancement is close to the sum of the individual effects of RHPC (20%) and the accelerator (20%) from previous sections 5.3.2 and 5.3.3. This means that the addition of an accelerator is helpful for RHPC to develop fast early-age strength.

By comparing Figure 5.9 to Figure 5.3 and 5.5, the combined effect has a longer duration of strength enhancement than that of the individual effects of RHPC/Accelerator after 1 day. Up to the third day, the mix with combined accelerating methods still has a higher strength than that of the baseline mix. The long-term strength is slightly lower than that of the baseline mix and the error bar suggests that there is no clear difference between the RHPC/accelerated mix and the baseline mix at later ages.

Elastic modulus development:

By using Equation 2.5, the predicted increase of the elastic modulus is expected to be 12% when the compressive strength is 40% higher. In Figure 5.10, the 1-day elastic modulus

has a 11% improvement after using both RHPC and the accelerator. The actual results demonstrate that the combination of these two methods has a positive effect on the elastic modulus, and the magnitude of this effect is predictable by using an empirical formula based on the compressive strength. After 3 days, the development of the elastic modulus has no significant difference between the two curves in Figure 5.10. Thus, the combined technique of using RHPC and an accelerator together does not have noticeable effects on the long-term elastic modulus, as expected.

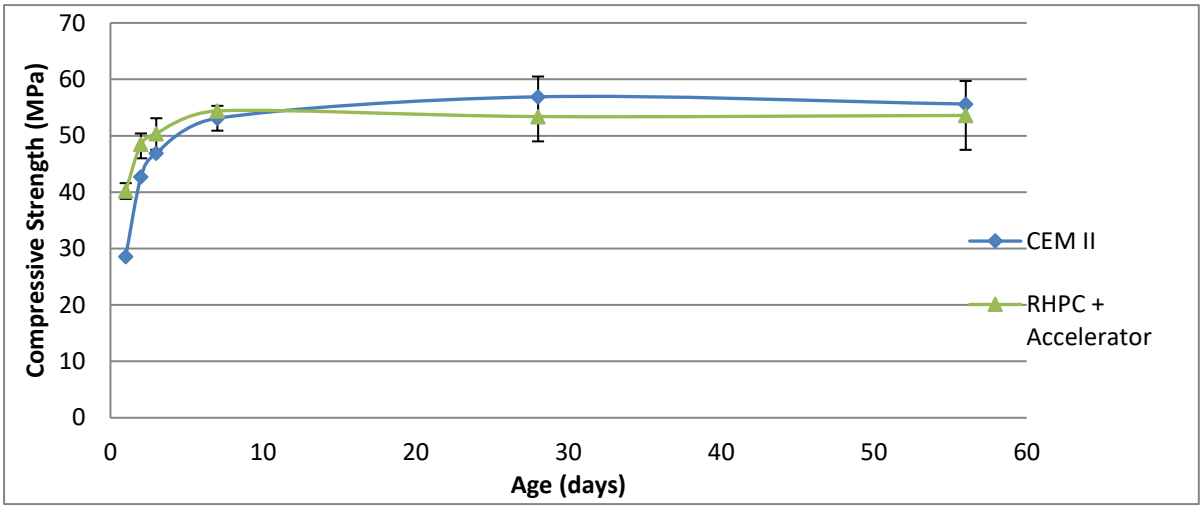

Figure 5.9 Compressive Strength vs Time for CEM II and RHPC + Accelerator

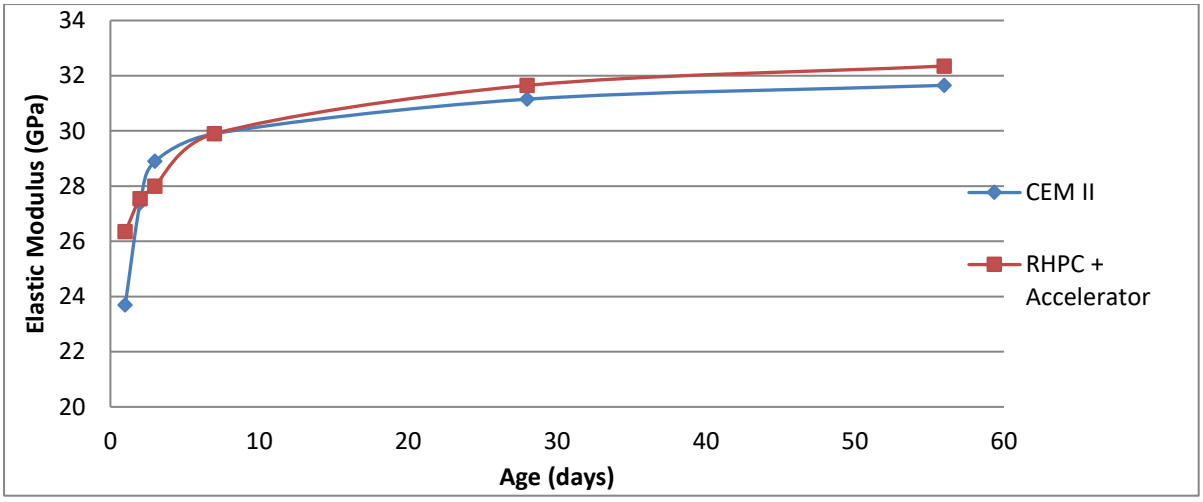

Figure 5.10 Elastic Modulus vs Time for CEM II and RHPC + Accelerator

5.3.6 Combined Effects of RHPC and Thermal Curing

In this section of testing, RHPC and thermal curing were used simultaneously in the concrete mix to evaluate the combined effects of these two methods. An identical procedure to that performed in section 5.3.4 was carried out again in the laboratory, except the CEM II/A-L cement was replaced by RHPC this time.

Strength Development:

The combined effect of RHPC and thermal curing improves the early-age strength significantly in Figure 5.11. The 1-day compressive strength is 40% higher than that of the baseline mix. However, the thermally cured CEM II/A-L shows a similar result in section 5.3.4. RHPC does not demonstrate a significant superiority over CEM II/A-L after the same thermal curing treatment. The first day strengths are 40.9MPa for CEM II/A-L and 41.3MPa

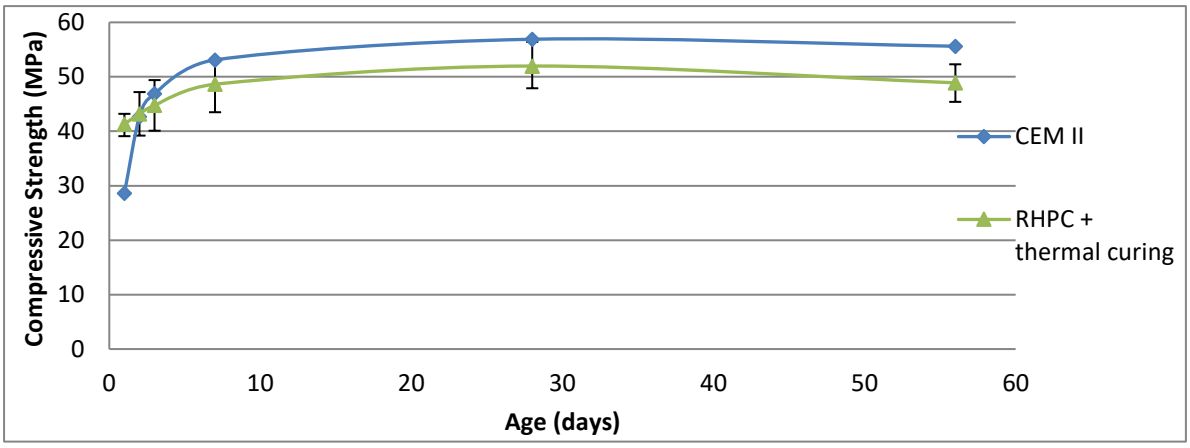

Figure 5.11 Compressive Strength vs Time for CEM II and RHPC + Thermal Curing

for RHPC respectively. The long-term strength drops largely at 28 days and 56 days due to the side-effects of this early-age acceleration by thermal curing.

The strength development is expected to last for years at an extremely slow rate after the concrete is made. However, the natural variation of experiment is greater than the expected strength gain from 28 days to 56 days, the actual 28-day results are slightly greater than the 56-day results in this case.

Elastic Modulus Development:

The 1-day elastic modulus is dramatically increased by applying RHPC and thermal curing together, and the result correlates the increase of compressive strength in Figure 5.11. The actual increase at 1-day is 17%, which is higher than the 13% prediction of using Equation 2.5.

The major difference between the strength and elastic modulus is that the thermal curing method shows no influence on the long-term elastic modulus compared with the different long-term strengths in Figure 5.11. Figure 5.12 demonstrates no variations between the baseline mix and thermally cured mix after 7 days.

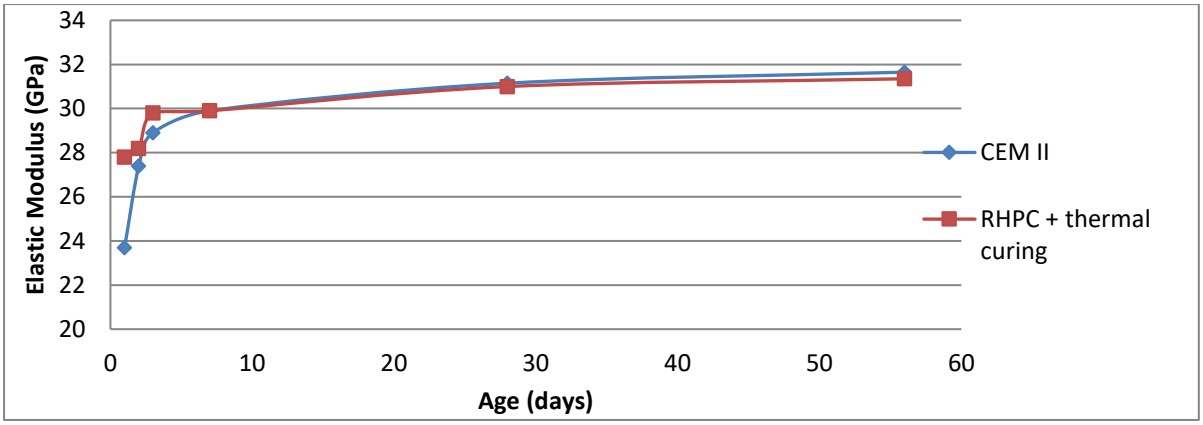

Figure 5.12 Elastic Modulus vs Time for CEM II and RHPC + Thermal Curing

5.3.7 Combined Effects of Three Methods

In this section of testing, all three accelerating methods were used simultaneously in the concrete mix to evaluate the combined. An identical procedure performed in section 5.3.4 was carried out again in the laboratory, except the CEM II/A-L cement was replaced by RHPC with an extra dosage of an accelerator.

Strength Development:

The development of compressive strength is almost identical to the sections 5.3.4 and 5.3.6. CEM II/A-L, RHPC and RHPC+Accelerator generated similar early-age strength after the same thermal curing procedure. Furthermore, the long-term strength is, again, reduced by a considerable proportion compared with baseline mix in Figure 5.13. This 35°C thermal curing procedure dominates the early-age development of concrete, whereas the other two methods show minor influences if they are used at the same time.

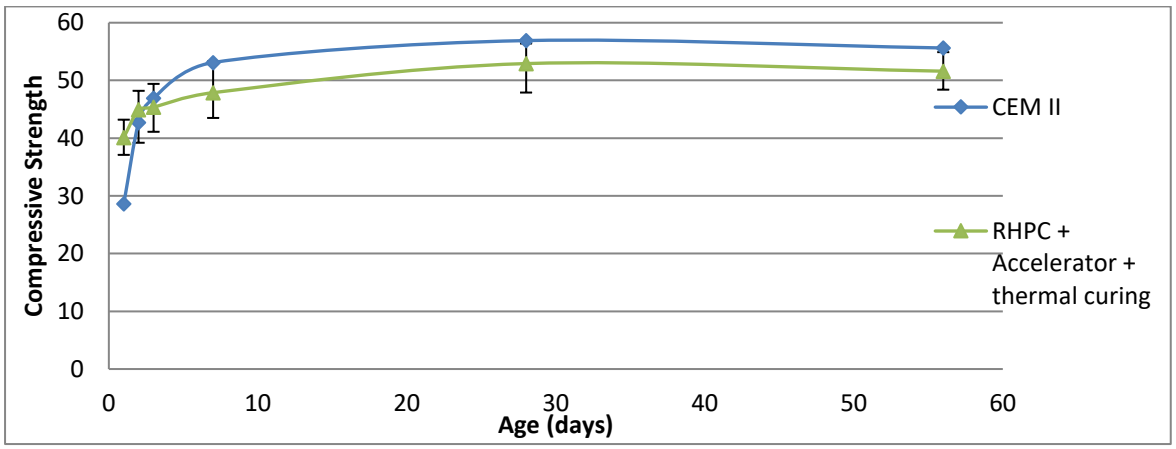

Figure 5.13 Compressive strength vs Time for CEM II and RHPC + Accelerator + Thermal Curing

Elastic Modulus Development:

The 1-day elastic modulus is increased by 19% after applying all three methods. The extra dosage of an accelerator slightly improves the early-age growth of elastic modulus compared with section 5.3.6, but not significantly.

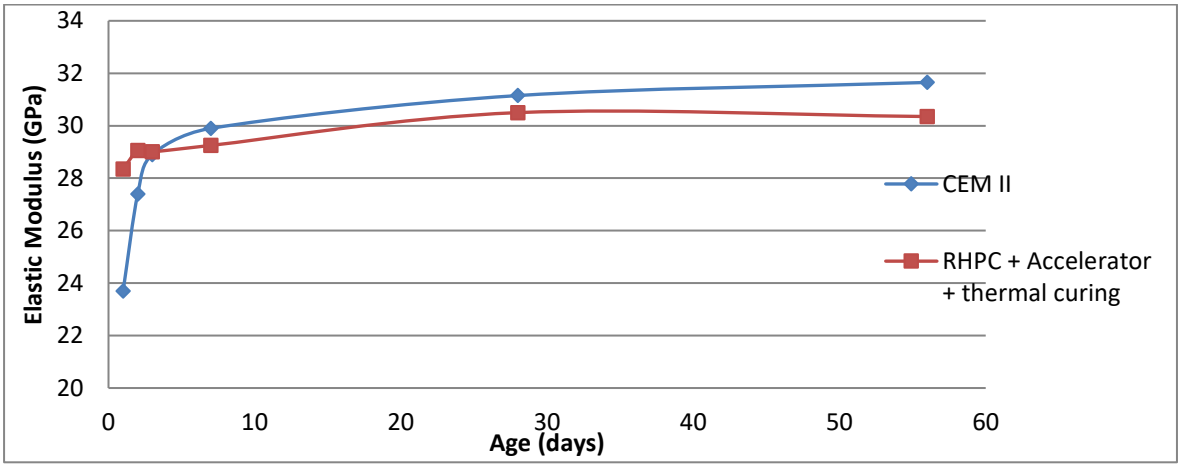

Figure 5.14 Elastic Modulus vs Time for CEM II and RHPC+ Accelerator + Thermal Curing

5.4 Effects of GGBS content with Acceleration Methods

In this section of testing, GGBS content is introduced into the concrete mixes for assessing the effectiveness of different accelerating methods. The CEM II/A-L cement is replaced by the GGBS content on a 1-to-1 basis at 30%, 50% and 70%. The efficiency factor of GGBS in concrete is found to be around 1.0 (Babu and Kumar, 2020). The technical sheet of GGBS (ECOCEM Ireland) also indicates that the activity index at 28 days of a 50/50 mix is at 103%. As the value is ~100% it gives justification for the 1-1 replacement. The mix design and accelerating methods remain the same as in the previous section 5.3. The effectiveness of each accelerating method will be investigated by numerical comparison to the results of baseline mixes at different proportions of GGBS.

5.4.1 Retardant Effects of GGBS

The rate of strength development of concrete with GGBS content decreases since the rate of reaction of GGBS is significantly slower than the hydration process of CEM II/A-L or RHPC. It is required to find out how the blended cement behaves with/without the accelerating methods discussed previously.

Firstly, only GGBS content is used to analyse the retardant effects of GGBS on the compressive strength and elastic modulus. 30%, 50% and 70% of CEM II/A-L cement was replaced by the GGBS to examine the degrees of this effect.

Figure 5.15 displays a significant early-age decrease of the compressive strength of the 30% GGBS mix compared with the baseline mix. Especially within 3 days, the compressive strength of the hydrated blended cement is approximately 30% lower than that of the pure CEM II/A-L cement. After 7 days, the development curve of the 30% GGBS mix is gradually approaching the baseline curve and ends on a similar level by 28 days. Indeed, the baseline mix is exceeded by 56 days.

Figure 5.16 shows of the development trend of the elastic modulus which is approximately 10% lower than that of the baseline mix within 3 days. Similarly, to the previous situations, the decreased level of the elastic modulus is much less than that of the compressive stress. In this case, the influence of GGBS content demonstrates the expected slower early-age development of both the compressive strength and elastic modulus.

As the GGBS content is increased to 50% and 70% in Figures 5.17 to 5.20 respectively, the slower rates on both of the compressive strength and elastic modulus development are also becoming more significant. Comparing with the baseline mix, the reductions in percentage particularly at 1-day, 2-day and 3-day are shown in Table 5.6 and Table 5.7.

According to Table 5.6, the reduction of the first day strength is approximately equal to the percentage of GGBS in the mix. Considering the effects of previous accelerating methods, the 1-day strength and stiffness has potential to be brought back to baseline levels when the replacement of GGBS is below a certain proportion. For any mix with 50% GGBS or higher, it would be more challenging to achieve this task.

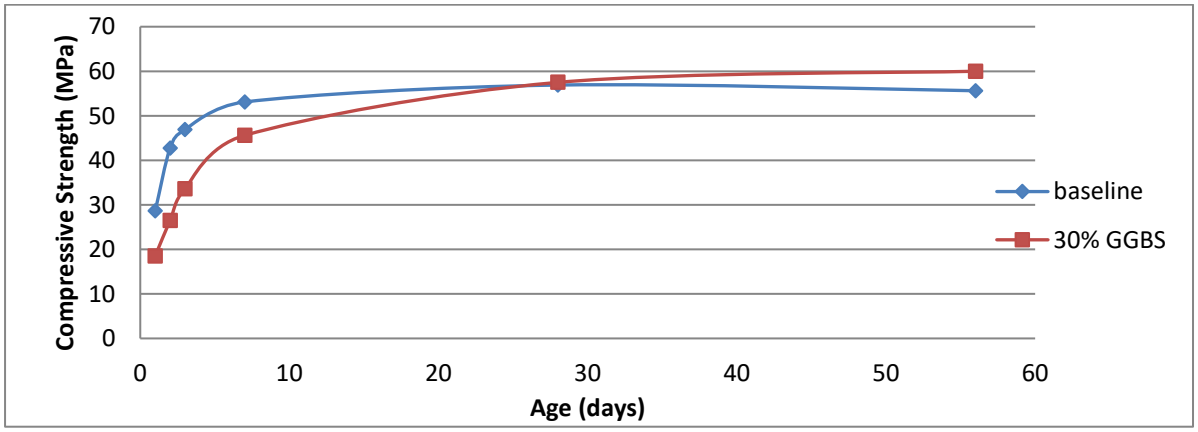

Figure 5.15 Compressive strength vs Time for Baseline mix and 30% GGBS mix

After 1 day, the influence of GGBS content on the elastic modulus is quickly becoming less pronounced. The compressive strength of 30% GGBS mix approached the 1-day compressive strength of the baseline mix at 2 days, while the 70% GGBS mix took 4 days to gain the similar strength due to a higher influence of more GGBS. At 3 days, the elastic modulii of the 3 mixes in Figures 5.16, 5.18 and 5.20 are all about 10% less than the baseline result. After 3 days, the difference between the baseline mix and mixes with GGBS becomes much less significant through to 56 days.

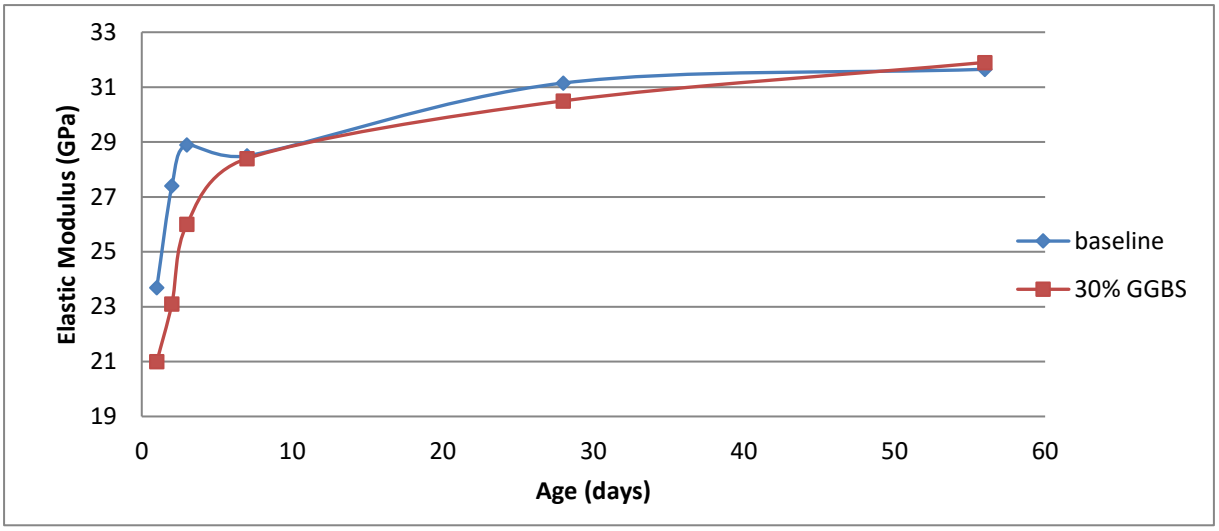

Figure 5.16 Elastic Modulus vs Time for Baseline mix and 30% GGBS mix

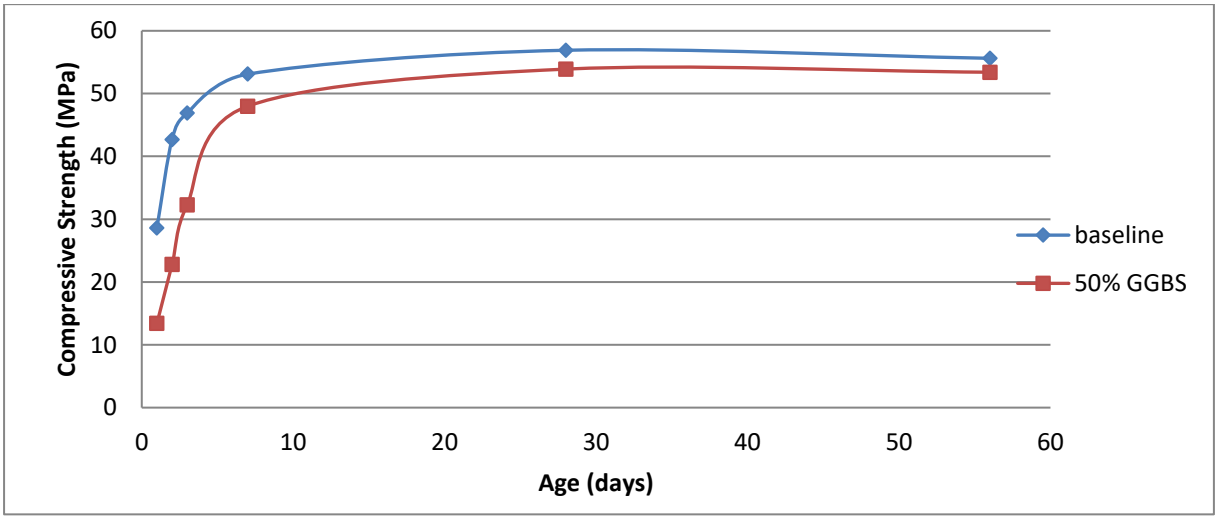

Figure 5.17 Compressive Strength vs Time for Baseline mix and 50% GGBS mix

The quantitative reductions of the compressive strength and elastic modulus listed in Tables 5.6 and 5.7 can cause serious consequences to practical work of concrete manufacture. The striking time of precast concrete has to be prolonged to withstand the self-weight of concrete. As a result, the productivity in a precast plant is lower as the production circle becomes longer due to weak early-age strength.

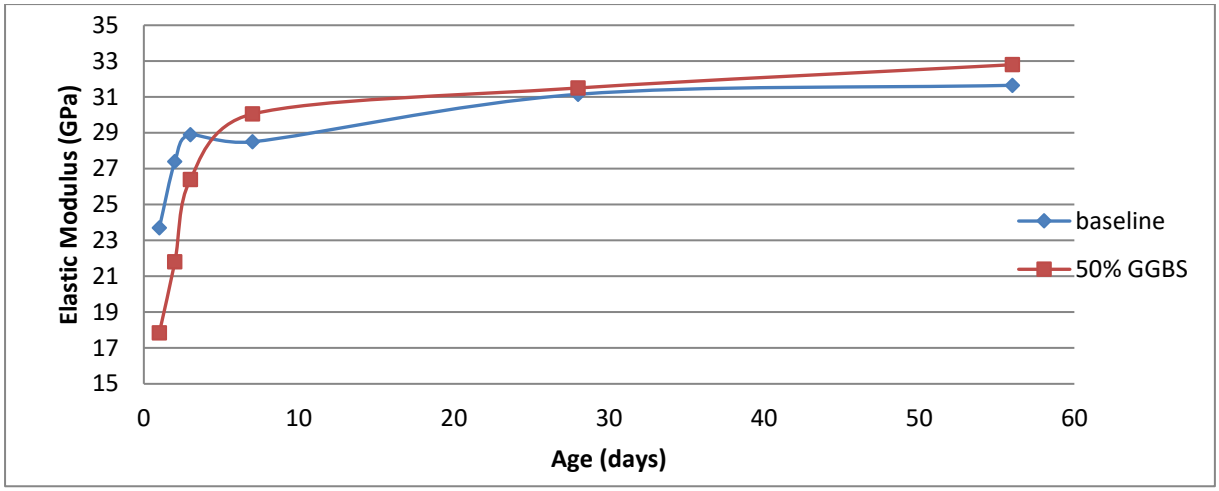

Figure 5.18 Elastic Modulus vs Time for Baseline mix and 50% GGBS mix

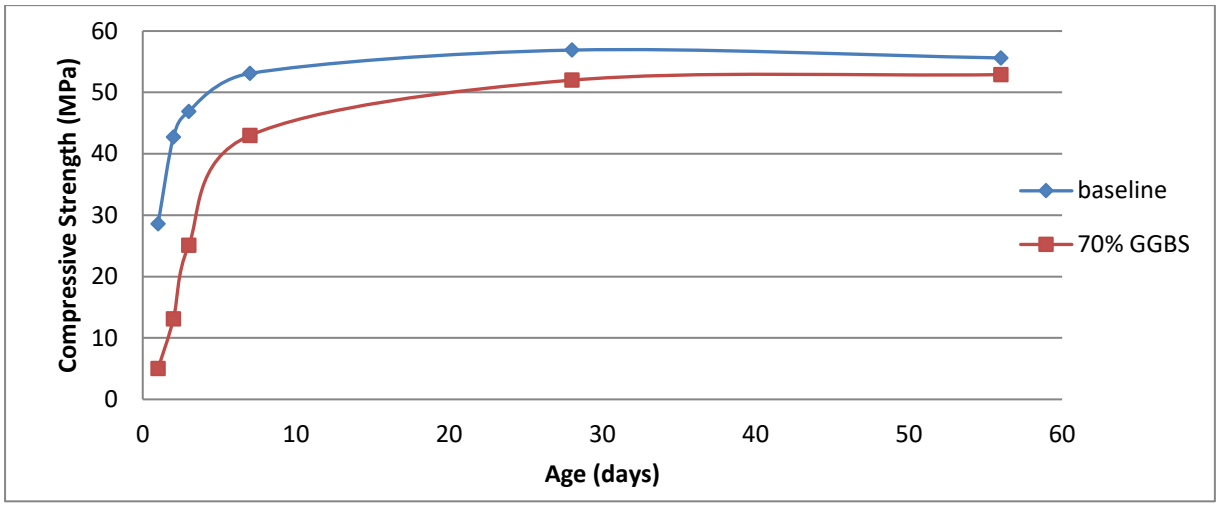

Figure 5.19 Compressive Strength vs Time for Baseline mix and 70% GGBS mix

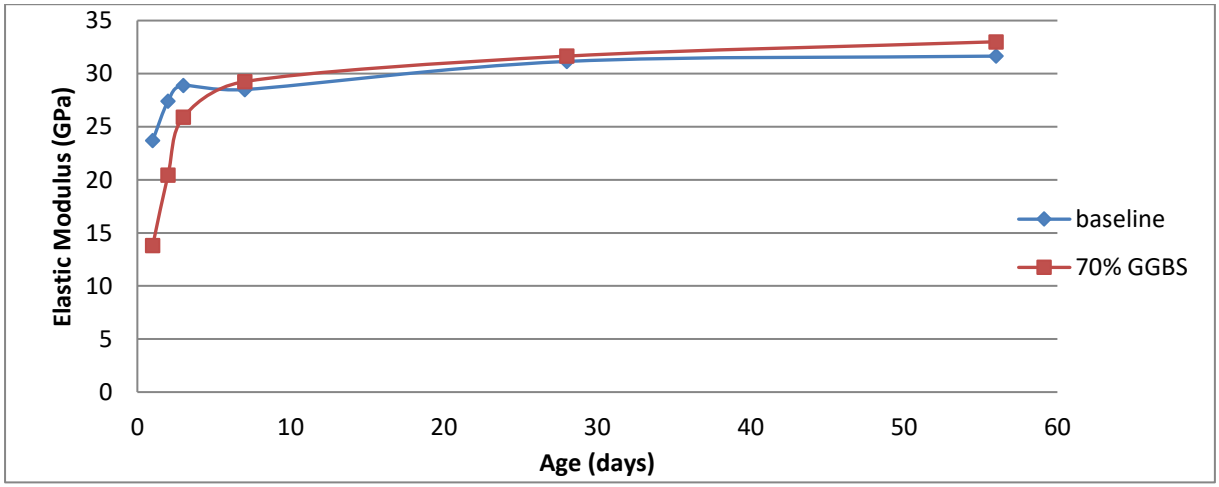

Figure 5.20 Elastic Modulus vs Time for Baseline mix and 70% GGBS mix

The 1-day elastic modulus of 70% GGBS mix in Figure 5.20 is only about 60% of the original value of baseline mix. Such a significant reduction in the elastic modulus can

cause serious prestress loss at transfer due to elastic shortening of concrete. Therefore, the release time of the prestressed tendon has to be delayed for the GGBS concrete to gain sufficient stiffness.

	1-day	**2-day**	**3-day**
30% GGBS	-36%	-36%	-28%
50% GGBS	-53%	-47%	-32%
70% GGBS	-82%	-69%	-46%

Table 5.6 Percentage reduction of compressive strength within 3 days of pouring

	1-day	**2-day**	**3-day**
30% GGBS	-12%	-15%	-10%
50% GGBS	-25%	-21%	-9%
70% GGBS	-42%	-25%	-11%

Table 5.7 Percentage reduction of elastic modulus within 3 days of pouring

5.4.2 Effects of Rapid Hardening Portland Cement on GGBS Concrete

In this section of testing, the CEM II/A-L cement is replaced by the RHPC to blend with GGBS content. It is required to investigate the combined effect of RHPC and GGBS at different proportions of GGBS content. Again, the results of the baseline mix are used for comparison to assess the effectiveness of RHPC in terms of accelerating the early-age development of concrete with GGBS content. These comparison graphs are shown in Figure 5.21 to 5.26.

As higher dosages of GGBS are used, lower quantities of RHPC remain in the blended cement, unlike the other two cases of accelerator and temperature application. Consequently, the effect of RHPC is expected to be less effective from a 30% GGBS mix to a 70% GGBS one. The figures show that RHPC did not provide significant improvement over CEM II/A-L and only a small improvement at low GGBS dosages. When there is 30% GGBS in the blended cement, the 1-day strength is slightly improved from 64% to 68%, comparing to the baseline mix.

Comparing Figure 5.15 to 5.21, the change of cement did not affect the influence of GGBS content significantly. In 30% GGBS mix, the compressive strength improvements from 1 day to 3 days by using RHPC are 4%, 10% and 11% respectively. Especially, the 4% increase of 1-day results did not show any apparent improvement when using RHPC, while there is a 20% increase discussed in section 5.3.2 previously.

The summary of strength and stiffness improvement within 3 days is included in Table 5.8 and Table 5.9, evaluated in percentage terms as follows:

Strength/Stiffness improvement = (RHPC mix - CEM II/A-L mix)/ CEM II/A-L mix × 100% (Eqn 5.3)

As the GGBS content is increased to 50% and 70%, the RHPC still has a lower performance by comparing Tables 5.6 and 5.7 to Table 5.8 and 5.9 due to the low proportion of RHPC in the mix. The 1-day compressive strength shows no improvement in Table 5.8 for the 70% GGBS mix. Therefore, as more RHPC is replaced by GGBS content, the effectiveness and significance of using RHPC becomes less important and indeed negligible.

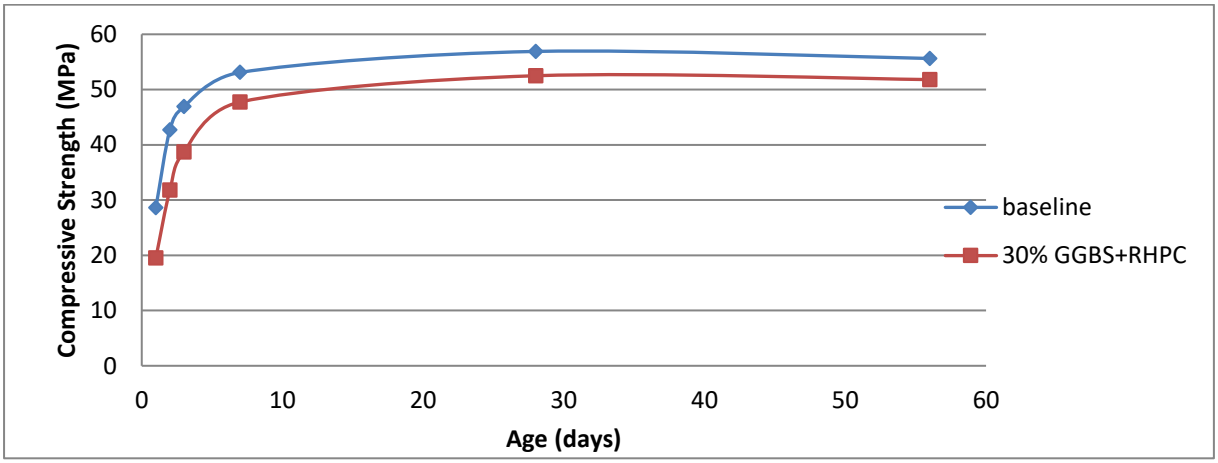

Figure 5.21 Compressive Strength vs Time for Baseline mix and 30% GGBS + RHPC mix

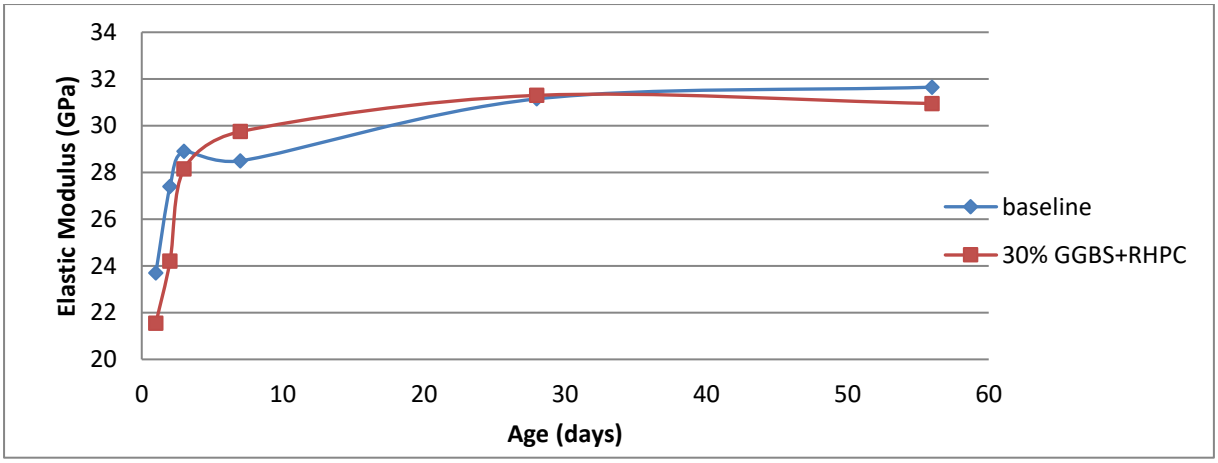

Figure 5.22 Elastic Modulus vs Time for Baseline mix and 30% GGBS + RHPC mix

The improvements of RHPC on the elastic modulus are slightly better than those on the compressive strength, about 3% to 5% at 1 day in Table 5.9. Consider the magnitudes of

reductions in Table 5.7 (12% - 42%), the general conclusion is that it is not possible to bring the elastic modulus back to the level of baseline mix by the application of RHPC alone.

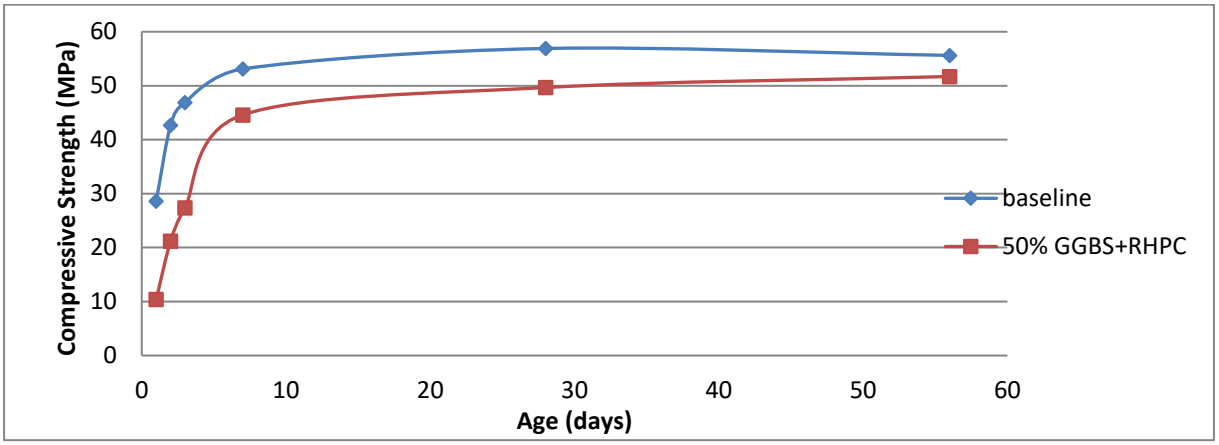

Figure 5.23 Compressive Strength vs Time for Baseline mix and 50% GGBS + RHPC mix

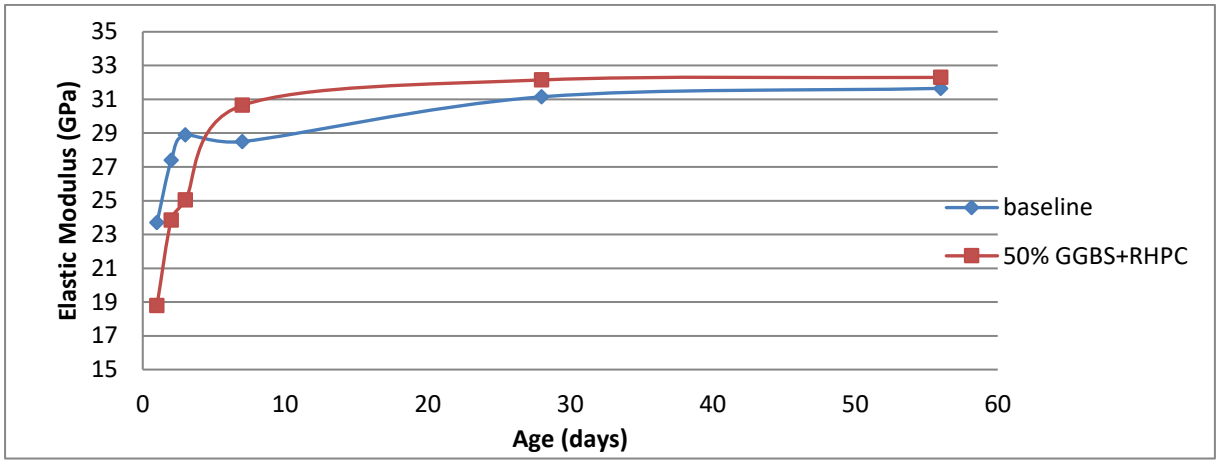

Figure 5.24 Elastic Modulus vs Time for Baseline mix and 50% GGBS + RHPC mix

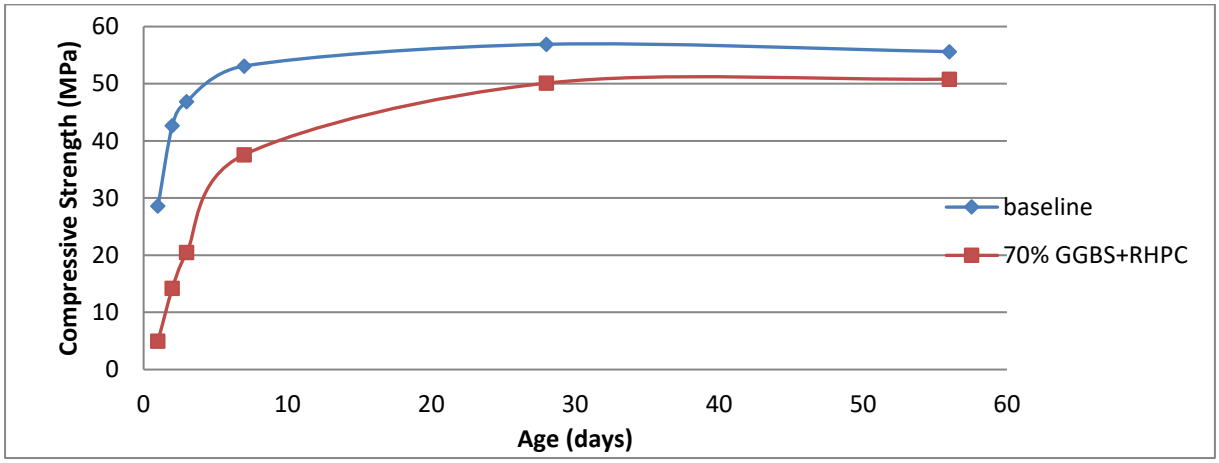

Figure 5.25 Compressive Strength vs Time for Baseline mix and 70% GGBS + RHPC mix

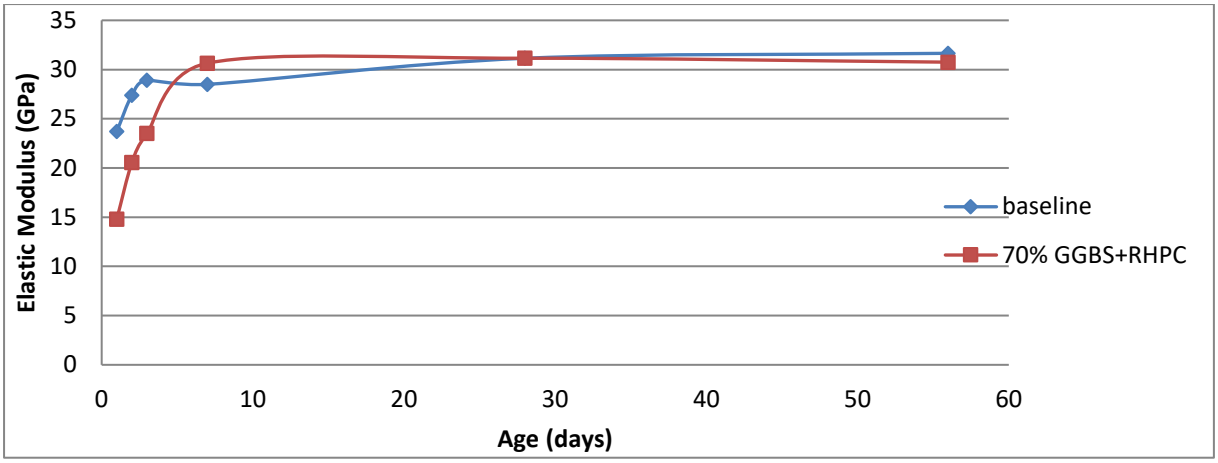

Figure 5.26 Elastic Modulus vs Time for Baseline mix and 70% GGBS + RHPC mix

	1-day	2-day	3-day
30%GGBS+RHPC	+4%	+10%	+11%
50%GGBS+RHPC	-10%	-3%	-9%
70%GGBS+RHPC	0%	+2%	-10%

Table 5.8 Percentage improvement of compressive strength by using RHPC within 3 days

	1-day	2-day	3-day
30%GGBS+RHPC	+3%	+4%	+8%
50%GGBS+RHPC	+5%	+7%	-4%
70%GGBS+RHPC	+5%	0%	-7%

Table 5.9 Percentage improvement of elastic modulus by using RHPC within 3 days

5.4.3 Effects of Accelerator on GGBS Concrete

In this section, an accelerator was added into the concrete mixes with different proportions of GGBS content. The combined effects of GGBS content and the accelerator are required to be investigated by comparing the results with the baseline mix.

The comparison graphs in Figure 5.27 to Figure 5.32 show that the result of using an accelerator is similar to the RHPC discussed in section 5.4.2. This accelerating method is also not capable to bring up the early-age concrete growth to the same level of the baseline mix. At 30% GGBS in Figure 5.27 and 5.28, the 1-day compressive strength is 23% lower than that of the baseline mix and the 1-day elastic modulus is 5% lower. Compared to the 30% GGBS mix without this accelerator, these reduction ratios are 36% and 12% for the compressive strength and elastic modulus respectively. This benefit of using the accelerator is relatively more effective than the previous method of using RHPC. As the GGBS content is increasing to 50% and 70%, the gaps between the baseline mix and the GGBS mix during the early age are, again, large enough to overwhelm the influence of the accelerator.

Table 5.10 and 5.11 show the numerical results of the strength/stiffness improvement by using the accelerator, calculated as follows:

Strength/Stiffness improvement = (CEM II/A-L mix with Accelerator - CEM II/A-L mix)/Baseline mix × 100% (Eqn 5.4)

Although the addition of an accelerator can be overcome by the retardant effect of using GGBS, the influence of the accelerator is relatively more significant than that of the RHPC by comparing Table 5.10 and 5.11 to Table 5.8 and 5.9. For example, the effect of the accelerator on the 1-day compressive strength has consistently positive influence by 7% - 13% at difference percentages of GBBS content, while RHPC shows insignificant or even negative effects on the 1-day compressive strength at 50% and 70% GGBS. Thus, this comparison suggests that the influence of the accelerator has similar effects on the cement+GGBS concrete mix no matter what the ratios between them. Only the 1-day strength shows a small decrease of the effect of accelerator with more GGBS content. However, the RHPC has a decreasing effect as the proportion of GGBS content is increasing for obvious reasons.

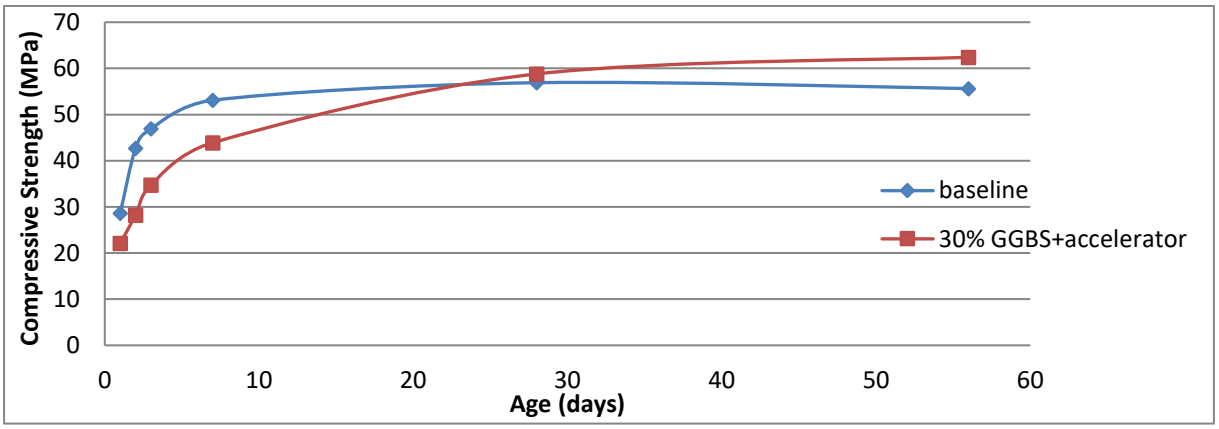

Figure 5.27 Compressive Strength vs Time for Baseline and 30% GGBS + Accelerator mix

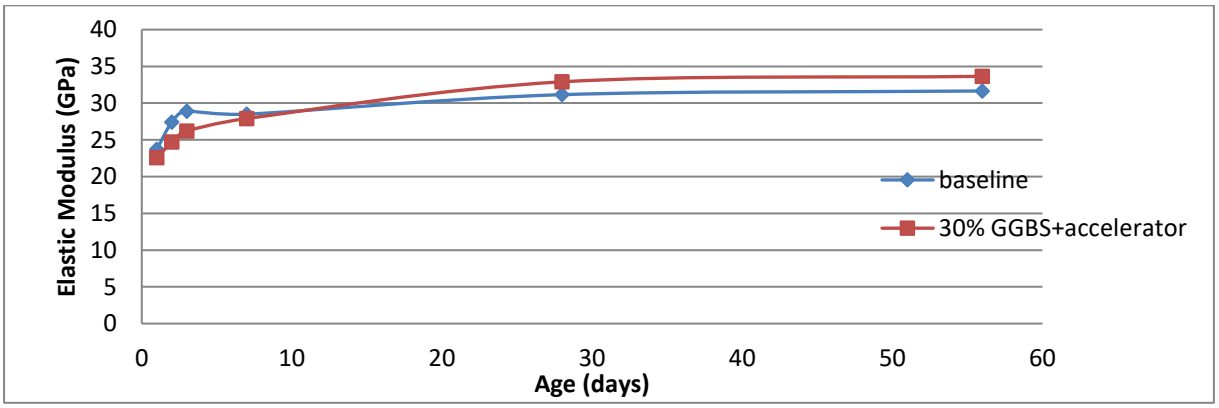

Figure 5.28 Elastic Modulus vs Time for Baseline and 30% GGBS + Accelerator mix

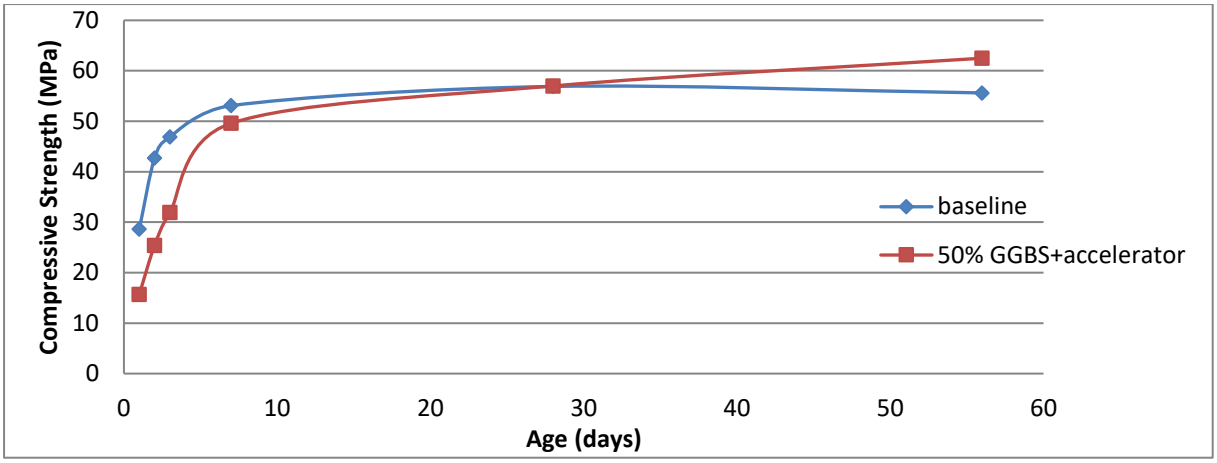

Figure 5.29 Compressive Strength vs Time for Baseline and 50% GGBS +Accelerator mix

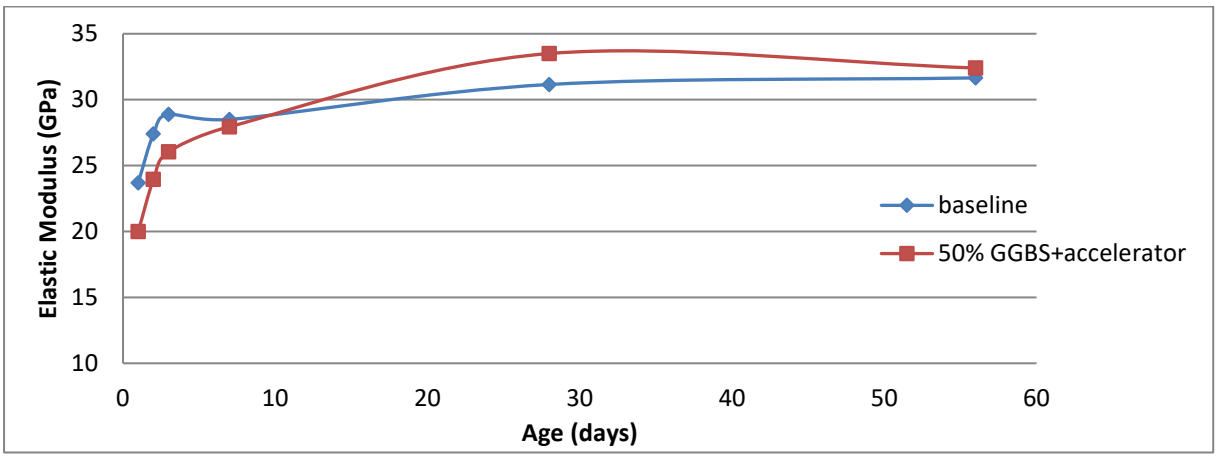

Figure 5.30 Elastic Modulus vs Time for Baseline mix and 50% GGBS + Accelerator mix

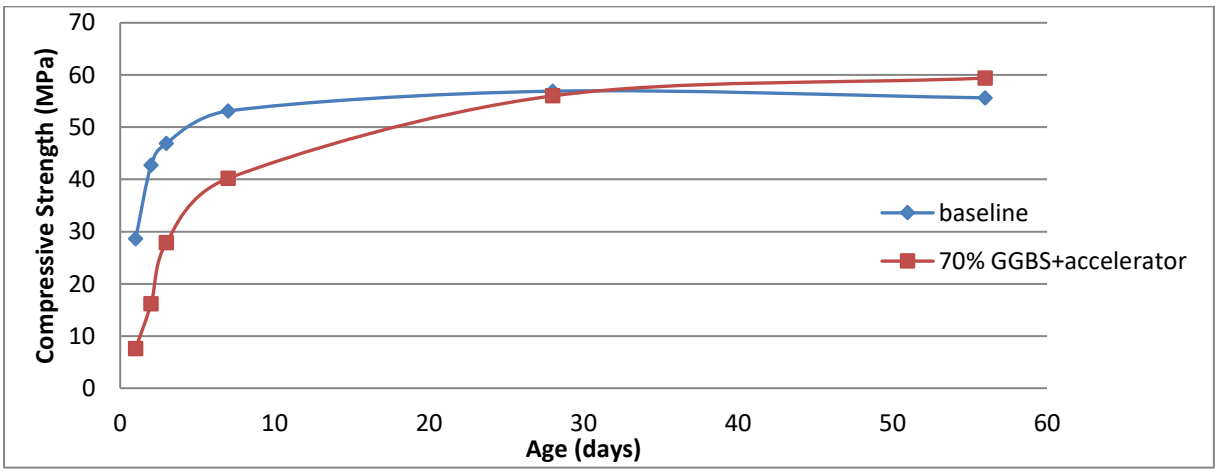

Figure 5.31 Compressive Strength vs Time for Baseline and 70% GGBS + Accelerator mix

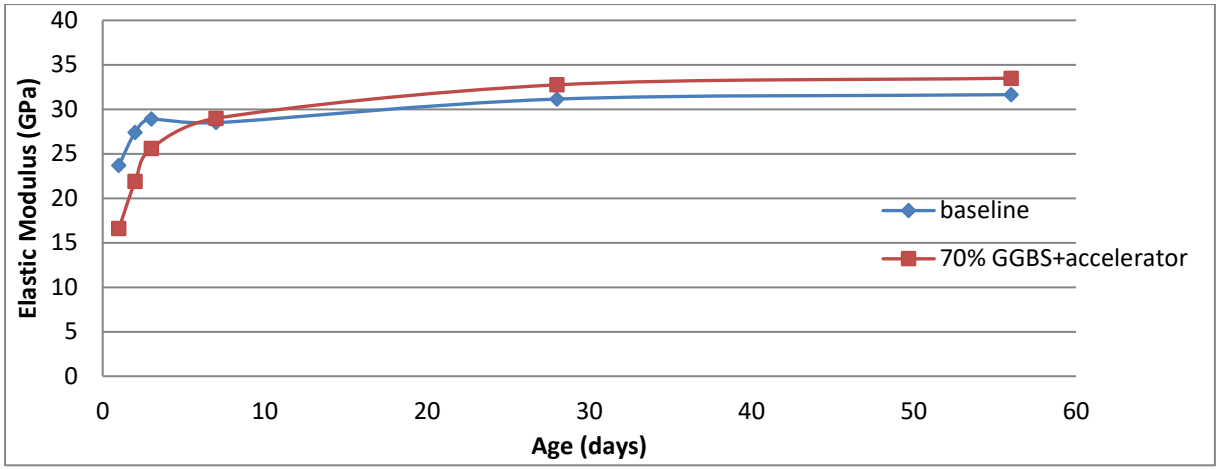

Figure 5.32 Elastic Modulus vs Time for Baseline and 70% GGBS + Accelerator mix

	1-day	2-day	3-day
30%GGBS+Accelerator	+13%	+2%	+1%
50%GGBS+Accelerator	+7%	+6%	0%
70%GGBS+Accelerator	+8%	+6%	+5%

Table 5.10 Percentage improvement of compressive strength by using Accelerator within 3 days

	1-day	2-day	3-day
30%GGBS+Accelerator	+7%	+5%	+2%
50%GGBS+Accelerator	+9%	+7%	-1%
70%GGBS+Accelerator	+12%	0%	+1%

Table 5.11 Percentage improvement of elastic modulus by using Accelerator within 3 days

5.4.4 Effects of Thermal Curing on GGBS concrete

In this section of testing, the thermal curing method was applied on the mixes made from CEM/A-L cement and 30-70% GGBS. It is required to find out the influence of thermal curing on strength and elasticity of concrete mixes with GGBS.

Figure 5.33 to 5.38 demonstrate the comparison between the thermally cured mixes and the baseline mix at different proportions of GGBS content. The most significant feature from these graphs is the high effectiveness of the thermal curing method during early-age, particularly on the first day as observed previously. In Figure 5.33, the 1-day compressive strength of the mix with 30% GGBS is almost same to the baseline mix after 20-hour thermal curing. At 50% and 70% GGBS, the 1-day reductions of the compressive strength compared to the baseline mix are 14% and 28% respectively which are dramatically better than the original 50% and 70% GGBS mixes. This leads to the conclusion that the

addition of 30% GGBS would have no adverse effect if combined with conventional thermal curing.

Previously, the gaps between curves of the specified mix and baseline mix are decreasing over time from early-age to long-term. This implies that GGBS concrete is developing at a higher rate comparing to the pure CEM II/A-L concrete. However, in this case, the development of thermal curing mixes is slower than that of the baseline mix after 1 day. Thus, the gaps between the two curves are becoming larger and reach the maximum around 7 days. Then, they remain at a steady level and slowly decrease from 7-day to 56-day. This phenomenon can be explained by the maturity method. The actual maturing of specimens through an early-age thermal curing is equivalent to the maturity at an older age. Thus, the growth rate during 1-day to 2-day of such specimens is also similar to later stage of concrete development which can be much slower. Consequently, the later strength and stiffness of concrete mixes after thermal curing are moderately lower than the relative results of the baseline mix. The numerical improvement by using a thermal curing method within 3 days is shown in Table 5.12 and 5.13, calculated as follows:

Strength/Stiffness improvement = (Thermal curing mix- CEM II/A-L mix)/Baseline mix × 100% (Eqn 5.5)

There is one exception result shown in Figure 5.35 for 50% GGBS concrete. The compressive strength has an unexpected large growth from 28-day to 56-day. This unusual result is likely caused by testing errors rather than a prove that GGBS content can contribute to a much better long-term compressive strength when used in concrete mix.

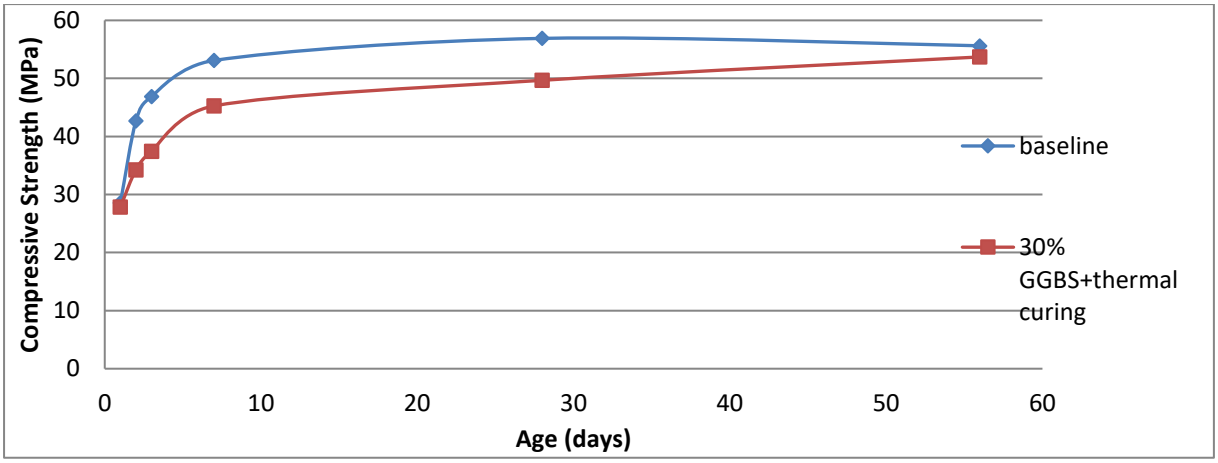

Figure 5.33 Compressive Strength vs Time for Baseline and 30% GGBS + thermal curing

The magnitude of the thermal curing benefit is considerably greater than that of the previous two methods to a large extent. Especially, the 1-day improvements are ranging

from 33% to 54% which are close to the previous expectation of 40% from section 5.3.4. As the GGBS content is increasing from 30% to 70%, the effectiveness of thermal curing is also growing to a higher degree. The thermal curing is even more helpful in bringing up the elastic modulus than the compressive strength. However, it is worth noting that the 1-day compressive strengths are still 14% and 28% lower than that of the baseline mix at 50% and 70 % dosages of GGBS respectively, while the 1-day elastic modulus is almost the same as the result of the baseline mix.

The differences between the baseline mix and GGBS mixes in the early-age elastic modulus are almost neutralised by the effect of the thermal curing treatment across all the proportions of GGBS in Figure 5.34, 5.36 and 5.38. Even though the 1-day compressive strength of 70% GGBS mix is still lower than the original strength by 28%, the concrete can provide similar stiffness as the non-GGBS concrete for structural design at 1 day after the treatment of thermal curing.

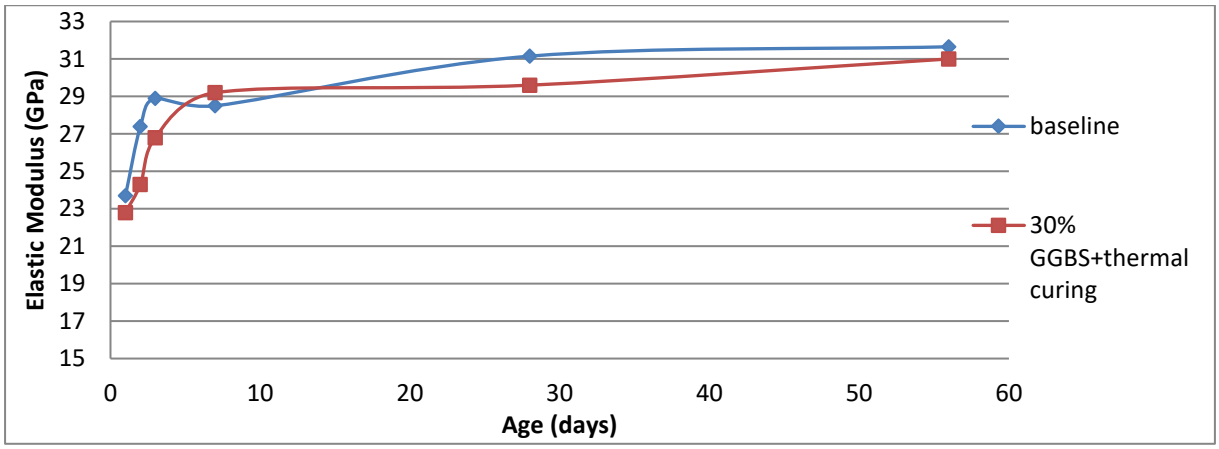

Figure 5.34 Elastic Modulus vs Time for Baseline and 30% GGBS + thermal curing

On the other hand, because the growth rate of thermally cured specimens is slower than that of the baseline mix after 1 day, as discussed before, the improvement by using thermal curing is rapidly reducing from 1 day to 3 days, even though, the 3-day performance of the thermal curing method is still better than the previous two methods. However, so far as lifting precast units is concerned, the 1-day strength is the most relevant property of concrete manufacturing.

Numerical results in Tables 5.12 and 5.13 demonstrate an increasing trend of the effectiveness of thermal curing method from a 30% GGBS mix to a 70% one within 2 days, while the other two methods provide constant or decreasing trends along the increasing dosages of GGBS. This would suggest that GGBS benefits more than CEM II/A-L from thermal curing.

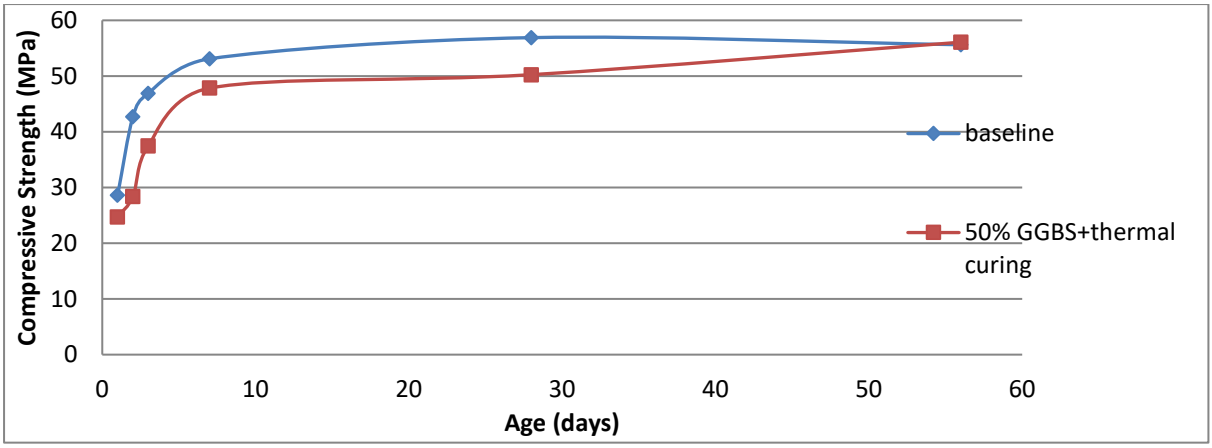

Figure 5.35 Compressive Strength vs Time for Baseline and 50% GGBS + thermal curing

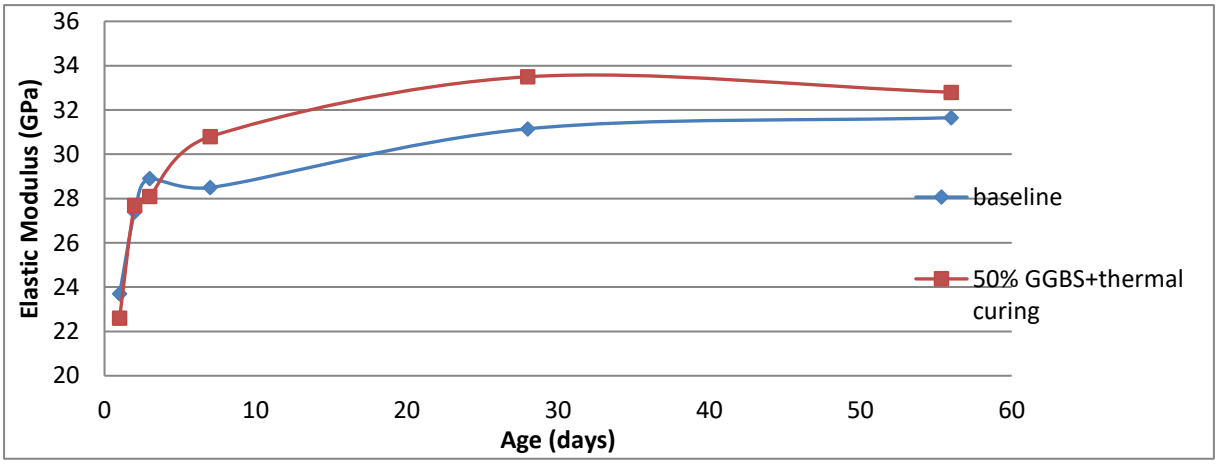

Figure 5.36 Elastic Modulus vs Time for Baseline and 50% GGBS + thermal curing

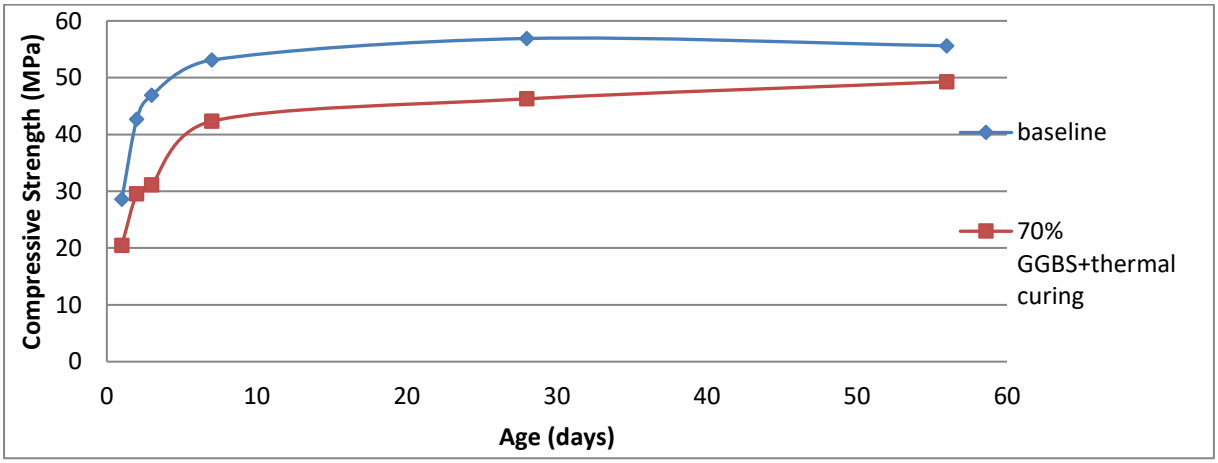

Figure 5.37 Compressive Strength vs Time for Baseline and 70% GGBS + thermal curing

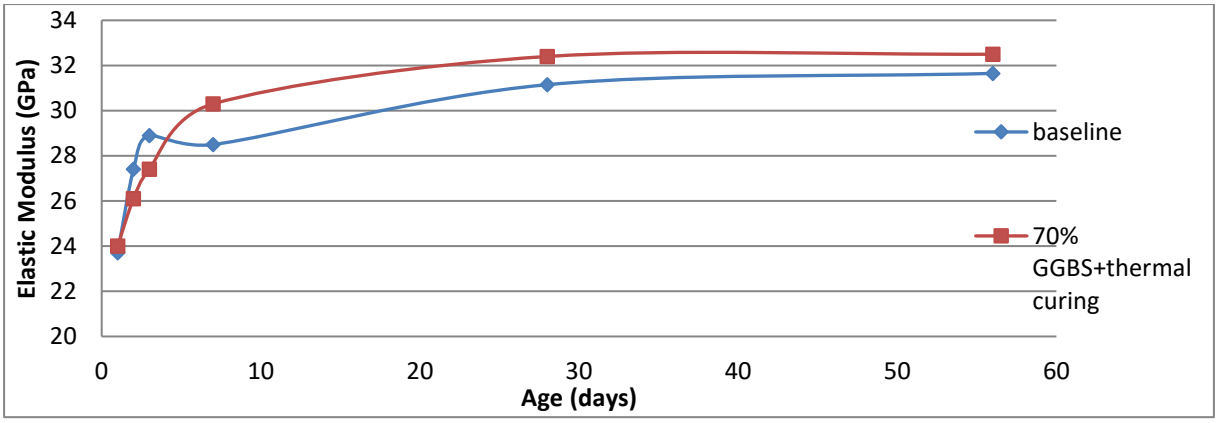

Figure 5.38 Elastic Modulus vs Time for Baseline and 70% GGBS + thermal curing

	1-day	2-day	3-day
30%GGBS+Thermal Curing	+33%	+17%	+8%
50%GGBS+ Thermal Curing	+39%	+14%	+12%
70%GGBS+ Thermal Curing	+54%	+38%	+13%

Table 5.12 Percentage improvement of compressive strength by using Thermal Curing within 3 days

	1-day	2-day	3-day
30%GGBS+Thermal Curing	+8%	+4%	+4%
50%GGBS+ Thermal Curing	+20%	+22%	+6%
70%GGBS+ Thermal Curing	+48%	+20%	+6%

Table 5.13 Percentage improvement of elastic modulus by using Thermal Curing within 3 days

5.5 Effects of GGBS content with Combined Acceleration Methods

In this section, two or three accelerating methods were applied simultaneously to investigate the combined effects on the compressive strength and elastic modulus. The results of the baseline mix are still used as the comparison target to numerically assess the scales of these combined methods at different percentages of GGBS content.

5.5.1 Effects of RHPC and Accelerator on GGBS Concrete

The combination of RHPC and the accelerator was tested and evaluated in this section. From previous analysis of results, neither RHPC nor an accelerator can significantly improve the early-age development of GGBS concrete, while the performance of the

accelerator is slightly better than that of RHPC. Especially at high dosages of GGBS, both of these accelerating methods are incapable of bringing the compressive strength and elastic modulus close to the baseline level.

At 30% dosage of GGBS content, Figures 5.39 and 5.40 demonstrate that the combined methods provide optimal results during early-age. The 1-day compressive strength is about 90% of the baseline value, and the 1-day elastic modulus is almost the same as the baseline value. Thus, at low dosage of GGBS, using RHPC and an accelerator simultaneously is a possible solution to compensate for the retardant effect of GGBS addition. However, as the dosage of GGBS content is increased to 50% and 70%, Figures 5.41 to 5.44 show that the results are not significantly influenced by this combined accelerating method. In Figure 5.43, the 1-day compressive strength at 70% GGBS is, again, decreased to a distinctly lower value due to the reduced proportion of RHPC in the total cementitious material.

Comparing Table 5.14 to Table 5.8 and 5.10, it can be observed that the improvement of 1-day compressive strength through the use of RHPC and an accelerator is 24% which is much greater than the sum of 4% (by RHPC alone) and 13% (by accelerator alone) at 30% dosage of GGBS. As the proportion of RHPC is decreased to 50% and 30%, the effectiveness of this combined method is returned to a similar level of the method of using an accelerator alone. Thus, at high dosages of GGBS content, it is not suggested to be worthwhile to replace the CEM II with RHPC to improve the early-age strength, considering the cost efficiency.

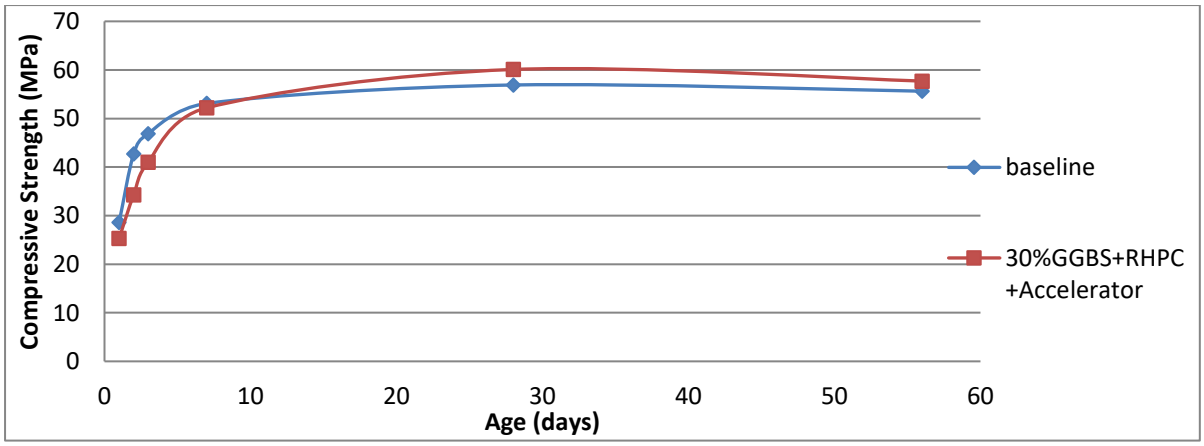

Figure 5.39 Compressive strength vs Time for Baseline and 30% GGBS + RHPC +accelerator

Comparing Table 5.15 to Table 5.9 and 5.11, there is no significant difference between the values from these tables. Whether using the combined method or RHPC/accelerator alone, the improvement of elastic modulus remains in the range between 0% - 10% across

different dosages of GGBS content. There is no evidence that could demonstrate the superior performance of this combined method. The combined effect of using RHPC and an accelerator together does not improve the early-age properties of concrete with high dosages of GGBS content. The method of using an accelerator alone almost provides a similar effect.

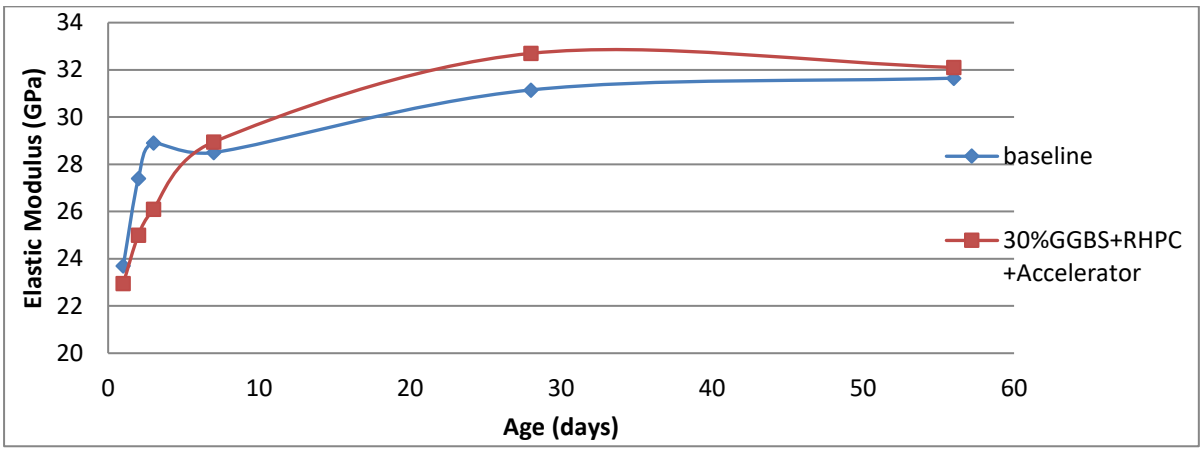

Figure 5.40 Elastic modulus vs Time for Baseline and 30% GGBS + RHPC +accelerator

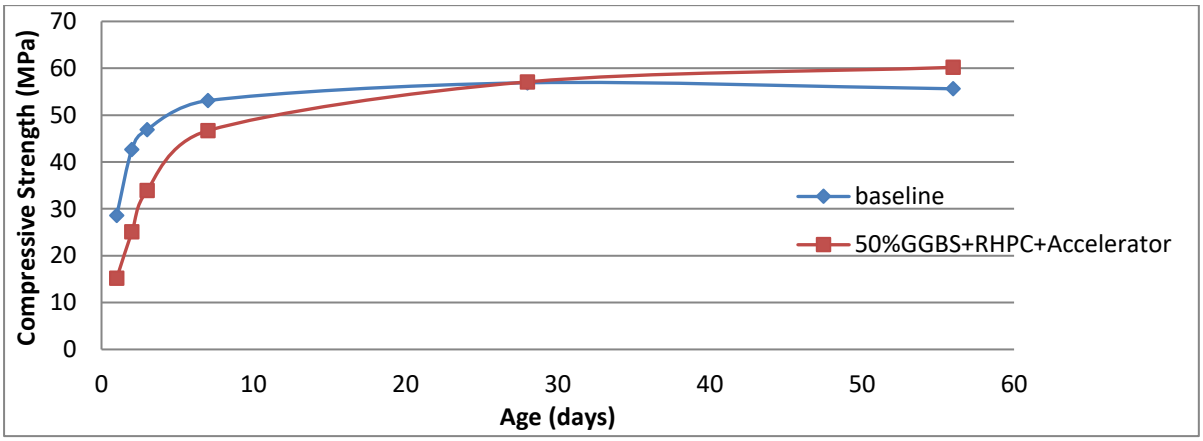

Figure 5.41 Compressive strength vs Time for Baseline and 50% GGBS + RHPC +accelerator

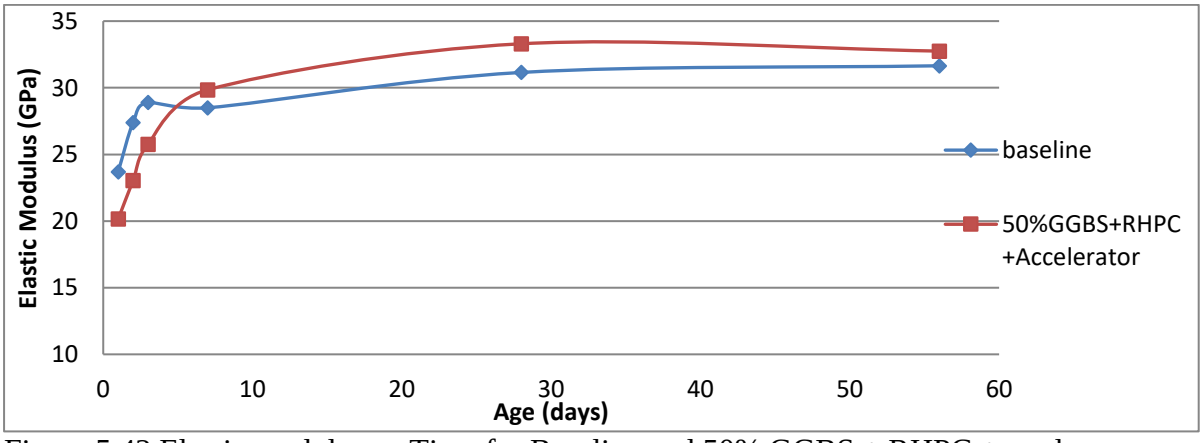

Figure 5.42 Elastic modulus vs Time for Baseline and 50% GGBS + RHPC +accelerator

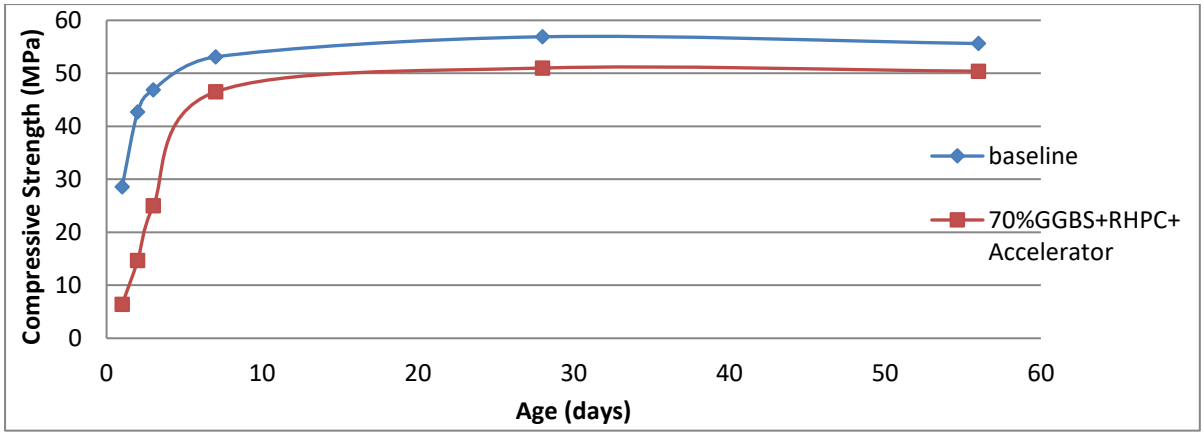

Figure 5.43 Compressive strength vs Time for Baseline and 70% GGBS+RHPC +accelerator

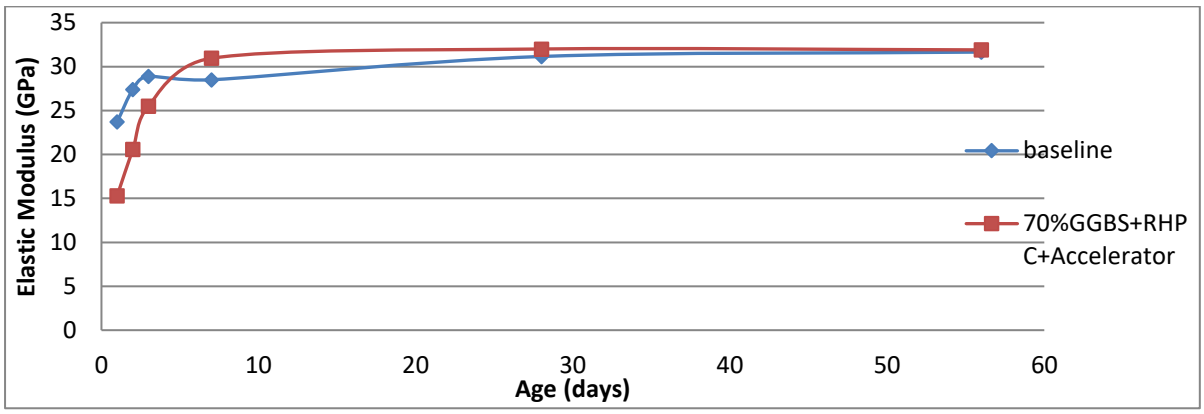

Figure 5.44 Elastic modulus vs Time for Baseline and 70% GGBS + RHPC +accelerator

	1-day	2-day	3-day
30%GGBS+RHPC+Accelerator	+24%	+16%	+14%
50%GGBS+RHPC+Accelerator	+7%	+5%	+4%
70%GGBS+RHPC+Accelerator	+4%	3%	0%

Table 5.14 Percentage improvement of compressive strength by using RHPC + accelerator

	1-day	2-day	3-day
30%GGBS+RHPC+Accelerator	+9%	+6%	0%
50%GGBS+RHPC+Accelerator	+10%	+5%	+1%
70%GGBS+RHPC+Accelerator	+11%	+1%	0%

Table 5.15 Percentage improvement of elastic modulus by using RHPC + accelerator

5.5.2 Effects of RHPC and Thermal Curing on GGBS Concrete

The combined effects of using RHPC and thermal curing was assessed in this section. Based on the previous results, the influence of thermal curing on the early-age

development has a large superiority over the effects of using RHPC. It is anticipated that the results from this section will be dominated by the thermal curing method.

Figures 5.45 and 5.46 show that, at 30% dosage of GGBS content, both the 1-day compressive strength and 1-day elastic modulus are greater than the baseline results. This acceleration effect of combined RHPC and thermal curing method is the most powerful result so far. In Figures 5.47 and 5.49, the 1-day compressive strengths are lower, but close to the baseline results, compared with previous graphs at 50% and 70% dosages of GGBS content. However, the 1-day elastic modulus in Figures 5.48 and 5.50 show similar or even higher values, compared to the baseline curve. Thus, this combined method has more positive impact on the elastic modulus than that on the compressive strength.

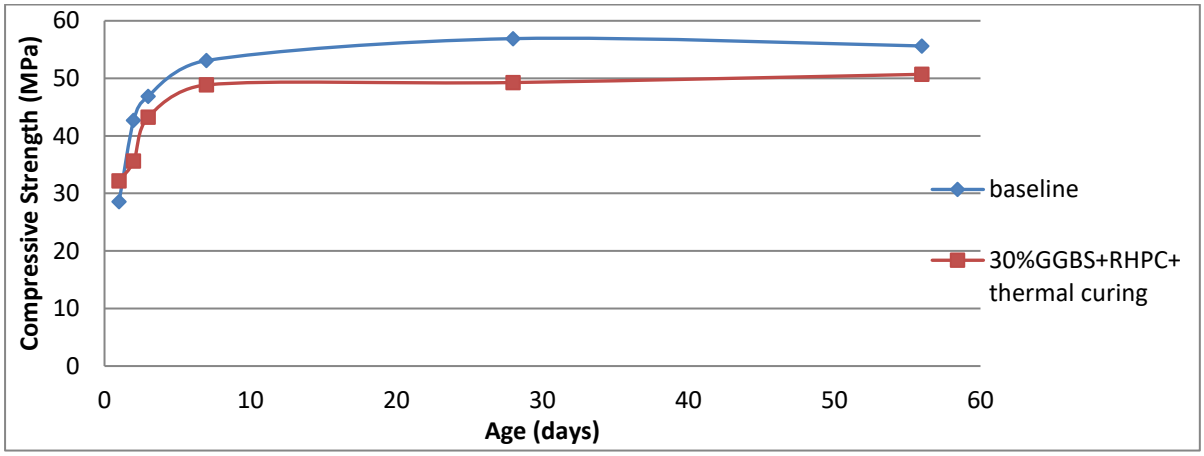

Figure 5.45 Compressive strength vs Time for Baseline and 30% GGBS + RHPC + thermal curing

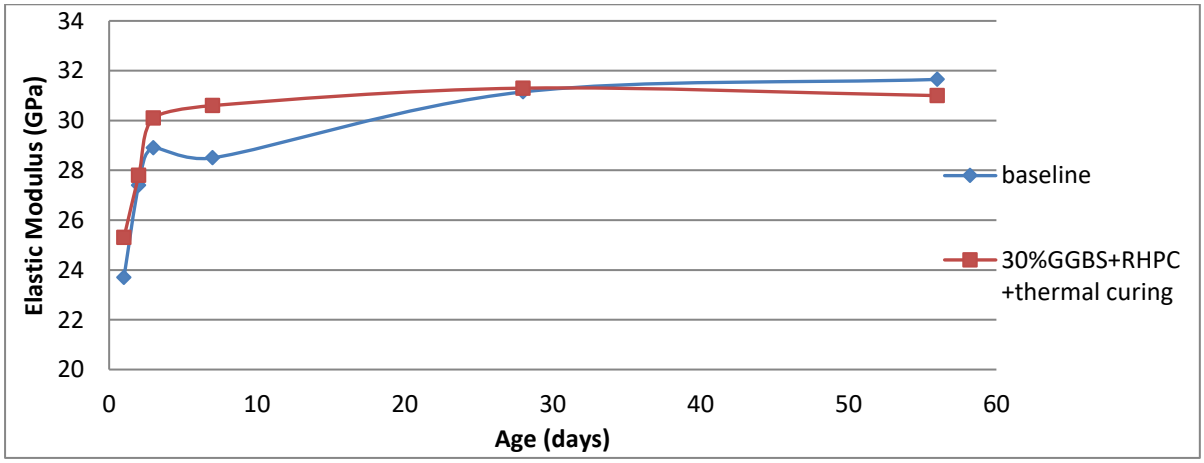

Figure 5.46 Elastic modulus vs Time for Baseline and 30% GGBS + RHPC + thermal curing

It is noticeable that the long-term compressive strength is significantly reduced after the combined effect of RHPC and thermal curing, especially at 70% dosage of GGBS content. On the other hand, the elastic modulus has a minor difference between the baseline mix and thermally cured mixes after 28 days. The first reason for this feature is that the elastic modulus is largely determined by the properties of aggregates. The baseline mix and the thermally cured mix have the same proportion and type of aggregates, but different cementitious materials and maturity history. Thus, a similar elastic modulus but different compressive strength appears in the long-term. Another possible explanation is that the harmful internal cracking and incomplete microstructure caused by thermal curing do not influence the modulus testing significantly because the testing strength is only at one third of the ultimate strength. These defects normally do not occur during the modulus testing. However, these harmful effects of thermal curing significantly reduce the results for a compressive strength test under the ultimate load.

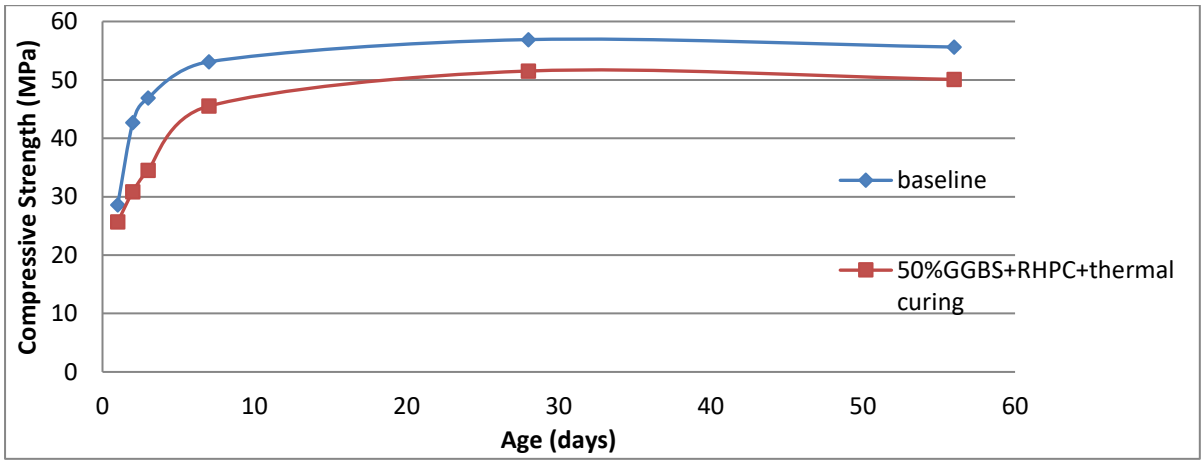

Figure 5.47 Compressive strength vs Time for Baseline and 50% GGBS + RHPC + thermal curing

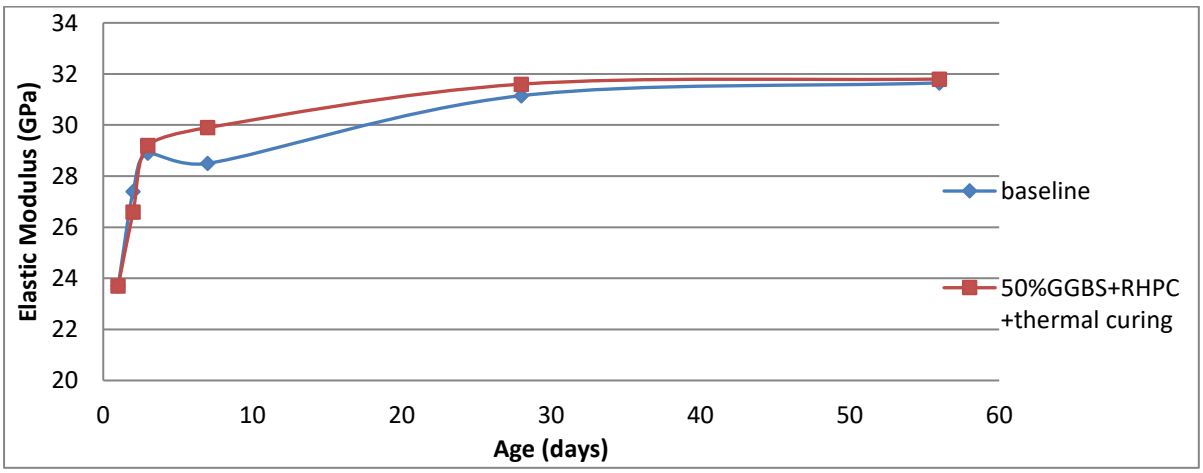

Figure 5.48 Elastic modulus vs Time for Baseline and 50% GGBS + RHPC + thermal curing

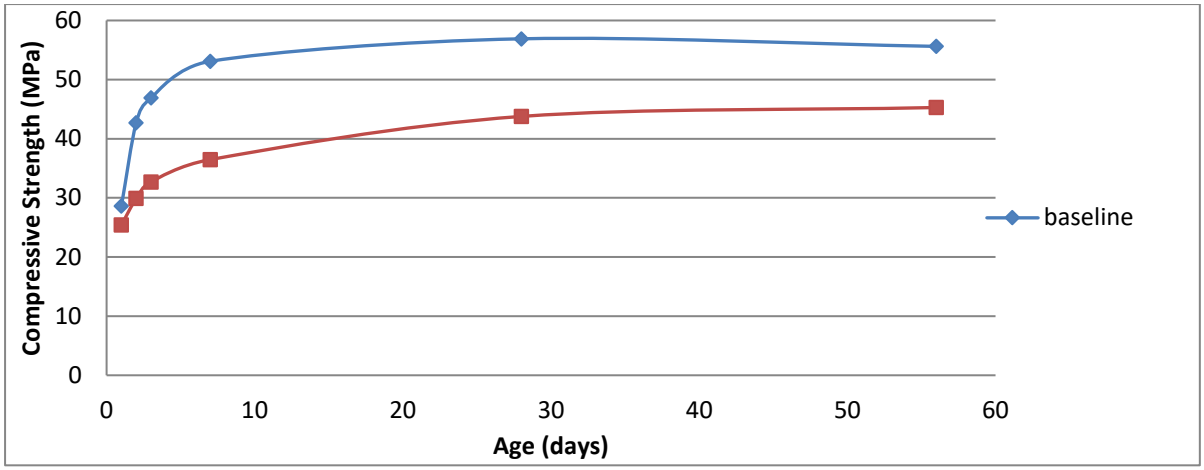

Figure 5.49 Compressive strength vs Time for Baseline and 70% GGBS + RHPC + thermal curing

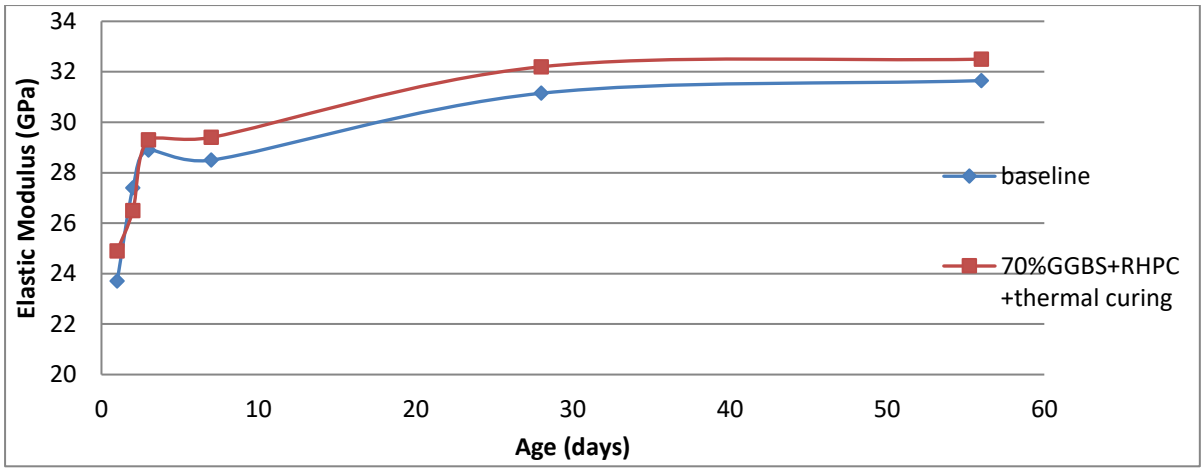

Figure 5.50 Elastic modulus vs Time for Baseline and 70% GGBS + RHPC + thermal curing

Comparing Table 5.16 and 5.17 to Table 5.8 and 5.9, the combined effects of the two methods are significantly larger than the solo effect of RHPC to a large extent. Thus, it is essential to compare the combined effects and the solo effect of thermal curing in Table 5.11 and 5.12. At 30% dosage of GGBS content, the 1-day compressive strength is improved by 48% which is larger than the sum of the two individual effects (4% and 33% respectively). At a higher dosage of 70% GGBS content, the combined method increases the 1-day compressive strength by 70%, while the individual effects are 0% for RHPC and 54% for thermal curing. Under the thermal curing conditions, the effect of RHPC shows a steady performance through 30% to 70% dosages. This property of RHPC is considerably different from previous results. Based on the previous results in Tables 5.9 and 5.13, the improvements on the elastic modulus of the combined method are approximately equal to the sum of the effects of two individual methods for the 1-day results.

	1-day	2-day	3-day
30%GGBS+RHPC+Thermal Curing	+48%	+20%	+20%
50%GGBS+RHPC+Thermal Curing	+43%	+19%	+6%
70%GGBS+RHPC+Thermal Curing	+70%	+39%	+16%

Table 5.16 Percentage improvement of elastic modulus by using RHPC and Thermal Curing

	1-day	2-day	3-day
30%GGBS+RHPC+Thermal Curing	+19%	+16%	+14%
50%GGBS+RHPC+Thermal Curing	+25%	+18%	+10%
70%GGBS+RHPC+Thermal Curing	+52%	+22%	+12%

Table 5.17 Percentage improvement of elastic modulus by using RHPC and Thermal Curing

5.5.3 Effects of Combined Three Methods on GGBS Concrete

In this section, all three accelerating methods were applied simultaneously to one concrete mix which is 70% GGBS+30% RHPC + Accelerator under the thermal curing treatment. The objective is to examine the combined effect of all three methods at high dosage of GGBS content. It is required to assess the effect of the extra addition of an accelerator by comparing section 5.5.2 to 5.5.3.

Comparing Figures 5.49 and 5.51, the extra addition of an accelerator did not visibly improve the 1-day compressive but slightly reduced the result from 25.4MPa to 22.7MPa. On the contrary, the 1-day elastic modulus is slightly increased from 24.9GPa to 25.7GPa which is probably not statistically significant. Tables 5.18 and 5.19 also show similar results compared with Tables 5.16 and 5.17.

Based on the limited results of using the accelerator and thermal curing together, there is no determined evidence to prove a beneficial effect of the accelerator under the thermal curing treatment. The basic functionality of an accelerator is to increase the speed of hydration of cement after the mixing process due to a higher internal temperature. As the concrete is already heated in the 35°C water, this effect of temperature rising is almost negligible during the first day after pouring. Thus, it is advisable to use an extra dose of accelerator if the concrete will be thermally cured after pouring to make the combined

effect more significant, or a specific activator for GGBS should be used to replace the conventional accelerator for concretes with a high percentage of GGBS.

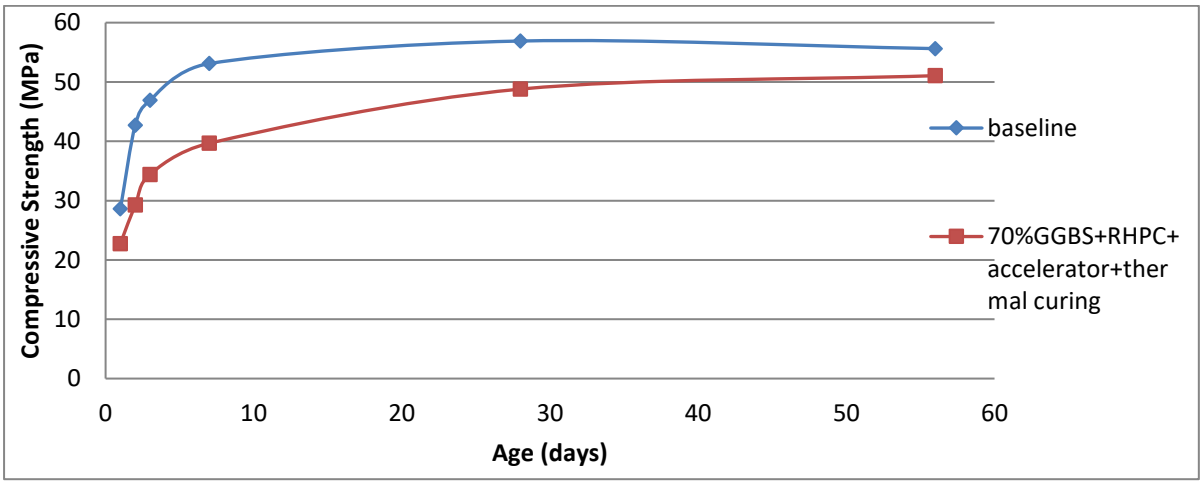

Figure 5.51 Compressive strength vs Time for Baseline and 70% GGBS + RHPC + Accelerator + thermal curing

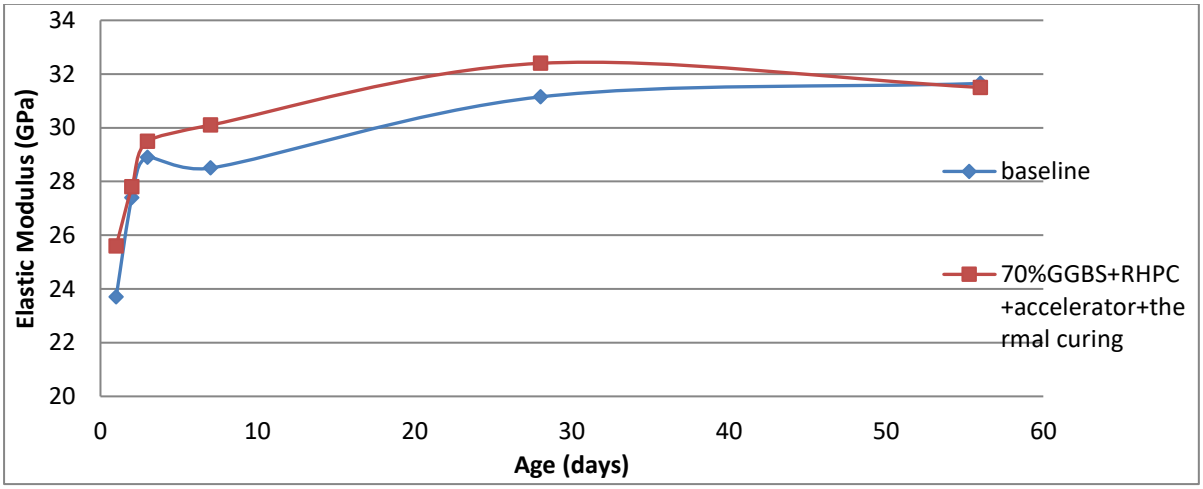

Figure 5.52 Elastic modulus vs Time for Baseline and 70% GGBS + RHPC + Accelerator + thermal curing

	1-day	2-day	3-day
70%GGBS+RHPC+Accelerator +Thermal Curing	+62%	+38%	+19%

Table 5.18 Percentage improvement of compressive strength by using RHPC + Accelerator + Thermal Curing within 3 days

	1-day	2-day	3-day
70%GGBS+RHPC+Accelerator +Thermal Curing	+55%	+26%	+13%

Table 5.19 Percentage improvement of elastic modulus by using RHPC + Accelerator + Thermal Curing within 3 days

5.6 Summary of Early-age Concrete Development

A complete growth trend of concrete development from 1 day to 56 days was assessed for each concrete mix design with a series of different combinations of conventional constituents. As this thesis is concerned with the importance of early-age properties of concrete, it is necessary to develop a full picture of all 1-day results for comparing the effectiveness of different accelerating methods.

5.6.1 Compressive Strength:

Table 5.20 contains all the 1-day results of compressive strength from previous sections. The result of the baseline mixes with pure CEM II/A-L and no GGBS content at 1 day is used for comparison with other values. Figures in brackets indicate the percentage increments/decrements for that particular mix, accepting there is some experimental variability in any one average result.

By viewing the results horizontally, there are dramatic reductions of compressive strength due to the cement replacement of GGBS content from 30% to 70% for each mix combination. The degree of strength reduction scales proportionally to the amount of GGBS dosage. From 0% to 70% GGBS, the compressive strength of baseline mix drops by 80% approximately. This retardant effect of GGBS will normally delay the striking time of precast concrete significantly due to insufficient strength.

The accelerator performs slightly better than the RHPC when GGBS is introduced into the mix at a low dosage of GGBS. However, at a high dosage of GGBS, the reduction ratio of 1-day strength is still relatively large compared with the baseline mix even when the accelerator is used. The biggest contrast occurs at the mix with a combination of RHPC and an accelerator where the 1-day strength drops from 40.2MPa (141%) at 0% GGBS to 6.4MPa (22%) at 70% GGBS. Thus, the effects of both of RHPC and the accelerator are becoming negligible as the dosage of GGBS is increasing. When thermal curing is applied, this decreasing trend is considerably reduced. The 1-day strength of the mix with a combination of RHPC and thermal curing drops from 41.3MPa (145%) at 0% GGBS to 25.4MPa (89%) at 70% GGBS.

Assessing the results vertically gives a full picture of comparison of these accelerating methods. Without the addition of GGBS content, all three methods and the combinations of them have significant beneficial effects on the compressive strength. Although RHPC

and the accelerator have less significant effects compared to the thermal curing at 35°C, their combination shows a similar 1-day result as that of the mix after thermal curing.

The addition of accelerator to the RHPC + Thermal Curing mix does not improve the 1-day strength visibly. The negative effect in this case, 25.4MPa to 22.7MPa, could be caused by the ineffectiveness of the accelerator and random error together.

However, with the addition of GGBS content, thermal curing provides significantly greater influence than the other two methods. At 30% GGBS, the 1-day strengths of mixes after thermal curing are brought back to the same level of the baseline mix. At 70% GGBS, the 1-day strengths of mixes with normal curing are 73% to 82% lower than that of the baseline mix, while the results of mixes thermally cured are 11% to 28% lower. It is notable that at 70% GGBS content no single or combined effect fully restores the baseline (0% GGBS) compressive strength.

1-day Compressive Strength (MPa)	Dosage of GGBS content			
	0%	30%	50%	70%
CEM II	28.6 (±0%) Baseline	20.5 (-28%)	13.4 (-53%)	5.0 (-79%)
Single Acceleration Method:				
RHPC	34.5 (+21%)	19.5 (-32%)	10.4 (-64%)	5.1 (-82%)
CEM II +Accelerator	33.4 (+16%)	22.1 (-23%)	15.7 (-45%)	7.6 (-73%)
CEM II + Thermal Curing	40.9 (+43%)	27.8 (-3%)	24.7 (-14%)	20.5 (-28%)
Multiple Acceleration Method:				
RHPC + Accelerator	40.2 (+41%)	25.3 (-12%)	15.2 (-47%)	6.4 (-78%)
RHPC + Thermal Curing	41.3 (+44%)	32.2 (+12%)	24.7 (-14%)	25.4 (-11%)
RHPC + Accelerator + Thermal Curing	40.1 (+40%)	n/a	n/a	22.7 (-21%)

Table 5.20 Summary of 1-day compressive strengths

To ensure safe lifting and handling of precast members, a minimum strength of 15MPa is required to avoid concrete failure during the moving. Based on the results in Table 5.20, a 1-day demoulding can be achieved for 30% GGBS concrete when RHPC and accelerator are used. However, these two techniques are not enough to grow enough strength when

50%GGBS or more is used in the concrete mix. Only the thermal curing method can be used to ensure the precasters a 1-day turnover period for safe production.

5.6.2 Elastic Modulus:

The equivalent results for elastic modulii in Table 5.21 show some similarities and some differences compared with the compressive strength.

For mixes with normal curing, neither the RHPC nor the accelerator individually deliver a strong improvement on the 1-day elastic modulus. The results are decreasing largely as the dosage of GGBS is increasing, where the percentages of reductions shown in the brackets are relatively smaller than those of the compressive strengths shown in Table 5.20. The nature of these concrete properties is anticipated by using the empirical formula (Equation 2.5) discussed previously.

1-day Elastic Modulus (GPa)	Dosage of GGBS content			
	0%	30%	50%	70%
Baseline				
CEM II	23.7 (±0%)	21.0 (-11%)	17.9 (-24%)	13.5 (-43%)
Single Acceleration Method:				
RHPC	24.5 (+3%)	21.6 (-9%)	18.8 (-21%)	14.8 (-38%)
CEM II +Accelerator	23.8 (+1%)	22.6 (-5%)	20.0 (-16%)	16.6 (-30%)
CEM II + Thermal Curing	27.5 (+16%)	22.8 (-4%)	22.4 (-5%)	24.0 (+1%)
Multiple Acceleration Method:				
RHPC + Accelerator	26.4 (+11%)	23.0 (-3%)	20.2 (-15%)	15.3 (-35%)
RHPC + Thermal Curing	27.8 (+17%)	25.3 (+7%)	23.7 (0%)	24.9 (+5%)
RHPC + Accelerator + Thermal Curing	28.4 (+20%)	-	-	25.6 (+8%)

Table 5.21 Summary of 1-day elastic modulii

For mixes with thermal curing, the 1-day elastic modulus is significantly increased when there is no GGBS content. As GGBS content is introduced into the mixes, the thermal

curing method can enhance the elastic modulus to a similar level as the baseline mix at different proportions of GGBS dosages. From 30% to 70% GGBS, thermally cured mixes remain around the baseline results of 23.7GPa which is within experimental error, while the compressive strength is reduced from 40.9MPa at 0% GGBS to 20.5MPa at 70% GGBS. However, this feature of the elastic modulus contradicts the previous empirical relationship between the compressive strength and elastic modulus, though it is indeed expected to be a lesser effect with GGBS dosages.

Unlike the previous case some multiple acceleration methods do appear to improve the elastic modulus above the baseline when 70% GGBS is used. However, in other cases, singular acceleration methods are not enough to overcome the retardation effect of high GGBS dosages on the elastic modulus at 1 day and this information may prove especially usefully for precast manufacturers.

CHAPTER 6. NUMERICAL ANALYSIS AND PREDICTION

6.1 Introduction

The development of the mechanical properties of hardened concrete at a particular age mainly depends on various factors, such as the type of cementitious materials, mix proportions, water/cement ratio, additions of admixtures and temperature history. In this research, the influences of types of cementitious materials, addition of an accelerator and temperature effects are the main focus being investigated, while other parameters were fixed throughout the whole testing process. After the discussion of experimental results in Chapter 5, numerical methods of strength and elastic modulus predictions will be established and examined in this chapter.

6.2 Theoretical Prediction of Strength Development

In Chapter 5, the actual test data were analyzed to demonstrate how the strength development of concrete varies under certain conditions. It is necessary to theoretically calculate the magnitudes of these influencing factors to utilise the empirical formulae proposed by EC2. Furthermore, modified formulae with new coefficients will be proposed for more accurate prediction based on the experimental results.

6.2.1 Determination of Coefficients

According to EC2 and Model Code 2010, the compressive strength of concrete at various ages can be predicted by the 28-day mean strength for several different types of cement. For a mean temperature of 20°C curing in accordance with EN-12390, the mean compressive strength is calculated from the following equations (see equations 2.1 and 2.2 in Chapter 2):

$$f_{cm}(t) = \beta(t)\, f_{cm} \qquad \text{(Eqn 6.1)}$$

$$\text{where } \beta(t) = \exp\left(s\left(1-\left(\frac{28}{t}\right)^{n}\right)\right) \qquad \text{(Eqn 6.2)}$$

$f_{cm}(t)$ is the mean concrete compressive strength at an age of t days

f_{cm} is the mean compressive strength at 28 days

$\beta(t)$ is a coefficient which depends on the age of the concrete

t is the age of the concrete in days

s is a coefficient which depends on the type of cement.

n is assumed to be 0.5 in EC2.

The coefficient s is key factor that determines the growth trend of compressive strength. Both EC 2 and Model Code 2010 propose a suggested list of the values for s for different classes of cement and hardening characteristics, as shown in Table 6.1. The suggested values of s are decreasing when the cement class is changing from 32.5N to 52.5R, which implies the rate of strength growth is higher at a lower value of coefficient s. The suggested value of coefficient s for CEM II/A-L 42.5N is 0.25. To examine the appropriateness of this suggested value of coefficient s, it is necessary to compare the predicted compressive strength and the actual results of the baseline mix.

Strength Class of cement	32.5 N	32.5 R 42.5 N	42.5 R 52.5 N 52.5 R
Values of coefficient 's'	0.38	0.25	0.20

Table 6.1 Values of coefficient s to be used in Equation 6.1 and 6.2 (I.S. EN-1992-1-1, 2005)

In Figure 6.1, the continuous curve is calculated using Equation 2.1 and 2.2 where s = 0.25 and 28-day mean strength $f_{cm}(28)$ = 56.9MPa from the test result of the baseline mix (no GGBS, RHPC, accelerator or thermal curing) discussed in Chapter 5. Thus, the predicted curve must pass through the 28-day testing value on the graph due to the mathematical nature of Equation 6.2. It is obvious that the actual compressive strength develops at a faster rate than the prediction during the first 7 days. Even the lower boundary of testing results is generally higher than the prediction curve for all the testing ages before 28 days.

In this case, the accuracy of such predictions is quite inadequate because of the large gaps between testing values and estimated ones. The R=0.851 is the result of low accuracy of theoretical prediction. To reduce the degree of errors in Figure 6.1, a new value of s is required to be determined for more precise predictions. A series of prediction curves can be drawn on the same chart to demonstrate how the s values affect the behaviour of Equation 6.2. In Figure 6.2, a series of values of coefficient s are selected to draw different prediction curves on the same graph. Between the period of 1-day to 7-day, a decreasing value of coefficient s causes the prediction curves to rise significantly and vice versa. Due to the inherent mathematical nature of Equation 6.2, all the curves must converge at 28 days. By visual observation, the actual testing points are generally

distributed around two curves which are derived from equations that have s values of 0.10 and 0.15 respectively.

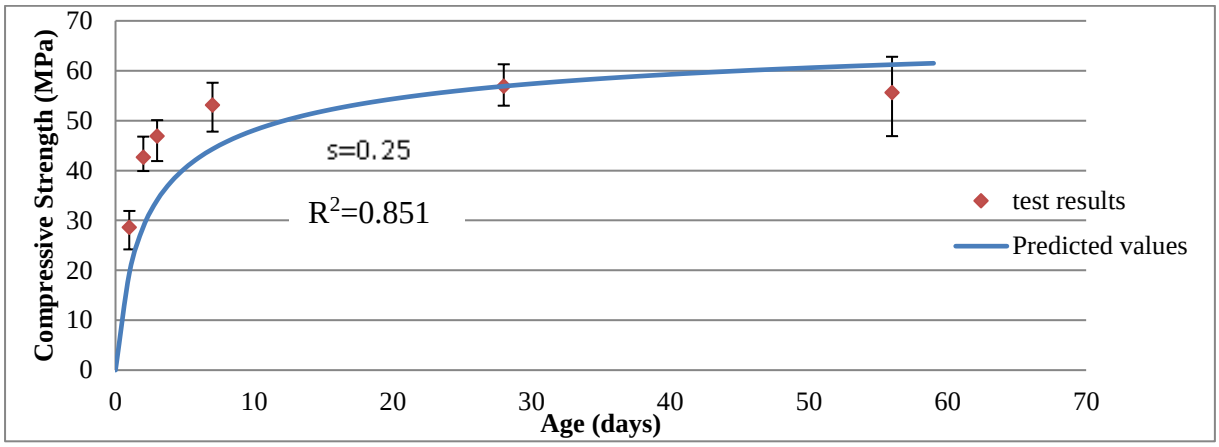

Figure 6.1 Comparison of predicted and actual compressive strength vs ages for baseline mix

To find the best regression curve, a numerical calculation of the least squares method is used to determine the exact value of s that minimise the errors between the prediction curve and actual testing results (Colin and Windmeijer 1997). The result of calculation indicates that the best fitted curve occurs when s is reduced to 0.13 which is significantly lower than the suggested value of 0.25 by EC2 and Model Code 2010. The coefficient of determination, R squared, is required to be acquired as a key factor that determines the accuracy of a prediction curve at any particular value of s. When s is equal to 0.13, the value of R squared is calculated to be 0.899 and demonstrates that this curve does not closely fit the testing results even if it is better than the original value of 0.25. The reason for this problem is because the shape of the prediction curve is predetermined by the index of (28/t) from Equation 6.2 and more importantly the experimental data is imperfect.

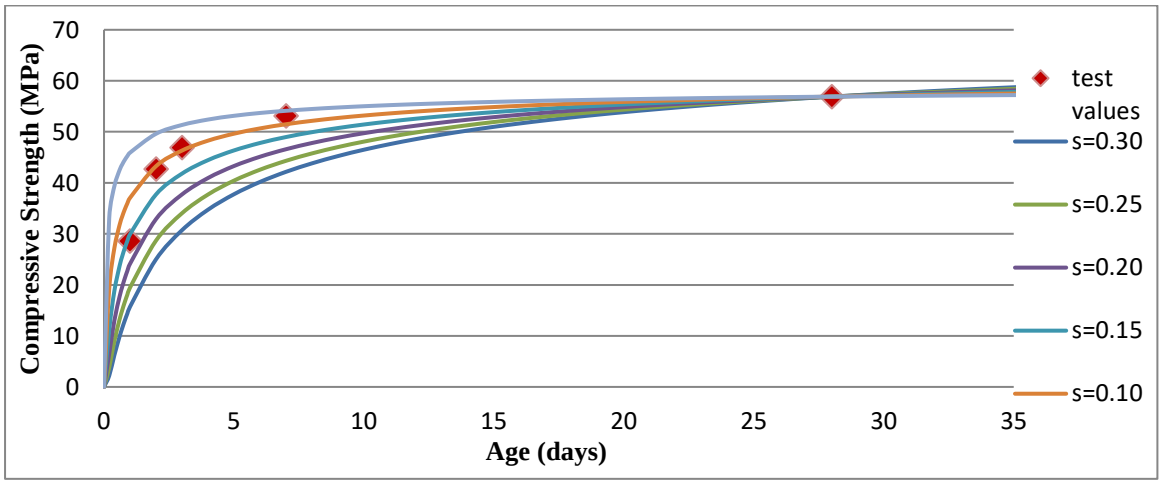

Figure 6.2 Prediction curves with different values of coefficient s and actual compressive strength vs ages

6.2.2 Influence of GGBS

When GGBS is introduced into the concrete mix, the early-age development of compressive strength is significantly slower than that of the baseline mix based on the discussion from Chapter 5. Although there is no suggested value of s from EC2 or Model Code 2010 in this case, it is anticipated that the value of s should be higher for the blended CEM II/A-L and GGBS.

Following the same method of finding best regression curves from the last section, Figure 6.3 demonstrates the best prediction curve of the mix with 30% GGBS where the value of s is selected to be 0.26. The plot of actual compressive strength is near the prediction curve in Figure 6.3 with a high R squared value of 0.996. Thus, the empirical equations 6.1 and 6.2 are viable as a means to predict the growth trend of a concrete mix made from blended cementitious materials with an appropriate value of coefficient s. This value of s is close to the suggested value 0.25 but significantly greater than the previous result of 0.13 for the pure CEM II/A-L mix.

The overall 56-days results do not demonstrate that there is a systematic growth of concrete development after 28 days. Comparing to the 28-days results, there are irregular increments or decrements of the compressive strength at 56 days for different concrete mixes. Therefore, it is necessary to eliminate this irrelevant influence involved in the calculation process of finding best fitting curves. Further analysis will focus on the concrete ages between 1 day to 28 days instead of 1 day to 56 days.

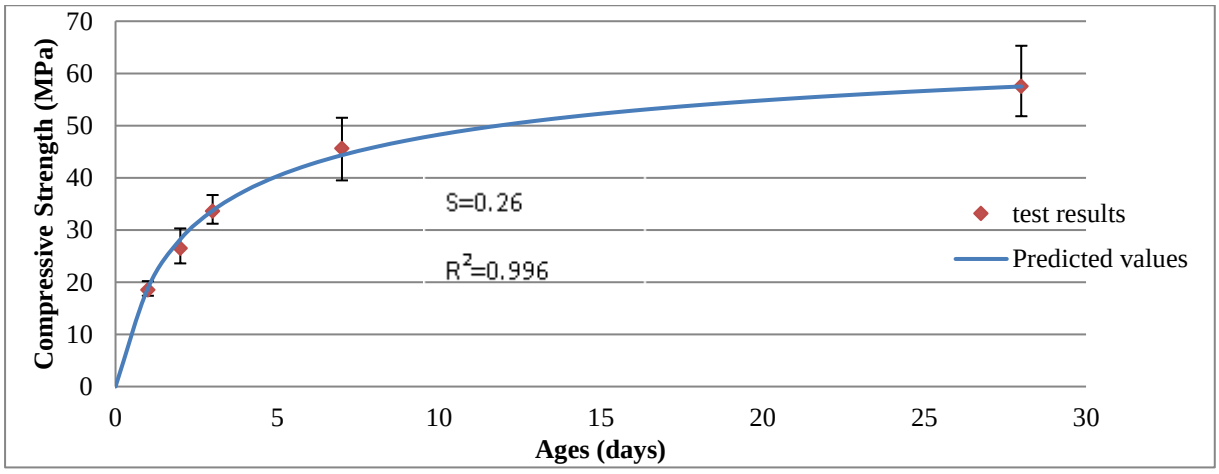

Figure 6.3 Prediction curve and testing points for 70% CEMII/A-L + 30% GGBS

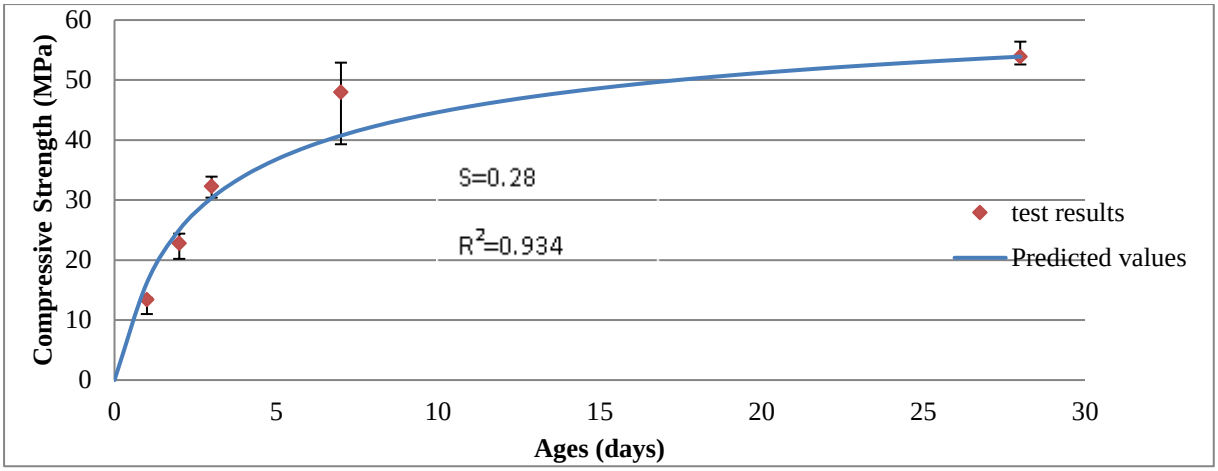

Figure 6.4 Prediction curve and testing points for 50% CEMII/A-L + 50% GGBS

As the proportion of GGBS is increasing to 50% and 70%, the values of coefficient s also increased to 0.28 and 0.35 in Figures 6.4 and 6.5 respectively. With a few unexpected data points in these figures, the prediction curves do not fit the testing results properly as well, with low values of R^2 at 0.934 and 0.930 respectively compared to 0.996 in Figure 6.3.

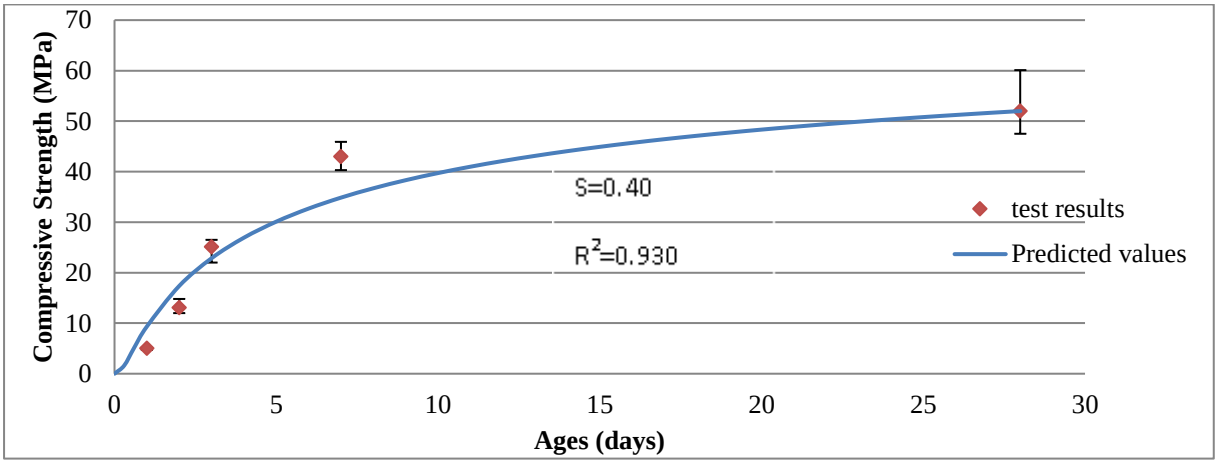

Figure 6.5 Prediction curve and testing points for 30% CEMII/A-L + 70% GGBS

As the coefficient n is fixed at 0.5, it is not possible to draw prediction curves that are better than those in Figures 6.4 and 6.5 by modifying coefficient s alone. However, a better regression curve could be achieved when a different value of coefficient n is selected. Different values of coefficient n are mathematical assumptions to find the best fitting curves. Table 6.2 shows an increasing trend of s values from Figures 6.1 to 6.4 which reflects the effect of GGBS content on the early-age strength development, within experimental variability. These values of s are selected to achieve the best fitted curves based on Equation 6.1 and 6.2. The increase of coefficient s from 0.13 to 0.40 is caused by a lower growth rate when GGBS is used. This trend of coefficient s to the changes in

data is also demonstrated in Table 6.1. However, as the index n is fixed at 0.5, as proposed by EC2 and Model Code 2010, the low values of R^2 for mixes with at 0%, 50% and 70% GGBS indicate that another value of n might be required to achieve a better prediction of the strength development behaviour of 42.5N cement produced in Ireland.

		s	n	R^2
CEM II	0%GGBS	0.13	0.5	0.907
	30%GGBS	0.26	0.5	0.998
	50%GGBS	0.28	0.5	0.939
	70%GGBS	0.40	0.5	0.930

Table 6.2 Summary of coefficient s and R^2 when n is fixed at 0.5

To achieve a better approximation based on Equation 6.1 and 6.2, it is necessary to adjust the variables of s and n simultaneously to find the maximum values of R^2. As the index n is changed, the shape of the prediction curve can be modified to fit the imprecise testing values with a better approximation.

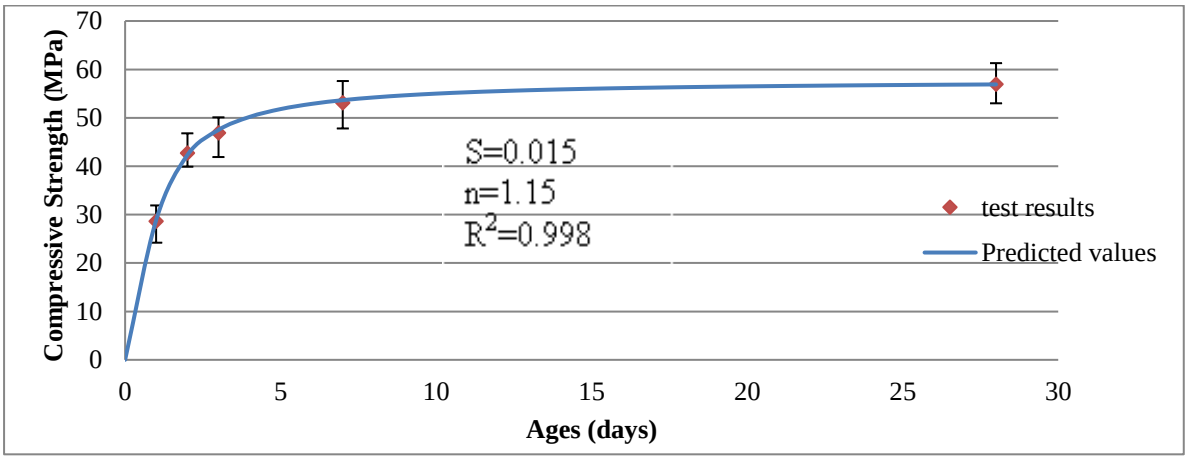

Figure 6.6 Prediction curve and testing points for 100% CEM II/A-L

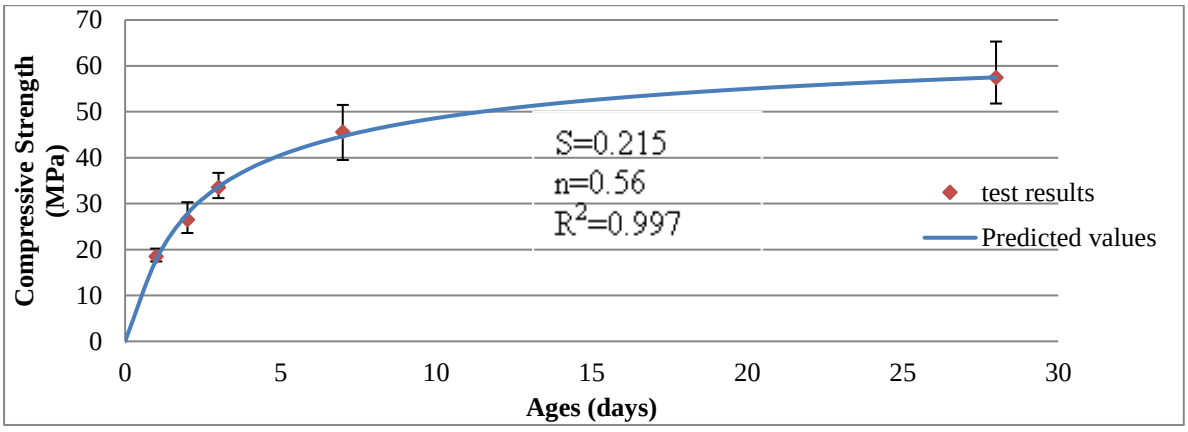

Figure 6.7 Prediction curve and testing points for 70% CEM II + 30% GGBS

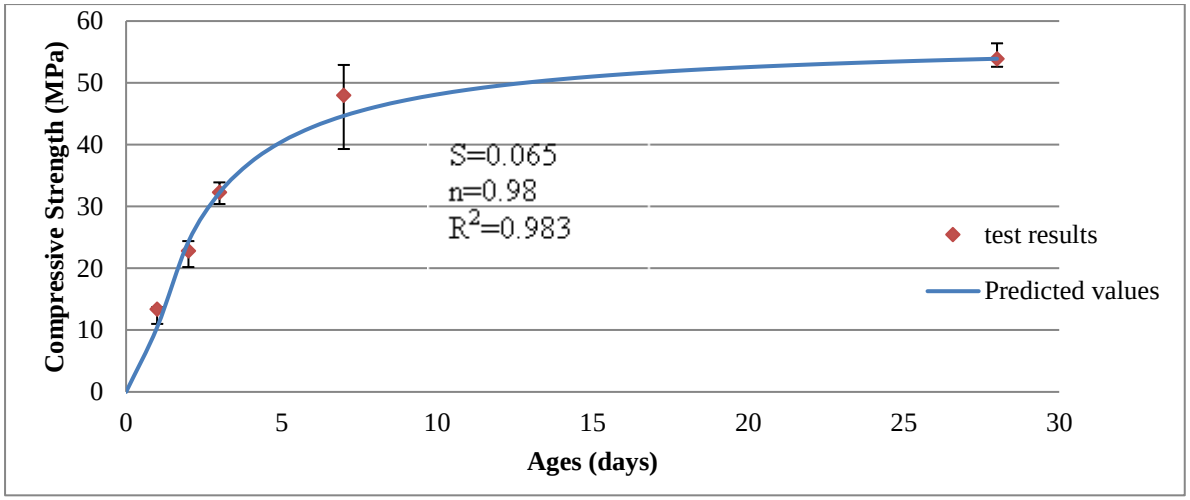

Figure 6.8 Prediction curve and testing points for 50% CEM II + 50% GGBS

Figure 6.6 to 6.8 demonstrate the results of the best combinations of s and n after a series of calculations to achieve the maximum values of R^2. These curves are generated by forcing them to approximate the actual testing data as much as possible. Comparing with previous Figures 6.2 to 6.5, these prediction curves fit the testing values at a significantly higher degree.

In Figure 6.6 and 6.7, each prediction curve almost goes through every testing plot with an R^2 value higher than 0.99. In Figure 6.8, an unexpected plot detracts from the prediction curve slightly whereas the resulting value of R^2 = 0.983 is still significantly greater than the previous result of 0.934 in Figure 6.4.

Although the method of achieving maximum R^2 by modifying both coefficients s and n gives significantly better approximation to testing values, a varying coefficient of n results in an irregular distribution of coefficient s from a pure CEM II/A-L mix to a mix with 70% GGBS as summarised in Table 6.3. In this case, the values of coefficient s or n cannot be consistently used as parameters to reflect the effect of GGBS content in a regular pattern. In part this is because a best fit is being forced upon imperfect experimental data with inevitable errors.

In Figure 6.9, legend 0%-P represents the prediction curve of the mix without GGBS, and legend 30%-T represents the testing plots of the mix with 30% GGBS. Figure 6.9 demonstrates the irregular shapes of prediction curves due to varying values of coefficients s and n. Thus, without a standardised value of coefficient n, it is not possible to determine a series of successive values of coefficient s to demonstrate the effects of GGBS content or, subsequently, any accelerating method. Therefore, a new normalised

value of n, different from the original one of 0.5 given by EC2, is required to be investigated for more accurate predictions.

		s	n	R squared
CEM II	0%GGBS	0.015	1.15	0.997
	30%GGBS	0.215	0.56	0.999
	50%GGBS	0.065	0.98	0.983
	70%GGBS	0.055	1.2	0.993

Table 6.3 Summary of coefficient s and R^2 when n varies

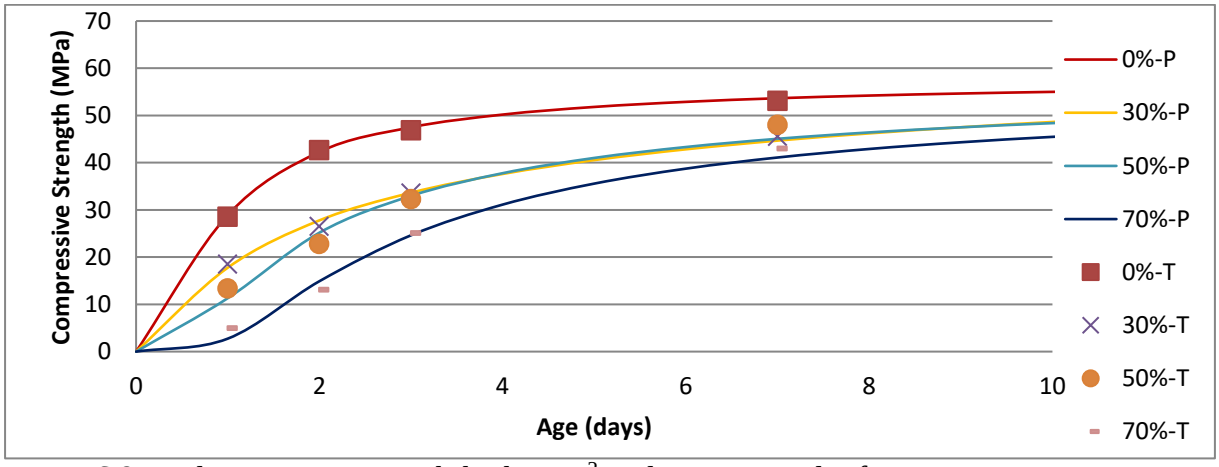

Figure 6.9 Predictions curves with highest R^2 and testing results for various proportions of GGBS content

In this case, a new trial coefficient n equal to 1 is selected based on the results in Table 6.3 where the best fitting curve occurs around n=1 except for the 30% GGBS mix. With this new index, Equation 6.2 is rewritten as:

$$\beta(t) = \exp(s(1-(\frac{28}{t}))) \qquad \text{(Eqn 6.3)}$$

Thus, a series of s values can be calculated by the least squared method again and is shown in Table 6.4.

Comparing to Table 6.2, the new values of s are significant smaller than the previous results while the resulting values R^2 are generally above 0.98 and significantly higher than previous ones in Table 6.2, except the 30% GGBS mix. The similarity between the two series of results of coefficient s is an increasing trend as the proportion of GGBS content rises. Therefore, both of Equations 6.2 and 6.3 can be used to generate a series of values of coefficient s that reflects the effects of different percentages of GGBS content.

		s	n	R squared
CEM II	0%GGBS	0.025	1	0.993
	30%GGBS	0.055	1	0.947
	50%GGBS	0.060	1	0.982
	70%GGBS	0.090	1	0.987

Table 6.4 Values of coefficient s when n is fixed at 1.0

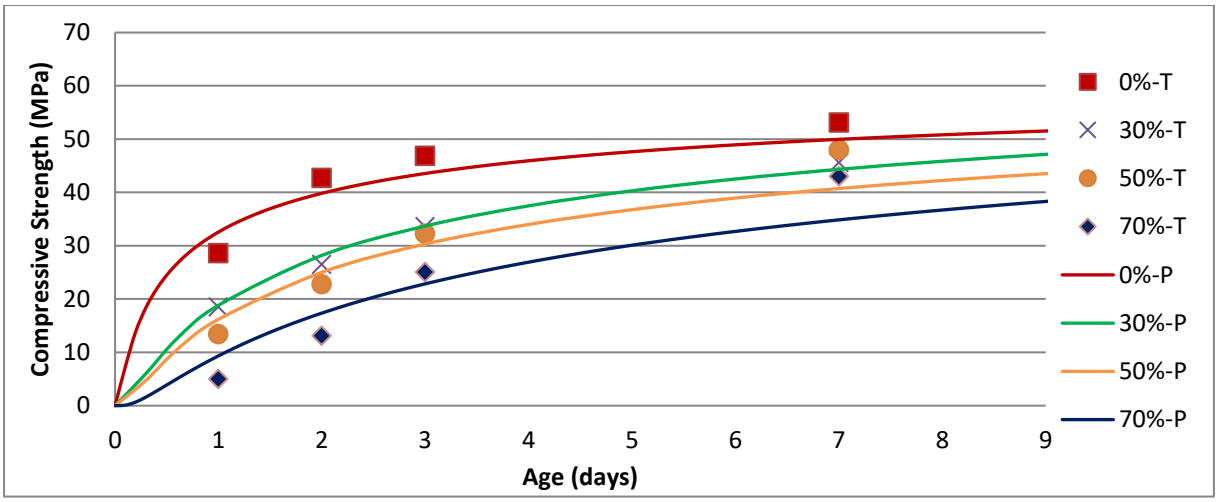

Figure 6.10 Comparison of prediction curves and testing results when n = 0.5

The increasing trends of s values from 0.15 to 0.44 in Table 6.2 and 0.025 to 0.090 in Table 6.4 demonstrate the effects of GGBS content on the strength development which significantly reduces the growth rates of compressive strength during early ages. If a linear relationship between the s values and the percentage of GGBS is assumed, the effects of GGBS content can be numerically evaluated. In section 6.2.5, this linear relationship will be discussed in detail when all the results of coefficient s are obtained by calculation.

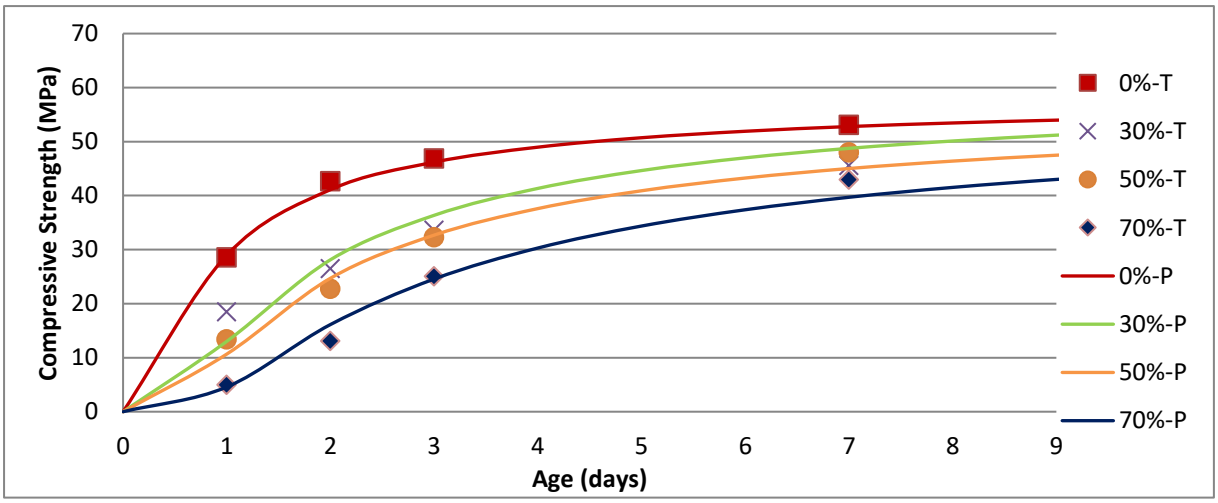

Figure 6.11 Comparison of prediction curves and testing results when n = 1.0

6.2.3 Influences of Accelerating Methods

Three accelerating methods will be examined in this section to demonstrate how they affect the strength development in terms of the variations of s values. Similar to the previous section, the coefficient n is set at 0.5 and 1.0 respectively to investigate the preferred value for predicting the strength development. It is expected to acquire reduced values of coefficient s as various accelerating methods are introduced into the concrete mixes, based on the mathematical property of Equation 6.2. Although the selected values of coefficient n may not generate the optimal prediction of strength development, fixing n does appear to give more predictable s values. Considering the inherent variability of test data, a very precise mathematical formulation for every individual curve is not likely to produce strong trends in coefficients s and n.

6.2.3.1 Influence of RHPC

As suggested by EC2, the value of s is reduced from 0.25 to 0.2 by changing a 42.5N cement to a 42.5R cement. Thus, it is expected that a lower value of coefficient s will be derived as RHPC is introduced into the concrete mix - that is, faster strength development is apparent. Numerical differences will be investigated for mixes of various proportions of GGBS during this part of the discussion.

Comparing Tables 6.2, 6.4 and Tables 6.5, 6.6, the values of coefficient s are indeed smaller when using RHPC instead of CEM II/A-L if the GGBS content is less than 30%. For instance, the values of coefficient s for mixes without GGBS content are reduced by 35% when n=0.5, and 36% when n=1.0, comparing to the corresponding figures in Tables 6.2 and 6.4. For mixes with 30% GGBS content, the values of coefficient s are reduced by 32% when n=0.5, and 31% when n=1.0. At high percentages of GGBS content, the proportions and accelerating effects of RHPC are consequently decreasing. Thus, replacing CEM II/A-L with RHPC shows insignificant influence on s values when GGBS content is over 50% in the total weight of cementitious materials. Results shown in Tables 6.5 and 6.6 illustrate that the effectiveness of using RHPC can only be achieved for mixes with low dosage of GGBS because high proportions of GGBS content dominate strongly the early-age development of concrete strength. When the coefficient n is changed from 0.5 to 1.0, the degree of the effect of RHPC on the coefficient s remains at a similar level (31%-36% reduction for ≤30%GGBS, minor differences for ≥50%GGBS). Thus, the increasing trends of s values with increasing proportions of GGBS in both cases are also similar.

The prediction curves in Figure 6.13 are generally closer to the test results than those in Figure 6.12 for each concrete mix with various proportions of GGBS content. Thus, for the RHPC mixes, a better prediction of strength growth can be generated when n = 1.0 compared with the case of n = 0.5. In the previous discussion of the baseline mix, n = 1.0 is also a better choice for more precise prediction.

		s	n	R squared
RHPC	0%GGBS	0.085	0.5	0.907
	30%GGBS	0.185	0.5	0.938
	50%GGBS	0.293	0.5	0.932
	70%GGBS	0.430	0.5	0.974

Table 6.5 Values of coefficient s when n = 0.5 for RHPC mixes

		s	n	R squared
RHPC	0%GGBS	0.016	1.0	0.984
	30%GGBS	0.038	1.0	0.998
	50%GGBS	0.063	1.0	0.982
	70%GGBS	0.100	1.0	0.996

Table 6.6 Values of coefficient s when n = 1.0 for RHPC mixes

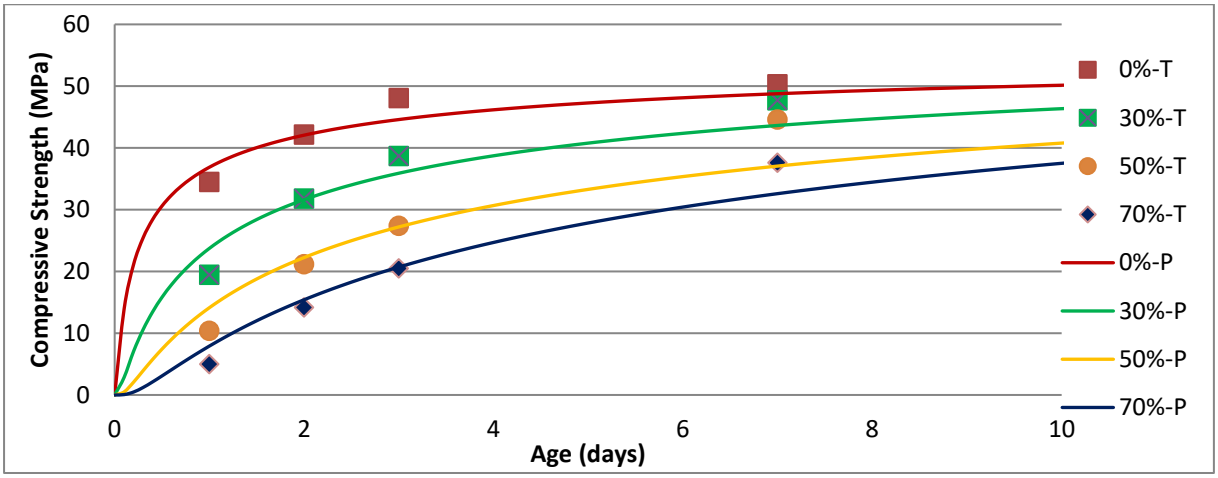

Figure 6.12 Comparison of prediction curves and testing results when n = 0.5 for RHPC mixes

In Figure 6.13, the prediction curve of the mix with 70% GGBS has an apparent turning point occurring when t is between 1 to 2 days. This turning point can be justified by the second derivative of Equation 6.3 shown in Appendix G. The second derivatives of Equation 6.2 and 6.3 both prove that there is a turning point for every prediction curve drawn by these equations. In most other cases, the turning point can be hardly observed on the chart because it is located close to 0 and the variation of the curve slope at this turning point is too small to be noticed. In this case, the turning point occurs when t=14×s

given by the second derivative of Equation 6.3 shown in Appendix G. In this case, the coefficient s is equal to 0.10, given in Table 6.6. Thus, the turning point is located at the plotting of t=1.4 (days), which confirms the visual observation in Figure 6.13 as well. This mathematical turning point of the curves around day 1 has no physical significance and does not represent the actual early-age development of concrete strength.

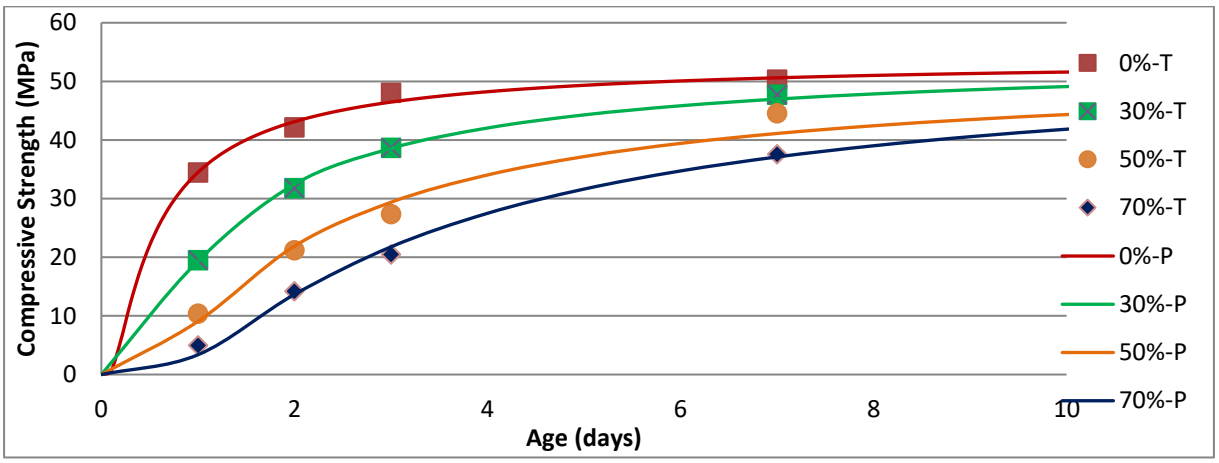

Figure 6.13 Comparison of prediction curves and testing results when n = 1.0 for RHPC mixes

6.2.3.2 Influence of Accelerator

The effects of using an accelerator in the concrete mix is mainly determined by its chemical compounds and manufacturer and how it interacts with the cementitious materials. Neither EC2 nor Model Code 2012 indicate the numerical effects on the strength development when an accelerator is used yet it clearly does have an impact on the strength development at an early age. The comparison of coefficient s of mixes with/without the accelerator could be used to analyse the effectiveness of this particular chemical admixture used during this research.

Comparing Tables 6.7 and 6.8 with previous Tables 6.2 and 6.4 of baseline mixes, only mixes without GGBS have a considerably lower value of coefficient s after the accelerator was added into the concrete mix. The resulting s value is reduced from 0.13 in Table 6.2 to 0.09 when n=0.5. Similar results occurs when n=1.0, where the s value drops from 0.025 in Table 6.4 to 0.017. When GGBS is introduced into the concrete mixes from 30% to 70%, the values of coefficient s have strong deceasing trends in both of Tables 6.7 and 6.8. However, comparing to the corresponding figures in Table 6.2 and 6.4 at one particular percentage of GGBS, there are no significant changes of coefficient s with or without the accelerator. The addition of GGBS content performs as a dominating role comparing to the influence of the accelerator.

As a result, the influence of the accelerator mainly exists for concrete mixes without GGBS or at a low dosage of GGBS at an early age only, which is similar to the case of RHPC discussed in the last section. The accelerating effect is significantly neutralized by the GGBS content, suggesting that this chemical admixture has a weak effect on the blended cement with 30% GGBS or higher. Although there is no indication about how an accelerator can influence the GGBS content in the concrete mix, the practical results show a weak impact of using this accelerator for concrete mixes with only 30% GGBS.

		s	n	R squared
CEM II+Accelerator	0%GGBS	0.090	0.5	0.928
	30%GGBS	0.253	0.5	0.988
	50%GGBS	0.275	0.5	0.961
	70%GGBS	0.400	0.5	0.980

Table 6.7 Values of coefficient s when n = 0.5 for CEM II + Accelerator mixes

		s	n	R squared
CEM II+Accelerator	0%GGBS	0.017	1.0	0.998
	30%GGBS	0.051	1.0	0.862
	50%GGBS	0.058	1.0	0.974
	70%GGBS	0.090	1.0	0.988

Table 6.8 Values of coefficient s when n = 1.0 for CEM II + Accelerator mixes

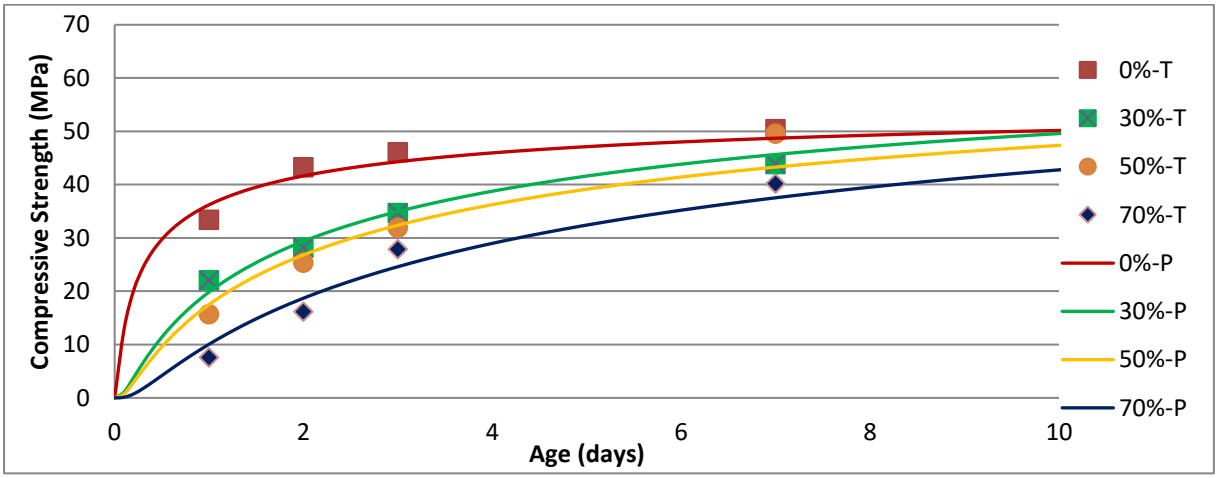

Figure 6.14 Comparison of prediction curves and testing results when n = 0.5 for CEM II + Accelerator mix

Comparing Figure 6.14 and 6.15, the strength development formula adopting n = 1.0 produces a curve with a better approximation to the test points on these charts for the mix without GGBS. However, the curve of the 30% GGBS mix in Figure 6.15 has much greater error (R^2=0.862) than the corresponding curve in Figure 6.14. At 50% and 70%

GGBS, the prediction curves in both Figures 6.14 and 6.15 at different values of coefficient n have a similar degree of accuracy with a slight advantage towards the situation when n=1.0. It can be seen that test points of 30% mix at 2-day 3-day are relatively close to those of 50% mix in Figure 6.14 and 6.15. Therefore, this exception might be caused by unexpected low values of the 30% mix at these two ages due to random experimental errors.

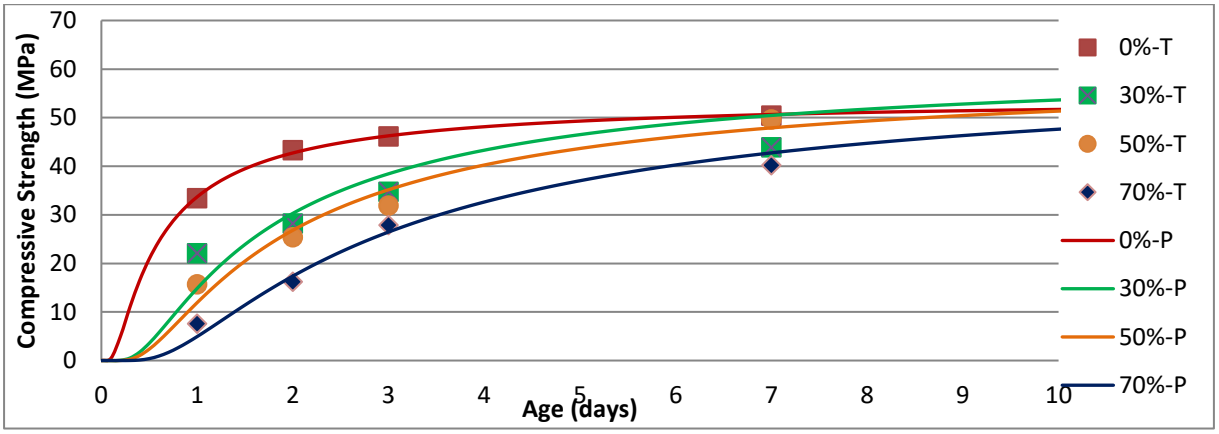

Figure 6.15 Comparison of prediction curves and testing results when n = 1.0 for CEM II + Accelerator mix

When n=0.5 in Figure 6.14, the errors in the prediction curve are showing positive values compared with the testing results at 1 day, whereas these curves are below the testing points with negative errors at 7 days. When n=1.0 in Figure 6.15, the opposite situations applied due to the change of coefficient n. Thus, the application of Equation 6.3 produces a more conservative prediction of early-age strength development than that which Equation 6.2 does. In conclusion, the prediction curves in Figure 6.15, with n=1.0, are reasonably acceptable.

6.2.3.3 Influence of Thermal Curing

As the thermal curing method is applied to the concrete mixes during early-age, a dramatic rise of the early-age compressive strength is achieved in Figures 6.16 and 6.17. Recalling the results from Chapter 5, the compressive strength of a cylinder thermally cured after 7 days is generally lower than those of mixes under normal curing due to reduced surface area of hydrated products and a coarser pore structure (Kjellsen 1996). Combining these two opposite influences due to thermal curing, the rate of strength gain of thermally cured mixes between 1 to 10 days is slower and the shapes of strength growth trends are consequently less steep in Figure 6.16 and 6.17. This variation of the growth trends could cause some changes to the predicting accuracies of both Equation 6.2 and 6.3.

The results for coefficient s for Table 6.9 and 6.10 are significantly lower than the results of concrete mixes without thermal curing in Table 6.2 and 6.4. When n=0.5, the percentage reductions of s values in Table 6.9 ranged from 41% to 63%. Similarly for the situation of n=1.0, the percentage reductions of s values are ranged from 47% to 68%. The previous effects of RHPC and accelerator demonstrate significantly less influence on the coefficient s in terms of numerical reduction. Furthermore, the thermal curing method also has a great impact on the concrete mixes even with high percentage dosage of GGBS content up to 70%.

		s	n	R squared
Thermal Curing	0%GGBS	0.047	0.5	0.924
	30%GGBS	0.131	0.5	0.989
	50%GGBS	0.164	0.5	0.917
	70%GGBS	0.175	0.5	0.963

Table 6.9 Values of coefficient s when n = 0.5 for thermal curing mixes

		s	n	R squared
Thermal Curing	0%GGBS	0.008	1.0	0.849
	30%GGBS	0.025	1.0	0.940
	50%GGBS	0.032	1.0	0.921
	70%GGBS	0.034	1.0	0.958

Table 6.10 Values of coefficient s when n = 1.0 for thermal curing mixes

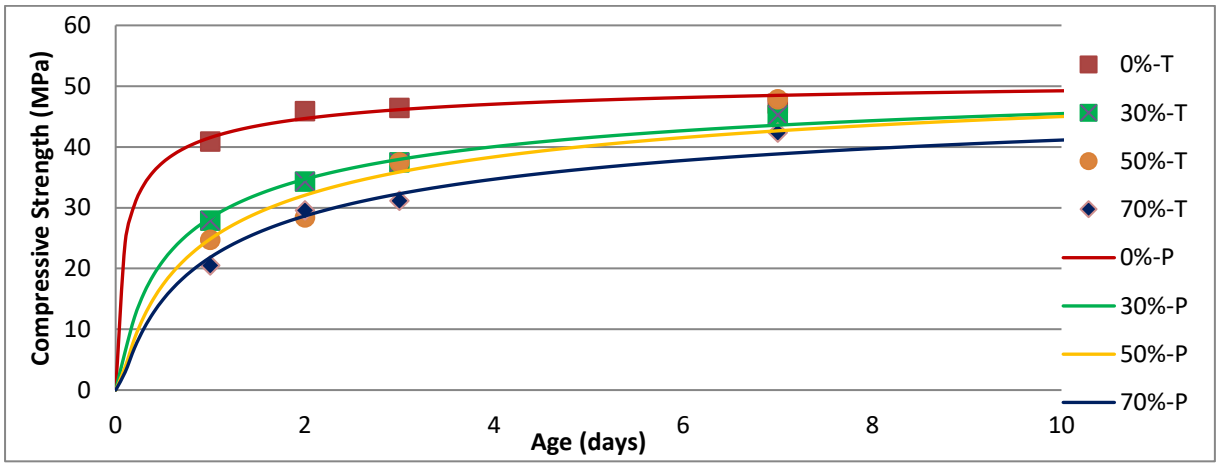

Figure 6.16 Comparison of prediction curves and testing results when n = 0.5 for thermal curing mixes

For mixes without GGBS content, the test points are close to prediction curves in both figures between 1-day to 3-day. However, the 7-day result has a large error in the prediction curve in Figure 6.17, which causes a significantly lower value of R squared in Table 6.10. For the 30% GGBS mix, the deviations of 1-day and 3-day in Figure 6.17 results in another low value of R squared due to its large error in the prediction curve. For

mixes with 50% and 70% GGBS content, there are similar errors for both prediction curves in Figure 6.16 and 6.17. In general, when thermal curing is applied, prediction curves drawn by Equation 6.2 have better accuracies than those drawn by Equation 6.3. However, previous discussions show opposite observations for mixes under normal curing. The differences between two equations in terms of prediction accuracy could be caused by the different shapes of strength development trends and the reduced values of coefficient s throughout all the thermally cured mixes, while the other two accelerating methods cannot significantly affect any mix with more than 50% GGBS. Thus, thermal curing is the most effective method of enhancing early age strength, across all GGBS dosages, of those strength enhancement methods under study.

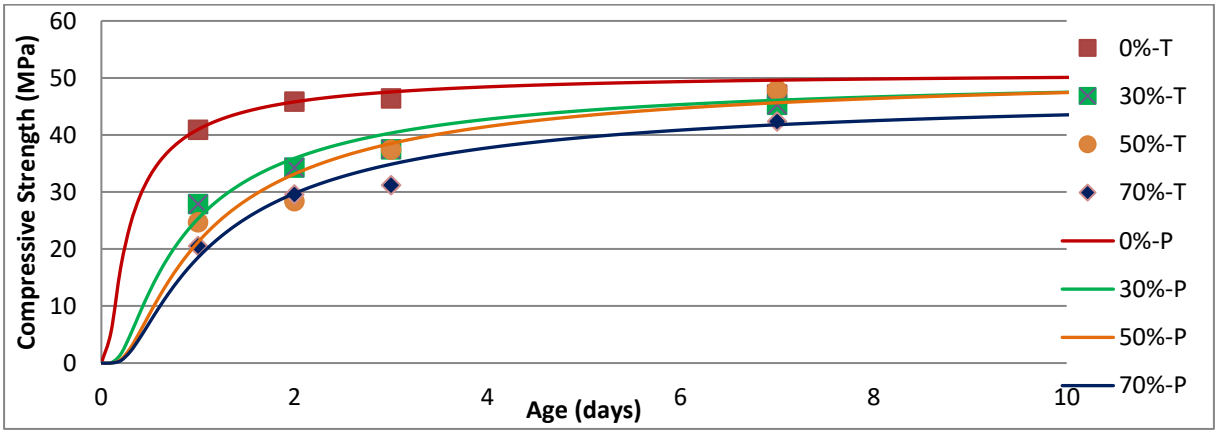

Figure 6.17 Comparison of prediction curves and testing results when n = 1.0 for thermal curing mixes

6.2.4 Influence of Combined Accelerating Methods

As multiple accelerating methods are applied in the experiment in a combined way, it is necessary to investigate the collective effects of combined methods by the following numerical analysis in this section. To achieve this objective, the optimal value of coefficient s is the important parameter to be calculated by the two prediction equations used previously. Despite the fact that all three accelerating methods have demonstrated their effectiveness under certain circumstances individually, the influence from a less effective method might not be a significant factor and may be outweighed by another strongly effective method.

6.2.4.1 Influence of RHPC + Accelerator

The influences of RHPC and accelerator individually were discussed in sections 6.2.3.1 and 6.2.3.2 respectively. Both methods have achieved similar accelerating effects in terms of a reduced value of coefficient s for concrete mixes without GGBS content. For 30%

GGBS mixes, RHPC applied a more significant effect on the early-age development of concrete, resulting in a lower value of coefficient s. Neither of them showed considerable influence on the numerical results when GGBS content is over 50%. This part of the analysis is expected to investigate the combined effect of RHPC and accelerator in the same concrete mix.

In Tables 6.11 and 6.12, the s values after using this combined method indicate an anticipated result based on the previous discussion. The combined effect of using two accelerating methods concurs with the additive result of two individual effects discussed previously. For mixes without GGBS content, the combined effect is stronger than both individual effects with a 65% reduction of coefficient s compared to the solo effects of 35% for RHPC and 31% for accelerator. There is no apparent interaction between RHPC and the accelerator that reduces the effectiveness of these two accelerating methods.

For mixes with GGBS content, the ineffective influences of both methods discussed previously also result in a small influence from this combined method. For 30% GGBS mix, this combined effect is similar to the single accelerating effect by using RHPC because using the accelerator is an ineffective method when the dosage of GGBS is higher 30% as discussed in section 6.2.3.2. For mixes with 50% to 70% GGBS, results in Table 6.11 and 6.13 are almost identical to those of the baseline mixes in Table 6.2 and 6.4 because both accelerating methods become ineffective when the dosage of GGBS is higher than 30%. In general, the chemical accelerator behaves similarly, but independently of RHPC as it does for CEM II/A-L with or without GGBS.

		s	n	R squared
RHPC+Accelerator	0%GGBS	0.046	0.5	0.742
	30%GGBS	0.195	0.5	0.988
	50%GGBS	0.280	0.5	0.981
	70%GGBS	0.360	0.5	0.896

Table 6.11 Values of coefficient s when n = 0.5 for mixes with RHPC and accelerator

		s	n	R squared
RHPC+Accelerator	0%GGBS	0.009	1.0	0.901
	30%GGBS	0.038	1.0	0.962
	50%GGBS	0.058	1.0	0.985
	70%GGBS	0.082	1.0	0.965

Table 6.12 Values of coefficient s when n = 1.0 for mixes with RHPC and accelerator

When n = 0.5 in Figure 6.18, the prediction curves are inadequately simulating the growth trends of testing values for mixes with 0% and 70% GGBS. The poor performance of

Equation 2.2 results in significantly lower values of R squared at 0.742 and 0.896 in Table 6.11. The unexpected high values from testing at 7 days are probably the main reason causing large errors for the cases with 0% GGBS and 70% GGBS. In contrast, the other two curves in the same graph have considerably better predictions when compared to the test values. Therefore, it is not possible to conclude on the accuracy of Equation 6.2 based on the percentages of GGBS in Figure 6.18. By observing the shapes of these prediction curves, the general trends of strength development are still consistent from the 0% GGBS curve to the 70% GGBS curve, as evidenced by the trend in the s values in Table 6.11.

When n = 1.0 in Figure 6.19, the prediction curves are generally closer to the plots of the test results compared with the chart in Figure 6.18. Although errors still exist due to a couple of unexpected results at 7 days, the average value of R squared in Table 6.12 is significantly higher than that in Table 6.11. Especially for concrete mixes with 0% and 70% GGBS, the prediction curves in Figure 6.19 fit the test points better and more accurate shapes are obtained than those from Figure 6.18. This observation, that the prediction is more accurate based on n = 1.0, complies with previous situations of mixes with CEM II/A-L, RHPC and CEM II/A-L + accelerator. The only exception occurred when the concrete mixes were thermally cured.

In general, none of RHPC, the chemical accelerator or the combined method using both of them proves to be an effective method to compensate for the strength development for concrete mixes with GGBS content of more than 30%.

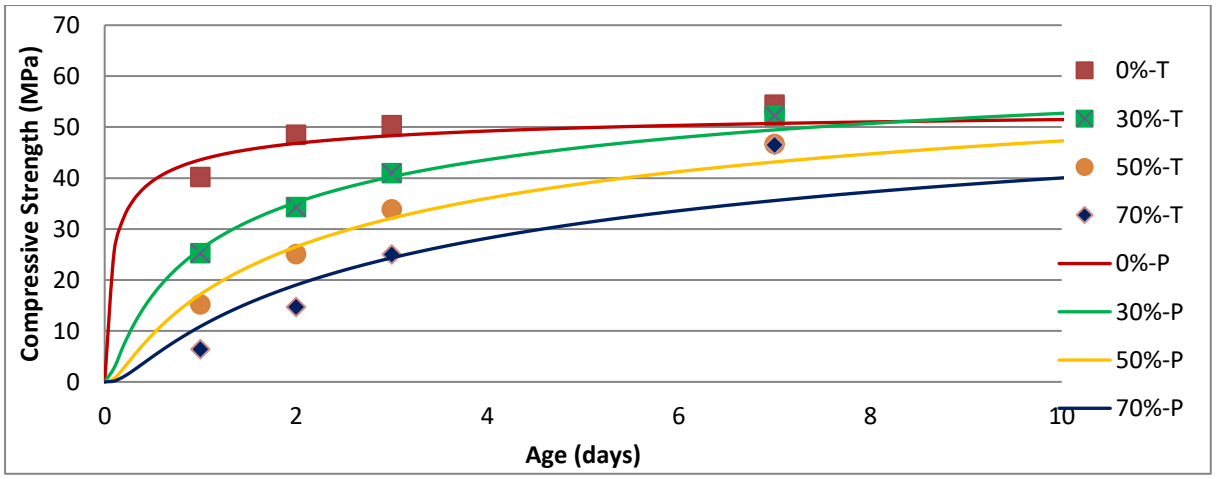

Figure 6.18 Comparison of prediction curves and testing results when n = 0.5 for mixes with RHPC and accelerator

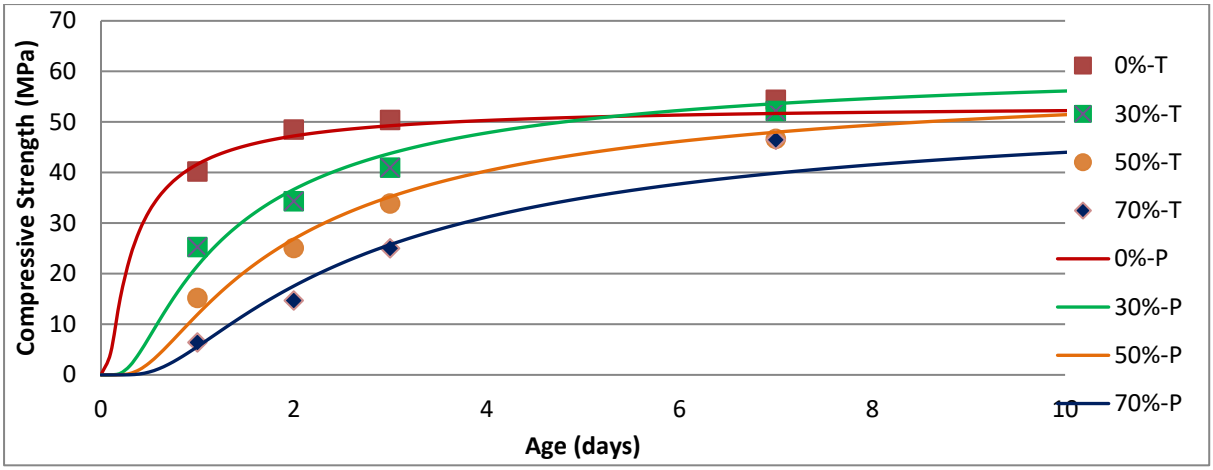

Figure 6.19 Comparison of prediction curves and testing results when n = 1.0 for mixes with RHPC and accelerator

6.2.4.2 Influence of RHPC + Thermal Curing

In this part of the discussion, the concrete mixes made from RHPC with thermal curing treatment are analysed to investigate the combined effects of these two accelerating methods. Based on previous discussions, the values of coefficient s after using the thermal curing method are smaller than those from mixes using RHPC. Thus, thermal treatment may be a dominant factor in the behaviour of strength development and causes the influence of RHPC to be indistinct in the combined results, especially for high GGBS substitution rates. To evaluate the combined effect, it is necessary to compare the results from previous discussions that involves the thermal curing alone.

Comparing Table 6.13 with Table 6.9, the combined effect of RHPC and thermal curing is indecisive due to the irregular results of those mixes at different proportions of GGBS. For mixes with 0% and 50% GGBS, the combined two methods exert less effect than the single thermal curing method due to higher values of coefficient s. However, the other two mixes with 30% and 70% GGBS behave in an opposite manner in that they have a stronger effect with a reduced value of coefficient s. Therefore, under thermal curing treatment, the comparison between RHPC and CEM II/A-L does not demonstrate a significant difference in terms of strength development rate.

		s	n	R squared
RHPC + Thermal Curing	0%GGBS	0.061	0.5	0.952
	30%GGBS	0.092	0.5	0.876
	50%GGBS	0.177	0.5	0.983
	70%GGBS	0.153	0.5	0.953

Table 6.13 Values of coefficient s when n = 0.5 for mixes with RHPC and thermal curing

		s	n	R squared
RHPC + Thermal Curing	0%GGBS	0.011	1.0	0.724
	30%GGBS	0.018	1.0	0.915
	50%GGBS	0.034	1.0	0.914
	70%GGBS	0.029	1.0	0.734

Table 6.14 Values of coefficient s when n = 1.0 for mixes with RHPC and thermal curing

The increasing trends of s values from a lower percentage of GGBS to a higher percentage in Tables 6.13 and 6.14 end at the 50% GGBS dosage, which is different from all the previous cases. It is possible that random errors cause unexpectedly high early-age strength of the mix with 70% GGBS. Thus, the test points in Figures 6.20 and 6.21 show that the experimental results from both mixes with 50% and 70% GGBS are unusually close to each other. In this case, the strength development of 70% GGBS mixes demonstrates unusual behaviour in Figures 6.20 and 6.21 that cause the values of coefficient s of the 70% GGBS mix to be lower than that of 50% GGBS mix. This decrease of coefficient s from 50% GGBS dosage to 70% GGBS dosage never happened in previous cases and may be caused by expected testing errors. Similarly, in Tables 6.9 and 6.10, the differences of coefficient s between 50% GGBS and 70% GGBS are also significantly smaller than those of mixes without thermal curing. Therefore, the increasing retardation effect by introducing more GGBS content might be significantly reduced by the thermal curing treatment.

Comparing Figure 6.20 to 6.21 in terms of the consistency and accuracy of these prediction curves, Figure 6.20 demonstrates a generally superior performance when n is selected to be 0.5. The inaccurate prediction in Figure 6.21 causes significantly low values of R squared in Table 6.14 and the curves are inevitably further away from the test points comparing to the curves in Figure 6.20.

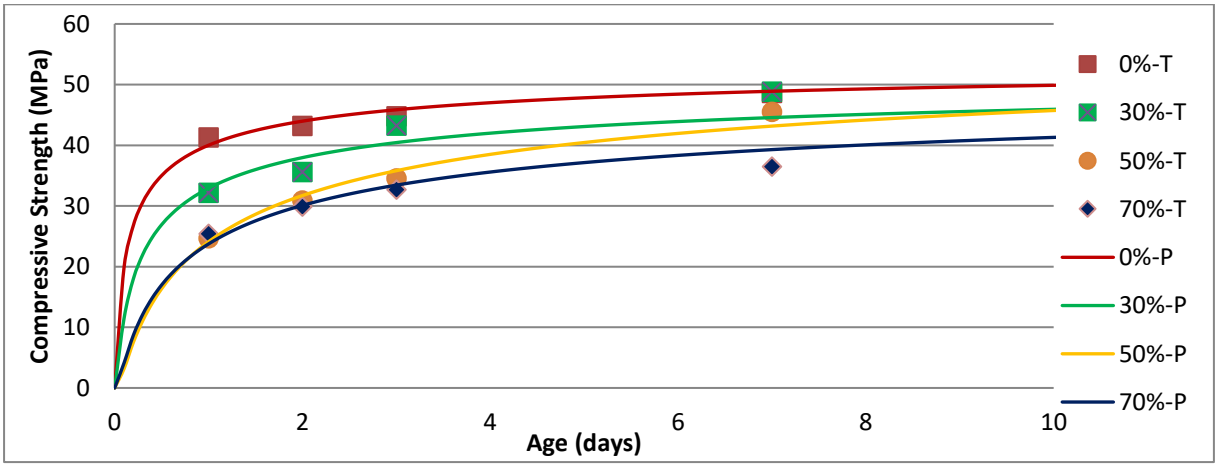

Figure 6.20 Comparison of prediction curves and testing results when n = 0.5 for mixes with RHPC and thermal curing

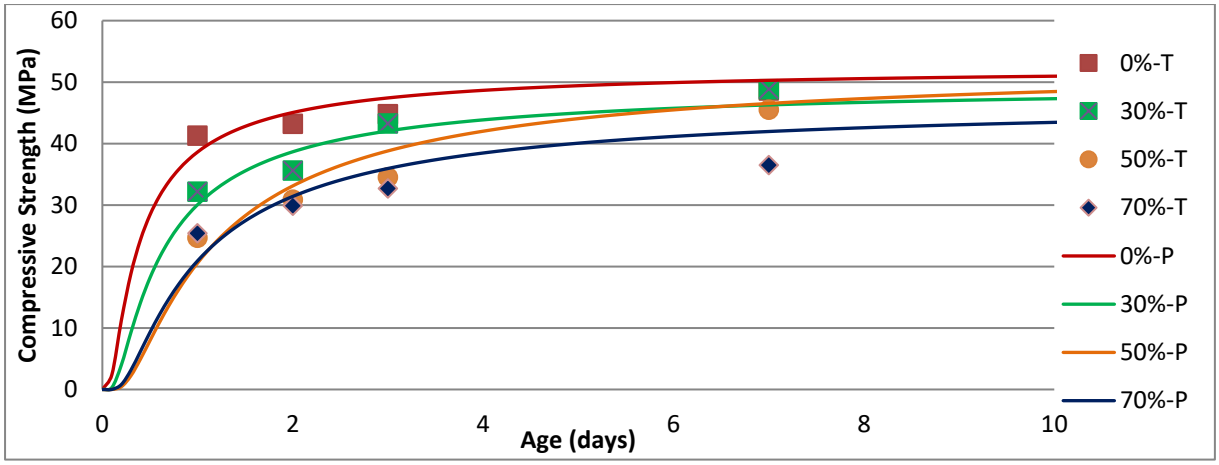

Figure 6.21 Comparison of prediction curves and testing results when n = 1.0 for mixes with RHPC and thermal curing

Based on previous discussions, the modified Equation 6.3 with an assumed value of n = 1.0 shows better or similar performances as Equation 6.2 with the default value of n = 0.5 for mixes under normal curing conditions. However, in this section and section 6.2.3.3, the original Equation 6.2 is more accurate for mixes under thermal curing treatment to draw a series of prediction curves with better consistency and accuracy based on the comparisons of R squared values. This phenomenon will be examined again in the next section and causes will be discussed in the conclusions.

6.2.4.3 Influence of RHPC + Accelerator + Thermal Curing

This part of the discussion will focus on two mixes with all three accelerating methods applied simultaneously. The above discussion indicated that RHPC has an indecisive influence on concrete mixes under thermal curing treatment. Similarly, the extra addition of the accelerator may be not as effective as it was previously under normal curing treatment. Thus, it is required to compare the combined effect of RHPC and accelerator for mixes with or without thermal curing treatment. In particular, whether the retarding effect of adding high GGBS dosages can be fully compensated for by the accelerating effect of the combined three methods is of interest.

For the mix without GGBS content, the value of coefficient s in Table 6.15 is greater than that from a mix with CEM II/A-L and thermal curing in Table 6.9. This greater value of coefficient s demonstrates that the accelerating methods of using RHPC and the accelerator under thermal curing are not significantly effective in terms of increasing the strength growth rate, whilst section 6.2.4.1 indicates that the combined effect of RHPC and accelerator is an effective method to achieve higher growth rate under normal curing

conditions. The possible explanation is that the effects of both RHPC and the accelerator are outweighed by the greater influence of thermal curing in this combined method.

For the mix with 70% GGBS, there is a 10% reduction of s values for using RHPC and accelerator together compared with the mix with CEM II/A-L. Again, the application of RHPC and accelerator is not a significant factor of strength growth if the thermal curing method is carried out. Both of the concrete mixes without GGBS and with high percentage GGBS show insignificant influences of RHPC and the accelerator when combined with a thermal curing treatment.

		s	n	R squared
RHPC + Thermal Curing + Accelerator	0%GGBS	0.059	0.5	0.692
	70%GGBS	0.159	0.5	0.994

Table 6.15 Values of coefficient s when n = 0.5 for mixes with all accelerating techniques

		s	n	R squared
RHPC + Thermal Curing + Accelerator	0%GGBS	0.010	1.0	0.297
	70%GGBS	0.031	1.0	0.984

Table 6.16 Values of coefficient s when n = 1.0 for mixes with all accelerating techniques

Similarly, to the previous discussion, Equation 6.2 in Figure 6.22 shows two prediction curves with better approximations than those in Figure 6.23 drawn using Equation 6.1. Again, for the mixes under thermal curing treatment, the default value of coefficient n = 0.5 is superior for the prediction of strength growth than the modified value of n = 1.0. Especially for the mix without GGBS, the low value of R squared in Table 6.16 demonstrates that the n = 1.0 case is not an acceptable value for this case. For the mix with 70% GGBS, the difference between two prediction curves is too small to determine which one is more accurate. In general, it is preferred to choose the default value of coefficient n to prediction the strength growth for a concrete mix that is treated by early-age thermal curing, especially for those mixes without any addition of GGBS content.

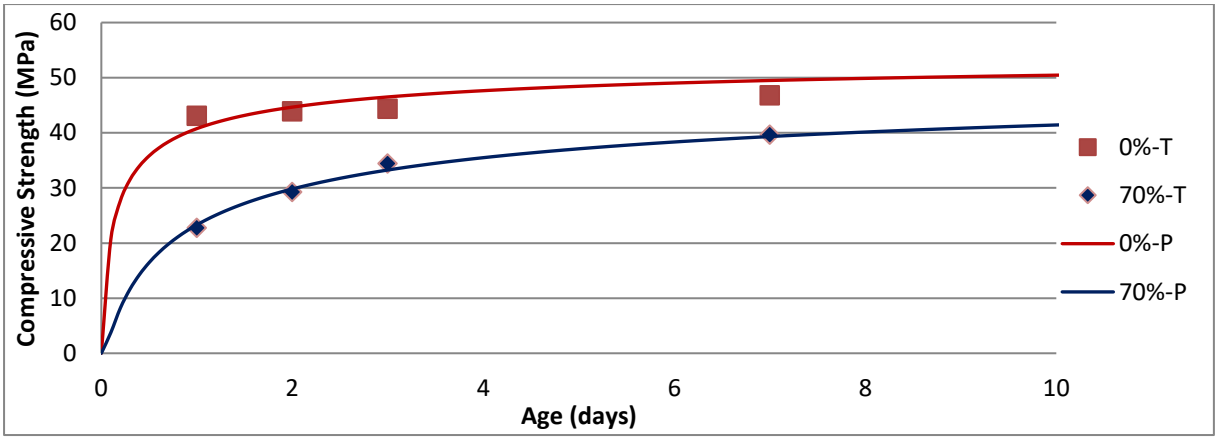

Figure 6.22 Comparison of prediction curves and testing results when n = 0.5 for mixes with RHPC, accelerator and thermal curing

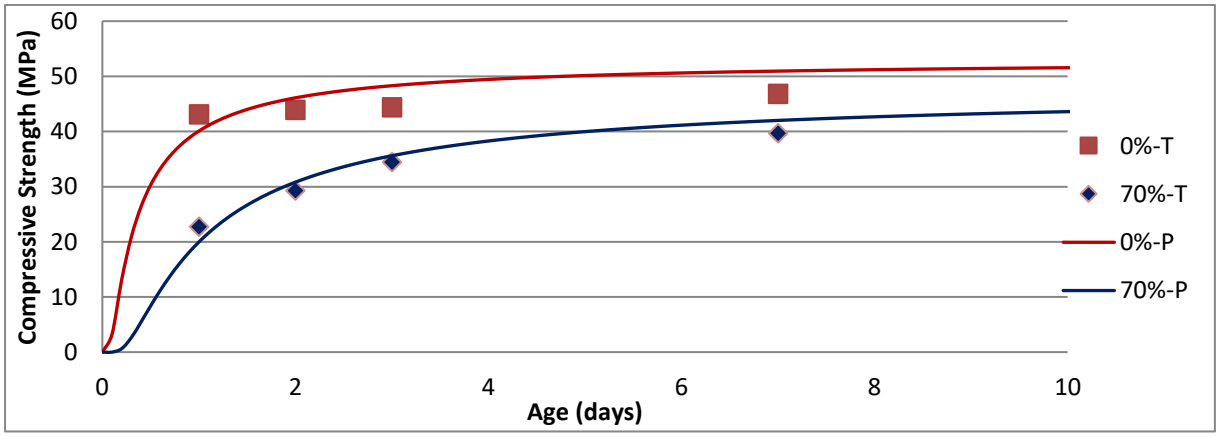

Figure 6.23 Comparison of prediction curves and testing results when n = 1.0 for mixes with RHPC, accelerator and thermal curing

6.2.5 Variations of Coefficient s under Various Conditions

Arising from the specific discussions of each concrete mix design in previous sections, it is necessary to present a comprehensive conclusion on the variation of coefficient s under various conditions. By analyzing all the data on the same graph, it is possible to identify the disturbance of random testing errors and approximate the specific influences of GGBS and three accelerating methods in a numerical form.

6.2.5.1 Comparison of Two Selected Values of Coefficient n

The previous discussions about how to evaluate the accuracy of prediction curves are based on the calculated R squared values. For some situations, the original value of coefficient n proposed by EC2 (0.5) contributes to relatively large errors for predicting the strength trend of concrete between 1 day and 28 days. One reason for a low value of R squared in some cases results from one exceptional test point due to uncertain random

factors occurring during the experiment. Another reason is due to the pre-determined shape of the prediction curves plotted by Equation 6.2 which cannot simulate the actual strength growth accurately no matter what value of coefficient s is selected. Therefore, another value of coefficient n is chosen to transform Equation 6.2 into Equation 6.3. The comparison of the two equations is also based on the magnitude of R squared values for various concrete mixes.

To demonstrate the distribution of R squared values, all the calculated results for each concrete mix are drawn in Figure 6.24 and categorized into two groups of vertical bars, indicating the magnitudes of R squared values from the baseline mix to the left to the mix with all treatments to the right. The captions on top of these bars represent the mix ingredients and/or curing method, each bar covers 4 vertical bars from 0% GGBS on left-hand side to 70% GGBS on the right-hand side. In general, the results calculated by Equation 6.2 and 6.3 do not present any consistent difference between each other. There are good predictions of R squared closed to 1 and poor predictions of R squared lower than 0.90 existing for both equations with different values of coefficient n. R squared values from each group are mainly distributed in the range of 0.9~1.0 with a few exceptionally low values. This implied that the chosen mathematical models are reasonable representations of the actual behaviour of strength development. Table 6.17 also suggests that the average results of R squared calculated by the two equations are almost the same. Thus, there is no evidence that can demonstrate the superiority of either equation from a general point of view for all the experimental work involved during this research.

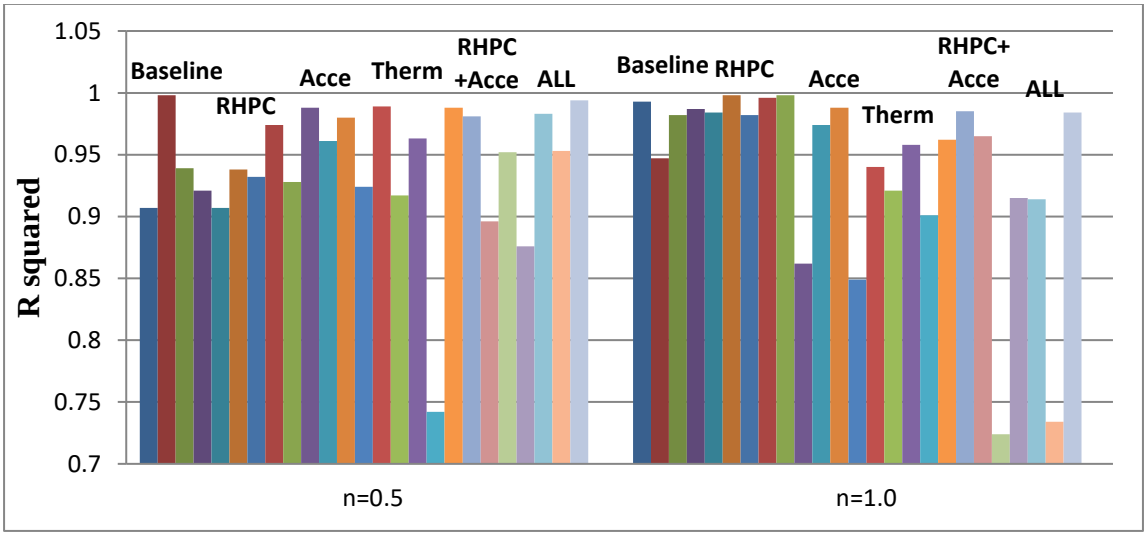

Figure 6.24 R squared values of prediction curves vs coefficient n for different mixes (RHPC: rapid hardening Portland cement. Acce: the admixture of accelerator. Therm: thermal curing by hot water. ALL: RHPC, the accelerator and thermal curing are used together.)

	Average R^2	Standard Deviation
n=0.5	0.939	0.054
n=1.0	0.936	0.075

Table 6.17 Average results of R squared and standard deviation

Considering the mix designs of all the concrete mixes, the early-age properties are the major difference among them. Thus, to present the distribution of R squared from another point of view, a chart plotted against the 1-day compressive strength is shown in Figure 6.25. In this chart, the average value of R squared is generally higher on the side of low 1-day strength. On the other hand, where the compressive strength is greater than 28.6MPa, which is the 1-day result of baseline mix, the values of R squared are dispersed in the range of 0.7 ~ 1.0.

Specifically, those plots which are below 0.90 in Figure 6.25 are all from concrete mixes applying one or two accelerating methods. It is possible that the original model of concrete development from Equations 6.2 and 6.3 does not fit an accelerated concrete mix perfectly due to the fast rate of early-age strength gain. Therefore, in terms of simulating the trend of concrete development, both prediction equations are less reliable for a concrete mix which applies accelerating methods.

Another feature shown in Figure 6.25 is the difference between Equations 6.2 and 6.3 in terms of predicting accuracy. For mixes with a 1-day strength lower than 20MPa, Equation 6.3 has a significantly higher values of R squared, and most results are above 0.95. In comparison to Equation 6.2, the results of R squared are varying in a larger range from 0.9 to 1.0. Thus, for mixes with low early-age strength, it is recommended to adopt the reformed equation for strength prediction. When the 1-day strength is greater than 20MPa, the comparison of two equations seems to be indistinctive for a clear conclusion.

Based on the previous discussion of the effects of accelerating methods, the thermal curing treatment is acting in a different way in terms of predicting accuracy. Thus, Figure 6.25 is separated into two charts (Figure 6.26 and 6.27) to demonstrate the different effects. Figure 6.26 includes all the results of mixes under normal curing conditions. Comparing to Figure 6.25, the superiority of Equation 6.1 is more observable throughout the whole chart, not only in the range of 1-day strength lower than 20MPa. Therefore, the reformed Equation 6.3 is more practical for mixes under normal curing conditions than the original Equation 6.2.

In contrast to Figure 6.26, results of mixes which have been thermally cured are shown in Figure 6.27 with the opposite situation arising. Figure 6.27 demonstrates that the original Equation 6.2 with n=0.5 has significantly better accuracy than Equation 6.3. Since all mixes which are thermally cured have their 1-day strengths higher than 20MPa and the trends in the accuracy of the two equations is shown to be reversed under different thermal methods, it is now understandable why the comparison of two predicting equations in Figure 6.25 is chaotic across the range of 20MPa to 40MPa.

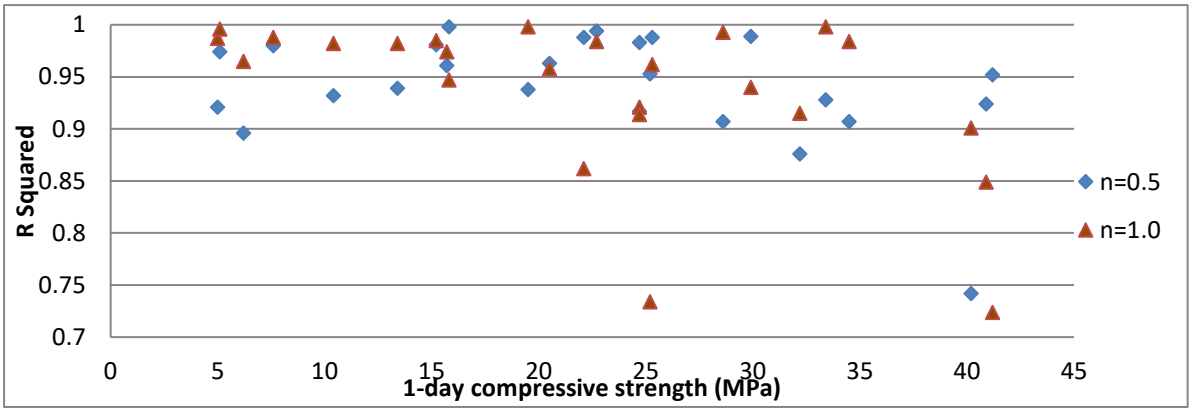

Figure 6.25 R squared values of prediction curves vs 1-day compressive strength

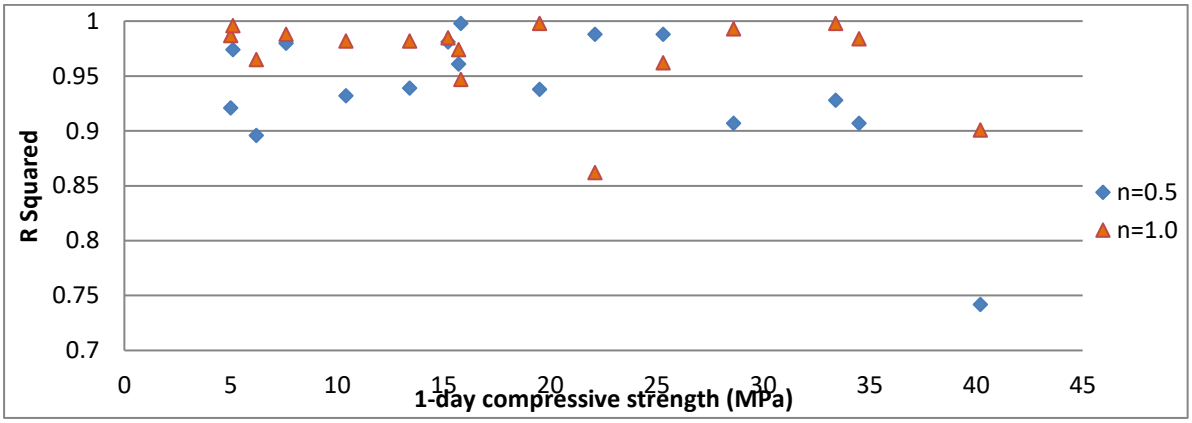

Figure 6.26 R squared values of prediction curves vs 1-day compressive strength without thermal curing

Therefore, the overall comparison of two values of coefficient n is not substantially clear in Figure 6.25 in terms of calculating accuracy. However, Figure 6.26 suggests that n = 1.0 is a better choice for all the mixes under normal curing conditions while Figure 6.25 suggests that the original value proposed by EC2 is better for thermally cured mixes.

6.2.5.2 Numerical Assessment of Coefficient s

In this part of the discussion, the numerical influences of accelerating methods and GGBS will be evaluated based on previous results of coefficient s under various mix designs.

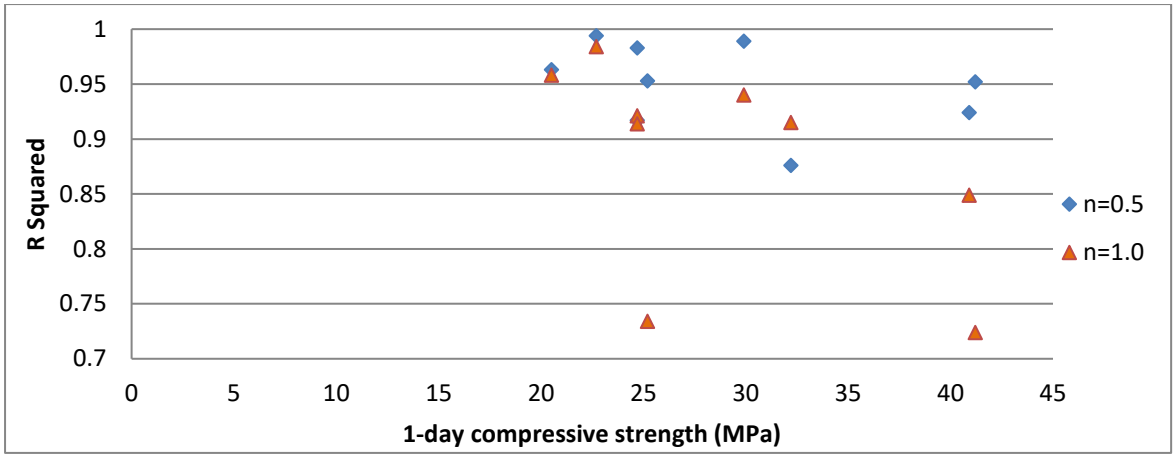

Figure 6.27 R squared values of prediction curves vs 1-day compressive strength with thermal curing

Considering the general increasing trend of s values alone with the addition of GGBS content, Figure 6.28 is plotted by coefficient s against the percentages of GGBS for mixes made from CEM II/A-L. Although the results calculated by Equation 6.2 and 6.3 show large differences in the numerical figures, they present similar trends of s values which are influenced by percentages of GGBS content. Thus, further discussion will be focused on the results calculated by Equation 6.2, and the concluded results for Equation 6.3 will be given afterwards.

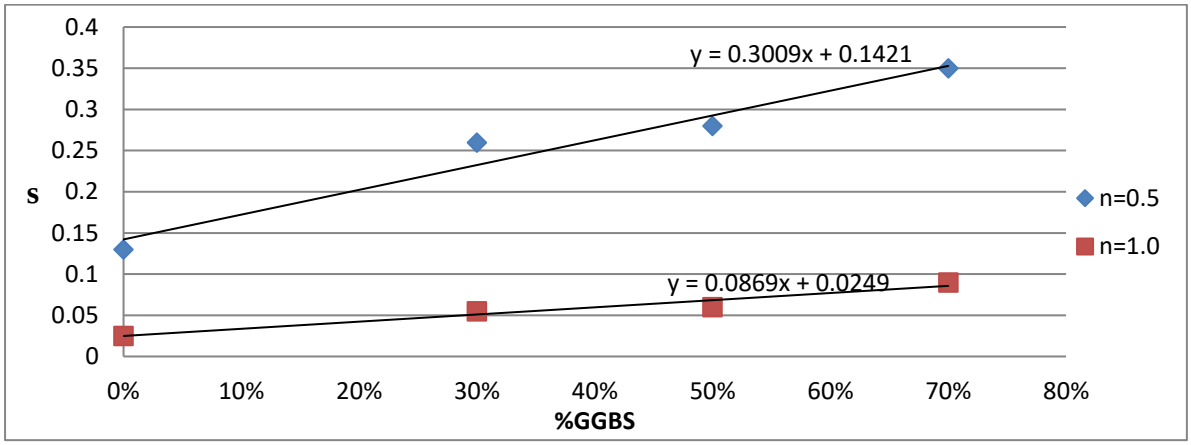

Figure 6.28 Coefficient s vs %GGBS for CEM II mixes

Supposing that the increments of coefficient s and the proportion of GGBS have a linear relationship, then a trend line joining the data points with minimal errors can be drawn in Figure 6.28 to demonstrate this relationship numerically. The formula for this trend indicates both the starting value of coefficient s for the mix without any GGBS and the growing rate of s values along with GGBS content. Thus, all the other values of s at any particular proportion of GGBS can be calculated by the starting value and increasing rate.

For other mix designs with various accelerating methods, similar plots and formulae are included in Appendix H.

To compare the baseline mix and to other accelerated mixes, all the trend lines from various mix designs are displayed collectively in Figure 6.29 to generate a complete picture of all the values of coefficient s. The numerical results are also based on the formulae of these trend lines and given in Table 6.18. Although the interception points on those trend line are slightly different from the actual plots, they can provide more consistent values of coefficient s to summarize the general influences of each accelerating method or combined methods.

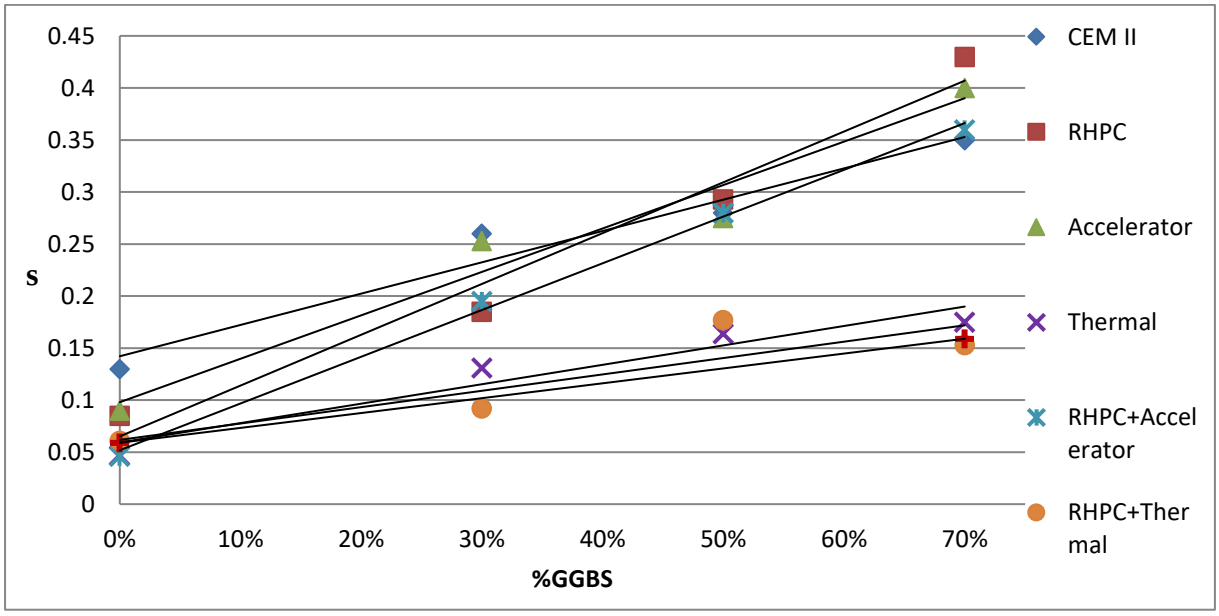

Figure 6.29 Coefficient s vs % GGBS for all mixes when n = 0.5

The first important feature in Figure 6.29 is a demonstration that all the accelerating methods have proved to be effective in accelerating the strength development with reduced values of coefficient s when there is no GGBS content involved. Along the 0%GGBS axis, the initial value of coefficient s from the baseline mix is reduced from 0.142 to a range of 0.098~0.051 regarding to various accelerating techniques. The application of an accelerator appears to have the least effectiveness among all the accelerating methods. When RHPC and thermal curing treatment are applied, values of coefficient s are reduced to 0.065 and 0.059 respectively. The combined method of RHPC and accelerator seems to be relatively more effective (s=0.51) than each method individually. However, any combined method involving thermal curing does not show any significant improvement over the single thermal curing method. The concrete mix with all three methods has an identical result of coefficients s compared with the value of the mix which is only thermally cured. It can be explained that the strong thermal curing

process out weights the less significant effects of RHPC and the accelerator, within experimental error.

When GGBS content is involved, these trend lines disperse largely as the proportions of GGBS is increasing. Based on the trend line of CEM II/A-L, for every 10% cement is replaced by GGBS, coefficient s is increased by approximately 0.03. On the top of Figure 6.29, all the mixes under normal curing conditions are converging to a similar value at a high percentage of GGBS. As a result, the effects of RHPC and accelerator are becoming less significant along the horizontal axis. When a certain amount of GGBS is added, approximately 35%-40%, both RHPC and accelerator almost have no significant influence in terms of values of coefficient s because both effects of RHPC and the accelerator are becoming less important when the proportion of CEM II/A-L is decreasing. The influence of GGBS dominates the strength development no matter what method is used.

The trend line of the combined method of RHPC and accelerator is slightly lower than both lines of a single accelerating method, and the effectiveness lasts until 50% GGBS is added into the concrete mix. Since the variation of coefficient s is greater for mixes accelerated by RHPC or an accelerator, the increment of coefficient s per 10% GBBS is also increased to approximately 0.045.

In the lower margin of this chart, three trend lines of mixes thermally cured show dramatically different features from those lines above them. The thermal curing method has strong influences over concrete mixes even when high percentages of cement are replaced by GGBS. This counter effect against GGBS by thermal curing is much greater than those by the other two methods. Thus, the increasing rate of coefficient s is significantly slower along the horizontal axis for mixes thermally cured.

When 70% GGBS is added into the concrete mixes, values of coefficient s rise to 0.35~0.40 for mixes under normal curing conditions. However, the thermal curing method reduces these figures by more than a half amount, to approximately 0.15~0.20. Consequently, the increasing rate of coefficient s per 10% GGBS is only about 0.015. The thermal curing method cannot fully compensate for GGBS addition, but it ameliorates the influence of GGBS significantly.

When the thermal curing method is combined with RHPC or RHPC+accelerator, the combined methods achieve similar effects to the thermal curing alone. The slight improvements with the inclusion of RHPC or an accelerator at 70% GGBS cannot confirm with certainty the superiority of these combined methods, considering their

inefficiencies at high percentages of GGBS, which is discussed above. Thus, it is concluded that RHPC and the accelerator have relatively insignificant effects on concrete mixes which are thermally cured with or without GGBS content and their influence in concrete mixes is not merited except for very early age enhancement.

To sum up, a series of values of coefficient s are proposed in Table 6.19 as a reference for possible practical work in future. To generate a series of values in proper conformity, several necessary assumptions are required for the calculation procedures. Firstly, RHPC and the accelerator are assumed to be effective factors on the coefficient s only if the proportion of GGBS is less than 40% in a concrete mix based on the observation of Figure 6.29. The trend line of baseline mix intercepts with those of RHPC and accelerator mixes near 40% GGBS. If GGBS content is equal to 40% or more, all the results in Table 6.19 are assumed to be more or less identical for mixes under normal curing conditions.

	s values without GGBS	s values at 70%GGBS	Slopes of trend lines
baseline mix CEM II/A-L	0.142	0.352	0.30
RHPC	0.065	0.406	0.49
Accelerator	0.098	0.389	0.42
RHPC + Accelerator	0.051	0.365	0.45
Thermal curing	0.059	0.189	0.18
Thermal curing+RHPC	0.061	0.171	0.15
Thermal curing+RHPC+Accelerator	0.059	0.158	0.14

Table 6.18 Values of coefficients based on trend lines in Figure 6.29

	Percentage of GGBS							
	0%	10%	20%	30%	40%	50%	60%	70%
Baseline	0.14 (0.25) *	0.17	0.20	0.23	0.26	0.29	0.32	0.35
RHPC	0.07 (0.20) *	0.12	0.17	0.22	0.26	0.29	0.32	0.35
Accelerator	0.10	0.14	0.18	0.22	0.26	0.29	0.32	0.35
RHPC+Accelerator	0.06	0.11	0.16	0.21	0.26	0.29	0.32	0.35
Mixes thermally cured	0.060	0.075	0.090	0.105	0.120	0.135	0.150	0.165

Table 6.19 Proposed values of coefficient s when n=0.5. *() includes original figure proposed by EC2

Another assumption is made based on the overwhelming influence of the thermal curing method. There is no strong evidence to determine the effects of RHPC or an accelerator if they are applied with thermal curing method simultaneously. As a result, three mix designs involving thermal treatment are assumed to be more or less identical in terms of the prediction of coefficient s, despite other accelerating methods being applied as well. Results in Table 6.19 are drawn in Figure 6.30 as a comprehensive view of the full distribution of coefficient s. This chart could be useful to determine a suitable value of s under various situations where a theoretical prediction of concrete development is required.

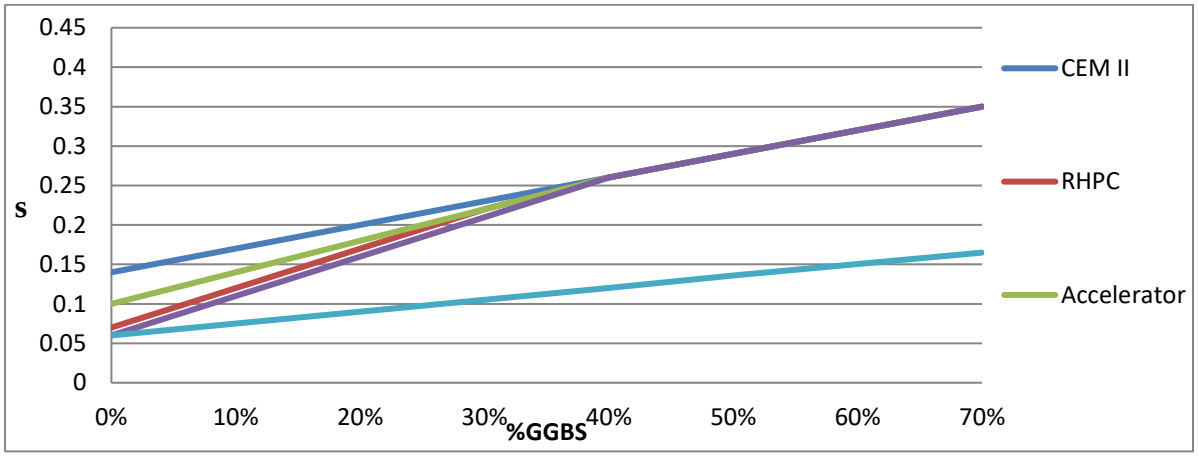

Figure 6.30 Proposed distribution of coefficient s when n=0.5

A similar process of calculation is performed for the situation where n=1.0. The resulting values are significantly smaller than those from the previous situation and are shown in Table 6.20. However, in both situations, coefficient s is affected by various conditions in a similar trend which is shown in Table 6.19 and Figure 6.30. Again, previous assumptions for introducing proposed values of coefficient s in Table 6.19 are also applied in this case for calculating the values in Table 6.20.

	Percentage of GGBS							
	0%	10%	20%	30%	40%	50%	60%	70%
Baseline	0.024	0.032	0.040	0.048	0.056	0.064	0.072	0.080
RHPC	0.011	0.022	0.033	0.044	0.056	0.064	0.072	0.080
Accelerator	0.017	0.027	0.037	0.047	0.056	0.064	0.072	0.080
RHPC+Accelerator	0.010	0.021	0.032	0.043	0.056	0.064	0.072	0.080
Mixes thermally cured	0.010	0.013	0.016	0.019	0.022	0.025	0.028	0.031

Table 6.20 Proposed values of coefficient s when n=1.0

Results in Table 6.20 are drawn in Figure 6.31 where the chart is almost the same shape as that in Figure 6.30, whereas the vertical dimensions of these plots in Figure 6.31 are only about a fifth of those in Figure 6.30. When Equation 6.3 is required to replace Equation 6.2 for a more appropriate prediction of concrete development based on previous discussions, this chart can be applied to replace Figure 6.30 at the same time as acquiring appropriate values of coefficient s for further calculation.

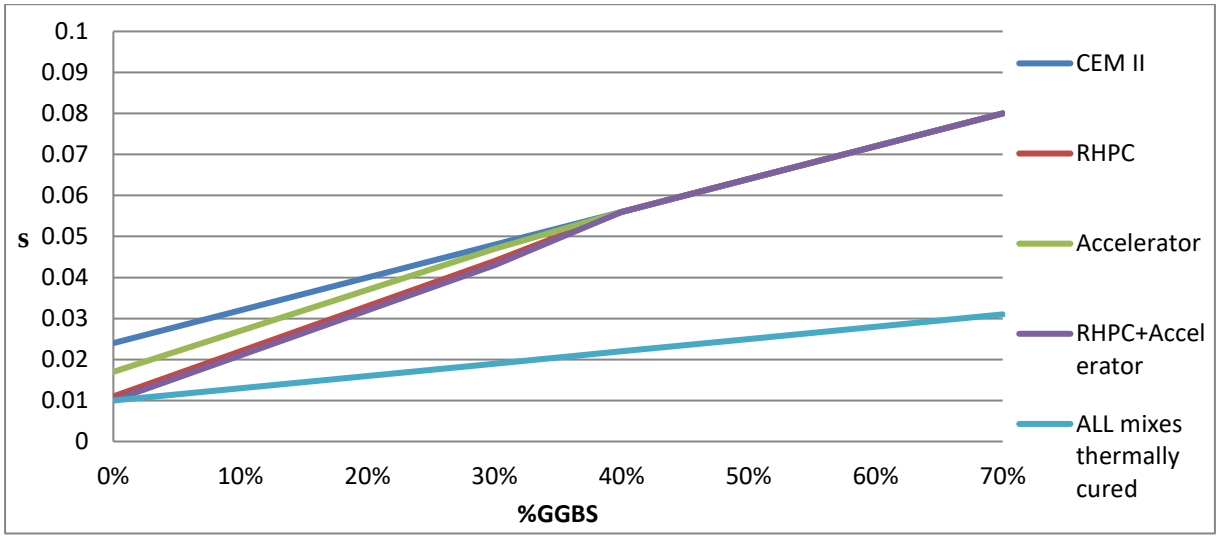

Figure 6.31 Proposed distribution of coefficient s when n=1.0

6.3 Theoretical Predictions of Elastic Modulus

In Chapter 4, the relationship between the elastic modulus and the compressive strength was discussed through various concrete mixes made from different types of coarse aggregates. The suggested formulae used in Chapter 4 for predicting the elastic modulus are mainly used to establish that relationship for concrete mixes at a particular age. In this part of the discussion, time-based models of predicting the elastic modulus will be established by using the empirical equations optimized under various conditions. The influences of GGBS and the three accelerating methods on the elastic modulus will also be assessed numerically in a comprehensive overview.

6.3.1 Formulae for Theoretical Predictions

The prediction of elastic modulus requires an empirical formula based on the relationship between the elastic modulus and the compressive strength at a particular age of concrete. EC2 has proposed such formulae that can be used to establish this relationship in a power function format shown in Equation 6.4 (from Equation 4.7). This formula assumes that the elastic modulus is proportional to the compressive strength to the power of 0.3.

$E_{cm} = 22\times\alpha\ (f_{cm}/10)^{0.3}$ (Eqn 6.4)

To predict the elastic modulus at any age during the development of concrete, a time based formula is required for achieving this objective. Thus, Equation 6.5 is established by assuming that the relationship between the elastic modulus and compressive strength is constant at any age of concrete development.

$E_{cm}(t) = 22\times\alpha\ (f_{cm}(t)/10)^{0.3}$ (Eqn 6.5)

Substituting Equation 6.2 into Equation 6.5, a new time-based formula for predicting the elastic modulus can be derived as Equation 6.6. This new formula establishes a relationship between the elastic modulus at various ages and the 28-day compressive strength. The values of coefficient s were calculated throughout the previous Section 6.2, and those results of coefficient s will be used again in this section instead of the standard values proposed by EC2.

$E_{cm}(t) = 22\times\alpha\times((f_{cm}\times\exp(s(1-(\frac{28}{t})^{0.5}))/10)^{0.3}$ (Eqn 6.6)

Equation 6.6 can be also written in another format to predict the elastic modulus at any time based on the 28-day elastic modulus. In Equation 6.7, the influence of coarse aggregate can be ignored once the 28-day elastic modulus is known. Theoretically, if the relationship between f_{cm} and E_{cm} exactly follows Equation 6.4 shown above, Equation 6.6 and 6.7 should provide identical results of predicted $E_{cm}(t)$. However, if both of the compressive strength and elastic modulus are known, experimental results show different answers when different equations are chosen. Further analysis will compare these two methods in terms of accuracy of prediction.

$E_{cm}(t) = \exp(s(1-(\frac{28}{t})^{0.5})\ )^{0.3}\times 22\times\ \alpha\ (f_{cm}/10)^{0.3}$

$= \exp(0.3\times s(1-(\frac{28}{t})^{0.5}))\times E_{cm}$ (Eqn 6.7)

6.3.2 Prediction of Elastic Modulus Based on 28-day Compressive Strength

In this section, Equation 6.6 will be used to predict the elastic modulus based on the 28-day compressive strength. It is common that the testing facility can only test the compressive strength of concrete and lacks the ability of strain measuring unlike the work here. Thus, the strength-based prediction could be a more convenient method for practical work.

6.3.2.1 Determination of Coefficient α

The first step involves using Equation 6.6 to determine a more accurate value of coefficient α for the limestone aggregate used in this project. The coefficient α is an inherent property of a certain type of the coarse aggregate as discussed in Chapter 4. Thus, the value of α should be consistent throughout this project because limestone was the only coarse aggregate type for all the concrete mixes. The suggested value of α is set at 0.9 by both of EC2 and Model Code 2010. However, an experimental value of α is necessary for more precise mathematical calculation, as observed previously in Chapter 4.

To determine the value of α for further analysis, the baseline mix without any influence of GGBS and accelerating methods should be used as the standard mix. The predicted results of the elastic modulus can be calculated by Equation 6.6 to draw a continuous curve in Figure 6.32. The actual testing values are also plotted in Figure 6.32 for comparison.

For this prediction curve, the value of α is set at 0.9 as suggested by EC2. The comparison between the prediction and test values noticeably shows large errors at all the testing ages where the entire prediction curve is an over-estimation of the experimental results by a considerable proportion. Thus, to achieve better prediction, it is necessary to modify the default value of α from 0.9 to a suitable level. Figure 6.33 shows how the coefficient α affects the prediction curves by changing the value from 0.7 to 1.0. A visual observation suggests that reducing α from 0.9 to 0.8 can adjust the prediction curve to a more accurate level. However, due to variability of test results at 7 days, fitting curves in Figure 6.33 show a misleading impression that there is no further growth of modulus of elasticity after 7 days. Therefore, the curves in Figure 6.33 do not represent the further development of elastic modulus in the long term.

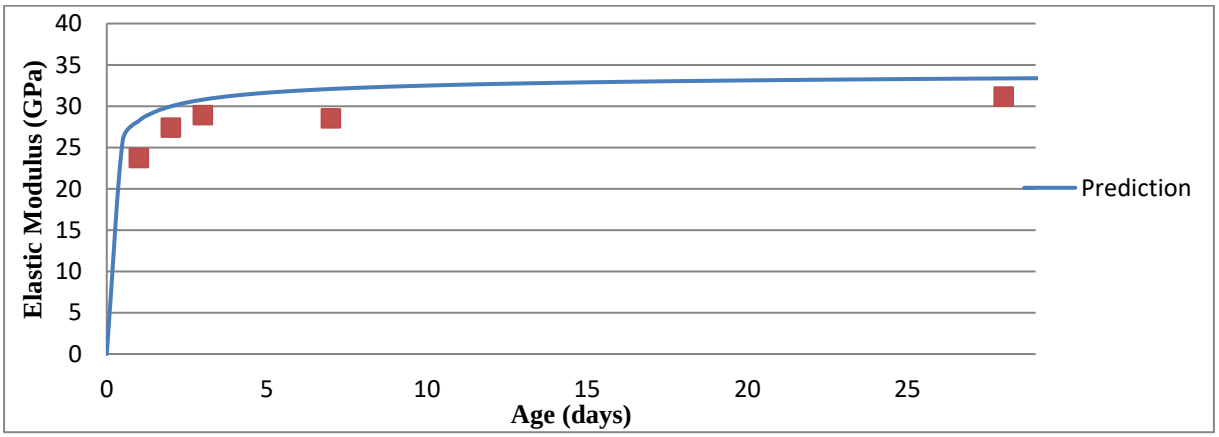

Figure 6.32 Comparison of predicted and actual elastic modulus for the baseline mix when α=0.9

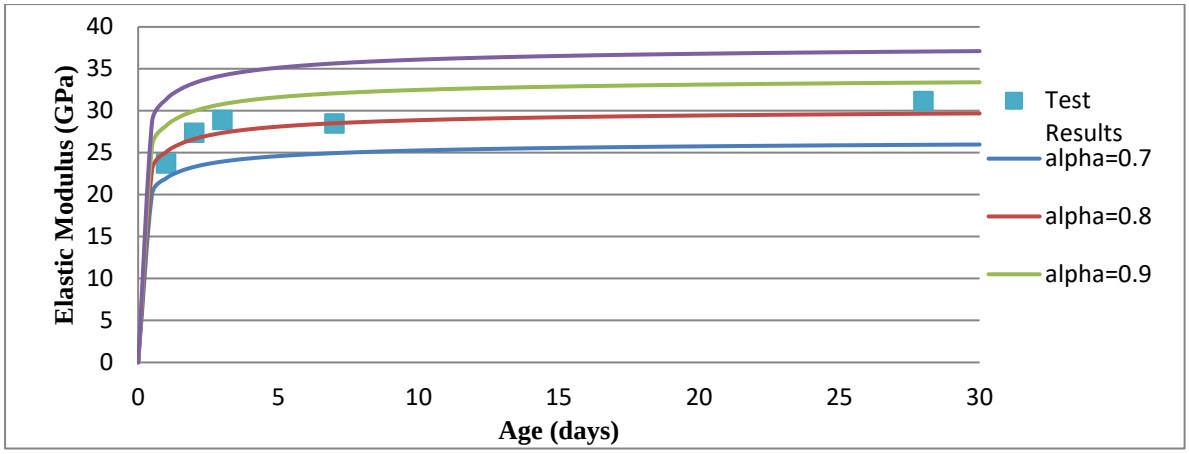

Figure 6.33 Various prediction curves when α is changing from 0.7 to 1.0

Again, using the least square method can be used to find the best fitted curve by calculating and maximizing the R squared value. As the value of α is reduced from 0.9 to a lower value, the R squared values are significantly improved and reach the maximum value when α=0.82, as shown in Table 6.21. Thus, the calculation suggests that the best fitting curve occurs when α=0.82, and Figure 6.34 shows that this best fitting curve is significantly closer to the test results than the previous one in Figure 6.32.

α	0.89	0.88	0.87	0.86	0.85	0.84	0.83	0.82	0.81	0.80	0.79
R^2	-0.30	-0.03	0.21	0.41	0.57	0.68	0.76	0.81	0.80	0.76	0.68

Table 6.21 Modifying the coefficient of α to find out the best fitting curve

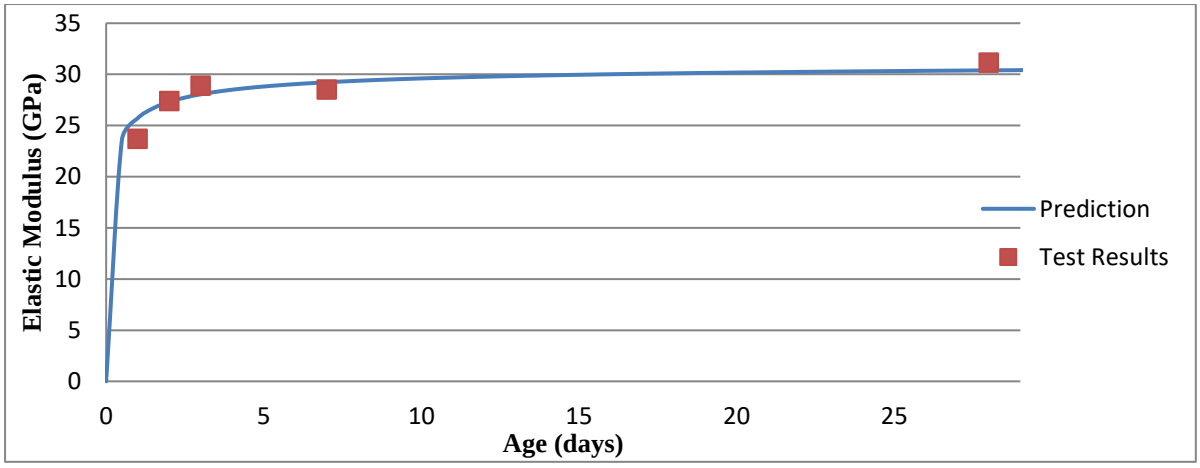

Figure 6.34 Comparison of predicted and actual elastic modulus for the baseline mix when α=0.82

Therefore, for this aggregate type of limestone, the default value of α is set at 0.82 for further analysis to achieve a better accuracy of theoretical predictions. This value is lower

than that suggested by EC2, and in Chapter 4, experimental results demonstrate that the EC2 generally overestimates all types of building stone.

6.3.2.2 Influence of GGBS

Figure 6.35 plots the predicted curves of the elastic modulus calculated by Equation 6.6 for CEM II/A-L mix with 70% GGBS. The large error between testing points and the predicted curve demonstrates poor curve fitting by using Equation 6.6 directly for a concrete mix with high percentage GGBS. To find a better fitting curve based on Equation 6.6, a new coefficient m is introduced in Equation 6.8 to modify the index value of $f_{cm}(t)/10$ which is 0.3 by default.

$$E_{cm}(t) = 22\times\alpha\times((f_{cm}\times\exp(s(1-(\frac{28}{t})^{0.5}))10)^{m} \qquad \text{(Eqn 6.8)}$$

By modifying the value of coefficient m, a better fitting curve can be found and drawn in Figure 6.36. A series of values of m are input into an excel table which outputs the R^2 values for each value of m. In this case, the R^2 value reaches the maximum when m is increased to 0.360. The visual comparison between Figure 6.35 and 6.36 demonstrates a significant improvement by reducing the errors of the prediction curves to a considerably lesser degree. Consequently, the R squared value reaches the peak at 0.859 in Figure 6.36, compared with the previous one of 0.793 in Figure 6.35. It is accepted, however, that there is experimental error in the data points.

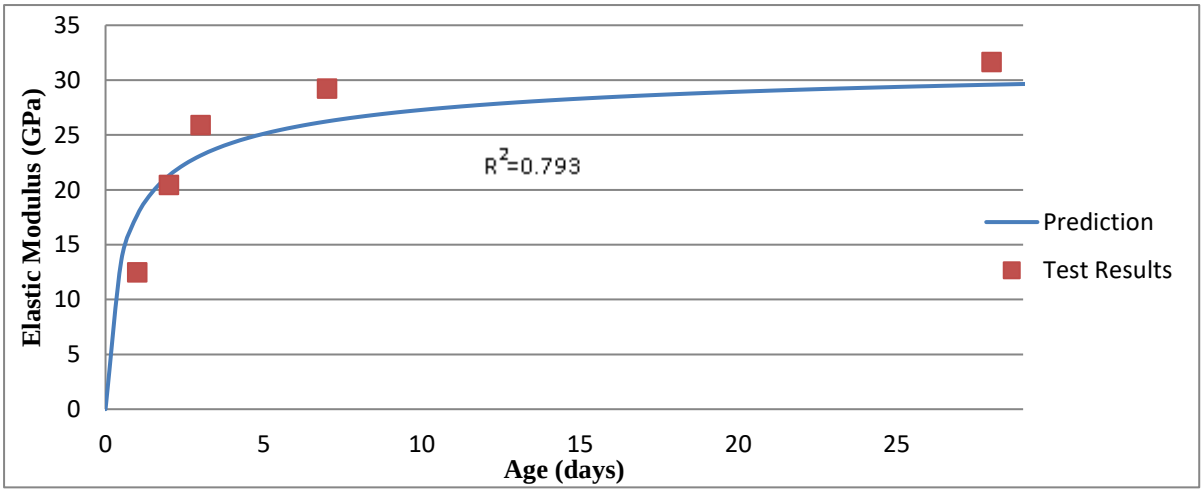

Figure 6.35 Comparison of prediction curve and testing results for the CEM II/A-L mix with 70% GGBS when m=0.300

In further discussions, best fitting curves will be determined by the same method of modifying coefficient m, using a consistent value of α of 0.82.

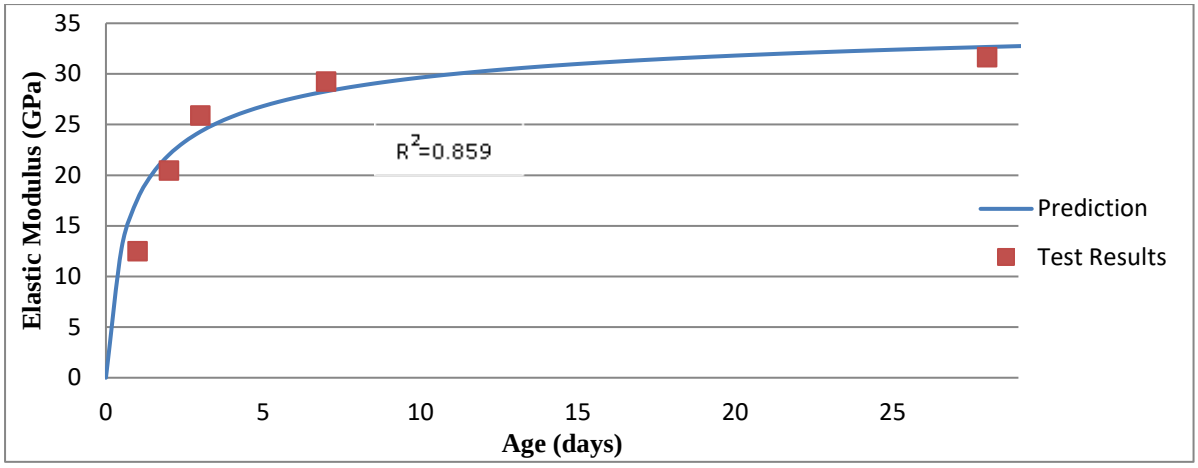

Figure 6.36 Comparison of prediction curve and testing results for the CEM II/A-L mix with 70% GGBS when m=0.360, using a constant value of α of 0.820

Figure 6.37 demonstrates all best fitting curves of the four CEM II/A-L mixes with different proportions of GGBS content and Table 6.22 shows the relative values of coefficient m and R squared values of each mix. The general accuracy of these prediction curves is not ideal because of the large gaps between the testing points and the prediction curve. Only the mix 30% GGBS has a relatively good result compared to the other three mixes. The visual comparison matches the results in Table 6.22 where the 30% GGBS mix has the largest R squared value of 0.954. It should be remembered, again, that the experimental results do have random variations which affect the fitted m values.

On the early-age side, large errors appeared mainly on the first day of concrete development which is highly relevant here. Figure 6.37 shows that the theoretical predictions overestimated the 1-day and 2-day elastic modulii, especially for the mix with 70% GGBS. Therefore, Equation 6.8 cannot achieve an entirely consistent prediction during the early age of concrete development. When the 1-day elastic modulus is significantly reduced by a high dosage of GGBS content, the error of Equation 6.8 is even greater than the case without GGBS content.

In the long-term, the test results are relatively close to each other regardless of the dosages of GGBS content. Thus, the GGBS content shows insignificant effect on the 28-day elastic modulus from 0% dosage to 70% dosage. However, the prediction curves do not converge as they went through the age of 28 days. Particularly, the 70% GGBS curve will diverge from the other curves and cause large errors if the prediction is needed at a much later age.

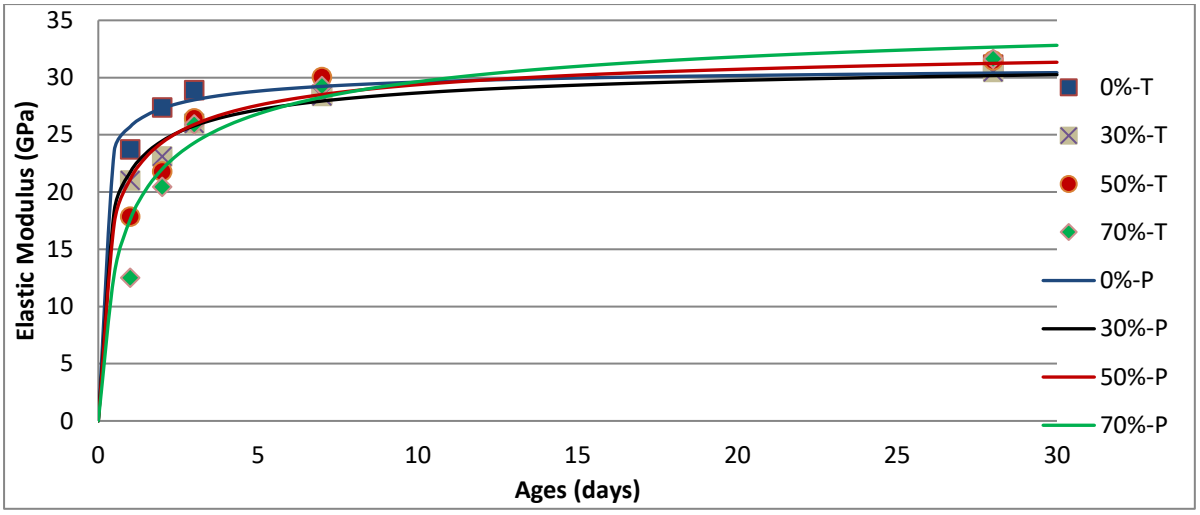

Figure 6.37 Comparison of prediction curves and testing results for CEM II/A-L mixes with various proportions of GGBS content

	0% GGBS	30% GGBS	50% GGBS	70% GGBS
m	0.300	0.294	0.326	0.360
R^2	0.803	0.954	0.848	0.859

Table 6.22 Values of coefficient m and R squared values for CEM II/A-L mixes

Values of coefficient m in Table 6.22 demonstrate a generally increasing trend along with the rising proportions of GGBS content. For mixes containing 0% GGBS and 30% GGBS, the optimal values of m are almost the same to the default 0.3 proposed by EC2. When 50% and 70% GGBS are introduced into the concrete mixes, the values of coefficient m are required to be increased to 0.326 and 0.360 respectively to achieve the best fitting curves.

The higher values (>0.3) of coefficient m for concrete mixes with high proportions of GGBS imply that there is a significant difference between compressive strength and elastic modulus in terms of the influence of GGBS content. As the proportion of GGBS content rises over 50%, both the compressive strength and elastic modulus have been reduced significantly during the early-age concrete development. However, the compressive strength undergoes a greater reduction compared to the elastic modulus. Thus, the prediction based on the 28-day compressive strength is consequently lower than the testing results. Therefore, a higher value of m is required to compensate for the error by lifting the prediction curve in Figure 6.35 to a higher range in Figure 6.36. The adjustment of coefficient m also implies that the modelling equation of elastic modulus, which is based on the compressive strength, may not be appropriate. Other influencing factors could be introduced for more accurate predictions in future research, e.g., cement types or water/cement ratio.

6.3.2.3 Influence of Acceleration Methods

RHPC:

Figure 6.38 displays the prediction curves of RHPC mixes with different proportions of GGBS content from 0% to 70%. The overall test results of early-age elastic modulus are enhanced by the effects of using RHPC compared with Figure 6.37, while this accelerating effect faded away after 3 days.

It appears that the errors in the prediction curves in Figure 6.38 are generally smaller than previous case of mixes with CEM II/A-L except the 0 %GGBS mix. For 50% GGBS and 70% GGBS mixes, Table 6.23 shows that the R squared values are significantly improved to 0.947 and 0.930 from 0.848 and 0.859 respectively, previously.

Comparing the values of coefficient m in Table 6.22 and 6.23, there is no obvious influence of RHPC. Thus, the methods of predicting elastic modulus by Equation 6.8 are similar for both types of cement. Again, the effect of GGBS content causes an increasing trend of coefficient m from 0.305 for the 0% GGBS mix to 0.371 for the 70% GGBS mix.

	0% GGBS	30% GGBS	50% GGBS	70% GGBS
m	0.305	0.320	0.366	0.371
R^2	0.655	0.936	0.947	0.930

Table 6.23 Values of coefficient m and R squared values for RHPC mixes

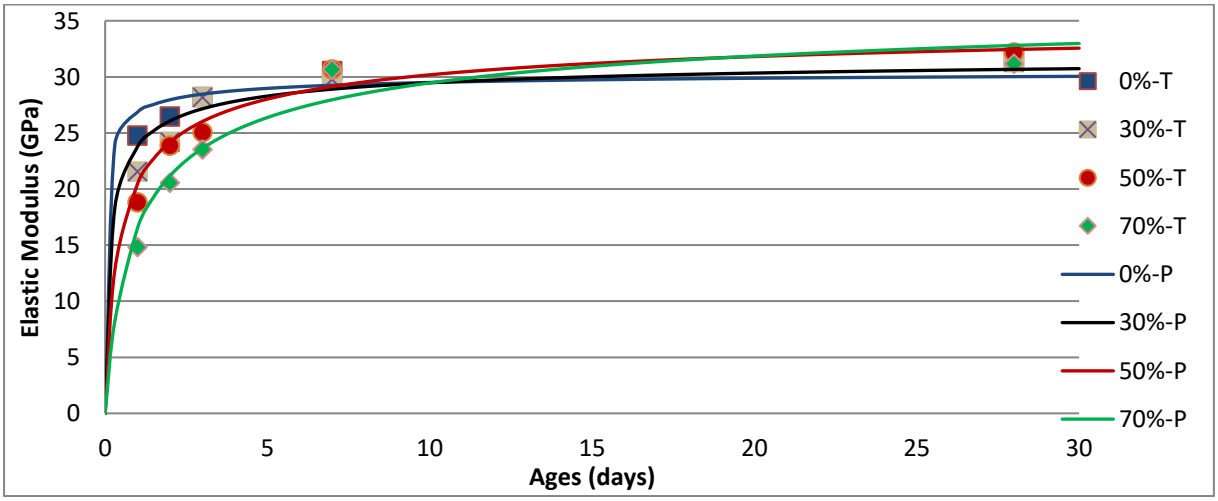

Figure 6.38 Comparison of prediction curves and testing results for RHPC mixes with various proportions of GGBS content

Accelerator:

When the accelerator is introduced into the CEM II/A-L concrete mixes, the early-age elastic modulus is generally higher in Figure 6.39 than that in Figure 6.37. Also, the differences between mixes with various proportions of GGBS content are smaller in Figure 6.39. Similarly, to the RHPC concrete mixes, the prediction curves for three mixes with GGBS content are relatively accurate and close to the testing point. Only the curve for the mix without GGBS content has large errors on both of the early-age and long-term sides.

Values of coefficient m in Table 6.24 have similar features with previous discussions. Primarily, the extra addition of GGBS content has a large impact on the coefficient m, while the accelerator does not influence it significantly, as observed when comparing Table 6.22 and Table 6.24.

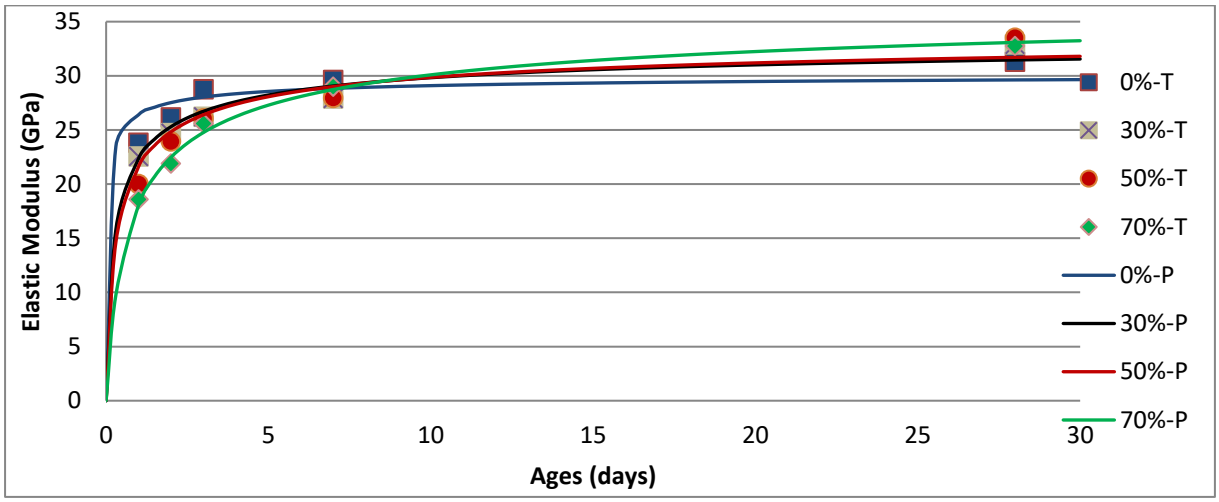

Figure 6.39 Comparison of prediction curves and testing results for CEM II/A-L + accelerator mixes with various proportions of GGBS content

	0%GGBS	30% GGBS	50% GGBS	70% GGBS
m	0.297	0.314	0.324	0.352
R^2	0.640	0.933	0.921	0.988

Table 6.24 Values of coefficient m and R squared values for CEM II/A-L + accelerator mixes

Thermal curing:

Figure 6.40 demonstrates that the influence of thermal curing on the elastic modulus is greater than those of RHPC and the accelerator. On the early-age side, mixes with 30%, 50% and 70% GGBS have relatively close test results. Some testing points of the 70% GGBS mix are even higher than those of the 50% GGBS mix, which is within experimental error. Thus, for the modulus of elasticity, the reduction effect of GGBS content is largely offset by the thermal curing method. This is also largely due to the narrowing of differences between calculated values mathematically as a consequence of the index m being significantly less than 1 in Equation 6.8.

On the long-term side, the 28-day results did not converge to a narrow range as the previous ones in Figures 6.37, 6.38 and 6.39 did. The greater values of coefficient m (0.363 and 0.373) for mixes with 50% and 70% GGBS cause significant variations of theoretical predictions at 28 days because the other two mixes still have the coefficient m close to the initial value of 0.3. As a result, the prediction curves for mixes with 50% and 70% GGBS are considerably higher than the other two curves on the long-term side in Figure 6.40. The side-effect of using thermal curing methods causes random and noticeable errors in the 28-day elastic modulus prediction. Again, the mix without GGBS has the largest error of the prediction curve with the lowest result of R squared value in Table 6.25.

Although the thermal curing method has a strong impact on the elastic modulus, the distribution of coefficient m across different proportions of GGBS content in Table 6.25 is still similar to the initial result of coefficient m in Table 6.22. Therefore, the initial value of 0.3 of coefficient m can be applied for concrete mixes with all the three accelerating methods without modification. A different value of coefficient m is only necessary when a different GGBS content is used into the mix.

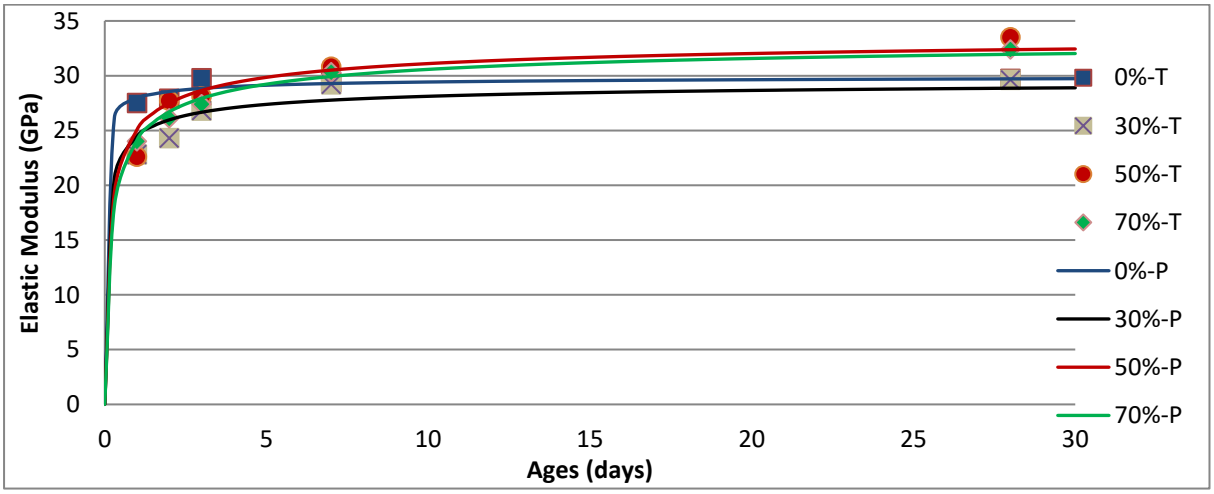

Figure 6.40 Comparison of prediction curves and testing results for thermal curing mixes with various proportions of GGBS content

	0%GGBS	30%GGBS	50%GGBS	70%GGBS
m	0.307	0.293	0.363	0.373
R^2	0.682	0.768	0.880	0.977

Table 6.25 Values of coefficient m and R squared values for thermal curing mixes

6.3.2.4 Influence of Combined Methods

RHPC + Accelerator:

Comparing Figure 6.38 and 6.41, the combined effect of RHPC and the accelerator provides little improvement to the concrete mixes with RHPC alone. Only the mix without GGBS content shows some improvements during the first 2 days of concrete development. The largest error among these prediction curves in Figure 6.41 still comes from the 0% GGBS mix with a low R squared value of 0.503. No matter what value of coefficient m is selected, the prediction curve cannot fit the test point better on both early-age and long-term sides simultaneously because the function shape of Equation 6.8 is predetermined by the coefficient s which is calculated in the previous section on strength prediction. This problem will be solved in further discussions where a new equation based on the 28-day elastic modulus will replace Equation 6.8 that is based on 28-day compressive strength.

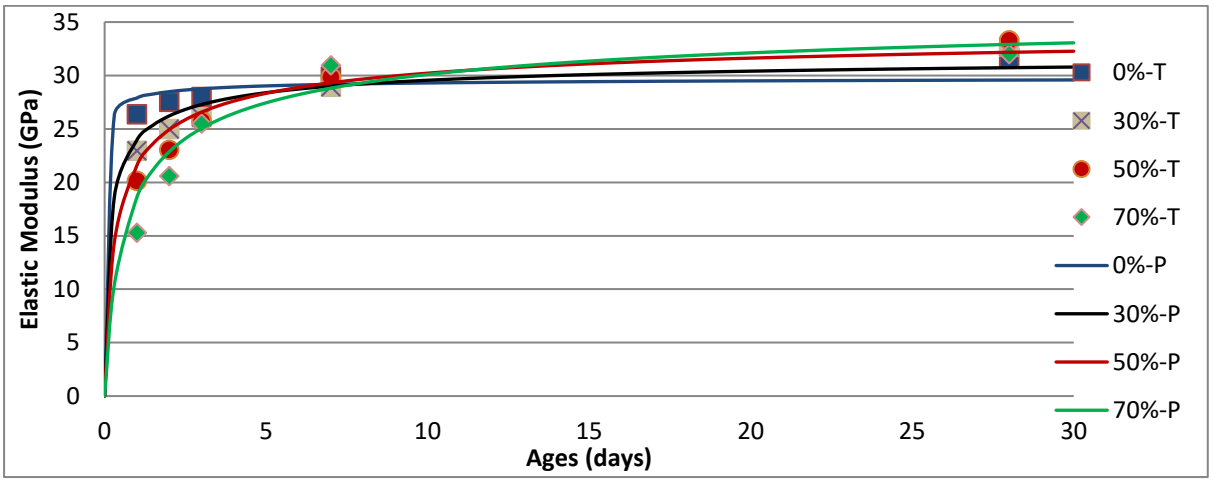

Figure 6.41 Comparison of prediction curves and testing results for RHPC + accelerator mixes with various proportions of GGBS content

The combined method requires similar values of coefficient m to generate the best fitting curve compared with the single accelerating method discussed above. GGBS content is still the dominating factor for the variation of coefficient m based on the results in Table 6.26.

	0% GGBS	30% GGBS	50% GGBS	70% GGBS
m	0.296	0.297	0.322	0.369
R^2	0.503	0.864	0.929	0.891

Table 6.26 Values of coefficient m and R squared values for RHPC + accelerator mixes

RHPC + Thermal curing:

When the thermal curing method is applied to the RHPC mixes, the test points in Figure 6.42 are significantly higher than those in Figure 6.37 by a large proportion. The difference between the 50% GGBS and 70% GGBS mixes is visually indecisive in Figure 6.42 since the effect of high dosage of GGBS content is offset by the combined methods.

The prediction curves of 50% GGBS and 70% GGBS mixes are relatively accurate in following the trend of the test points. In this case, the R squared value of 30% GGBS mix is the lowest in Table 6.27 since there is an unexpectedly high testing results at 3 days.

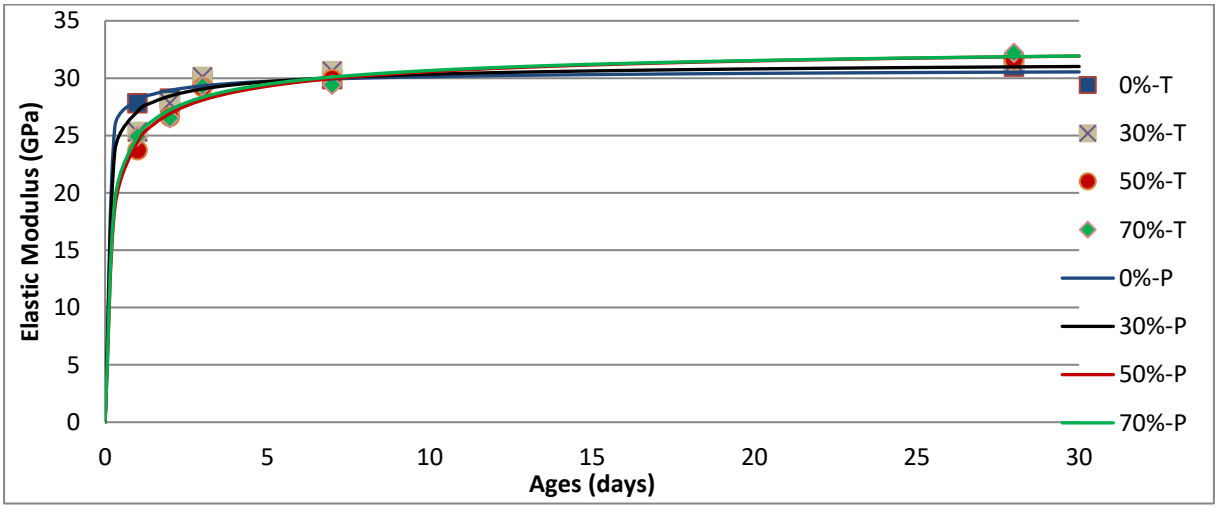

Figure 6.42 Comparison of prediction curves and testing results for RHPC + thermal curing mixes with various proportions of GGBS content

	0% GGBS	30% GGBS	50% GGBS	70% GGBS
m	0.319	0.339	0.347	0.374
R^2	0.846	0.786	0.947	0.935

Table 6.27 Values of coefficient m and R squared values for RHPC + thermal curing mixes

RHPC + Thermal curing + Accelerator:

The early-age development of the elastic modulus of the 70% GGBS mix in Figure 6.43 is even faster than that of the baseline mix without GGBS in Figure 6.37 when three accelerating methods are applied together. The difference between the 0% GGBS and 70% GGBS mixes in Figure 6.43 is also smaller than the corresponding difference in Figure 6.37 since the effect of high dosage GGBS can be reduced by these three accelerating method to a large extent. The increments of the elastic modulus from 1 day to 3 days in Figure 6.43 is also much smaller than those in Figure 6.37 because the early-age effect of GGBS is compensated for much better with all three techniques.

Both prediction curves are accurate by visual observation, and the results of R squared values in Table 6.28 are greater than 0.930 and relatively good. Again, a higher value of coefficient m for better prediction is needed for the mix with a higher dosage of GGBS. For the concrete mix without GGBS, the best result of coefficient m is slightly greater than the initial value 0.3.

	0% GGBS	70% GGBS
m	0.313	0.346
R^2	0.931	0.947

Table 6.28 Values of coefficient m and R squared values for mixes under all accelerating methods

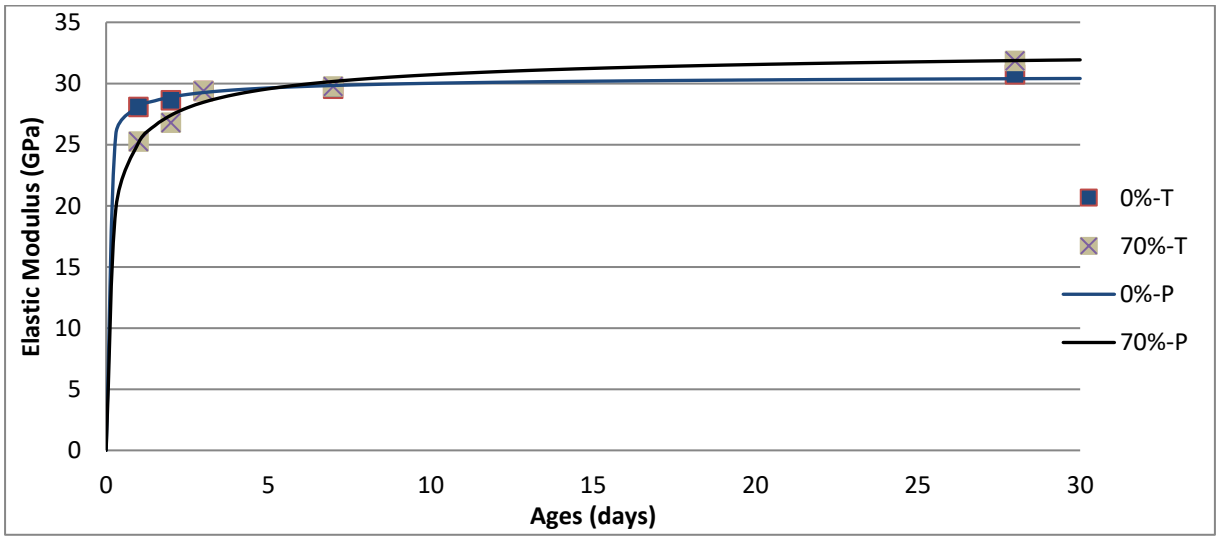

Figure 6.43 Comparison of prediction curves and testing results for mixes under all accelerating methods with various proportions of GGBS content

6.3.2.5 Summary of Coefficient m:

Table 6.29 demonstrates an overall view of the numerical results of coefficient m across various mix designs and different proportions of GGBS content. Analysing this table in a vertical view, most results of coefficient m locate around the average value with small deviations which are generally lower than 5%. The specific influence of each accelerating method or any combined method on the coefficient m are generally indecisive through this summary table. This is mainly due to the nature of Equation 6.8 which is entirely based on the 28-day compressive strength and previous prediction results of strength development. The influences of various accelerating techniques are already taken into account before the predicting calculation of elastic modulus. Concerning the practical work, it is viable to assume that these accelerating method have little influence to the coefficient m and an average result can be used for all cases.

	GGBS			
	0%	30%	50%	70%
Baseline	0.300	0.294	0.326	0.360
RHPC	0.305	0.320	0.366	0.371
Accelerator	0.297	0.314	0.324	0.352
Thermal curing	0.307	0.293	0.362	0.373
RHPC+accelerator	0.296	0.297	0.332	0.369
Thermal Curing + RHPC	0.319	0.339	0.347	0.374
Thermal Curing + RHPC + accelerator	0.313	n/a	n/a	0.346
Average	0.305	0.310	0.343	0.364

Table 6.29 Results of coefficient m

However, to find out average values of coefficient m, it is necessary to consider the effect of GGBS content. As discussed previously, a higher value of coefficient m is required to allow for the effect of GGBS, especially for concrete mixes with high dosages of GGBS content. Figure 6.44 plots the relationship between the coefficient m and the percentage of GGBS with a rising trend line. The function of this trend expresses this relationship in a numerical way. Therefore, Equation 6.8 can be rewritten into Equation 6.9 to include this influencing factor:

$$E_{cm}(t) = 22\times\alpha\times((f_{cm}\times\exp(s(1-(\frac{28}{t})^n))/10)^{(0.3+0.08p)} \quad \text{(Eqn 6.9)}$$

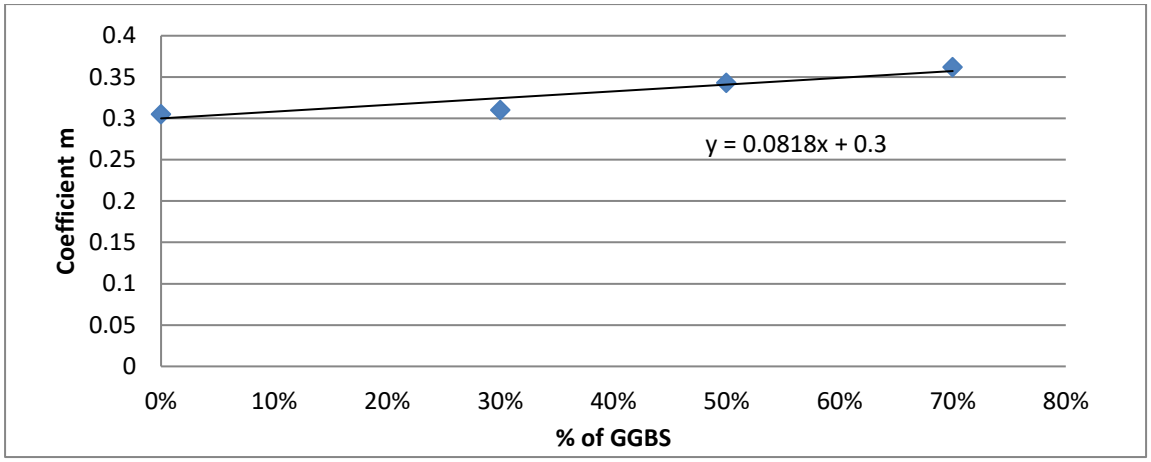

Figure 6.44 Coefficient m vs percentages of GGBS

where p is the percentage of GGBS content in the cementitious materials, $\alpha = 0.82$ and $n = 0.5$. The constant 0.08 is slope of trend line in Figure 6.44.

6.3.3 Prediction of Elastic Modulus Based on 28-day Elastic Modulus

When the 28-day elastic modulus can be acquired through practical tests, Equation 6.7 is an alternative time-based formula to predict the elastic modulus. The advantage of Equation 6.7 is that the influence of coarse aggregate is removed from the prediction formula. Thus, this formula can be used for concretes with various types of coarse aggregate without the initial determination of coefficient α.

$$E_{cm}(t) = (\exp(0.3\times s(1-(\frac{28}{t})^{0.5}))\times E_{cm} \qquad \text{(Eqn 6.7)}$$

Figure 6.45 plots the prediction curve calculated by Equation 6.7 from 1 day to 30 days. This curve certainly meets the test point at 28 days since Equation 6.7 is based on the 28-day elastic modulus. The accuracy of the prediction curve is reasonably good at 2 days and 3 days shown in Figure 6.45. However, the overestimations at 1 day and 7 days reduce the overall accuracy significantly and result in a low R squared value of 0.681.

To improve the overall accuracy of prediction, a new variable v is necessary to be introduced to replace constant (0.3×s). Thus, Equation 6.7 is transformed into a new form of function. This new equation has the same format as Equation 6.2 which is used to predict the development of compressive strengths, except with a different variable v, instead of s.

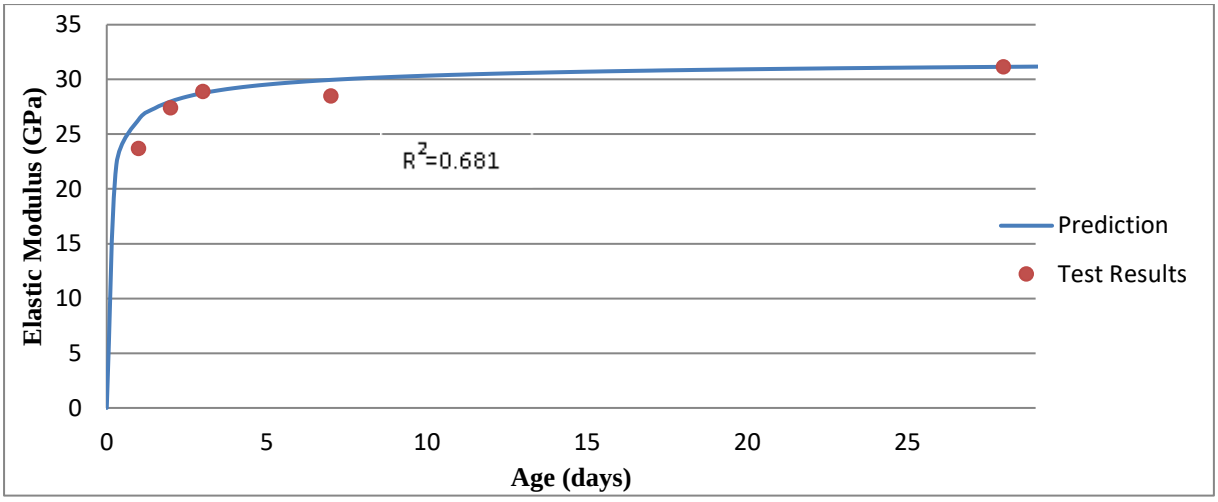

Figure 6.45 Comparison of prediction curve and testing results for the baseline mix

A varying coefficient v has a similar effect on the prediction curve discussed in Figure 6.2 previously. Therefore, by modifying the values of coefficient v, a best fitting curve can be acquired and is shown in Figure 6.46 when v = 0.056. The prediction curve is located in between the testing points from 1 day to 7 days and has a significantly better result of R squared value (0.882).

$$E_{cm}(t) = (\exp(v(1-(\frac{28}{t})^{0.5}))\times E_{cm} \qquad \text{(Eqn 6.10)}$$

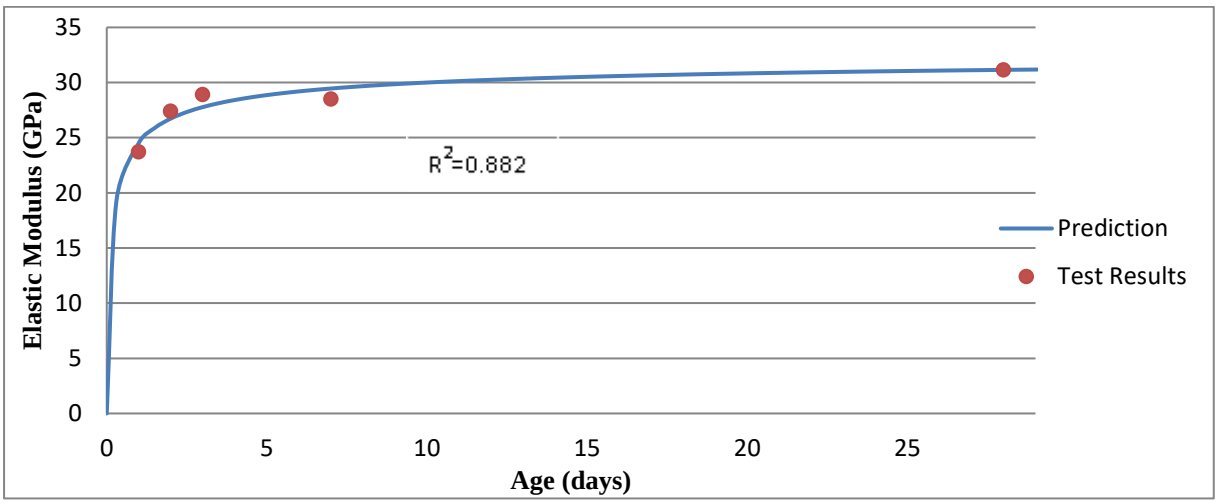

Figure 6.46 Comparison of prediction curve and testing results for the baseline mix when v=0.056

6.3.3.1 Influence of GGBS

For CEM II/A-L mixes with different proportions of GGBS, Figure 6.47 demonstrates all the best fitting curves drawn by Equation 6.10. Comparing to the corresponding curves drawn by Equation 6.8 in Figure 6.37, Equation 6.10 has significantly improved

performance in term of accuracy for all the mixes. The shapes of these curves are similar to each other and are more reliable to demonstrate the consistent effect of GGBS from 0% to 70% dosages. The first reason for this better performance of Equation 6.10 is that all the curves are fixed at points for their individual 28-day values, while curves drawn by Equation 6.8 can deviate significantly at the long-term side if the tested 28-day compressive strength has an unexpected error. Secondly, the results of R squared values in Table 6.30 are all greater than the corresponding ones in Table 6.22. With greater values of R squared, the theoretical predictions in Figure 6.47 are closer to the test points than that of Figure 6.37 to reflect the tested elastic modulus in a more accurate way.

To find out the best fitting curves for these four different mixes, a series of values of coefficient v are required and are shown in Table 6.30. The coefficient v is increased from 0.056 to 0.162 as GGBS content is added to mixes from 0% to 70%. This increasing trend of coefficient v is determined for the proportions of GGBS in a similar way discussed previously for coefficient s. The corresponding values of coefficient s for CEM II/A-L mixes are 0.13, 0.26, 0.28 and 0.40 discussed in section 6.2.2, which is a similar geometric type of progression to that shown in Table 6.30 for coefficient v. Therefore, for both of the compressive strength and elastic modulus, the effect of GGBS on the numerical prediction causes similar increasing trends for both of the coefficients s and v.

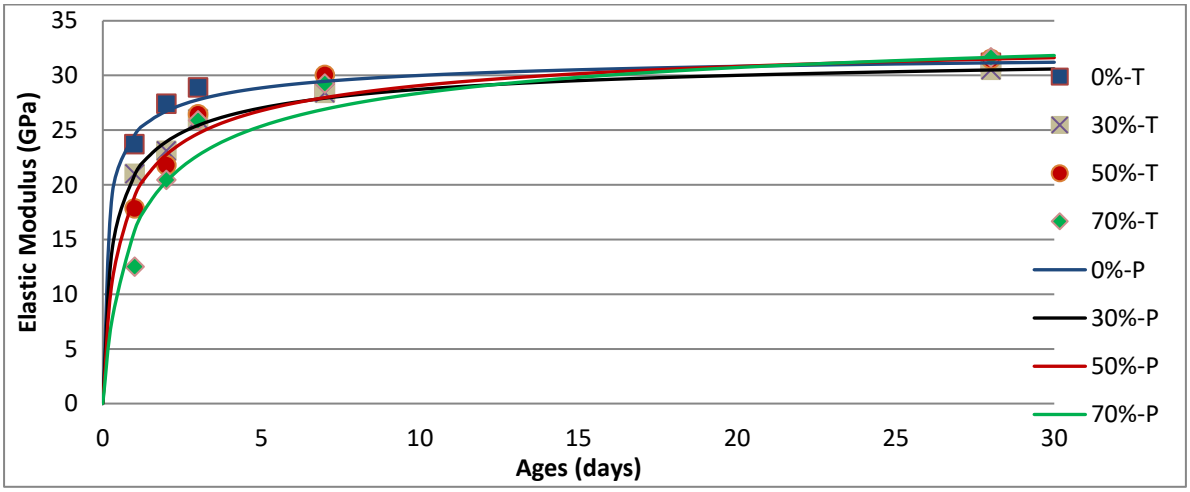

Figure 6.47 Comparison of prediction curves and testing results for CEM II/A-L mixes with various proportions of GGBS content by Equation 6.10

	0% GGBS	30% GGBS	50% GGBS	70% GGBS
v	0.056	0.088	0.119	0.162
R^2	0.882	0.979	0.927	0.886

Table 6.30 Values of R squared values for CEM II/A-L mixes

6.3.3.2 Influence of Acceleration Methods

RHPC:

As the early-age elastic modulus is considerably improved by the replacement of RHPC, the prediction curves in Figure 6.48 are also more accurate than those in Figure 6.38 drawn by Equation 6.8. Again, the 28-day elastic modulus based equation is significantly superior to the 28-day compressive strength based equation. The results of R squared values in Table 6.31 also confirms this fact with higher values for all mixes.

The increasing trend of coefficient v from 0.059 to 0.148 demonstrates the effect of GGBS once again. However, the comparison between CEM II/A-L and RHPC shows little differences in coefficient v even though the actual test results of elastic modulus have been improved by RHPC. It is not possible to conclude the systematic difference in coefficient v when RHPC is used because of the results in Table 6.31. Indeed, as the percentage of GGBS rises, it is not at all surprising that the change from CEM II/A-L to RHPC has a decreasing influence on coefficient v. Therefore, for the prediction of elastic modulus by Equation 6.10, there is no need to modify the coefficient v to suit the replacement of CEM II/A-L with RHPC.

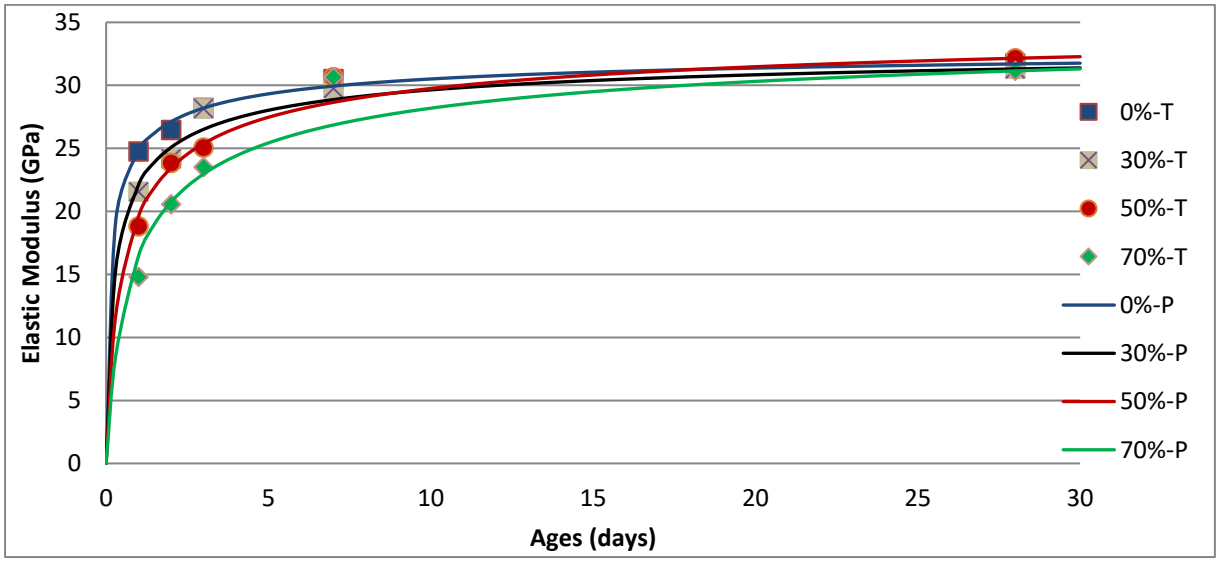

Figure 6.48 Comparison of prediction curves and testing results for RHPC mixes with various proportions of GGBS content by Equation 6.10

	0% GGBS	30% GGBS	50% GGBS	70% GGBS
v	0.059	0.081	0.115	0.148
R^2	0.979	0.929	0.958	0.909

Table 6.31 Values of R squared values for RHPC mixes

Accelerator:

Equation 6.7 produces accurate prediction curves in Figure 6.49 for CEM II/A-L mixes with an accelerator once again. However, the greater differences among the 28-day elastic modulii result in larger variations of prediction curves in the long-term. The continuously high result of R squared values in Table 6.32 suggests that Equation 6.10 is relatively adequate for concrete mixes influenced by this accelerating admixture.

The coefficient v is still increasing as more cement is replaced by GGBS content in Table 6.32. The effect of the accelerator slightly increases the coefficient v for mixes with 0%, 30% and 50% GGBS. However, the 70% GGBS mix contradicts this trend with a reduced coefficient v of 0.145. Again, a comparison between Table 6.30 and 6.32 cannot determine a clear influence of the accelerator in terms of coefficient v due to the magnitudes of differences.

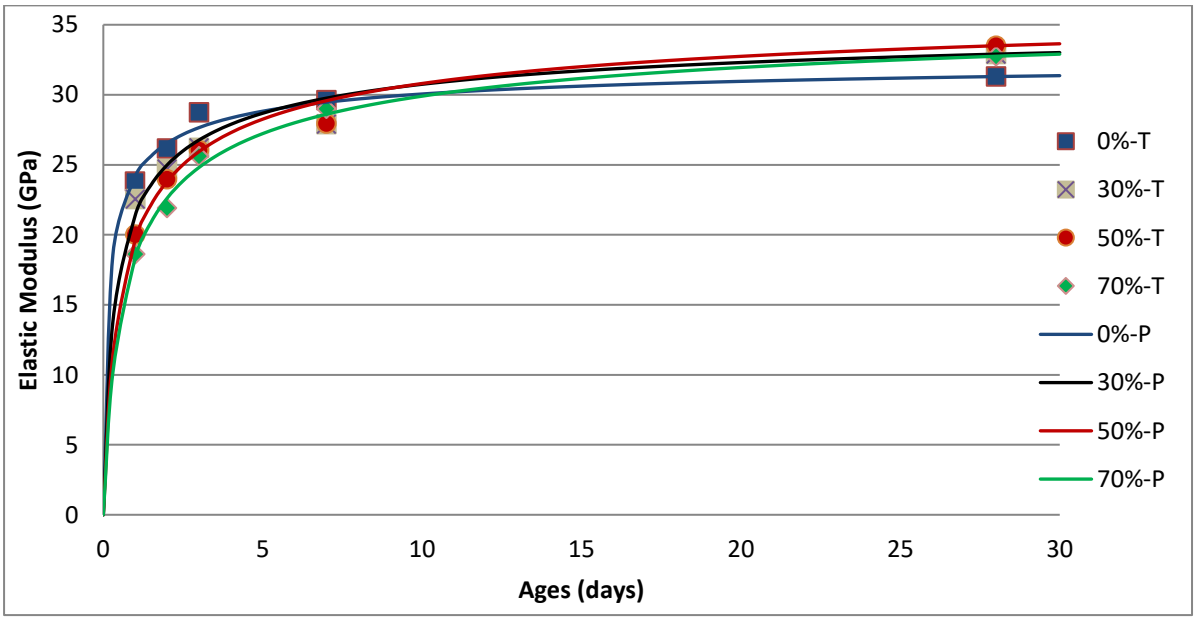

Figure 6.49 Comparison of prediction curves and testing results for CEM II/A-L + accelerator mixes with various proportions of GGBS content by Equation 6.10

	0% GGBS	30% GGBS	50% GGBS	70% GGBS
v	0.060	0.100	0.125	0.145
R^2	0.957	0.915	0.972	0.989

Table 6.32 Values of R squared values for CEM II/A-L + accelerator mixes

Thermal Curing:

For mixes thermally cured, large differences among the 28-day elastic modulus cause irregular shapes of prediction curves in Figure 6.50. Especially for the mix without GGBS content, an unexpected high value of 3-day elastic modulus reduces the R squared values of this prediction to 0.698. The other three prediction curves are still more accurate than those calculated by Equation 6.8.

A significantly large reduction of coefficient v in Table 6.33 demonstrates the thermal curing method has a greater impact on the numerical prediction than the other two accelerating methods.

Similarly, the coefficient s also experienced such reduction when thermal curing was applied. For mixes without GGBS, the values of coefficient v are reduced to 0.026 from 0.056 by the effect of thermal curing and results in a prediction curve with a highly reduced slope in Figure 6.50.

	0% GGBS	30% GGBS	50% GGBS	70% GGBS
v	0.026	0.059	0.084	0.074
R^2	0.698	0.921	0.973	0.988

Table 6.33 Values of R squared values for thermal curing mixes

As the test points of the 70% GGBS mix is even higher than those of the 50% GGBS mix, the increasing trend of coefficient v also reverses in Table 6.33 from 0.084 to 0.074. The possible reason is that the thermal curing method can strongly enhance the early-age development of concrete mixes with high percentages of GGBS and reduce early-age gaps between the mixes containing 50% and 70% GGBS.

Within an acceptable experimental error, the 1-day elastic modulus of 70% GGBS mix can be higher than that of the 50% GGBS mix because the systematic difference between these two mixes is smaller than the random variations.

6.3.3.3 Influence of Combined Methods

RHPC+Accelerator:

Figure 6.51 plots the prediction curves for RHPC mixes with an accelerator. In general, Equation 6.10 performs better than Equation 6.8 in terms of accuracy with an appropriate value of coefficient v again. The results of R squared values in Table 6.34 are all above 0.9, indicating good fits of these prediction curves. To achieve the best fitting curves, values of coefficient v are listed in Table 6.34 for each mix.

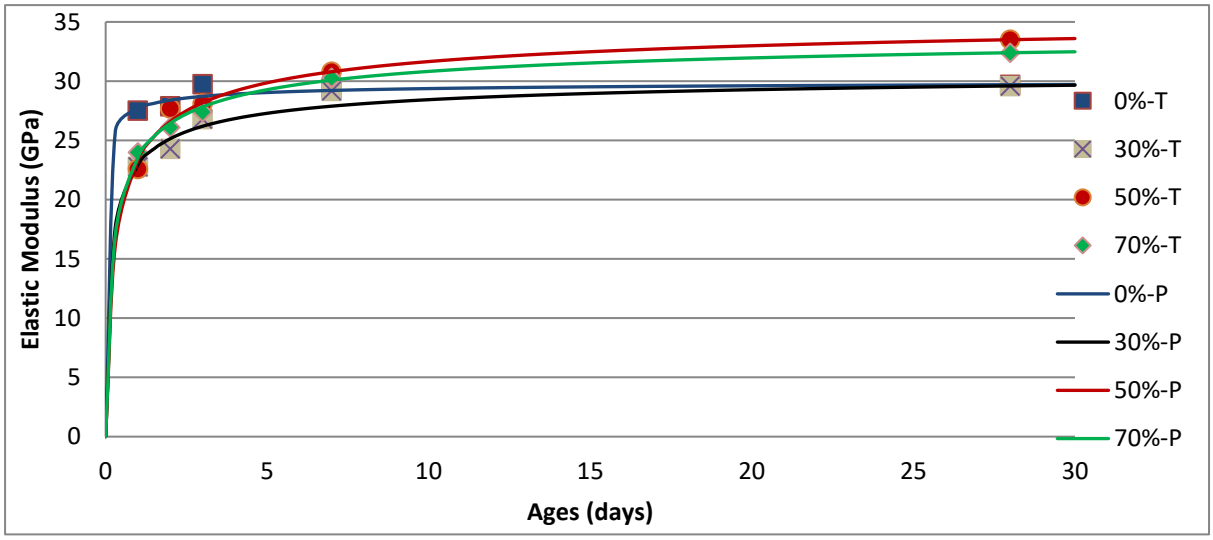

Figure 6.50 Comparison of prediction curves and testing results for thermal curing mixes with various proportions of GGBS content

	0% GGBS	30% GGBS	50% GGBS	70% GGBS
v	0.048	0.093	0.123	0.146
R^2	0.947	0.953	0.991	0.909

Table 6.34 Values of R squared values for RHPC + accelerator mixes

Comparing these values to those of the CEM II/A-L mixes in Table 6.30, two of them (0% and 70%) are lower than previous results whereas the other two (30% and 50%) indicate opposite results. It is difficult to conclude definitely the effect of this combined method in terms of coefficient v based on the limited quantity of results. The systematic influence of this combined accelerating method could be still less than the experimental error.

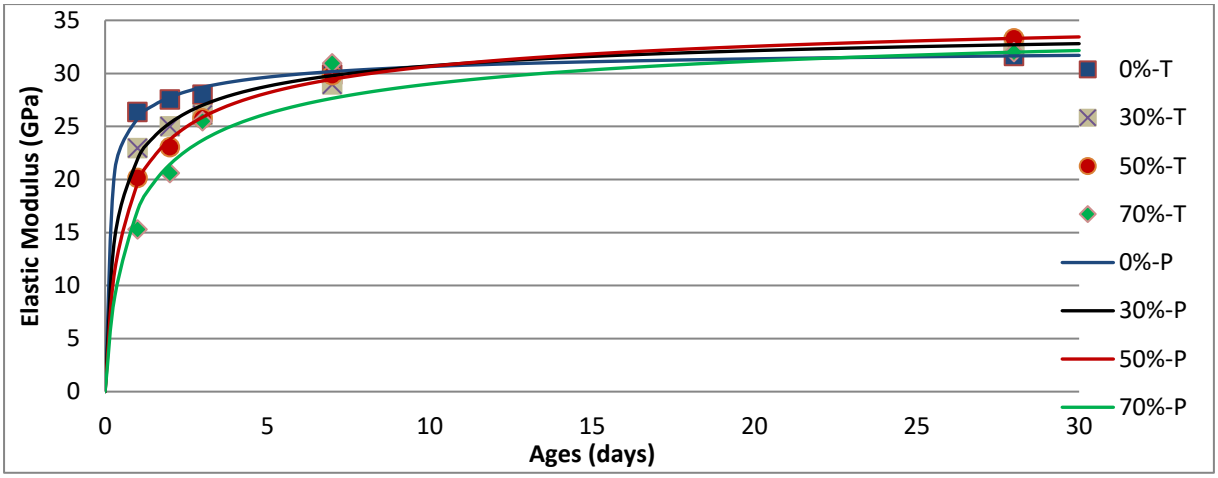

Figure 6.51 Comparison of prediction curves and testing results for RHPC + accelerator mixes with various proportions of GGBS content

RHPC + Thermal curing:

Figure 6.52 shows a series of excellent prediction curves which are close to each other due to the combined effect of RHPC and thermal curing treatment. The retardation effect of GGBS content on the elastic modulus is largely reduced by this combined accelerating method from a 30% dosage to a high dosage of 70% GGBS.

The corresponding values of coefficient v in Table 6.35 to achieve these curves are similar to the results in Table 6.33 where only thermal curing is applied. Thus, both groups of concrete mixed under thermal curing treatment have significantly lower results of coefficient v than other concrete mixes under normal curing process. The replacement of cement from CEM II/A-L to RHPC did not affect the results strongly in this combined method.

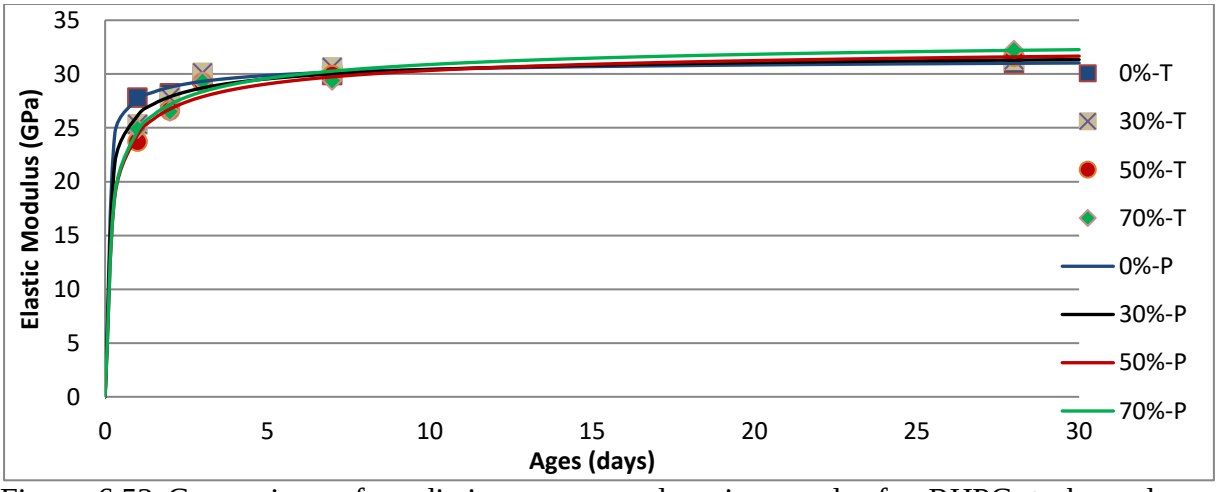

Figure 6.52 Comparison of prediction curves and testing results for RHPC + thermal curing mixes with various proportions of GGBS content

	0% GGBS	30% GGBS	50% GGBS	70% GGBS
v	0.027	0.042	0.061	0.062
R^2	0.902	0.877	0.943	0.933

Table 6.35 Values of R squared values for RHPC + thermal curing mixes

RHPC + Thermal curing + Accelerator:

All the accelerating methods were applied simultaneously for two concrete mixes which contained no GGBS and 70% GGBS. These two predicted curves in Figure 6.53 are grouped closely during the early age with approximately 10% variation at 1 day. The retardation effect of this high dosage of GGBS can be overcome by this combined method of all three techniques and is accurately predicted by the mathematical model of Equation 6.10.

This combined method requires the lower values of coefficient v to draw the best fitting curves in Figure 6.53. For all the mixes with 70% GGBS, the value of coefficient v of 0.55 is the smallest one compared to previous results. The accuracy of these prediction curves are visibly good in Figure 6.53, and are proved to be acceptable based on the R squared values (0.919 and 0.947) in Table 6.36.

	0% GGBS	70% GGBS
v	0.023	0.055
R^2	0.919	0.947

Table 6.36 Values of R squared values for mixes under all accelerating methods

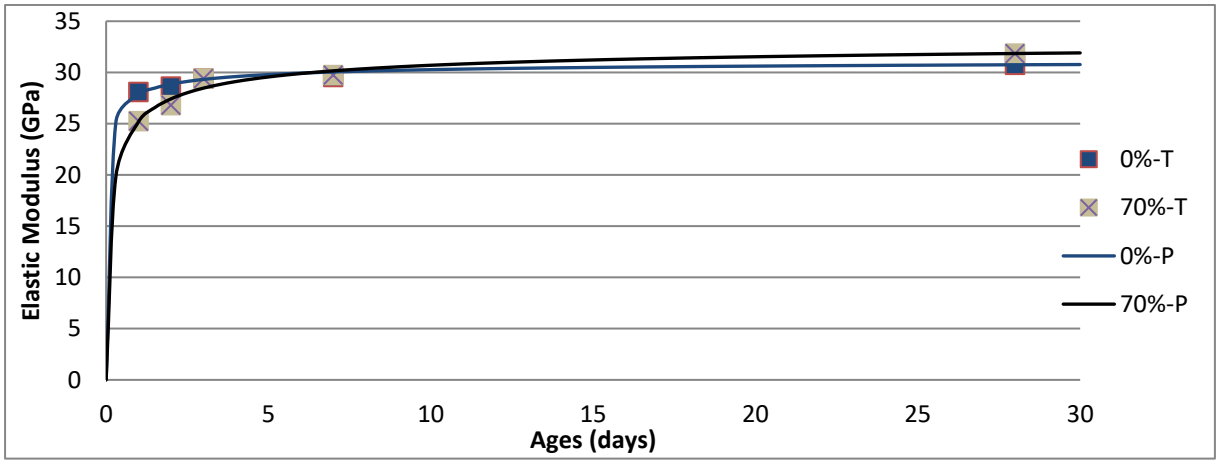

Figure 6.53 Comparison of prediction curves and testing results for mixes under all accelerating methods with various proportions of GGBS content

6.3.3.4 Summary of Coefficient v

The role of coefficient v in Equation 6.10 is relatively similar to the coefficient s in Equation 6.2. When GGBS content is adding to concrete mixes, a higher value of coefficient is required to compensate for the retardation effect of GGBS. On the other hand, lower values of coefficient v might be needed for concrete mixes accelerated by extra materials or treatment. Furthermore, the thermal curing methods is a significantly greater factor that influences this coefficient than the other two accelerating method. To analyse the suggested values of coefficient v for any mix design, Figure 6.54 demonstrates the results in a general picture to show an overall distribution of coefficient v into two categories, those which have little influence on coefficient v and those that significantly change the values of v for any given GGBS content.

Based on the trend lines shown in Figure 6.54, results can be separated into two categories. The first group of results contain all the concrete mixes under normal curing conditions. Unlike the previous condition of coefficient s, neither of RHPC, nor the accelerator demonstrate a strong influence on the coefficient v compared to the original CEM II/A-L mixes. The similarity is persistent through different proportions of GGBS content. Even the combined result of these two accelerating methods cannot achieve lower values of coefficient v.

For these concrete mixes, only the proportions of GGBS are the deciding factor on how the coefficient v varies for different conditions. Therefore, an empirical formula can be assumed to calculate the suggested values of coefficient v.

$$v = 0.15p + 0.05 \quad \text{(Eqn 6.11)}$$

where p is the percentage of GGBS.

The second groups of results involve the results of concrete mixes which were thermally cured. There is a quite distinct gap between the trend lines of these concrete mixes and the others above them. The thermal curing treatment strongly changes the growing path of the elastic modulus. As a result, the shape of prediction curve has also been changed by a significantly low value of coefficient v.

The thermal curing method has also been proved to be strongly effective for concrete mixes containing high dosage of GGBS. Therefore, as GGBS content is adding into the concrete mixes, the growing rate of coefficient v is also slower than the other trend lines

above. With the help of RHPC and the accelerator, the thermally treated mixes have a further reduction of coefficient v in Figure 6.54. The following empirical formulae can be used to assume an appropriate value of coefficient v under different accelerating methods.

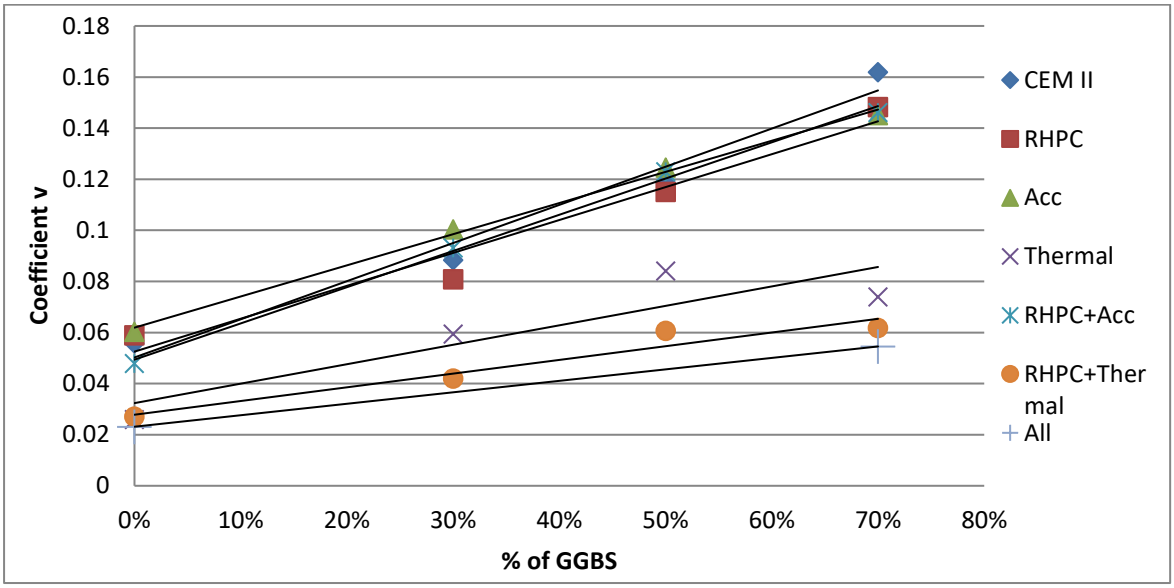

Figure 6.54 Coefficient v vs percentage of GGBS

For thermal curing method alone: $v = 0.75p + 0.035$ (Eqn 6.12)

For thermal curing + RHPC: $v = 0.55p + 0.027$ (Eqn 6.13)

For thermal curing +RHPC +accelerator: $v = 0.45p + 0.023$ (Eqn 6.14)

6.3.4 Comparison of Strength Based Equation and Elastic Modulus Based Equation

Section 6.3.2 and 6.3.3 mainly discussed the theoretical prediction of elastic modulus based on Equation 6.8 and 6.10 respectively. By the demonstration of figures and numerical tables, these two equations have shown respectively features in terms of accuracy and consistency.

Since both equations are time-dependent formula with fixed ends at 28 days, the consistency of predictions of different concrete mixes are mainly determined by the test results of 28-day compressive strength and elastic modulus. Large variations on the 28-days ends could cause the shapes of prediction curves to be distinct from each other significantly. For example, the prediction curves in Figures 6.40 and 6.50 are inconsistent to demonstrate the growing path of elastic modulus of different concrete mixes. To reduce the effect of this problem, it is necessary to eliminate the errors of tested 28-day results as much as possible.

In terms of accuracy, the elastic modulus based on Equation 6.10 is significantly better than the compressive strength based on Equation 6.8 at various mix designs. Table 6.37 shows the average values of R^2 calculated for these two equations respectively for different mix designs. The overall results of Equation 6.10 are above 0.9 and visual observations from previous figures also demonstrate excellent prediction curves. On the other hand, the average R squared values calculated by Equation 6.8 range around 0.80 to 0.87. These values are appropriate to produce good predictions but inaccurate in some cases. The gaps between the predictions and testing results are shown to be larger in Section 6.3.2 than those in Section 6.3.3. Again, natural experimental errors play a part in the quality of these correlations.

The superior prediction by Equation 6.10 requires the practical results of 28-day elastic modulus which is more difficult to acquire than the 28-day compressive strength in most situations. When the test conditions are not sufficiently capable of testing the elastic modulus, Equation 6.8 is also acceptable and easier to implement.

	Average R^2	
	Equation 6.8	**Equation 6.10**
CEM II/A-L	0.866	0.919
RHPC	0.842	0.944
CEM II/A-L + accelerator	0.868	0.958
CEM II/A-L + thermal curing	0.827	0.895
RHPC + accelerator	0.798	0.950
RHPC + thermal curing	0.878	0.914
RHPC + thermal curing + accelerator	0.939	0.933
average	0.859	0.930

Table 6.37 Comparison of Equation 6.8 and 6.10 by average R^2

6.4 Conclusions

The main objective of this chapter is to develop existing equations which predict the compressive strength and elastic modulus of concrete under various conditions through a continuous period. There are established empirical formulae proposed by EuroCode 2 and Model Code 2010 to achieve this goal, while modified equations with newly introduced parameters are also necessary for more accurate predictions and wider applicability.

The strength prediction was based on Equation 6.2 and Equation 6.3 which is a modified version of the previous equation with a different index value of (28/t). The results for coefficient s calculated by Equation 6.2 have demonstrated the relative influences of each acceleration technique and combined methods compared with the baseline mix in a

numerical format. However, the absolute values of all the calculated coefficient s are much smaller than the suggested ones in EuroCode 2, approximately half of the original values. The influence of using RHPC or the accelerating admixture can be observed from the numerical results but are not as significant as the strong impact of using the thermal curing treatment. In a combined method, the effect of thermal curing dominates the resulting outcomes by a large proportion compared with the other two methods.

When Equation 6.3 is applied for theoretical calculation with a different value of n, the effect on coefficient s is reduced by approximately 50% compared with the results calculated by Equation 6.2. Therefore, the comparison of the magnitude of coefficient s is pointless in this case. However, the trends of coefficient s influenced by various accelerating methods are similar to the previous cases. The primary comparison between the two equations is the accuracy of prediction curves. The conclusive results show that Equation 6.3 is more accurate for all the concrete mixes under normal curing conditions, whereas the original Equation 6.2 performs better when thermal curing treatment is introduced.

The prediction of elastic modulus is achieved by two equations, namely Equation 6.8 based on the 28-day mean compressive strength and Equation 6.10 based on the 28-day mean elastic modulus. Equation 6.8 is derived from the assumption that the elastic modulus is proportional to the corresponding compressive strength to the power of index m. As the index m is much less than 1, all the differences of elastic modulus among different ages, mix designs and curing conditions are smaller than those of compressive strength. The actual variations of index m are not significant enough to demonstrate a systematic influence of each accelerating method because Equation 6.8 also includes the previous prediction results of coefficient s which partly reflects those influences. Only the addition of GGBS content plays a decisive role that causes an increasing trend of index m when more GGBS is used.

Equation 6.10 is based on the 28-day mean elastic modulus and a new coefficient v which combines the index m and coefficient s. The prediction curve is forced to go through the actual 28-day result of elastic modulus and the shape of this curve is more flexible with different values of coefficient v. As a result, predictions by Equation 6.10 are generally more accurate than those calculated by Equation 6.8. The coefficient v can also reflect all the varying parameters in a numerical format, not only the influence of GGBS as Equation 6.8. Thus, a new equation to replace those in EC2 and Model Code 2010 is proposed for use, especially when GGBS is combined with conventional techniques for accelerating strength development in precast works.

7. CONCLUSIONS

7.1 Research Conclusions

Phase 1:

For the same mix proportions, concrete made from basalt is stronger than the other four types of coarse aggregates. The performances of sandstone and quartzite are similar to each other and slightly lower than the basalt aggregate. Concretes made from limestone and granite are generally weaker than other concretes at the same water/cement ratio. Water/cement ratio also affects the growth rate of concrete strength significantly, though this is not reflected in the equation in EC2. At 0.28 water/cement ratio, concrete made from RHPC gains approximately 85% of 28-day strength at 3 days, while this percentage rates drop to 77% and 71% for water/cement ratios of 0.36 and 0.41 respectively.

For the modulus of elasticity, the coarse aggregate type is the main varying factor under a given mix design. Similarly, as in the case of compressive strength, concrete made from basalt is stiffer than that of all the other concretes. However, concrete made from limestone with a lower compressive strength has a greater elastic modulus than those of concretes made from sandstone and quartzite. The performances of sandstone and quartzite on elastic modulus are, again, similar to each other. The granite aggregate contributes to a significantly lower stiffness compared to other types of aggregates.

The comparison of test results and calculated predictions indicates that the currently proposed values of coefficient α in EC2 and Model Code 2010 are inaccurate for some types of coarse aggregate. The original values of 0.9 and 0.7 for limestone and sandstone respectively are reasonably suitable for theoretical predictions. The stiffness of concretes made from basalt and quartzite is considerably overestimated by approximately 20%. Therefore, the corresponding values of coefficients α need to be reduced to 1.0 and 0.7 for these Irish local aggregates, dropped from 1.2 and 1.0 respectively. The α value for granite is not specified in either standard. Thus, a suitable assumption of a value for coefficient α for granite is set at 0.6 based on the numerical calculation of experimental results under different strength classes.

Phase 2:

When the initial CEM II/A-L was replaced by RHPC, there is an 20% increase of compressive strength the first day after mixing. This enhancement effect of RHPC rapidly

diminished after 2 days. The influence of RHPC on the long-term compressive strength shows no significant advantage or disadvantage. There is also an enhancement effect of RHPC on the elastic modulus at 1 day. But the magnitude of increase of elastic modulus in percentage is only 4%, that is, within experimental error, and significantly smaller than that of compressive strength.

Adding an accelerator to a CEM II/A-L concrete mix has a similar effect to the replacement of RHPC. The early-age strength enhancement is about 20% at 1 day and rapidly disappears after 3 days. However, the experimental results show no improvement in the elastic modulus at all ages. Considering the small effect of RHPC, the actual enhancement of the accelerator on the elastic modulus might be outweighed by random variations in testing.

The thermal curing treatment at 35˚C demonstrates large increases in both the compressive strength and elastic modulus of 40% and 16% respectively after 1 day of mixing, which is much larger than the previous two methods. However, the side-effect of thermal curing treatment reduced the long-term strength and stiffness by a significant proportion due to the reduced surface area of the hydrated products and a coarser pore structure formed during the early-age treatment.

The combined effect of RHPC and the accelerator is significantly stronger than either individual method so that this type of accelerator has a similar effect on both CEM II/A-L and RHPC. However, the combined effect of [RHPC + thermal curing] and [accelerator + thermal curing] are similar to the effect of the single thermal curing treatment. Therefore, the less effective methods can be outweighed by the stronger thermal curing method. Even in the case of all three methods together, RHPC and the accelerator showed minor influences on both compressive strength and elastic modulus.

GGBS content was blended with CEM II/A-L at 30%, 50% and 70% to test the retardation effect on both compressive strength and elastic modulus. This retardation effect of GGBS is increasing with the proportions of GGBS in the total cementitious material. The percentage of reduction on 1-day compressive strength increased from 36% to 82% when the proportion of GGBS is increased from 30% to 70%. The corresponding results for the elastic modulus also showed an increasing trend but of lesser magnitudes, from 12% to 42%.

Although the long-term properties of concrete with various proportions of GGBS are similar to those of pure cement concrete, the 82% reduction on 1-day compressive strength significantly affects the functionality of precast concrete containing 70% GGBS

within the first 2 weeks of mixing. Therefore, the three accelerating methods were expected to compensate for this reduction effect. It should be noted that as the GGBS percentage rises the effectiveness of using RHPC to enhance the early-age strength is reduced.

When the three methods were used together, the 1-day compressive strength and elastic modulus of concrete with 70% can be improved to almost the same level of strength as concrete without GGBS.

Numerical Analysis:

The theoretical prediction of compressive strength is mainly determined by Equation 6.1 and 6.2 from EC2. Using the suggested values of coefficients s for 42.5N and 42.5R cements, large errors occurred between the calculated values and test results where the predicted strength is significantly less than the actual strength during the early period of hydration. Therefore, a modified value of coefficient s is needed to minimise the total difference between the calculated growth curve and test points. This modified coefficient s is significantly smaller than the suggested value by EC2 for the baseline mix using CEM II/A-L cement.

When GGBS is added into a concrete mix, the value of coefficient s needs to be increased for accurate predictions to reflect the influence of GGBS. On the other hand, the application of any accelerating method reduced the value of coefficient s to a level in accordance with the effectiveness of this method. Thus, the modified values of coefficient s can be used as an indicator that quantifies various influencing factors on strength development with age. The suggested values of coefficient s are summarized by two graphs in Figure 6.30 and 6.31.

To further improve the accuracy of the prediction curve of compressive strength, the index number n in Equation 6.2 is also required to be changed to a suitable value. Therefore, the case of n=1.0 was also examined to compare with the initial value of 0.5 to establish an appropriate one for Equation 6.2. In general, the average R squared values of all the prediction curves calculated by n=0.5 and n=1.0 are both around 0.94. However, for concrete mixes under normal curing, n=1.0 generated a more accurate prediction than n=0.5. If thermal curing is applied, n=0.5 is favourable for better prediction. There is no conclusive result for index n to achieve accurate predictions for all the different situations. Therefore, no change to the existing default value of 0.5 is recommended.

The first method of stiffness prediction is based on the 28-day compressive strength using Equation 6.8. To improve the accuracy of predicted curves of elastic modulus, the index m is set to be a modifier for different conditions. The results show any accelerating method or combined ones does not change the index m to a significantly different level because Equation 6.8 contains the previously discussed coefficient s. Thus, the influence of accelerating methods is already represented by the modified values of coefficient s. However, an increasing proportion of GGBS causes the index m to grow from 0.3 to 0.36 on average.

The second method of stiffness prediction is based on the 28-day elastic modulus by Equation 6.10. In this case, the prediction curve is set to pass through the 28-day elastic modulus. As a result, the average error between the prediction curve and test point is smaller than that of the previous method. In Equation 6.10, a combined coefficient v is introduced to represent the influences of different proportions of GGBS and accelerating methods. The distribution of coefficient v through all the concrete mixes is summarized in Figure 6.53. The value of coefficient v is determined by the proportions of GGBS and accelerating methods and can be calculated by Equation 6.11 to 6.14 for various conditions.

Finally, it is expected the conclusions of this research will feed into the development work of Technical Group 7 in Europe in their next report on time-dependent characteristics of hardened concrete.

7.2 Recommendations for Further Work

There are recommendations for further work to arise this research:

-The quantity of concrete specimens should be increased to a larger scale so that the systematic influence of any variable developed by more data cannot be outweighed by random experimental errors.

-With a larger concrete mixer and curing facility, all the concrete specimens from the same mix design can be mixed and poured at the same time to eliminate the experimental errors that arise from mixing procedures.

-Other accelerating techniques, conventional or unconventional, should be tested to widen the selection under different practical situations. For example: comparison of steam curing and hot water curing, heating the reinforcing steel in precast concrete using

electricity and autogenous curing with an insulated blanket, increasing the constituents' temperatures before mixing and using an alkali-activator to promote early-age GGBS hydration.

-The full stress-strain graph of concrete can be drawn to study and develop a more comprehensive understanding of the non-linear elastic behaviour of concrete.

-A wider range of the selections of curing temperature can be applied to concrete specimens to quantify the influence of temperature. Not only the accelerating effect of high temperature is important for precast concrete, the decelerating effect of a low temperature is also of importance for various environmental conditions. Furthermore, the temperature of all the constituents should be controlled to eliminate any possible error that may occur before the specimens are moved into the heating facility.

-A more thorough study is needed on the interactions between cementitious materials, their micro-structural analysis, the effect of an accelerating admixture and thermal curing on long term strength and durability beyond 28 days.

References:

BS 812-109, (1990). "Testing aggregates —Part 109: Methods for determination of moisture content." London, British Standards Institution,.

BS 812-110, (1990). "Testing aggregates - Part 110: Methods for determination of aggregate crushing value (ACV)." London, British Standards Institution,.

BS 812-111, (1990). "Testing aggregates - Part 111: Methods for determination of ten percent fines value (TFV)." London, British Standards Institution,.

BS 1881-108, (1983). " Methods of testing concrete. Method for making test cubes from fresh concrete" London, British Standards Institution.

BS 1881-110, (1983). " Methods of testing concrete. Methods for making test cylinders from fresh concrete" London, British Standards Institution.

BS 1881-121, (1983). "Method for determination of static modulus of elasticity in compression." London, British Standards Institution.

BS 1881-125, (2013). " Testing concrete — Part 125: Methods for mixing and sampling fresh concrete in the laboratory" London, British Standards Institution.

CEB-FIP (1993). "Model Code 1990: Design Code" Lausanne, Fédération internationale du béton.

fib-bulletin-42 (2008). "Constitutive modelling of high strength/high performance concrete." Lausanne, Fédération internationale du béton.

fib-bulletin-66 (2012). "Model Code 2010,Vol.1, Final Draft." Lausanne, Fédération internationale du béton.

I.S. EN-196-3, (2008). "Methods of testing cement -Part 3: Determination of setting times and soundness." Dublin, NSAI.

I.S. EN-197-1, (2011). "Cement - Part 1: Composition, specifications and conformity criteria for common cements." Dublin, NSAI.

I.S. EN-206-1, (2013). " Concrete - Part 1: Specification, performance, production and conformity." Dublin, NSAI.

I.S. EN-1992-1-1, (2005). "Eurocode 2: Design of concrete structures - Part 1-1: General rules and rules for buildings." Dublin, NSAI.

I.S. EN-13369, (2018). "Common rules of precast concrete products" Dublin, NSAI.

I.S. EN-15167, (2006). "Ground granulated blast furnace slag for use in concrete, mortar and grout." Dublin, NSAI.

I.S. EN 450-1, (2012). "Fly ash for concrete - Part 1: Definition, specifications and conformity criteria." Dublin, NASI.

I.S. EN 934-2, (2012). "Admixtures for concrete, mortar and grout - Part 2: Concrete admixtures - Definitions, requirements, conformity, marking and labelling." Dublin, NSAI.

I.S. EN 12620, (2013). "Aggregates for concrete." Dublin, NSAI.

I.S. EN 15167-1, (2006). "Ground granulated blast furnace slag for use in concrete, mortar and grout - Part 1: Definitions, specifications and conformity criteria." Dublin, NSAI.

IS EN-12350-8, (2010). "Testing fresh concrete. Self-compacting concrete. Slump-flow test." Dublin, NSAI.

IS EN-12390-1, (2012). "Testing hardened concrete — Part 1: Shape, dimensions and other requirements for specimens and moulds." Dublin, NSAI.

IS EN-12390-2, (2019). "Testing hardened concrete Part 2: Making and curing specimens for strength tests." Dublin, NSAI.

IS EN-12390-3, (2019). "Testing hardened concrete Part 3: Compressive strength of test specimens." Dublin, NSAI.

IS EN 1097-2, (2010). "Methods for the determination of resistance to fragmentation." Dublin, NSAI.

Abalaka, A. E. and Okoli, O. G. (2012). "Effects of curing conditions on high strength concrete." *Journal of Civil Engineering and Construction Technology* **3**(10): 273-279.

Ahmad, S. (2002). "Effect of fineness of cement on properties of fresh and hardened concrete." *27th Conference on Our World in Concrete & Structures*: 103-109. Singapore

Ahmad, J. Kontoleon, K.J. Majdi, A. Naqash, M.T. Deifalla, A.F. Ben Kahla, N. Isleem, H.F. Qaidi, S.M.A. (2022) "A Comprehensive Review on the Ground Granulated Blast Furnace Slag (GGBS) in Concrete Production." *Sustainability* **2022**, *14*, 8783.

Aitcin, P. C. (1995). "Developments in the application of high-performance concretes." *Construction and Building Materials* **9**(1): 13-17.

Aitcin, P. C. and Mehta., P. K. (1990). "Effect of Coarse Aggregate Characteristics on Mechanical Properties of High-Strength Concrete." *ACI Materials Journal* **87**(2): 103-107.

Aref Al-Swaidani, Andraos Soud, Amina Hammami. (2017). "Improvement of the Early-Age Compressive Strength, Water Permeability, and Sulfuric Acid Resistance of Scoria-Based Mortars/Concrete Using Limestone Filler". *Advances in Materials Science and Engineering*, vol. 2017, https://doi.org/10.1155/2017/8373518

A.S. Malaikah. (2005). "A Proposed Relationship for the Modulus of Elasticity of High Strength Concrete Using Local Materials in Riyadh" Journal of King Saud University - Engineering Sciences, Volume 17, Issue 2, Pages 131-141

Baalbaki, W., Aitcin, P.-C. and Ballivy, G. (1992). "On Predicting Modulus of Elasticity inHigh-Strength Concrete." *ACI Materials Journal* **89**(5): 517-520.

Baalbaki., W., Benmokrane., B., Chaallal, O. and Aitcin, P.-C. (1991). "Influence of Coarse Aggregate on Elastic Properties of High-Performance Concrete." *ACI Materials Journal* **88**(5): 499-503.

Ballim, Y. and Graham, P. (2009). "The effects of supplementary cementing materials in modifying the heat of hydration of concrete." *Materials and Structures* **42**(6): 803-811.

Baron, J. and Douvre, C. (1987). "Technical and Economical Aspects of the Use of Limestone Filler Additions in Cement." *World Cement* **18**(3): 100-104.

Beshr, H., Almusallam, A. A. and Maslehuddin, M. (2003). "Effect of coarse aggregate quality on the mechanical properties of high strength concrete." *Construction and Building Materials* **17**(2): 97-103.

Beushausen, H., Alexander, M. and Ballim, Y. (2012). "Early-age properties, strength development and heat of hydration of concrete containing various South African slags at different replacement ratios." *Construction and Building Materials* **29**: 533-540.

Brooks, J. J., Megat Johari, M. A. and Mazloom, M. (2000). "Effect of admixtures on the setting times of high-strength concrete." *Cement and Concrete Composites* **22**(4): 293-301.

Carino, N. and Lew, H. (2001). "The Maturity Method: From Theory to Application." *Structures 2001*: 1-19. Washington, D.C. USA

Cartuxo, F., de Brito, J., Evangelista, L., Jiménez, J. R. and Ledesma, E. F. (2015). "Rheological behaviour of concrete made with fine recycled concrete aggregates – Influence of the superplasticizer." *Construction and Building Materials* **89**: 36-47.

Changming Bu, Lei Liu, Xinyu Lu, Dongxu Zhu, Yi Sun, Linwen Yu, Yuhui OuYang, Xuemei Cao and Qike Wei. (2022). "The Durability of Recycled Fine Aggregate Concrete: A Review" *Material* 15(3): 1110.

Colin, C. A. and Windmeijer, F. A. G. (1997). "An R-squared measure of goodness of fit for some common nonlinear regression models." *Journal of Econometrics* **77**(2): 329-342.

Crook, R. N. and Day, R. I. (2016). "Concrete practice- guidance on the practical aspects of concreting" Concrete Society

Damtoft, J. S., Lukasik, J., Herfort, D., Sorrentino, D. and Gartner, E. M. (2008). "Sustainable development and climate change initiatives." *Cement and Concrete Research* **38**(2): 115-127.

Dongbing Jiang, Xiangguo Li, Yang Lv, Changjiao Li, Ting Zhang, Chenhao He, Difei Leng, Kai Wu. (2022). "Early-age hydration process and autogenous shrinkage evolution of high performance cement pastes" Journal of Building Engineering, Volume 45, 103436

Donza, H., Cabrera, O. and Irassar, E. F. (2002). "High-strength concrete with different fine aggregate." *Cement and Concrete Research* **32**(11): 1755-1761.

Fatma Shaker, Ahmed Rashad, Mohamed Allam. (2018). "Properties of concrete incorporating locally produced Portland limestone cement" *Ain Shams Engineering Journal*, **9**(4): 2301-2309.

Gyabaah, G. Miyazawa, S. Nito, N. (2022). "Effects of Gypsum and Limestone Powder on Fresh Properties and Compressive Strength of Concrete Containing Ground Granulated Blast Furnace Slag under Different Curing Temperatures" Construction Materials, 2, 114–126

Gidion Turu'allo. (2013). "Early Age Strength Development of GGBS Concrete Cured Under Different Temperatures" PhD Thesis, University of Livepool, UK

Higgins, Brendan. Curran, Michael. and Spillane, John P. (2020) "Maximising the Potential Use of Ground Granulated Blast-Furnace Slag (GGBS) in Cement: An Irish Investigation" (2020). *Civil Engineering Research in Ireland 2020*

Hu, J., Ge, Z. and Wang, K. (2014). "Influence of cement fineness and water-to-cement ratio on mortar early-age heat of hydration and set times." *Construction and Building Materials* **50**(1): 657-663.

Irassar, E. F., Violini, D., Rahhal, V. F., Milanesi, C., Trezza, M. A. and Bonavetti, V. L. (2011). "Influence of limestone content, gypsum content and fineness on early age properties of Portland limestone cement produced by inter-grinding." *Cement and Concrete Composites* **33**(2): 192-200.

Khan, M. I. (2012). "Predicting properties of High Performance Concrete containing composite cementitious materials using Artificial Neural Networks." *Automation in Construction* **22**(0): 516-524.

Kjellsen, K. O. (1996). "Heat curing and post-heat curing regimes of high-performance concrete: Influence on microstructure and C-S-H composition." *Cement and Concrete Research* **26**(2): 295-307.

Klemm, W. A. and Adams, L. D. (1990). "An investigation of the formation of carboaluminates." *Carbonate Additions to Cement*: 60-72.

Korde Chaaruchandra, Matthew Cruickshank, Roger P. West, Claudia Pellegrino. (2019). "Activated slag as partial replacement of cement mortars: Effect of temperature and a novel admixture" Construction and Building Materials, Volume 216, Pages 506-524

Korde, Chaaruchandra & Cruickshank, Matthew & West, Roger & Reddy, John. (2018). "Temperature and admixtures effects on the maturity of GGBS mortars for the precast concrete industry" Civil Engineering Research in Ireland 2018

Korde Chaaruchandra, Matthew Cruickshank, Roger P. West, (2020). "A technique for early age strength determination of hollowcore slab, enabling partial replacement with slag: Field and laboratory investigations" Construction and Building Materials, Volume 256, 119321

K Ganesh Babu, V Sree Rama Kumar. (2020) "Efficiency of GGBS in concrete" *Cement and Concrete Research*, 30(7): 1031-1036

Kourounis, S., Tsivilis, S., Tsakiridis, P. E., Papadimitriou, G. D. and Tsibouki, Z. (2007). "Properties and hydration of blended cements with steelmaking slag." *Cement and Concrete Research* **37**(6): 815-822.

Kumavat, H. R. and Patel, V. J. (2014). "Factors Influencing the Strength Relationship of Concrete Cube and Standard Cylinder." *International Journal of Innovative Technology and Exploring Engineering* **3**(8): 76-79.

Lindgård, J., Andiç ‐ Çakır, Ö., Fernandes, I., Rønning, T. F., & Thomas, M. D. A. (2012). "Alkali–silica reactions (ASR): Literature review on parameters influencing laboratory performance testing" Cement and Concrete Research, 42(2), 223 ‐ 243

Mamlouk, M. S. and Zaniewski, J. P. (2010). *Materials for civil and construction engineers*. New Jersey, USA, Prentice Hall.

Mehta, P. K. (2004). "High-Performance, High-Volume Fly Ash Concrete for Sustainable Development." *International Workshop on Sustainable Development and Concrete Technology*: 3-14.

Mehta, P. K. and Aitcin, P. C. (1990). "Principles Underlying the Production of High-Performance Concrete." *Cement, Concrete and Aggregates Journal* **12**(2): 70-78.

Memon, A. H., Radin, S. S., Zain, M. F. M. and Trottier, J.-F. (2002). "Effects of mineral and chemical admixtures on high-strength concrete in seawater." *Cement and Concrete Research* **32**(3): 373-377.

Navdeep Singh, Bhawana Sharma, Manali Rathee. (2002). "Carbonation resistance of blended mortars and industrial by-products: A brief review" Cleaner Materials, Volume 4, 100058

Nawy, E. G. (2001). *Fundamentals of High-Performance Concrete*. USA, John Wiley & Sons, Inc.

Neville, A. M. (2012). *Properties of concrete*. Essex, UK, John Wiley & Sons.

Nicholas J. Carino and Hai S. Lew. (2001). "The Maturity Method: From Theory to Application" *Structures Congress and Exposition 2001*, https://tsapps.nist.gov/publication/get_pdf.cfm?pub_id=860356.

Nielsen, C. V. (2015). "Concrete E-modulus: Is it overrated". *Global magazine of the Concrete Society*. **49:** 43-45.

Odler, I. (1991). "Strength of cement (final report)." *Materials and Structures* **24**(2): 143-157.

Ozioko, Hyginus. Ohazurike, Emeka. (2019). "Accelerated Curing of Concrete Cubes Using Warm Water." International Journal of Research and Innovation in Applied Science (IJRIAS) **4**(3), 2454-6194

Piotrowska, E., Malecot, Y. and Ke, Y. (2014). "Experimental investigation of the effect of coarse aggregate shape and composition on concrete triaxial behavior." *Mechanics of Materials* **79**: 45-57.

Ramachandran, V. S. (1984). *Accelerators In Concrete admixtures handbook: Properties, science, and technology*. Park Ridge, New Jersey, Noyes Publications.

Ramachandran, V. S. and Malhotra, V. M. (1984). *Superplasticizers In Concrete admixtures handbook: Properties, science, and technology*. Park Ridge, New Jersey, Noyes Publications.

Ravindra K.Dhir, Jorge de Brito, Ciarán J.Lynn, Rui V.Silva (2018). *Sustainable Construction Materials.* Woodhead Publishing. Page 139-195.

Rixom, M. R. and Mailvaganam, N. P. (1986). *Chemical admixtures for concrete*. Cambridge, England, The University Press.

R.N. Swamy, G.H. Lambert. (1983). "Mix design and properties of concrete made from PFA coarse aggregates and sand" International Journal of Cement Composites and Lightweight Concrete, Volume 5, Issue 4, Pages 263-275

Runxiao Zhang, Tanvir S. Qureshi, Daman K. Panesar. (2022). "Use of industrial waste in construction and a cost analysis" Handbook of Sustainable Concrete and Industrial Waste Management, Pages 615-635

Sarah Steiner, Tilo Proske, Frank Winnefeld, Barbara Lothenbach. (2022). "Effect of limestone fillers on CO2 and water vapour diffusion in carbonated concrete" Cement, Volume 8, 100027

Schindler, A. K. (2004). "Prediction of concrete setting." *International RILEM Symposium on Concrete Science and Engineering:* 19-32. Illinois. USA

Sideris, K. K., Manita, P. and Sideris, K. (2004). "Estimation of ultimate modulus of elasticity and Poisson ratio of normal concrete." *Cement and Concrete Composites* **26**(6): 623-631.

Sluijter, W. L. and Kreijger, P. C. (1997). "Corrosion of Reinforcement in Concrete due to Calcium Chloride." *Heron* **22**(1): 28-45.

Srinivasan, C. B., Narasimhan, N. L. and Ilango, S. V. (2003). "Development of rapid-set high-strength cement using statistical experimental design." *Cement and Concrete Research* **33**(9): 1287-1292.

Sulapha, P., Wong, S. F., Wee, T. H. and Swaddiwudhipong, S. (2003). "Carbonation of Concrete Containing Mineral Admixtures." *Journal of Materials in Civil Engineering* **15**(2): 134-143.

Tsivilis, S., Chaniotakis, E., Badogiannis, E., Pahoulas, G. and Ilias, A. (1999). "A study on the parameters affecting the properties of Portland limestone cements." *Cement and Concrete Composites* **21**(2): 107-116.

Vuk, T., Tinta, V., Gabrovšek, R. and Kaučič, V. (2001). "The effects of limestone addition, clinker type and fineness on properties of Portland cement." *Cement and Concrete Research* **31**(1): 135-139.

Wu, K.-R., Chen, B., Yao, W. and Zhang, D. (2001). "Effect of coarse aggregate type on mechanical properties of high-performance concrete." *Cement and Concrete Research* **31**(10): 1421-1425.

Yoshitake, I., Zhang, W., Mimura, Y. and Saito, T. (2013). "Uniaxial tensile strength and tensile Young's modulus of fly-ash concrete at early age." *Construction and Building Materials* **40**: 514-521.

Zhou, F. P., Lydon, F. D. and Barr, B. I. G. (1995). "Effect of coarse aggregate on elastic modulus and compressive strength of high performance concrete." *Cement and Concrete Research* **25**(1): 177-186.

Appendix A: Pouring Schedule of 2010

2010	Monday	Tuesday	Wednesday	Thursday	Friday	Saturday	Sunday
Week One	15 Mar	16 Mar	17 Mar	18 Mar	19 Mar	20 Mar	21 Mar
Mixing and pouring	03S50	28S50		28S60	03S60		
Cleaning and stripping		03S50	28S50		28S60	03S60	
Testing				03S50			
Storage of cylinders	0	6	12	6	12	18	18
Week Two	22 Mar	23 Mar	24 Mar	25 Mar	26 Mar	27 Mar	28 Mar
Mixing and pouring	03S75	03S85/28S85	28S75	28B50	03B50/03B60		
Cleaning and stripping		03S75	03S85/28S85	28S75	28B50	03B50/03B60	
Testing	03S60			03S75	03S85		
Storage of cylinders	12	18	30	30	30	42	42
Week Three	29 Mar	30 Mar	31 Mar	1 Apr	2 Apr	3 Apr	4 Apr
Mixing and pouring	03B75-f	28B60/03B75	28B85		-		
Cleaning and stripping		03B75-f	28B60/03B75	28B85			
Testing	03B50/03B60			03B75-f	03B75		
Storage of cylinders	30	36	48	48	42	42	42
Week Four	5 Apr	6 Apr	7 Apr	8 Apr	9 Apr	10 Apr	11 Apr
Mixing and pouring	-	03B85/28B75	28L50	28L60	03L60/03L50		
Cleaning and stripping	-		03B85/28B75	28L50	28L60	03L60/03L50	
Testing	-				03B85/		
Storage of cylinders		42	54	60	60	72	72

2010	Monday	Tuesday	Wednesday	Thursday	Friday	Saturday	Sunday
Week Five	12 Apr	13 Apr	14 Apr	15 Apr	16 Apr	17 Apr	18 Apr
Mixing and pouring	03L75	28L75	03L85/28L85				
Cleaning and stripping		03L75	28L75	03L85/28L85			
Testing	03L60/03L50	28S50		28S60/03L75		03L85	
Storage of cylinders	60	60	66	66	66	60	60
Week Six	19 Apr	20 Apr	21 Apr	22 Apr	23 Apr	24 Apr	25 Apr
Mixing and pouring		28Q50/28Q60	28Q85/28Q75	28G50	28G75/28G60		
Cleaning and stripping			28Q50/28Q60	28Q85/28Q75	28G50	28G75/28G60	
Testing		28S85	28S75	28B50			
Storage of cylinders	60	54	60	66	72	84	84
Week Seven	26 Apr	27 Apr	28 Apr	29 Apr	30 Apr	1 May	2 May
Mixing and pouring	28G85/03Q50	03Q60/					
Cleaning and stripping		28G8503Q50	03Q60/				
Testing		28B60	28B85	03Q50	03Q60/		
Storage of cylinders	84	90	90	84	78	78	78
Week Eight	3 May	4 May	5 May	6 May	7 May	8 May	9 May
Mixing and pouring	-	03Q75/	03Q85/03G50				
Cleaning and stripping	-		03Q75/	03Q85/03G50			
Testing	-	28B75	28L50	28L60	03Q75/	03Q85/03G50	
Storage of cylinders		72	72	78	72	60	60

2010	Monday	Tuesday	Wednesday	Thursday	Friday	Saturday	Sunday
Week Nine	10 May	11 May	12 May	13 May	14 May	15 May	16 May
Mixing and pouring	03G60/03G75	03G85					
Cleaning and stripping		/03G60/03G75	03G85				
Testing		28L75	28L85	/03G60/03G75/	03G85		
Storage of cylinders	60	66	66	54	48	48	48
Week Ten	17 May	18 May	19 May	20 May	21 May	22 May	23 May
Mixing and pouring							
Cleaning and stripping							
Testing		28Q50/28Q60	28Q85/28Q75	28G50	28G75/28G60		
Storage of cylinders	48	36	24	18	6	6	6
Week Eleven	24 May	25 May	26 May	27 May	28 May	29 May	30 May
Mixing and pouring							
Cleaning and stripping							
Testing	28G85						
Storage of cylinders	0						

B = Basalt
L = Limestone
S = Sandstone
Q = Quartzite
G = Granite
Prefix figure indicates the testing age.
Suffix figure indicates the strength class of concrete cubes.

Appendix B: Pouring Schedule of 2011

2011	Monday	Tuesday	Wednesday	Thursday	Friday	Saturday
Week 1	23-May	24-May	25-May	26-May	27-May	28-May
Mixing and pouring				00R01/07		
Cleaning and stripping					00R01/07	
Testing					00R01	
Storage of cylinders					5	5
Week 2	30-May	31-May	01-Jun	02-Jun	03-Jun	04-Jun
Mixing and pouring	00R02/03/28/56	30R03/07	30R01/02	30R28/56		
Cleaning and stripping		00R02/03/28/56	30R03/07	30R01/02	30R28/56	
Testing			00R02	00R07/03|30R01	30R03/02	
Storage of cylinders	5	25	30	25	25	25
Week 3	06-Jun	07-Jun	08-Jun	09-Jun	10-Jun	11-Jun
Mixing and pouring	Bank holiday	50R03/07	50R01/02		50R28/56	
Cleaning and stripping			50R03/07	50R01/02		50R28/56
Testing		30R07		50R01	50R02/03	
Storage of cylinders	25	20	30	35	25	35
Week 4	13-Jun	14-Jun	15-Jun	16-Jun	17-Jun	18-Jun
Mixing and pouring		70R03/07	70R01/02	70R28/56		
Cleaning and stripping			70R03/07	70R01/02	70R28/56	
Testing		50R07		70R01	70R03/02	
Storage of cylinders	35	30	40	45	45	45

2011	Monday	Tuesday	Wednesday	Thursday	Friday	Saturday
Week 5	20-Jun	21-Jun	22-Jun	23-Jun	24-Jun	25-Jun
Mixing and pouring			00C28/56			
Cleaning and stripping				00C28/56		
Testing		70R07				
Storage of cylinders	45	40	40	50	50	50
Week 6	27-Jun	28-Jun	29-Jun	30-Jun	01-Jul	02-Jul
Mixing and pouring			00C01/07			
Cleaning and stripping				00C01/07		
Testing	00R28			30R28/00C01		
Storage of cylinders	45	45	45	45	45	45
Week 7	04-Jul	05-Jul	06-Jul	07-Jul	08-Jul	09-Jul
Mixing and pouring	00C01/03	30C03/07	30C01/02	30C28/56		
Cleaning and stripping		00C01/03	30C03/07	30C01/02	30C28/56	
Testing		00C01	00C07	00C03/30C01	50R28/30C02/03	
Storage of cylinders	45	50	55	55	50	50
Week 8	11-Jul	12-Jul	13-Jul	14-Jul	15-Jul	16-Jul
Mixing and pouring	50C01/02			50C28/56		
Cleaning and stripping		50C01/02			50C28/56	
Testing		30C07/50C01	50C02	70R28		
Storage of cylinders	50	50	45	40	50	50

2011	Monday	Tuesday	Wednesday	Thursday	Friday	Saturday
Week 9	18-Jul	19-Jul	20-Jul	21-Jul	22-Jul	23-Jul
Mixing and pouring		70C03/07	70C01/02		70C28/56	
Cleaning and stripping			70C03/07	70C01/02		70C28/56
Testing			00C28	70C01	70C02/03	
Storage of cylinders	50	50	55	60	50	60
Week 10	25-Jul	26-Jul	27-Jul	28-Jul	29-Jul	30-Jul
Mixing and pouring			00RA01/02|30RA01/02			
Cleaning and stripping				00RA01/02|30RA01/02		
Testing	00R56	70C07		30R56|00RA01|30RA01	00RA02|30RA02	
Storage of cylinders	55	50	50	55	45	45
Week 11	01-Aug	02-Aug	03-Aug	04-Aug	05-Aug	06-Aug
Mixing and pouring		00RA03/07|30RA03/07	50RA01/02		50RA03/07	
Cleaning and stripping			00RA03/07|30RA03/07	50RA01/02		50RA03/07
Testing				30C28|50RA01	50R56|00RA03|30RA03|50RA02	
Storage of cylinders	45	45	65	65	45	55
Week 12	08-Aug	09-Aug	10-Aug	11-Aug	12-Aug	13-Aug
Mixing and pouring		70RA03/07	70RA01/02		00RA28/56|30RA28/56	
Cleaning and stripping			70RA03/07	70RA01/02		00RA28/56|30RA28/56
Testing	50RA03	00RA07|30RA07		70R56/50C28|70RA01	50RA07|70RA02/03	
Storage of cylinders	50	40	50	45	30	50

2011	Monday	Tuesday	Wednesday	Thursday	Friday	Saturday
Week 13	15-Aug	16-Aug	17-Aug	18-Aug	19-Aug	20-Aug
Mixing and pouring		-	-	-	-	
Cleaning and stripping						
Testing		70RA07	00C56		70C28	
Storage		45	40	40	35	35
Week 14	22-Aug	23-Aug	24-Aug	25-Aug	26-Aug	27-Aug
Mixing and pouring	00CA01/02		50RA28/56|70RA28/56		00CA03/07/28/56	
Cleaning and stripping		00CA01/02		50RA28/56|70RA28/56		00CA03/07/28/56
Testing		00CA01	00CA02			
Storage	35	40	35	55	55	75
Week 15	29-Aug	30-Aug	31-Aug	01-Sep	02-Sep	03-Sep
Mixing and pouring			30CA01/02		30CA03/07/28/56	
Cleaning and stripping				30CA01/02		30CA03/07/28/56
Testing	00CA03			30C56|30CA01	00CA07|30CA02	
Storage	70	70	70	70	60	80
Week 16	05-Sep	06-Sep	07-Sep	08-Sep	09-Sep	10-Sep
Mixing and pouring		50CA03/07		50CA28/56|70CA01/07		
Cleaning and stripping			50CA03/07		50CA28/56|70CA01/07	
Testing	30CA03			50C56	00RA28|30RA28|30CA07|50CA03|70CA01	
Storage	75	75	85	80	75	75

2011	Monday	Tuesday	Wednesday	Thursday	Friday	Saturday
Week 17	12-Sep	13-Sep	14-Sep	15-Sep	16-Sep	17-Sep
Mixing and pouring		50CA01/02|70CA02/03		70CA28/56		
Cleaning and stripping			50CA01/02|70CA02/03		70CA28/56	
Testing		30CA07	50CA01	70CA02/07|50CA02	70C56|70CA03	
Storage	75	70	85	70	70	70
Week 18	19-Sep	20-Sep	21-Sep	22-Sep	23-Sep	24-Sep
Mixing and pouring						
Cleaning and stripping						
Testing			50RA28|70RA28		00CA28	
Storage	70	70	60	60	55	55
Week 19	26-Sep	27-Sep	28-Sep	29-Sep	30-Sep	01-Oct
Mixing and pouring						
Cleaning and stripping						
Testing					30CA28	
Storage	55	55	55	55	50	50
Week 20	03-Oct	04-Oct	05-Oct	06-Oct	07-Oct	08-Oct
Mixing and pouring						
Cleaning and stripping						
Testing				50CA28	00RA56|30RA56	
Storage	50	50	50	45	35	35

2011	Monday	Tuesday	Wednesday	Thursday	Friday	Saturday
Week 21	10-Oct	11-Oct	12-Oct	13-Oct	14-Oct	15-Oct
Mixing and pouring						
Cleaning and stripping						
Testing				70CA28		
Storage	35	35	35	30	30	30
Week 22	17-Oct	18-Oct	19-Oct	20-Oct	21-Oct	22-Oct
Mixing and pouring						
Cleaning and stripping						
Testing			50RA56|70RA56		00CA56	
Storage	30	30	20	20	15	15
Week 23	24-Oct	25-Oct	26-Oct	27-Oct	28-Oct	29-Oct
Mixing and pouring						
Cleaning and stripping						
Testing					30CA56	
Storage	15	15	15	15	10	10
Week 24	31-Oct	01-Nov	02-Nov	03-Nov	04-Nov	05-Nov
Mixing and pouring						
Cleaning and stripping						
Testing				50CA56		
Storage	10	10	10	5	5	5

2011	Monday	Tuesday	Wednesday	Thursday	Friday	Saturday
Week 25	07-Nov	08-Nov	09-Nov	10-Nov	11-Nov	12-Nov
Mixing and pouring						
Cleaning and stripping						
Testing				70CA56		
Storage	5	5	5	0		

C = Cem II/A-L
R = Rapid Hardening Portland Cement
A = Accelerator
Prefix figure indicates the percentage of GGBS used in the total cementitious content.
Suffix figure indicates the testing age.

Appendix C: Pouring Schedule of 2012

2012	Monday	Tuesday	Wednesday	Thursday	Friday	Saturday
Week 1				14/06	15/06	16/06
Mixing and pouring				00CH01/07		
Cleaning and stripping					00CH01/07	
Testing					00CH01	
Storage quantity				0	5	5
Week2	18/06	19/06	20/06	21/06	22/06	23/06
Mixing and pouring	00CH02/03		00CH28/56			
Cleaning and stripping		00CH02/03		00CH28/56		
Testing			00CH02	00CH03/07		
Storage quantity	5	15	10	10	10	10
Week 3	25/06	26/06	27/06	28/06	29/06	30/06
Mixing and pouring	30CH03/07		30CH01/02		30CH28/56	
Cleaning and stripping		30CH03/07		30CH01/02		30CH28/56
Testing				30CH03/01	30CH02	
Storage quantity	10	20	20	20	15	25
Week 4	02/07	03/07	04/07	05/07	06/07	07/07
Mixing and pouring	50CH03/07					
Cleaning and stripping		50CH03/07				
Testing	30CH07			50CH03		
Storage quantity	20	30	30	25	25	25

2012	Monday	Tuesday	Wednesday	Thursday	Friday	Saturday
Week5	09/07	10/07	11/07	12/07	13/07	14/07
Mixing and pouring	50CH01/02			50CH28/56	70CH03/07	
Cleaning and stripping		50CH01/02			50CH28/56	70CH03/07
Testing	50CH07	50CH01	50CH02			
Storage quantity	20	25	20	20	30	40
Week 6	16/07	17/07	18/07	19/07	20/07	21/07
Mixing and pouring	70CH01/02		70CH28/56			
Cleaning and stripping		70CH01/02		70CH28/56		
Testing	70CH03	70CH01	00CH28/70CH02		70CH07	
Storage quantity	35	40	30	40	35	35
Week7	23/07	24/07	25/07	26/07	27/07	28/07
Mixing and pouring	00RH03/07		00RH01/02		00RH28/56	
Cleaning and stripping		00RH03/07		00RH01/02		00RH28/56
Testing				00RH01/03	30CH28/00RH02	
Storage quantity	35	45	45	45	35	45
Week 8	30/07	31/07	01/08	02/08	03/08	04/08
Mixing and pouring			30RH28/56			
Cleaning and stripping				30RH28/56		
Testing	00RH07					
Storage quantity	40	40	40	50	50	50

2012	Monday	Tuesday	Wednesday	Thursday	Friday	Saturday
Week 9	06/08	07/08	08/08	09/08	10/08	11/08
Mixing and pouring		30RH03/07				
Cleaning and stripping			30RH03/07			
Testing				50CH28	30RH03	
Storage quantity	50	50	60	55	50	50
Week 10	13/08	14/08	15/08	16/08	17/08	18/08
Mixing and pouring	30RH01/02		50RH01/02		50RH03/07	
Cleaning and stripping		30RH01/02		50RH01/02		50RH03/07
Testing		30RH07/01	00CH56/70CH28/30RH02	50RH01	50RH02	
Storage quantity	50	50	35	40	35	45
Week 11	20/08	21/08	22/08	23/08	24/08	25/08
Mixing and pouring	50RH28-56		70RH01/02			
Cleaning and stripping		50RH28/56		70RH01/02		
Testing	50RH03			70RH01	30CH56/00RH28/50RH07/70RH02	
Storage quantity	40	50	50	55	35	35
Week12	27/08	28/08	29/08	30/08	31/08	01/09
Mixing and pouring				00RHA28/56		
Cleaning and stripping					00RHA28/56	
Testing			30RH28			
Storage quantity	35	35	30	30	40	40

2012	Monday	Tuesday	Wednesday	Thursday	Friday	Saturday
Week 13	03/09	04/09	05/09	06/09	07/09	08/09
Mixing and pouring	00RHA01/07					
Cleaning and stripping		00RHA01/07				
Testing		00RHA01		50CH56		
Storage quantity	40	45	45	40	40	40
Week 14	10/09	11/09	12/09	13/09	14/09	15/09
Mixing and pouring		00RHA02/03		70RHA28/56		
Cleaning and stripping			00RHA02/03		70RHA28/56	
Testing	00RHA07		70CH56	00RHA02	00RHA03	
Storage quantity	35	35	40	35	40	40
Week 15	17/09	18/09	19/09	20/09	21/09	22/09
Mixing and pouring	70RHA03/07			70RHA01/02		
Cleaning and stripping		70RHA03/07			70RHA01/02	
Testing	50RH28			70RHA03	00RH56/70RHA01	70RHA02
Storage quantity	35	45	45	40	40	35
Week 16	24/09	25/09	26/09	27/09	28/09	29/09
Mixing and pouring						
Cleaning and stripping						
Testing	70RHA07		30RH56	00RHA28		
Storage quantity	30	30	25	20	20	20

2012	Monday	Tuesday	Wednesday	Thursday	Friday	Saturday
Week 17	01/10	02/10	03/10	04/10	05/10	06/10
Mixing and pouring						
Cleaning and stripping						
Testing						
Storage quantity	20	20	20	20	20	20
Week 18	08/10	09/10	10/10	11/10	12/10	13/10
Mixing and pouring						
Cleaning and stripping						
Testing				70RHA28		
Storage quantity	20	20	20	15	15	15
Week 19	15/10	16/10	17/10	18/10	19/10	20/10
Mixing and pouring						
Cleaning and stripping						
Testing	50RH56					
Storage quantity	10	10	10	10	10	10
Week 20	22/10	23/10	24/10	25/10	26/10	27/10
Mixing and pouring						
Cleaning and stripping						
Testing				00RHA56		
Storage quantity	10	10	10	5	5	5

2012	Monday	Tuesday	Wednesday	Thursday	Friday	Saturday
Week 21	29/10	30/10	31/10	01/11	02/11	03/11
Mixing and pouring						
Cleaning and stripping						
Testing						
Storage quantity	5	5	5	5	5	5
Week 22	05/11	06/11	07/11	08/11	09/11	10/11
Mixing and pouring						
Cleaning and stripping						
Testing				70RHA56		
Storage quantity	5	5	5	0		

C = Cem II/A-L
R = Rapid Hardening Portland Cement
A = Accelerator
H= Thermal Curing
Prefix figure indicates the percentage of GGBS used in the total cementitious content.
Suffix figure indicates the testing age.

Appendix D: Monitor of Temperature and Humidity

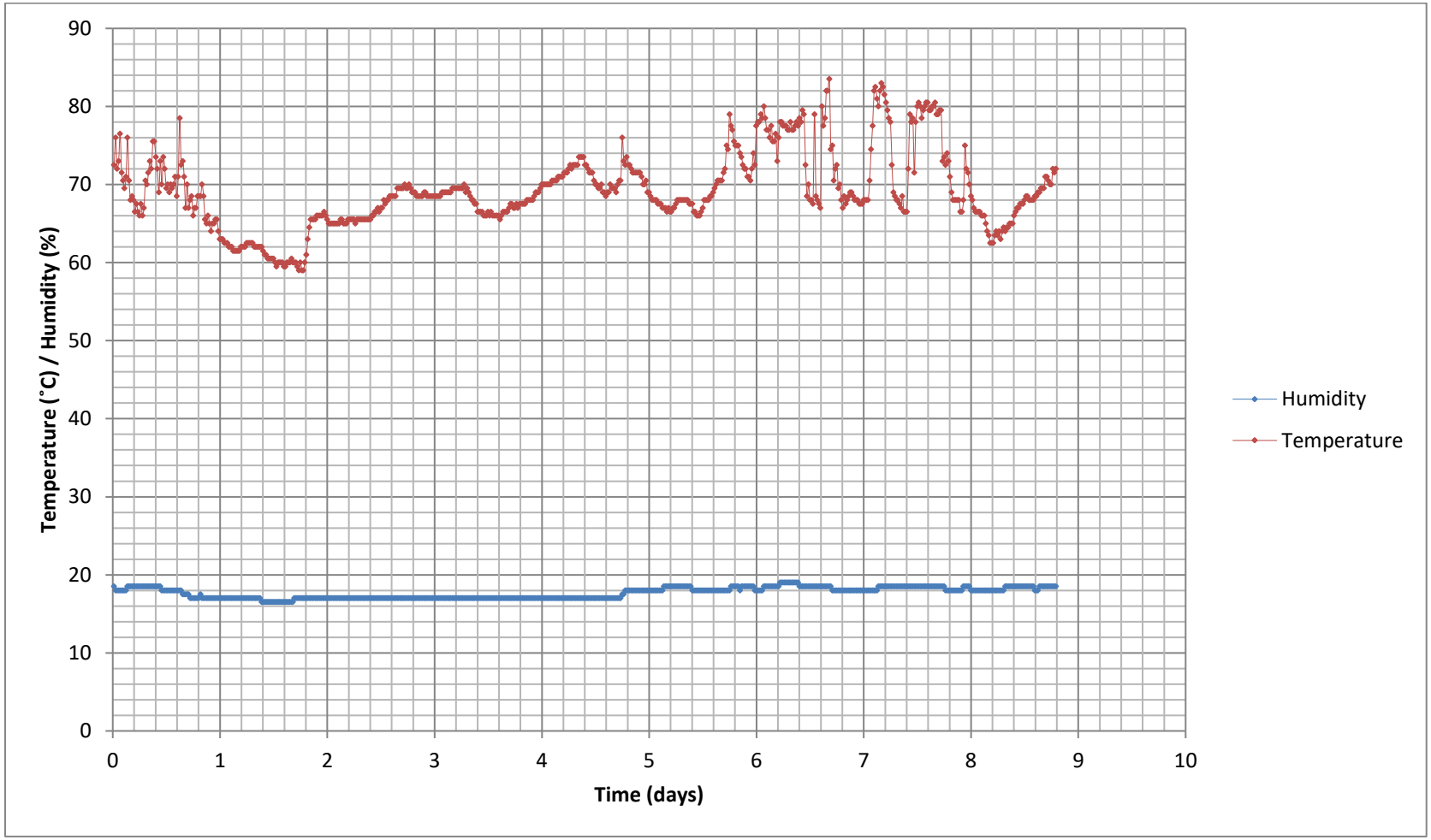

Figure D1 Temperature and humidity vs time

Appendix E: Graphs of E_{cm} vs f_{cm}

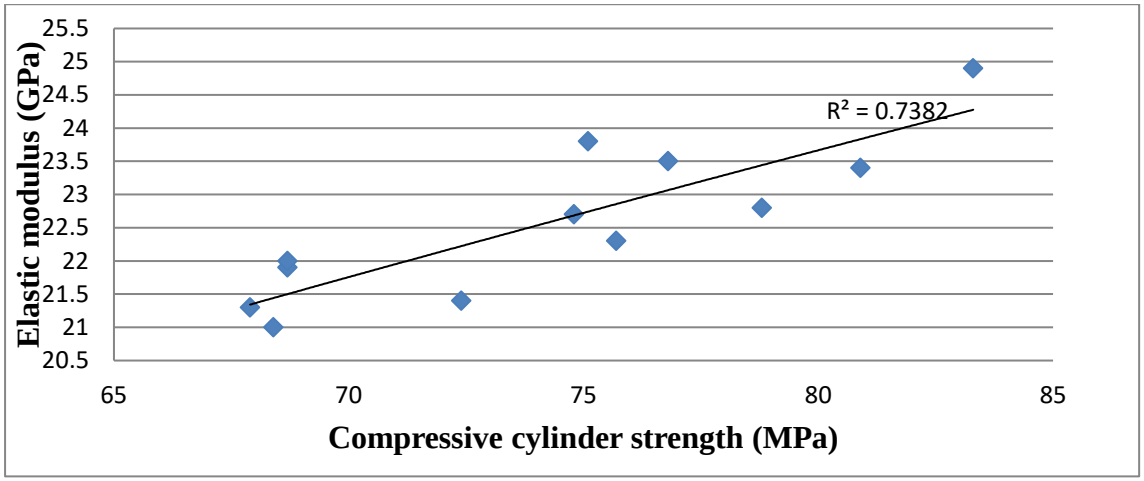

Figure E1 Modulus of elasticity (in GPa) against cylinder strength (in MPa) for 28-day granite specimens

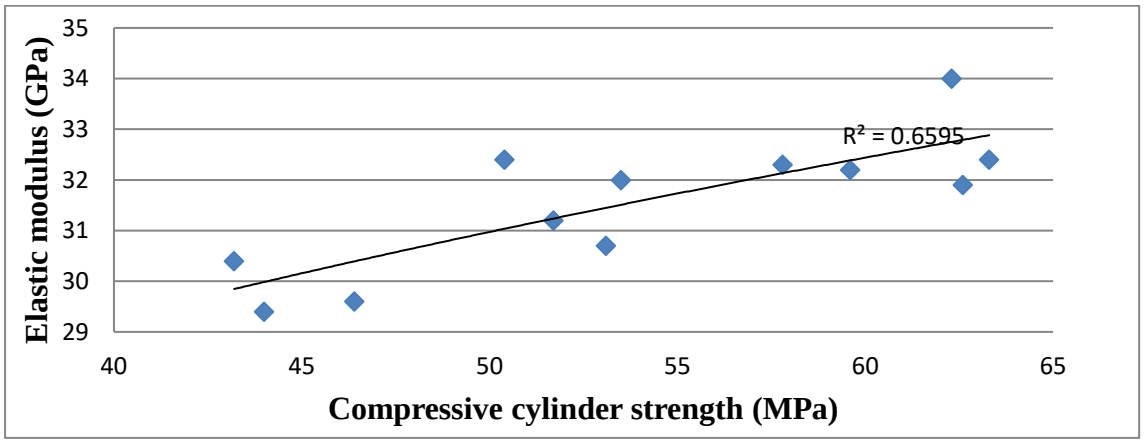

Figure E2 Modulus of elasticity (in GPa) against cylinder strength (in MPa) for 3-day limestone specimens

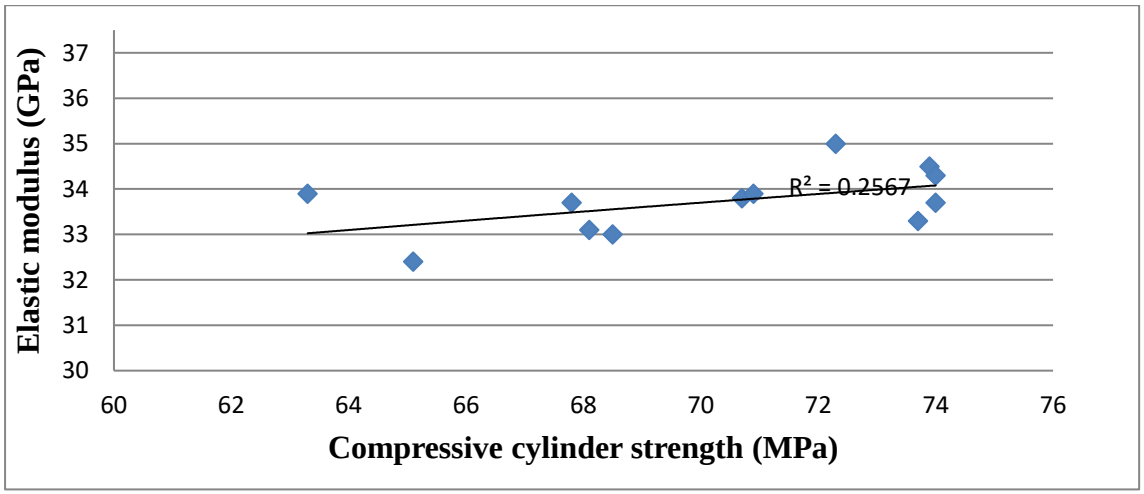

Figure E3 Modulus of elasticity (in GPa) against cylinder strength (in MPa) for 28-day limestone specimens

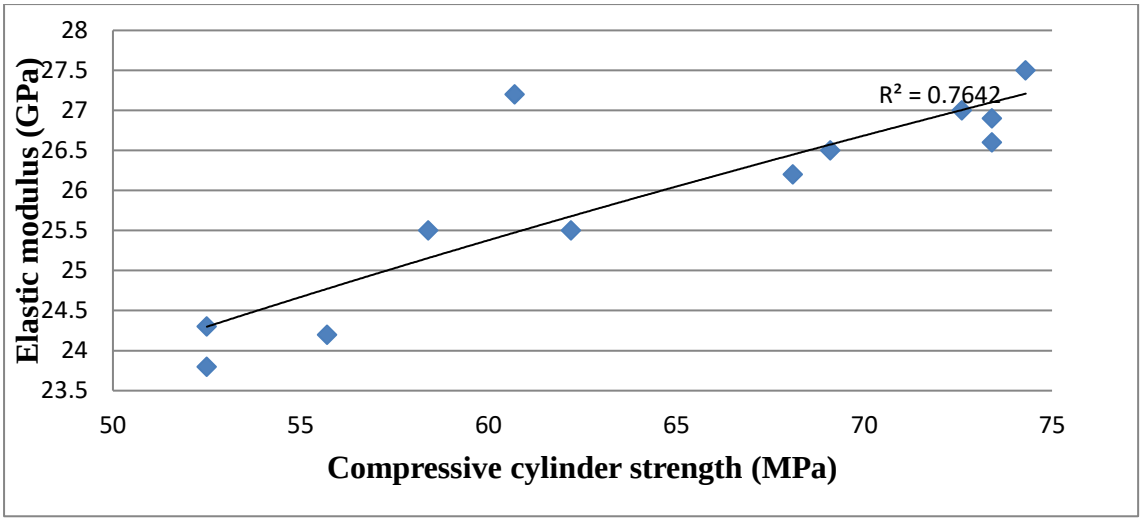

Figure E4 Modulus of elasticity (in GPa) against cylinder strength (in MPa) for 3-day quartzite specimens

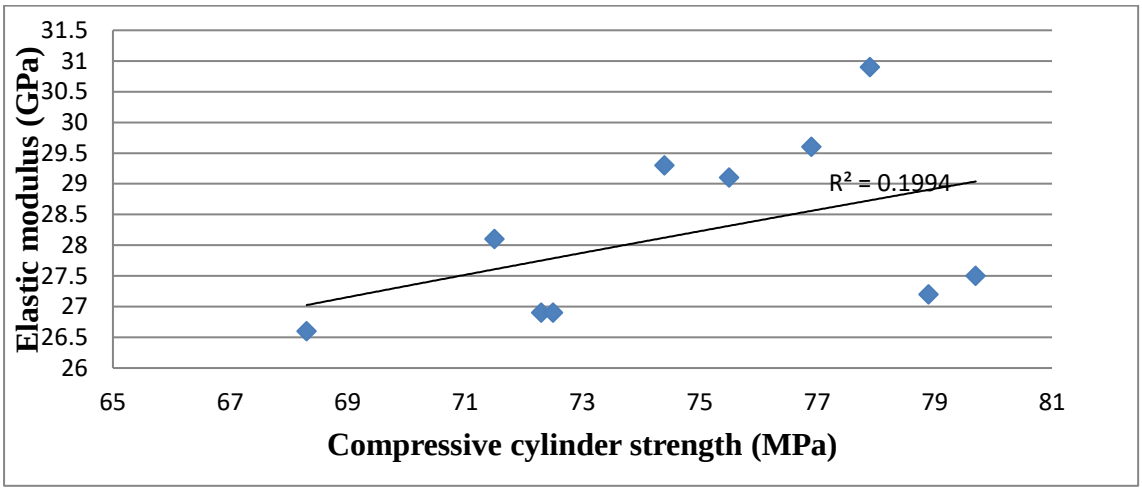

Figure E5 Modulus of elasticity (in GPa) against cylinder strength (in MPa) for 28-day quartzite specimens

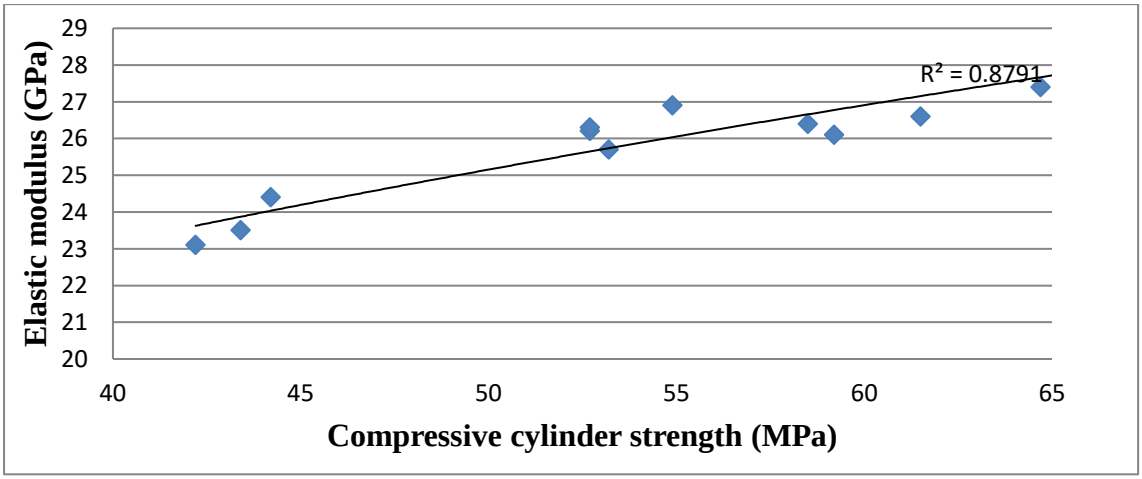

Figure E6 Modulus of elasticity (in GPa) against cylinder strength (in MPa) for 3-day sandstone specimens

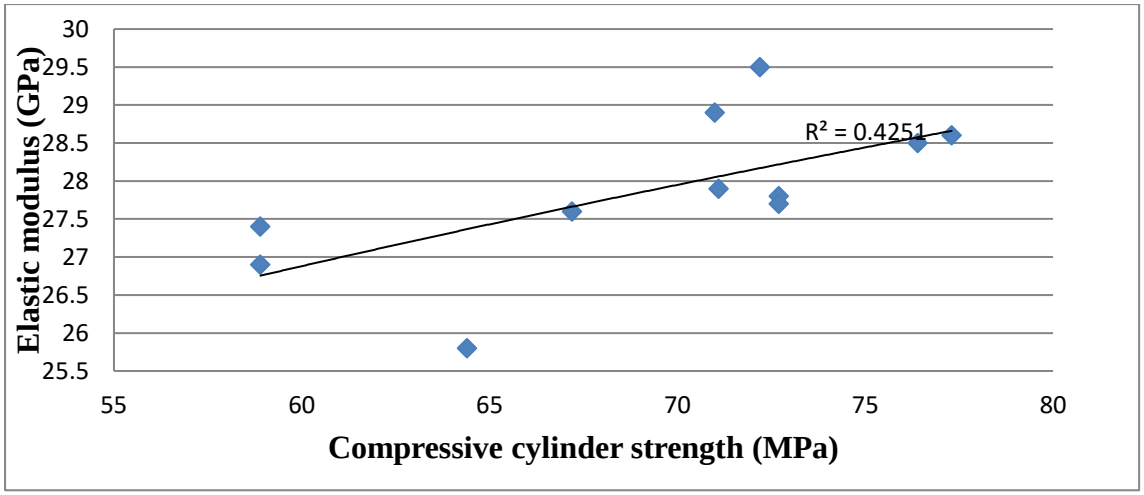

Figure E7 Modulus of elasticity (in GPa) against cylinder strength (in MPa) for 28-day sandstone specimens

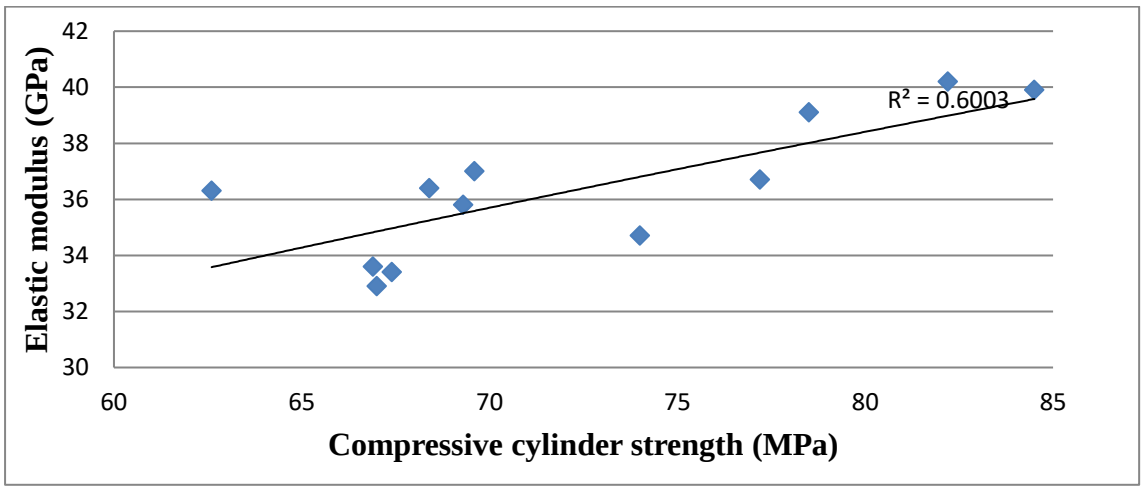

Figure E8 Modulus of elasticity (in GPa) against cylinder strength (in MPa) for 28-day basalt specimens

Appendix F: Comparison of Test Results and Calculated Values

		Sandstone	Basalt	Limestone	Quartzite	Granite
Measure mean value	f_{cm} (MPa)	54.6	52.6	51.7	60.4	57.3
Measure mean value	E_{cm} (GPa)	26.3	35.4	31.4	26.1	20
calculated values by EC2 without α	E_{cm}' (GPa)	36.6	36.2	36.0	37.7	37.1
calculated values by EC2 with α	E_{cm}' (GPa)	25.6	43.4	32.4	37.7	37.1
deviation from EC2	δ	-2.6%	+22.7%	+3.2%	+44.6%	+85.7%
calculated values by *fib* 42	E_{cm}' (GPa)	25.1	42.5	31.7	37.1	36.5
deviation from *fib* 42	δ	-4.5%	+20.2%	+1.0%	+42.2%	+82.4%
calculated values by *fib* 55	E_{cm}' (GPa)	26.4	44.6	33.3	38.9	38.2
deviation from *fib* 55	σ	+0.2%	+26.0%	+6.0%	+49.1%	+91.2%

Table F1 Modulus of elasticity of grade C50/60 at 3 days, assuming α= 1 for granite

		Sandstone	Basalt	Limestone	Quartzite	Granite
Measure mean value	f_{cm} (MPa)	55.8	65.2	58.5	73.7	61.7
Measure mean value	E_{cm} (GPa)	26.2	36.5	32	27	21.3
calculated values by EC2 without α	E_{cm}' (GPa)	36.8	38.6	37.4	40.1	38.0
calculated values by EC2 with α	E_{cm}' (GPa)	25.8	46.3	33.6	40.1	38.0
deviation from EC2	δ	-1.6%	+26.9%	+5.1%	+48.4%	+78.3%
calculated values by *fib* 42	E_{cm}' (GPa)	25.3	45.7	33.0	39.6	37.4
deviation from *fib* 42	δ	-3.4%	+25.1%	+3.3%	+46.8%	+75.5%
calculated values by *fib* 55	E_{cm}' (GPa)	26.5	47.9	34.7	41.6	39.2
deviation from *fib* 55	σ	+1.3%	+31.2%	+8.3%	+53.9%	+84.0%

Table F2 Modulus of elasticity of grade C60/75 at 3 days, assuming α= 1 for granite

		Sandstone	Basalt	Limestone	Quartzite	Granite
Measure mean value	f_{cm} (MPa)	63.9	62.9	61.1	69.9	64.5
Measure mean value	E_{cm} (GPa)	27.4	36.8	32.4	26.6	22.1
calculated values by EC2 without α	E_{cm}' (GPa)	38.4	38.2	37.9	39.4	38.5
calculated values by EC2 with α	E_{cm}' (GPa)	26.9	45.8	34.1	39.4	38.5
deviation from EC2	δ	-2.0%	+24.6%	+5.2%	+48.2%	+74.1%
calculated values by *fib* 42	E_{cm}' (GPa)	26.5	45.1	33.5	38.9	37.9
deviation from *fib* 42	δ	-3.4%	+22.6%	+3.5%	+46.4%	+71.6%
calculated values by *fib* 55	E_{cm}' (GPa)	27.8	47.3	35.2	40.8	39.8
deviation from *fib* 55	σ	+1.3%	+28.6%	+8.5%	+53.5%	+80.0%

Table F3 Modulus of elasticity of grade C70/85 at 3 days, assuming α= 1 for granite

		Sandstone	Basalt	Limestone	Quartzite	Granite
Measure mean value	f_{cm} (MPa)	60.7	69.5	65.6	71	68.3
Measure mean value	E_{cm} (GPa)	26.7	33.7	33.1	26.8	21.4
calculated values by EC2 without α	E_{cm}' (GPa)	37.8	39.4	38.7	39.6	39.2
calculated values by EC2 with α	E_{cm}' (GPa)	26.5	47.2	34.8	39.6	39.2
deviation from EC2	δ	-0.9%	+40.1%	+5.2%	+47.8%	+83.0%
calculated values by *fib* 42	E_{cm}' (GPa)	26.0	46.6	34.3	39.1	38.6
deviation from *fib* 42	δ	-2.5%	+38.4%	+3.7%	+46.1%	+80.6%
calculated values by *fib* 55	E_{cm}' (GPa)	27.3	48.9	36.0	41.1	40.5
deviation from *fib* 55	σ	+2.2%	+45.2%	+8.8%	+53.2%	+89.4%

Table F4 Modulus of elasticity of grade C40/50 at 28 days, assuming α= 1 for granite

		Sandstone	Basalt	Limestone	Quartzite	Granite
Measure mean value	f_{cm} (MPa)	73.4	66	71.8	76.7	72
Measure mean value	E_{cm} (GPa)	28.1	35.4	33.6	27.6	22
calculated values by EC2 without α	E_{cm}' (GPa)	40.0	38.8	39.7	40.5	39.8
calculated values by EC2 with α	E_{cm}' (GPa)	28.0	46.5	35.8	40.5	39.8
deviation from EC2	δ	-0.3%	+31.4%	+6.5%	+46.9%	+80.8%
calculated values by *fib* 42	E_{cm}' (GPa)	27.7	45.9	35.4	40.2	39.3
deviation from *fib* 42	δ	-1.4%	+29.5%	+5.2%	+45.5%	+78.8%
calculated values by *fib* 55	E_{cm}' (GPa)	29.1	48.1	37.1	42.1	41.2
deviation from *fib* 55	σ	+3.4%	+35.9%	+10.4%	+52.6%	+87.5%

Table F5 Modulus of elasticity of grade C50/60 at 28 days, assuming α= 1 for granite

		Sandstone	Basalt	Limestone	Quartzite	Granite
Measure mean value	f_{cm} (MPa)	72	72	72.3	76.7	78.4
Measure mean value	E_{cm} (GPa)	28.7	36.5	34.4	29.9	22.8
calculated values by EC2 without α	E_{cm}' (GPa)	39.8	39.8	39.8	40.5	40.8
calculated values by EC2 with α	E_{cm}' (GPa)	27.8	47.7	35.8	40.5	40.8
deviation from EC2	δ	-3.0%	30.8%	4.2%	35.6%	79.0%
calculated values by *fib* 42	E_{cm}' (GPa)	27.5	47.2	35.4	40.2	40.4
deviation from *fib* 42	δ	-4.1%	29.3%	3.0%	34.3%	77.4%
calculated values by *fib* 55	E_{cm}' (GPa)	28.9	49.5	37.2	42.1	42.4
deviation from *fib* 55	σ	0.6%	35.6%	8.1%	40.8%	86.0%

Table F6 Modulus of elasticity of grade C60/75 at 28 days, assuming α= 1 for granite

Appendix G: Mathematical Deduction of Equations 6.2 and 6.3

First and second derivatives of Equation 6.2:

$\beta(t) = \exp\{s[1-(\frac{28}{t})^{0.5}]\}$ (Equ 6.2)

$\frac{d(\beta(t))}{d\,t} = \sqrt{7}\cdot s\cdot t^{-1.5}\exp\{s[1-(\frac{28}{t})^{0.5}]\}$

$\frac{d^2(\beta(t))}{d\,t^2} = \sqrt{7}\cdot s\cdot t^{-3}\exp\{s[1-(\frac{28}{t})^{0.5}]\}\cdot(\sqrt{7}\cdot s - 1.5t^{-0.5})$

Hence, the turning point occurs when $t = 28s^2/9$

First and second derivatives of Equation 6.3:

$\beta(t) = \exp\{s[1-(\frac{28}{t})]\}$ (Equ 6.3)

$\frac{d(\beta(t))}{d\,t} = 28st^{-2}\exp\{s[1-(\frac{28}{t})]\}$

$\frac{d^2(\beta(t))}{d\,t^2} = 56st^{-4}\exp\{s[1-(\frac{28}{t})]\}\cdot(14s - t)$

Hence, the turning point occurs when $t = 14s$

Appendix H: Values of coefficient s vs proportions of GGBS

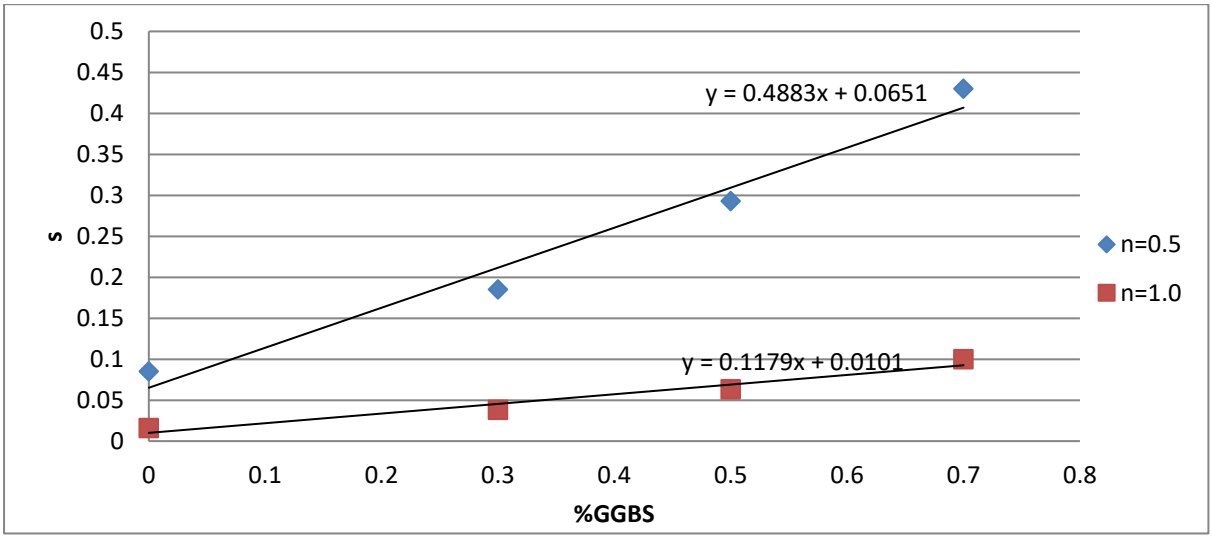

Figure H1 Coefficient s vs %GGBS for RHPC mixes

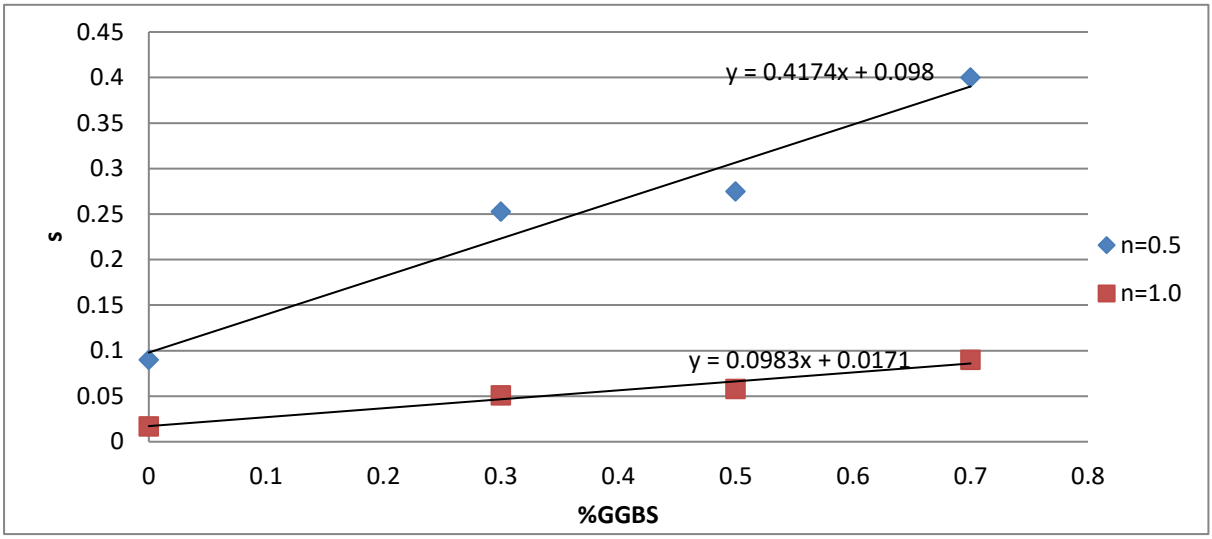

Figure H2 Coefficient s vs %GGBS for CEM II/A-L + Accelerator mixes

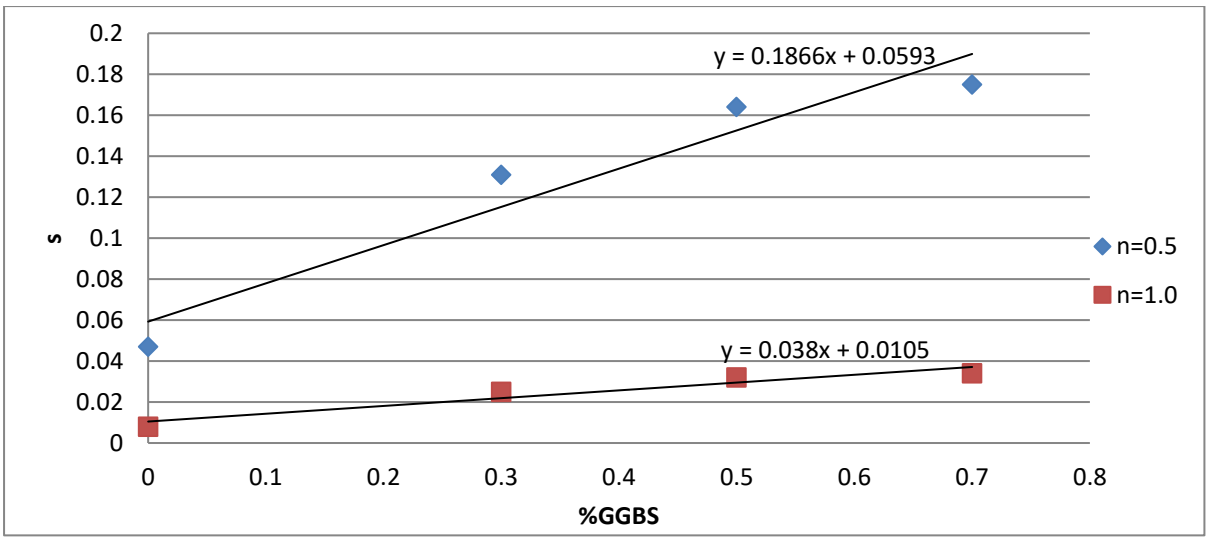

Figure H3 Coefficient s vs %GGBS for CEM II/A-L + Thermal Curing mixes

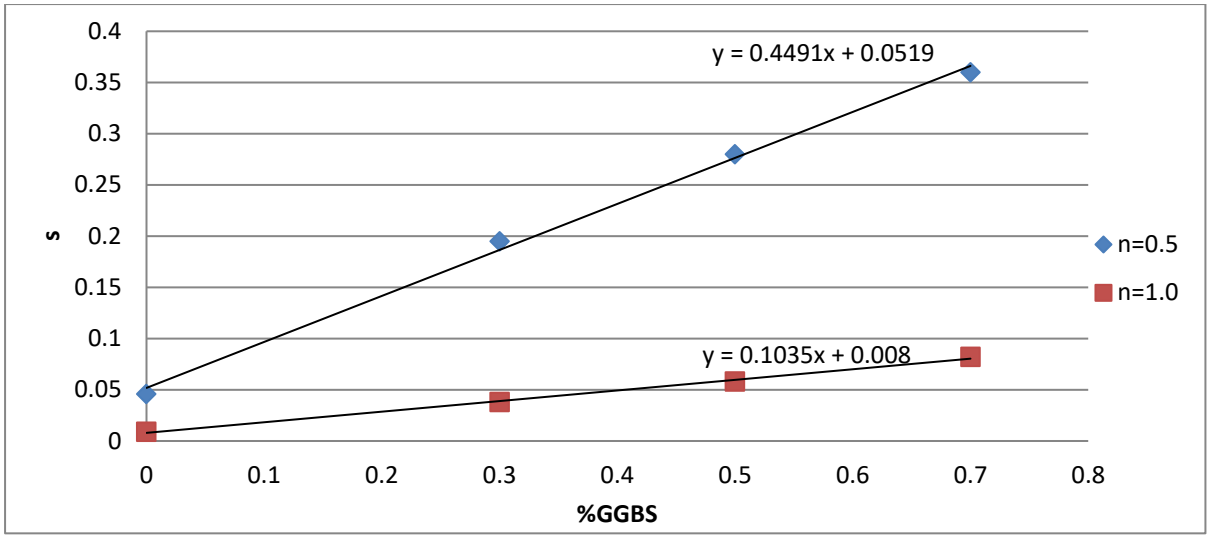

Figure H4 Coefficient s vs %GGBS for RHPC + Accelerator mixes

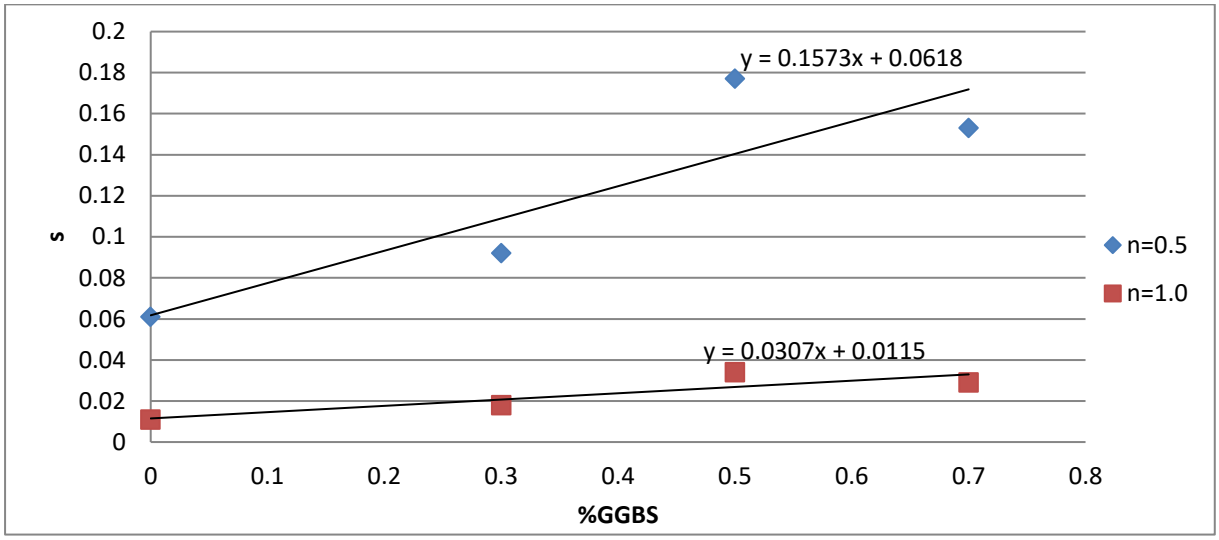

Figure H5 Coefficient s vs %GGBS for RHPC + Thermal Curing mixes

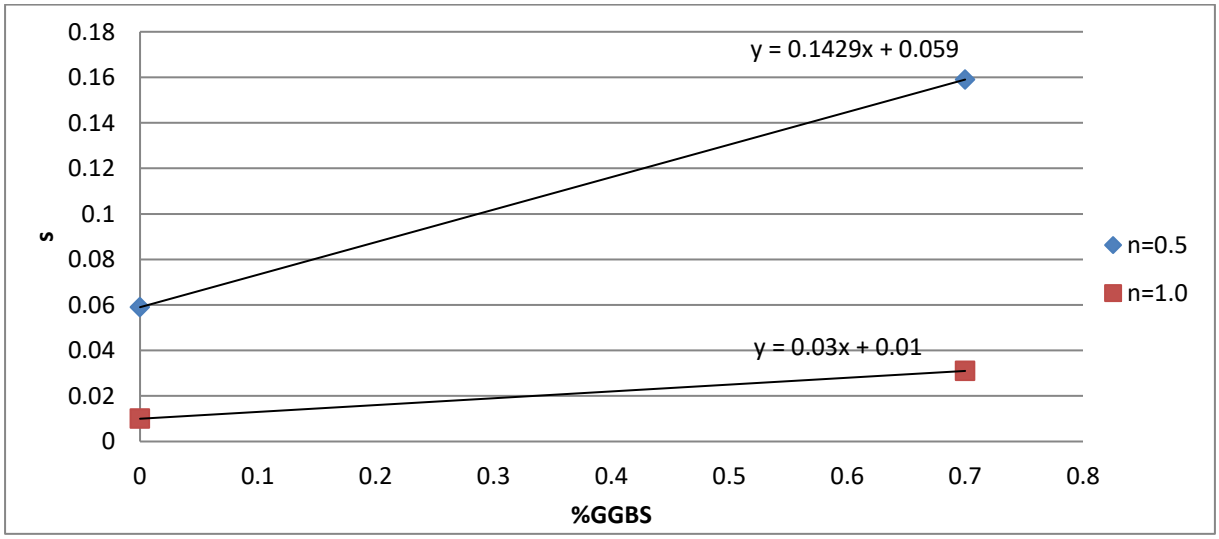

Figure H6 Coefficient s vs %GGBS for RHPC + Accelerator + Thermal Curing mixes